Theta phase precession and the temporal representation of space: Environmental and behavioural contributions to place cell firing in the rat

By

John R. Huxter

A dissertation submitted to the University of London in accordance with the requirements of the degree of PhD in the Faculty of Life Sciences

Department of Anatomy and Developmental Biology

University College London, 2004

Word Count: 60,357

Pages (not including figures): 162

Figures: 48

ProQuest LLC
789 East Eisenhower Parkway
P.O. Box 1346
Ann Arbor, MI 48106-1346

Abstract

Place cells" fire when a rat enters a particular region of the environment – a rate code for space. As the rat traverses the "place field", the place cell fires earlier in each successive cycle of the theta EEG oscillation – a temporal code, known as "phase precession". Simultaneous recordings were made of place cell action potentials and the local EEG in rats shuttling between the ends of a stationary treadmill for food reward. Probe trials involved 1) changing the height of the walls bounding the ends of the treadmill, 2) compressing the treadmill by bringing the end walls together, and 3) changing the speed at which the treadmill moved. The effects of natural variability in running speed and firing rate were also investigated.

Compressing the treadmill compressed place fields, with a proportional increase in phase precession slope. Phase precession was unaffected by other manipulations or natural variability in running speed and firing rate. The moving treadmill produced shifts in place field positions, suggesting that path integration based information plays a direct role in determining where place cells fire.

O'Keefe & Recce (1993) proposed that the interference pattern of two oscillatory inputs produced phase precession. Alternatively it has been suggested (Harris et al., 2003; Buzsáki et al., 2002) that increased depolarisation as the rat approaches the centre of the field allows the cell to fire earlier in the theta cycle, where it would normally be inhibited. Here, the rate and temporal codes were shown to be dissociable, suggesting that a depolarisation model is insufficient to explain phase precession. Firing phase probably encodes information about position in space, with the rate of visual change in the environment determining the rate of one of the oscillators in a dual oscillator model. Firing rate is free to encode other variables, such as running speed.

Acknowledgements

To my dear wife Judy, for following me to a strange and wonderful land across the ocean to do this work. Without her love and support this wouldn't have been possible. To my darling little girls, Holly and Emily, for tolerating the paternal absences completing it often required. To my parents, who never doubted this day would finally come. To the Goodenough College, for making our three-year stay in London a multicultural delight.

To the O'Keefe lab in general, for being a wonderful place to work. Specifically, and alphabetically... to Clive Barker, for fixing everything I broke. To Neil Burgess, for lending his statistical expertise, reviewing this manuscript, and for writing TINT. To Stephen Burton, brain-slicer extraordinaire, who never gets thanked enough. To Francesca Cacucci, my Italian co-conspirator and honorary Newfoundlander. To Jim Donnett, for making a fantastic multi-channel recording system and always having the time to answer questions about it. To Dave Edwards, for making microdrives that were works of art. To Colin Lever, my Interactive Ref-Man™ , who managed to (almost) always keep me humble. To my supervisor, John O'Keefe, for being John O'Keefe, and getting the balance just right. And to Tom Wills, for adding that healthy dose of cynicism to almost everything.

I would also like to thank Andras Czurkó, Bob Muller, and Yu Li, at the University of Bristol, for their helpful commentary.

This research was generously supported by the Rothermere Trust, a Graduate School Research Scholarship from UCL, and the Overseas Research Students Award Scheme (ORS).

Table of Contents

Table of Figures

Page numbers refer to the text page the figure follows.

Chapter 1: Introduction

1.1 Overview

In 1971 O'Keefe and Dostrovsky found that individual neurons in the hippocampus of awake, freely moving rats fire preferentially in response to the animal's position in its environment (the cell's place field). Alongside functional imaging, lesion studies, knockout mice and *in vitro* work using hippocampal slices, "place cell" methodology has contributed enormously to our understanding of the role the hippocampus plays in learning and memory in general, and spatial learning and navigation in particular. The notion that a neuron could encode something as abstract as a representation of "space" was something of an affront to the behaviourist tradition of the time. Nevertheless, this heretical idea culminated in O'Keefe & Nadel's influential *"The Hippocampus as a Cognitive Map"* (1978) - a work whose central thesis was that not only was a neuronal representation of space possible, but that it was indeed **the** primary evolutionary function of the hippocampus.

The cognitive map theory was augmented in 1993 by O'Keefe and Recce, with the discovery of the "phase precession" effect. The hippocampal theta EEG oscillation is characteristic of exploratory behaviour in the rat (Vanderwolf, 1969), and given its coherence throughout large portions of a given cell layer (Bullock, Buzsáki & McClune, 1990), can be thought of as a hippocampal "clock". O'Keefe and Recce observed that both firing rate and the precise timing of place cell firing relative to this "clock" were correlated with position - a temporal code for space. As the rat traverses a cell's place field, the cell fires at progressively earlier phases of each successive theta cycle. Position-dependent phase precession has several exciting implications, potentially compensating for natural variability in the rate code (Fenton & Muller, 1998) or even "freeing" firing rate to encode other aspects of the rat's environment or behaviour within the place field. Recently however, it has been proposed that rather than being independent, the timing of spike firing may in fact be determined by the level of place cell depolarization, as manifested by firing rate (Harris et al., 2002; Mehta, Lee & Wilson, 2002).

Despite these advances in our understanding of hippocampal function, many issues remain unresolved. Broadly speaking, the current investigation focused on two particular issues. 1) First, the role of behavioural parameters in defining the cognitive

map. It is generally assumed that both sensory and self-motion cues contribute to place cell firing, but most studies to date have focussed on sensory factors, while behavioural ones have received considerably less attention. Does running speed affect place field size, shape, or position, or the nature of the phase precession effect? Is there a motor efference contribution to place cell firing? I hypothesized that if hippocampal activity robustly codes for position in space, then the firing of place cells should be unaffected by natural variability in running speed. In contrast, if motor efference contributes to the positional firing properties of place cells, dissociation of motor output and spatial translation ought to produce a systematic change in place field position. 2) Second, are place cell firing rate and firing phase both manifestations of the depolarisation state of the cell? No direct attempt has yet been made to test this hypothesis in intact animals performing tasks on which the phase precession effect is manifested. I proposed that if the two are indeed reflecting the same phenomenon, then the firing rates of individual neurons, modulated as a result of manipulations or varying as a function of uncontrolled variables, should bear a consistent relationship with the preferred firing phase.

For the current experiment, I trained rats to shuttle for food reward on a linear track, and studied the changes in place fields and phase precession in response to natural (uncontrolled) variations in running speed and firing rate, and in response to experimental manipulations. These manipulations included altering the distance between the end walls of the runway (compressing the runway), lowering the height of the end walls, and having the rat perform the shuttling task on a moving treadmill. The results indicate that place field position is influenced by the dissociation of motor output and actual motion produced on the moving treadmill, providing direct evidence that the hippocampus performs a "path integration" function, which up until now has been speculated upon, but unproven. Place fields and phase precession were virtually unchanged by natural variations in running speed and firing rate, but runway compression reduced the size of the place fields, reduced firing rates, and increased the spatial derivative (but not the extent) of phase precession. This indicates that firing phase is indeed dissociable from firing rate (and by extension, cellular depolarization). Firing phase appears inextricably linked to the proportion of the place field traversed, while firing rate is influenced by, and may in fact code for, momentary running speed and alterations in the animal's environment. This represents a serious challenge to the depolarization model of phase precession, and maximises the theoretical utility of firing phase for encoding spatial information.

1.2 Hippocampal Morphology

1.2.1 Gross morphology

If one removes the overlying neocortex (including the entorhinal cortex), the rat hippocampal formation appears as a distinct bean-shaped structure, accounting for approximately 50% of the total cortical volume. Because of the way the structure is seated in the brain, both poles face forward, with the *septal* pole dorsal and anterior, and the *ventral* pole most posterior. Ammon's horn and the DG (see below) form a pair of c-shaped interlocking cell sheets, which, combined with the subiculum and bent in a curve, form the hippocampal "bean", as seen in Figure 1.1. In contrast, the human hippocampus lies "on its back", and is positioned much more ventrally in the brain. Consequently, the dorsal and ventral portions of the rat hippocampus are analogous to the posterior and anterior portions of the human hippocampus, respectively.

A variety of terms are used to refer to structures in or associated with the hippocampus, but they can be broadly separated into those which refer to either allocortex (3-layered) or neocortex (6-layered). This is the basis of the structural classification outlined by Witter et al. (2000), and the same classification will be used here. The *hippocampus*, or *hippocampus proper*, refers to Ammon's horn (Cornu Ammonis), which can be divided into the CA1, CA2 and CA3 fields (Lorente de Nó, 1934). Differentiation of subfields CA1-CA3 is based on the morphology and connectivity of these neurons, but generally speaking, CA1 and CA3 correspond with the upper and lower blades of Ammon's horn, with CA2 comprising the intermediate cells at the apex of the bend. The *hippocampal formation* (HF) is comprised of adjacent allocortical structures: namely, the hippocampus proper, the dentate gyrus (DG), and the subiculum. The *parahippocampal region* consists of neocortical structures which have extensive reciprocal connections with the HF, including the presubiculum (PrS), parasubiculum (PaS), entorhinal cortex (EC), perirhinal cortex, and postrhinal cortex.

It should be noted that the classification system proposed by Paxinos (1995) includes the PrS, PaS, and EC in the definition of the HF. This more liberal classification is based on the "unique and largely unidirectional projections" which link these structures, to form what appears to be a functional unit. The more conservative definition of "hippocampal formation" will be used here. It is also worth noting that the *postsubiculum* is sometimes defined as a separate structure from the presubiculum,

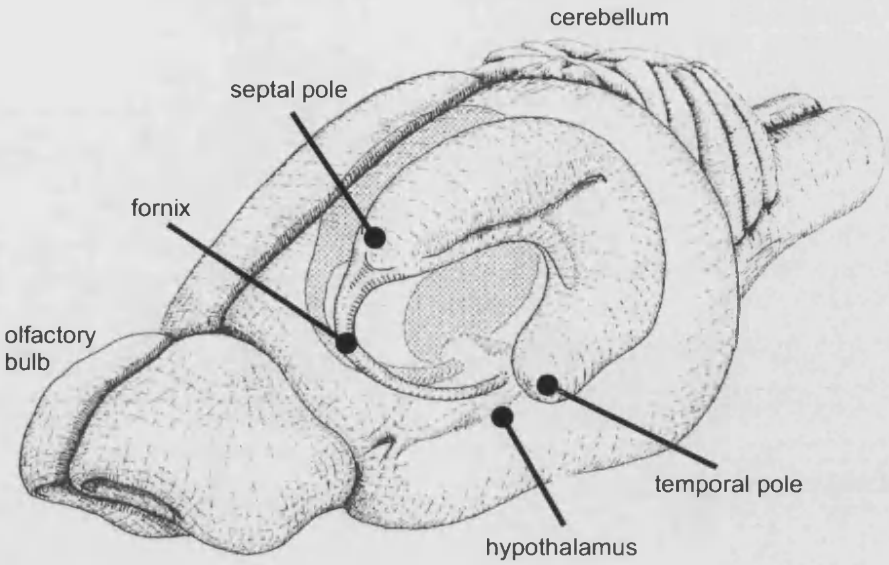

Figure 1.1. Basic hippocampal morphology: the position of the bean-shaped hippocampal formation in the rat brain, and highlights several other prominent structures. Adapted from Paxinos (1995).

but it is unclear whether this is a valid distinction, so the terms will be used interchangeably in this thesis.

1.2.2 Laminar structure

The naming convention for the laminar structure of the HF is directly related to the major morphological features of the principal hippocampal cells (see below), and follows the scheme used by Ramón y Cajal (1911). Approaching the CA1 sub-field from the dorsal brain surface, one encounters the *alveus* (axonal processes), *stratum oriens* (basal dendrites), *stratum pyramidale* (the pyramidal cell body layer), *stratum radiatum* (proximal apical dendrites), *stratum lacunosum-moleculare* (distal apical dendrites), and the *hippocampal fissure* (separating the hippocampus proper from the DG), The lower blade of Ammon's horn presents the same sequence of layers in reverse order for the CA3 pyramidal cells, with the addition of *stratum lucidium* between the pyramidal cell layer and stratum radiatum. The DG is divided into *stratum moleculare* (granule cell dendrites), the *stratum granulosum* (cell bodies) and the *polymorph layer* or *hilus* (granule cell axons). The *hilus* or *polymorph* layer is a morphologically distinct region where CA3 disappears just before intersecting concave surface of the DG (Blackstad, 1956; Amaral, 1978). The laminar structure of the hippocampus and principal neuronal types are illustrated in Figure 1.2.

1.2.3 Neuronal types

Hippocampal neurons can be broadly separated into principal cells, with large "pyramidal" cell bodies and excitatory projections between and beyond the different hippocampal sub-fields, and interneurons, with typically smaller cell bodies and inhibitory projections which in most cases extend only a short distance from the cell body (Ramón y Cajal, 1911; Lorente de Nó, 1934; Szentágothai, 1962, 1965a,b; Eccles, 1964; Andersen et al., 1971). Principal cells are considered to be the information-carriers of the central nervous system, while interneurons are thought to play an integral role in the gating of transmission, the production of extracellular EEG patterns and the entraining of large numbers of hippocampal neurons (more on that later). It should be noted that there are exceptions to these general criteria (e.g. Andersen et al., 1980; Freund & Buzsáki, 1996), which is why hippocampal neurons have often simply been referred to as either "pyramidal" or "non-pyramidal".

The principal neurons of the HF are the *pyramidal cells* of CA1 and CA3, and the *granule cells* of the DG (Ramón y Cajal, 1911; Paxinos, 1995). The densely packed cell bodies of these neurons comprise the pyramidal cell layer in CA1 and CA3, and the granule cell layer in DG. These cell layers are the most pronounced structures under cresyl violet staining, as is clearly evident in Figure 1.2a. Pyramidal cells are characterised by dense dendritic trees on either side of the cell body layer, while granule cell dendrites project only towards the outer surface of the curved dentate gyrus. *Mossy cells* are the principal excitatory cells of the hilus, insofar as the hilus is an ambiguously discrete region straddling the CA fields of Ammon's horn and the upper and lower blades of the DG "proper" (Amaral, 1978, Wenzel et al., 1997) .

There are numerous types of inhibitory hippocampal interneurons, which can be classified according to the positioning of their cell bodies, their efferent targets, and their immunoreactivity (Freund & Buzsáki, 1996). I will attempt only the broadest overview of the more well known classes here. *Basket cells* were perhaps the earliest identified interneuron in the hippocampus, and have cell bodies in the pyramidal cell layer of CA1, CA3, and DG (Ramón y Cajal, 1911, Lorente de Nó, R., 1934). These cells almost exclusively target the soma and proximal dendrites of pyramidal cells (Buhl et al., 1995) and granule cells (Kosaka, Hama & Wu, 1984), surrounding the cell body of their targets with an axonal "plexus" (hence their name). *Chandelier* (*axo-axonic*) cells are another class of pyramidal layer interneuron, but these make almost exclusive contact with the axon initial segment of their pyramidal and granule cell targets (Somogyi et al., 1985; Soriano & Frotscher, 1989; Li et al., 1992; Han et al., 1993). Oriens-lacunosum-moleculare cells (*O-LM)* and their DG counterparts, hilar perforant-path associated cells (*HIPP*), have cell bodies amongst the axonal arbour of the principal cells and target the apical dendrites associated with perforant path input to the HF (McBain, DiChiara & Kauer, 1994; Freund & Buzsáki, 1996). *Bistratified* and *trilaminar* interneurons innervate both the basal and proximal apical dendritic trees of their principal cell targets (Buhl et al.,1994; Sik et al., 1995; Halasy et al., 1996). There are also several classes of interneuron whose primary targets are other interneurons, instead of the principal cells, making them indirectly excitatory. I*nterneuron-selective* or *IS* cells (Freund & Buzsáki, 1996), while others project from one hippocampal field to another (e.g. *backprojection* interneurons; Sik et al, 1995), or to a wide range of interneuron targets throughout the dorso-ventral extent of the hippocampus and to extra-hippocampal structures like the medial septum (*hippocampo-septal* cells; Tóth et al., 1993; Gulyás et al, 2003).

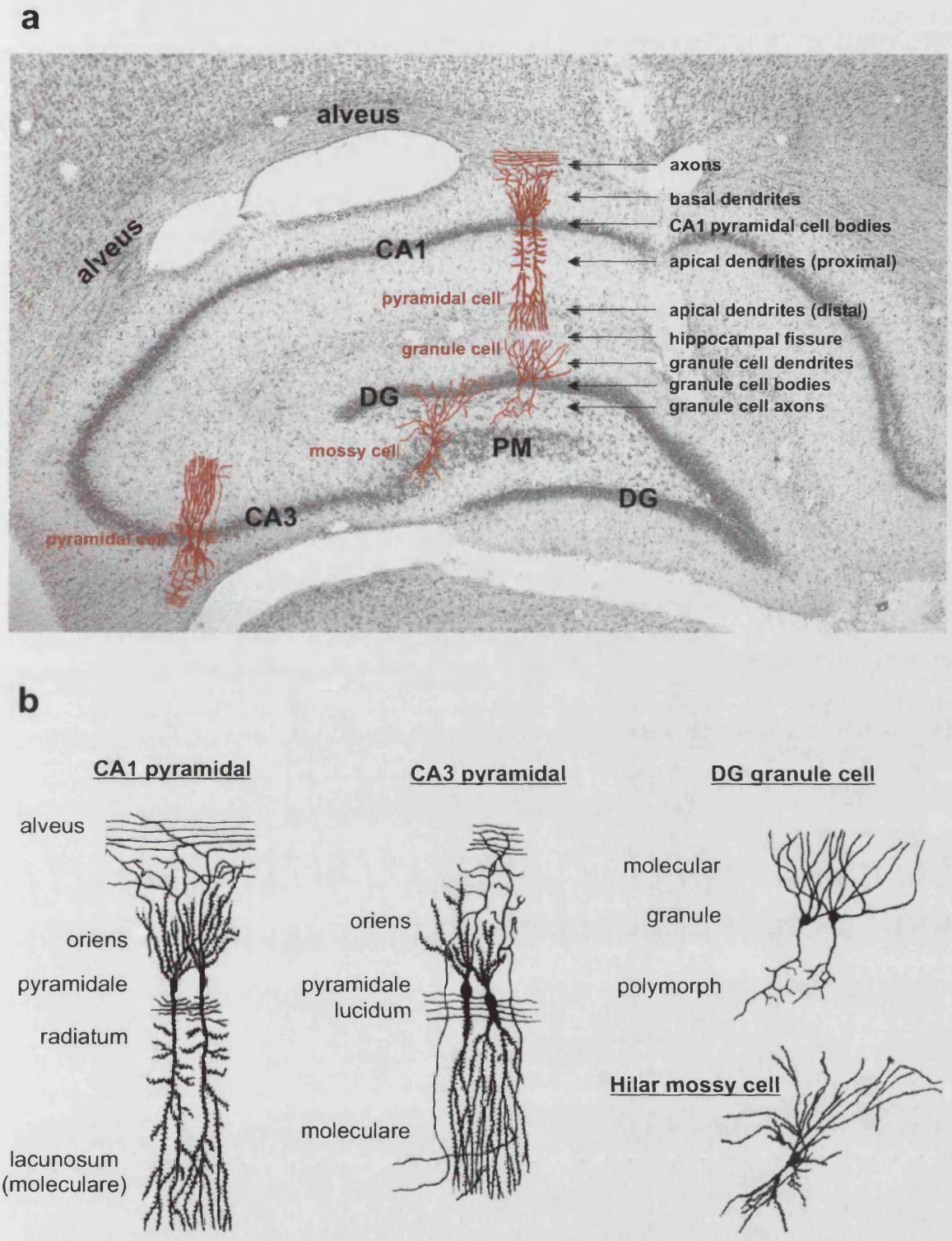

Figure 1.2. Laminar structure of the hippocampus, and principal cell types. **a:** Cresyll violet stained coronal cross section of the hippocampus, highlighting the principal cell bodies. Sub-fields CA1, CA3, dentate gyrus (DG) and hilus (polymorph area, PM) are labelled in bold text, along with the overlying alveus, the hippocampal fissure separating CA1 from the DG, and PM. Representations of the principal cell types in each subfield superimposed in red. Also indicated are the dorso-ventral position of the cell body and main processes of CA1 pyramidal cells. **b:** Principal cell types (Adapted from O'Keefe & Nadel, 1978 and Sharfman, 2003). Note that the CA3 pyramidal cell is presented "upside down" relative to the actual orientation shown in (**a**), in order to highlight the similarities with CA1 pyramidal cells.

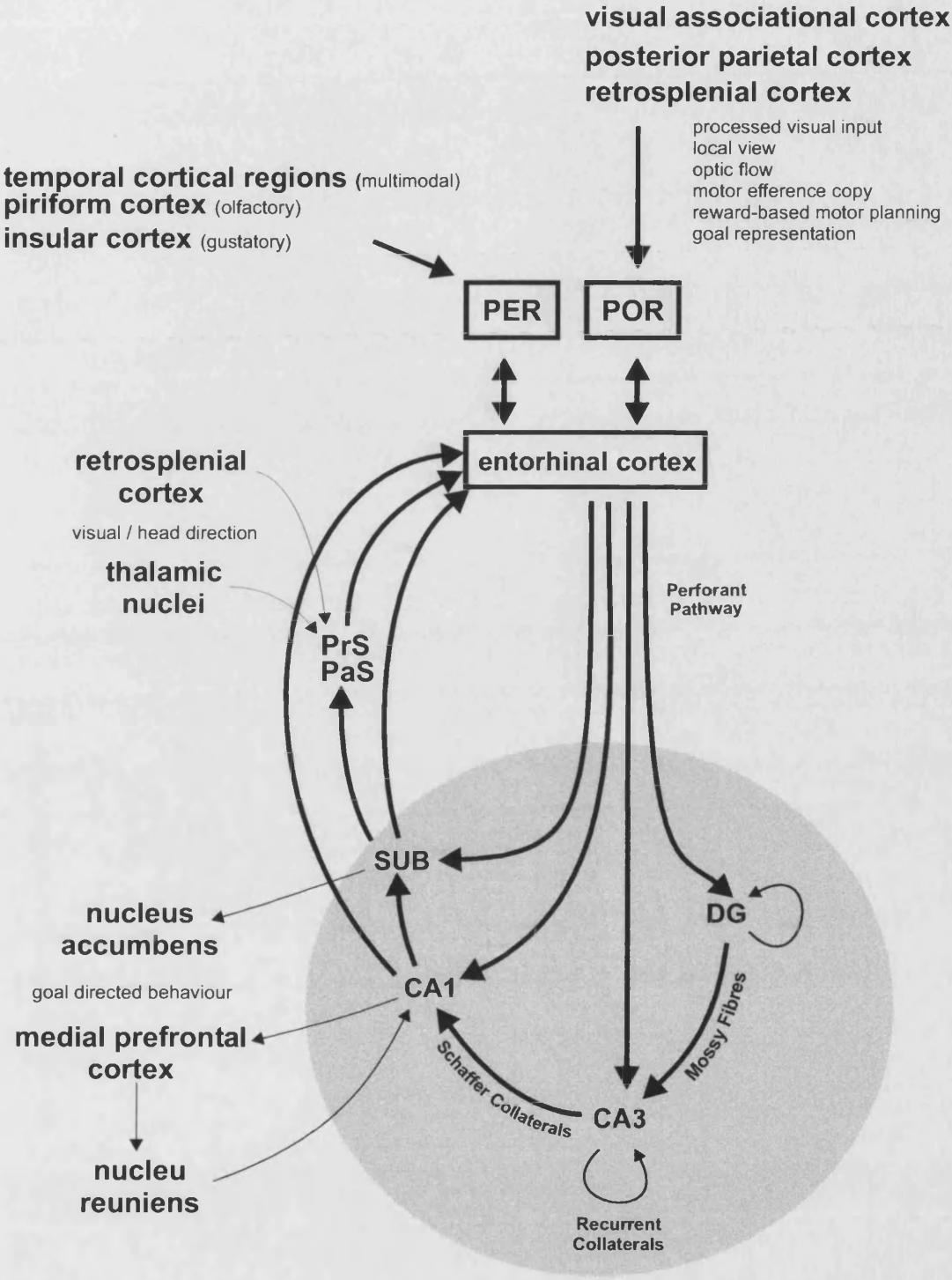

Figure 1.3. The major cortico-hippocampal pathways and hippocampal outputs likely to support goal directed behaviour. Structures of both the hippocampal formation and the parahippocampal region are included. Grey zone delimits the hippocampal formation.Most subcortical connections and some lesser or reciprocal connections are not illustrated. Abbreviations: **DG**: dentate gyrus. **PER**: perirhinal cortex. **POR**: postrhinal cortex. **PrS**: pres/postsubiculum. **PaS**: parasubiculum. **SUB**: subiculum. Adapted from Paxinos (1995) and Witter et al. (2000), with much augmentation.

1.3 Connectivity

In the discussion which follows, afferent, efferent and internal connections are in reference to the entire HF – that is, the hippocampus proper, DG, and subiculum. The pattern of connections to these structures offer some insight into the functions they may perform. Figure 1.3 is a summary of the connections described below. The global picture which emerges is of a structure with numerous internal and external loops, which is capable of integrating a huge array of highly processed sensory and/or mnemonic information, and of guiding behaviour.

1.3.1 Afferents

The most obvious and best documented route by which cortical information reaches the HF is via the EC and the *perforant path* - a dense fibre pathway arising from the superficial layers of the EC (layers II and III) and directly innervating all parts of the HF (DG, CA1, CA3 and subiculum). EC efferents terminate in stratum moleculare of the DG and stratum lacunosum-moleculare of CA1/CA3.

There is a high degree of convergence of information at the EC from subcortical regions and both unimodal and polymodal cortices (Burwell & Amaral, 1998). The *perirhinal cortex* (PER) projects primarily to the lateral EC, and itself receives projections from all sensory modalities, but in particular from the *piriform cortex* (olfactory; Haberly, 2001) and *insular cortex* (gustatory; Kiefer & Braun,1977; Kosar et al., 1986). In contrast, the *postrhinal cortex* (POR) projects to the medial EC, and receives its primary afferents from the *visual association cortex*, with substantial inputs from the ventral temporal associational area, retrosplenial cortex, and posterior parietal cortex as well. The posterior parietal – POR – EC route is one way by which vestibular and motor efference information regarding self motion may enter the hippocampus (Wiener & Berthoz, 1993; Andersen et al., 1997). PER and POR also project directly to the subiculum (e.g. Naber, Witter & Lopes da Silva, 2001), and pre- and parasubiculum both receive input from the visual cortex via retrosplenial cortex.

Subcortical regions target the hippocampus both directly and via the EC. For example, the amygdala, thalamic nuclei, dorsal raphe nucleus and *locus coeruleus* (LC) all project to EC. (Beckstead, 1978). The LC provides noradrenergic projections directly to the HF as well, particularly DG (Oleskevich, S., Descarries, L., & Lacaille, J.C., 1989). The amygdaloid complex targets both CA1 and subiculum, though

principally the ventral portions. The *medial septum* (MS) and vertical limb of the *diagonal band of Broca* (DBv) project strongly to virtually every structure in the hippocampal formation, including EC, DG, CA3, the subiculum, and to a lesser extent, CA1. MS/DBv input has been implicated in the generation of the hippocampal theta oscillation (Stewart & Fox, 1990), and can be subdivided into excitatory (cholinergic) targeting primarily pyramidal cells, and inhibitory (GABAergic) input targeting mostly inhibitory interneurons (Freund & Antal, 1988). Consequently, this pathway is a net excitatory one for hippocampal pyramidal cells. The anterior thalamic nucleus (ATN) and laterodorsal thalamic nucleus (LDN) project to the hippocampus via the cingulate cortex and subicular complex, but also have terminals in the deep layers of EC (Van Groen and Wyss, 1992, 1995) and the subicular complex (Shibata, 1993). These projections provide a potential route for head-direction information into the hippocampus (Mizumori & Williams,1993). A major thalamic projection from nucleus reuniens targets both CA1 and the subiculum (Wouterlood et al., 1990). This is a particularly interesting connection, as the nucleus reuniens receives a substantial projection from the *medial prefrontal cortex* (mPFC) – a brain region implicated in decision making and goal-directed behaviour (Vertes, 2002).

1.3.2 Efferents

Many of the projections from the hippocampal formation described above are, in fact, reciprocal connections. The principal path for information out of the hippocampus is via the subiculum (the major target for CA1), which in turn projects to pre- and parasubiculum and thence to the deep layers III-IV of EC (Witter et al., 1989). Both CA1 and subiculum also project directly to EC (Naber, Lopes da Silva & Witter, 2001). A similar system of back-projections from HF to EC has been identified in primates (Rolls, 2000). The main target of hippocampal output via the EC is the perirhinal cortex, and to a lesser degree, the motor, somatosensory, auditory, and visual cortices (Insausti et al., 1997).

Subcortical regions also receive projections from the hippocampus. The subicular complex, for example, projects to ADN and LDN (van Groen & Wyss, 1990). The fimbria/fornix represents a major fibre tract arising from pyramidal cell axons in the alveus, and targets basal forebrain structures such as the septal nuclei, and the diencephalon (Amaral & Witter, 1995). There is also a direct projection to nucleus accumbens from the ventral subiculum, which converges with fibres from prefrontal

cortex (French & Totterdell, 2002). This suggests a role for the hippocampus in guiding purposeful behaviour (Mogenson et al., 1983.; Groenewegen et al., 1991). Direct CA1 and subicular projections to cortical regions like the retrosplenial cortex and mPFC further reinforce the notion that the hippocampus plays a role in guiding behaviour (Jay & Witter, 1991).

The aforementioned afferents refer to processes arising from the principal cells in the output stages of the HF – namely pyramidal cells of CA1 and the subiculum. However, it is worth noting that there are also a class of backprojecting interneurons in the hippocampus (Alonso & Kohler, 1982; Freund & Buzsáki, 1996; Gulyás et al., 2003) which innervate interneurons in the MS/DBv. The existence of this interneuron pathway is suggestive of a feedback mechanism for regulating septal theta modulation in the HF.

1.3.3 Intrinsic connections

While the perforant path terminates in all of the HF subfields, the flow of information between the DG, CA3, CA1 and subiculum can be described as essentially unidirectional (see Amaral & Witter, 1995, for a review). The main glutaminergic pathway through the HF is as follows: Mossy fibres from DG granule cells target proximal dendrites of CA3 pyramidal cells in stratum lucidium, CA3 pyramidal cells give rise to Schaffer collaterals which project to CA1 pyramidal cell proximal dendrites in stratum radiatum, and CA1 efferents contact subicular pyramidal cells via the alveus. There are no significant excitatory projections within the HF running in the opposite direction, nor are there any major "short-cuts" from, say, DG to CA1, or from CA3 to subiculum.

There are two excitatory synaptic loops within the hippocampal formation which are hypothesised to support associative memory functions (e.g. Marr, 1971; Treves & Rolls, 1992; Lisman, 1999). 1) In the DG, granule cell mossy fibres have powerful excitatory input to hilar mossy cells, which in turn provide glutaminergic input back to granule cells and hilar GABAergic interneurons (Scharfman, et al., 1990; Buckmaster & Schwartzkroin, 1994; Wenzel et al., 1997). 2) In CA3, pyramidal cells give rise to recurrent collaterals which target other CA3 pyramidal cells at stratum radiatum. This is, in fact, the single strongest excitatory input to CA3 principal cells. (Amaral & Witter, 1989). CA1 has no such recurrent collateral system, but because both the subiculum and CA1 project to deep EC, connections between deep (input) and superficial (output)

layers of the EC (Lorente de Nó, R.,1933; Kloosterman et al., 2003.) make it theoretically possible for hippocampal output to be fed back in, forming a HF-EC loop.

1.4 Physiology

Broadly speaking, the EEG state of the awake rat brain can be said to shift between one of two conditions (Vanderwolf, 1969; Buzsáki, 1989) – *large irregular activity* (LIA) and *theta*, or rhythmic slow activity (RSA). The extracellular currents that experimenters refer to as the EEG are believed to arise from the coordination of membrane potential oscillations (MPOs) of the principal hippocampal neurons, and the synchronised firing of large populations of interneurons. Membrane potential oscillations may be driven by sub-threshold EPSPs or IPSPs, but may also reflect, or be amplified by, the natural tendency of hippocampal neurons to resonate at theta frequencies. These concepts will be explored in more detail in section 1.4.4. *Gamma oscillations*, which tend to be associated with theta (Bragin et al., 1995), will be discussed separately, in addition to the probability and timing of individual neuronal firing in relation to theta and LIA.

1.4.1 LIA

The term LIA was used by Vanderwolf (1969) to refer to arrhythmic large amplitude (1-3 mV) events, typically associated with automatic or non-voluntary behaviours like eating, quiet wakefulness, or slow wave sleep. Two phenomena associated with the LIA state are sharp waves (SPWs) and ripples. Both may reflect aspects of the same phenomenon, as they tend to occur together – sharp waves most notably in stratum radiatum, and ripples in the CA1 pyramidal cell layer (O'Keefe and Nadel 1978; Buzsáki et al., 1992). Sharp waves are abrupt deflections in EEG which are negative at stratum radiatum, and positive-going at or above the CA1 pyramidal cell layer, when visible at this depth. Ripples are 100-200 Hz sinusoidal bursts which become apparent as electrodes approach the CA1 pyramidal cell layer from the overlying cortex – they are often used as the first sign of approach to the hippocampus, as electrodes are lowered through the overlying cortex. Ripples can be seen to be superimposed on sharp waves in an unfiltered EEG recording. When recording from within the CA1 pyramidal cell layer, burst firing of many individual neurons can be seen

to be superimposed on the ripple oscillation. This is believed to result from a general disinhibition of pyramidal neurons during the LIA state.

Recent evidence suggests that sharp waves, ripples, and the associated population activity in CA1 are generated in CA3 (Csicsvari et al., 2000). These events may be facilitated by CA3's unique recurrent connectivity, an attenuation of cortical inputs to the hippocampus via EC layers II-III (Chrobak & Buzsáki, 1994), and disinhibition resulting from a reduction in the release of subcortical neuromodulators (Hasselmo et al., 1995). The resulting bursts of internally generated, synchronised hippocampal activity have been proposed as a mechanism for transferring processed packets of information from the hippocampus to cortical regions (Chrobak & Buzsáki, 1994; Ylinen et al., 1995; Siapas & Wilson,1998).

1.4.2 Theta - general properties

The second general hippocampal EEG state is *theta* - sometimes referred to as "rhythmical slow activity" (RSA), but here I will continue to use the more common designation of "theta". Figure 1.4a presents a theta EEG recording during a single traversal of the runway in the current experiment. Theta is a coherent 4-12 Hz hippocampal field potential oscillation in the rat, but was identified as a 3-7 Hz "arousal response" in the rabbit hippocampus by Green & Arduini (1954), who named it after the human EEG pattern of similar frequency. I will focus on theta oscillations in the HF of awake freely moving rats, but it should be noted that theta oscillations have been identified in other limbic structures associated with the hippocampus such as the cingulate cortex (Holsheimer, 1982; Leung & Borst, 1987), EC (Mitchell & Ranck, 1980); Alonso & Garcia-Austt, 1987) subiculum (Bullock et al, 1990; Anderson & O'Mara (2003), and amygdala (Pare & Collins, 2000; Seidenbecher et al., 2003).

Within a particular hippocampal cell layer, theta oscillations are believed to be phase-coherent across large areas of the hippocampus (Bland et al., 1975; Bullock et al., 1990; but see also Petsche, H & Stumpf, 1960). This broad coherence makes the theta oscillation a good candidate for a hippocampal clock, coordinating the activity of neurons from disparate regions of the hippocampus. In contrast with this coherence at a given recording depth, theta phase has a distinct depth profile along the axis of the individual principal neurons in CA1, CA3 and DG. Using multi-site recording electrodes, Bragin et al. (1995) simultaneously recorded theta EEG at a variety of depths in both the hippocampus and the DG, and noted a gradual phase inversion of approximately

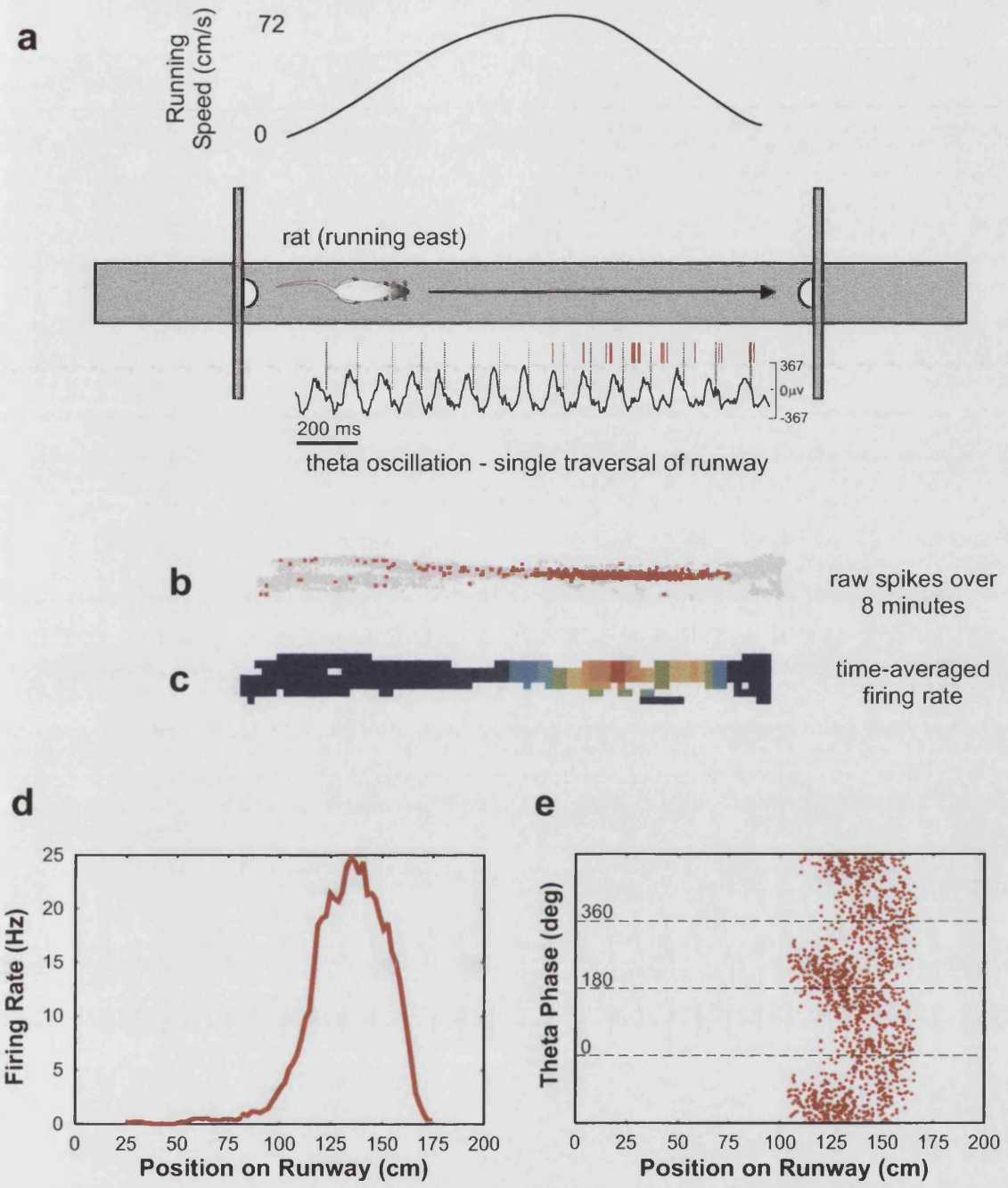

Figure 1.4. Place cells and theta phase precession as a rat runs from left (west) to right (east). **a:** A single eastbound traversal of the runway, with running speed, theta phase, and spike firing illustrated. Dashed lines indicate the beginning of theta cycles (zero-crossings). Note the spatially constrained firing pattern, the tendency for spikes to occur in bursts in the middle of the spike distribution, and the shift in firing to earlier portions of each successive theta cycle. **b:** Data summed over 8 minutes of eastbound traversals. Grey areas indicate areas the rat visited, while red pixels represent the rat's position when an action potential occurred. **c:** Autoscaled colour contour firing rate plot of the same data. This is the rate code for position, and is the typical way place fields are represented. **d:** A line-graph version of the preceding, with data collapsed in the Y-dimension as was the norm for this experiment. **e:** The phase precession effect. Individual spike firing from multiple traversals of the runway as a function of position and the phase of the local theta oscillation. Data is duplicated beyond the original 0-360^0 to compensate for the circular nature of the data, which normally obscurs the linear nature of the position vs. phase relationship.

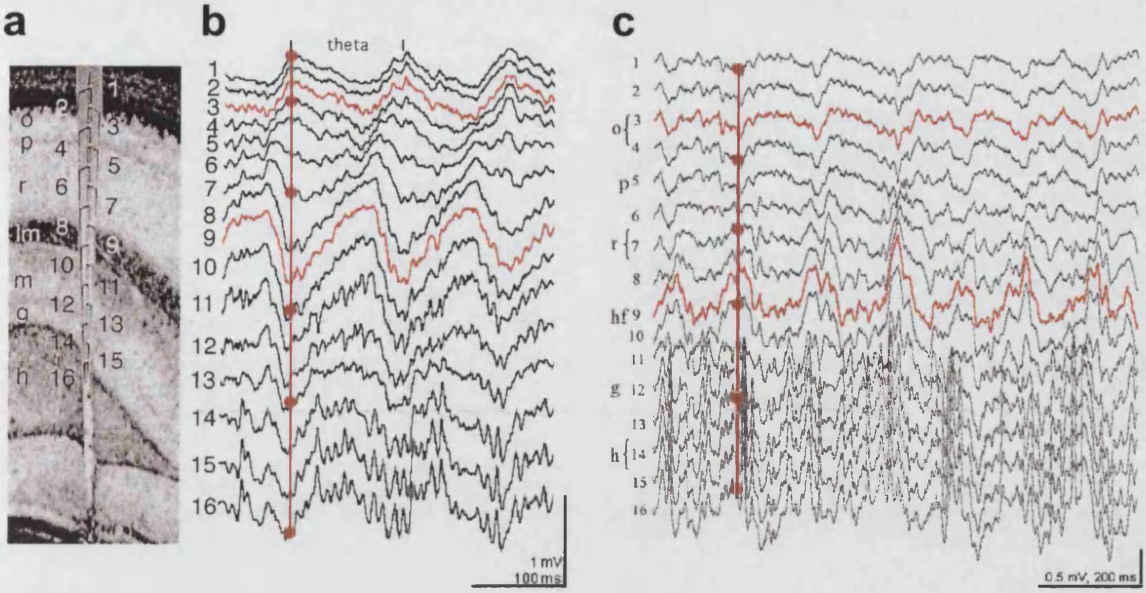

Figure 1.5. The laminar depth profile of the hippocampal theta EEG. **a:** Stained hippocampal section showing placement of a 16-site silicon probe used to record EEG simultaneously at 100μm intervals covering all layers of the hippocampus and dentate gyrus. **b,c:** EEG recordings, showing the gradual theta phase inversion between stratum oriens and the hippocampal fissure - traces from these two layers are indicated in red to highlight the 180^0 phase inversion. Trace numbering in **b** corresponds with recording site numbering in **a**. Each adjacent pair of nodes on the vertical red lines represent potential recording sites from tetrode pairs in the current experiment, which were separated by 300μm. Note that recording sites straddling the pyramidal cell layer (trace 5) exhibit inverted theta phase (peaks corresponding with valleys) while other pairs of nodes at this spacing do not. This feature of hippocampal physiology facilitates localisation of electrodes during recording. Figure adapted from Bragin et al., 1995 (**a,b**) and Kocsis et al., 1999 (**c**).

180^0 between theta power maxima at stratum oriens and the hippocampal fissure (see also Winson, 1974; Leung, 1984a). This laminar phase shift, which becomes apparent near stratum radiatum when lowering electrodes through the hippocampus, is frequently used as a physiological marker for electrode depth. The theta depth profile is illustrated in Figure 1.5. It is worth noting that theta power minima and maxima generally occur at the levels of principal cell soma and dendrites, respectively (Buzsáki et al., 1986).

1.4.3 Theta - behavioural correlates

In a classic study, Vanderwolf (1969) demonstrated three main correlates of hippocampal theta. 1) In the awake rat, theta is most reliably related to voluntary movements - such as rearing, walking, climbing, struggling or jumping, and disappeared during periods of motionlessness - and not "automatic" behaviours like grooming, or drinking, nor arousal states, unless the arousal was accompanied by movement. During periods of motionlessness, theta disappears. 2) In a shock avoidance task, theta was continuously present during the period of motionlessness just before jumping (when the rat appears focussed on the ledge it had to jump to), and increased in frequency just prior to jumping. 3) In the unconscious rat, theta is associated with paradoxical sleep, or REM. In humans at least, REM experiences often resemble waking periods of voluntary movement. Vanderwolf (1969) commented that cerebrospinal pathways are known to be active during REM sleep, and that physical movement is simply inhibited by descending pathways. In summary, rat-theta is directly related to voluntary movement through space, the preparation for such movement, and perhaps the dream-like experiences of motion (assuming of course that rats dream!).

Morris et al. (abstract, 1975) replicated Vanderwolf's shock avoidance experiment, noting that the increase in theta frequency was greatest during the launch and immediately thereafter, and that the magnitude of the increase was directly related to the height of the jump, but unaffected by the addition of a 50g weight fixed to the rat's back. This reinforces the notion that movement through space or preparation for it is directly related to theta, and that acceleration (but not the muscular effort required for it) might be a determinant of theta frequency. Some researchers have found a relationship between movement velocity and theta frequency in rats (Bland & Vanderwolf, 1972; McFarland et al., 1975; Oddie & Bland,1998; Slawinska & Kasicki, 1998) guinea pigs (Rivas et al., 1996) and dogs (Arnolds et al., 1979), while others

have not, instead noting a relationship between theta *amplitude* and core temperature (Whishaw & Vanderwolf, 1971,1973) or running-wheel speed (Czurkó et al., 1999). The relationship between theta frequency and the velocity and acceleration of an animal's motion through space remains ambiguous.

Theta oscillations have been most extensively studied in the rat, but have been identified in other mammalian species, including mice (Buzsáki et al., 2003), rabbits (Green, & Arduini, 1954), dogs, cats, and gerbils (Winson, 1972), pigeons (Siegel et al., 2000), monkeys (Crowne & Radcliffe,1975; Stewart & Fox, 1991) and humans (Meador et al., 1991; Kahana et al., 1999; Tesche & Karhu, 2000). Intra-cranial recordings from human epileptics suggests that, as with other species, theta accompanies simulated spatial behaviour in virtual reality tasks (Caplan et al., 2001), but there is also evidence that human theta is associated with non-spatial working memory (e.g. Raghavachari et al., 2001). Interestingly, Rugg & Dickens (1982) found that while verbal tasks increased the power of theta in both hemispheres, the increase during a visuospatial task was only evident in the right hemisphere. Such hemispheric differences have not been noted in other species. It should also be noted that humans are not the only species which, unlike rats, exhibit theta during non-movement, non-REM states. Specifically "non-spatial" theta has also been documented in rabbits (Green & Arduini, 1954), pigeons (Siegel et al., 2000), and cats (Golebiewski et al., 1999).

1.4.4 Generation of theta

Experiments by Vanderwolf and colleagues (Vanderwolf, 1975, Kramis et al., 1975) suggest that theta can be divided into atropine-sensitive and atropine-resistant types. Under urethane anaesthesia, theta can occur spontaneously or in response to a tail-pinch, but is abolished by cholinergic blockers like atropine sulphate. Consequently, this is referred to as "atropine sensitive" theta, and must be dependent on excitatory cholinergic input. In contrast, theta during walking could not be similarly abolished, and was termed "atropine resistant". The receptor or receptors mediating atropine resistant theta are still unknown although serotonergic (Vanderwolf, 1988) and glutaminergic pathways (Buzsáki, 2002) have been proposed. Only atropine-sensitive theta is present under deep anaesthesia, while both types of theta are presumably present simultaneously in the awake moving animal. However, the two types might be dissociable depending on the rat's behaviour. Specifically, Kramis et al. (1975)

observed that walking-related theta is atropine-resistant, while theta observed prior to planned movements is atropine-sensitive.

Given that MS/DBv is a major source of cholinergic projections to the entire HF (Lewis & Shute, 1967), that septal neurons fire in rhythmic bursts in time to hippocampal theta (Petsche et al., 1962) and that lesions of the medial septum completely abolish theta (Andersen, et al., 1979; Gray, 1971), it is not surprising that the MS/DBv came to be viewed as the principal theta "pacemaker" (see Stewart & Fox, 1990, for a review). The MS/DBv is in fact comprised of both cholinergic and GABAergic cells (Baisden et al., 1984; Kohler et al., 1984), but the muscarinic ACh receptors of pyramidal cells are too slow to generate a theta-frequency oscillation (Cole & Nicoll, 1983; Stewart & Fox, 1992). Therefore, only the GABAergic projections are capable of acting in the capacity of a theta rhythm generator. In support of this notion, following selective neurotoxic lesions of septal cholinergic projections to the hippocampus, CA1 theta frequency is preserved while power was considerably reduced (Buzsáki et al., 1986). It would appear that septal cholinergic innervation, which targets both pyramidal cells and local CA1 interneurons (Freund & Antal, 1988), may principally serve to provide a tonic level of depolarisation which permits rhythmicity to be expressed.

As mentioned previously, there is a distinct laminar profile to hippocampal theta, and current source density analyses have revealed three noteworthy theta dipoles in CA1- **1**) a current source at or near stratum pyramidale related to inhibition at the soma, **2**) a small current sink at stratum radiatum reflecting excitatory Schaffer collateral input from CA3, and **3**) and a large sink near the hippocampal fissure that corresponds with the perforant path excitatory input to the distal dendrites from the EC (Buzsáki et al., 1986; Brankack et al, 1993). Bilateral lesions of the EC abolish the theta dipole at lacunosum moleculare (Bragin et al., 1995), and the theta oscillations which remain following this type of treatment are completely abolished by atropine (Buzsáki et al, 1983). This implies that rhythmic somatic inhibition depends on cholinergic input from the MS/DBv, while the dipole at stratum lacunosum-moleculare requires additional (probably glutaminergic: Buzsáki, 2002) excitatory drive. Interestingly, Kocsis et al. (1999) determined that theta generated at stratum oriens and lacunosum-moleculare, while phase inverted, exhibited a high degree of coherence. In contrast, theta from radiatum was coherent with theta from the DG granule cell layer. Kocsis and colleagues also noted that bilateral EC lesions caused all theta signals in the CA1 field to become coherent, both above and below the cell layer.

These results suggest that there are two independent excitatory theta generators – one related to the EC, and the other to CA3, although neither of these structures need necessarily be the ultimate source of the rhythmicity observed in CA1.

Recent experiments cast some doubt on whether the MS/DBv is actually necessary for or even capable of acting as a hippocampal rhythm generator. capable, of producing coherent rhythmicity in the hippocampus. King, et al. (1998) found that GABAergic neurons in the MS/DBv, far from firing at a coherent phase relative to the hippocampal theta rhythm, are in fact a very diverse population. Some neurons do not fire phase locked to theta, while others do, and those that do exhibit a variety of preferred phases. Similar results were found by Dragoi et al. (1999), although in the latter case, the authors also suggested that a sub group of rhythmic septal cells, inhibited during LIA-associated sharp waves (SPW), are indeed phase locked to the negative peak of CA1 theta, and may form a functional group. The inhibition of this class of septal neurons by a hippocampal population phenomenon is presumably mediated by projections of HF GABAergic neurons to the septum (Alonso & Kohler, 1982; Gulyás et al., 2003). This same hippocampo-septal projection may have a role in regulating septal rhythmicity - the converse of the septal pacemaker hypothesis.

So, assuming for a moment that the MS/DBv does not give rise to a coherent theta oscillation in the hippocampus, where does the synchrony arise from? It has recently been discovered that numerous classes of hippocampal neurons are endowed with membrane properties which allow them to resonate at theta frequencies. Such intrinsic oscillations have been identified in pyramidal cells in interneurons and CA1 and CA3 pyramidal cells, and result in the expression of field potential oscillations in response to non-rhythmic excitation (MacVicar & Tse, 1989; Strata, 1998; Chapman & Lucille,1999; Fellous & Sejnowski, 2000; Magee, 2001). The cholinergic agonist carbachol can induce theta oscillations in hippocampal slices with (Fischer et al., 1999) or without (Fischer et al., 2002) the integrity of the septo-hippocampal pathway, these oscillations only propagate to CA1 via CA3. MacVicar & Tse (1989) noted that carbachol induced oscillations in CA3 depend on muscarinic receptors, do not require input from the DG, and are unaffected by NMDA, GABAa, or GABAb antagonists. CA3 pyramidal cells are endowed with a dense network of recurrent collaterals, which provides a hypothetical means for synchronising their oscillations. These results support the notion of an intrinsic theta rhythm generator in CA3,

In CA1, it has been proposed that interneuron networks could support oscillatory synchrony . Cobb et al., (1995) estimated that a single GABAergic interneuron could make contact with over 1000 pyramidal cells, entraining their intrinsic membrane oscillations. These interneurons may depend on input from the MS/DBv to coordinate their own firing. However, a recent experiment by Gillies et al. (2002) demonstrated that coherent, long lasting theta in CA1 slices can be produced with bath application of DHPG, a metabotropic glutamate receptor agonist. This glutamate-dependent oscillation was shown to be dependent on GABAergic input from intrinsically rhythmic stratum oriens interneurons to the distal dendrites of CA1 neurons. The dendritic spiking induced by rebound from this rhythmic inhibition was shown to be directly related to the field potentials which constituted the extracellular theta oscillation. Importantly, this oscillation was not dependent on input from CA3 or any other extra-hippocampal structure, was atropine resistant, and abolished by NMDAR blockade, making it very similar to the atropine resistant theta observed in intact waking rats.

In 1996, Skaggs et al. observed that individual putative CA1 interneurons fired in a phase locked manner relative to the local theta oscillation, but the preferred phase varied widely between cells. Expanding on this finding, Klausberger et al. (2003) demonstrated that different classes of morphologically identified CA1 interneurons fire at preferred phases of the local theta cycle in intact anaesthetized animals. The authors stress that by using a low dose of anaesthetic, the induced theta they observed was atropine-resistant, and therefore similar to theta in the waking animal. Under this preparation, O-LM interneurons were shown to fire preferentially in the negative phase of the local theta oscillations, making them likely candidates for the "phasing" of tonic input via the perforant path – in keeping with the findings of Gillies et al., 2002). Axo-axonic and basket cells, with their preferred firing phase at the peak and descending slope of the oscillation, respectively, may phase input from CA3 at stratum radiatum, or participate in synchronizing pyramidal cell firing during sharp waves. But at least one interesting consequence of discrete interneuron populations having different preferred firing phases is that it rejuvenates the potential role of the MS/DBv, with its variously phased projecting neurons, in pacing all of them.

1.4.5 Gamma oscillations

Gamma is a low amplitude, 30 -100 Hz oscillation which has peak power in the rat DG (Bragin et al., 1995), and has also been described in the EC of cats (Boeijinga & Lopes da Silva, 1988), visual cortex of monkeys (Kreiter & Singer, 1996) and from surface recordings and subdural recordings above the medial temporal lobe during sleep in humans (Llinas & Ribary, 1993; Uchida, et al., 2001). Gamma is coincident with theta in both intact animals and hippocampal slices, and in CA1 can be seen superimposed on the negative peak of the local theta cycle (Buzsáki et al., 1983; Gillies et al., 2002). Bragin and colleagues (1995) also found that changes in the frequency of theta and gamma oscillations in the rat were correlated, although recent research suggests that gamma oscillations do not depend on the presence of theta (Csicsvari et al., 2003). Pharmacologically induced gamma in hippocampal slices is dependent on ACh and AMPA receptors (Fisahn et al., 1998; Gillies et al., 2002).

In the hippocampus, Csicsvari et al. (2003) determined that there are two, independent gamma generators - one in the DG, which is dependent on EC input, and one in CA3, which entrains gamma oscillations in neighbouring CA1, and persists in the absence of entorhinal input. One can't help but note the similarities with findings regarding theta, as outlined above. Moreover, Csicsvari and colleagues found that both pyramidal cells and interneurons in the hippocampus fired phase-locked to local gamma oscillations. This supports the notion that hippocampal input may be "sorted" into gamma-interval packets, and retrieved in a similar fashion (Jensen & Lisman, 1996; Wallenstein & Hasselmo, 1997). Gamma oscillations have been proposed as a mechanism for attentional selection, perceptual integration ("binding"), and even consciousness (as reviewed by Engel and Singer, 2001).

1.4.6 Firing behaviour of pyramidal cells and interneurons

Early recordings from individual neurons in freely moving animals permitted differentiation of two basic cell types - "complex spike" cells and "theta" cells (Ranck, 1973; Fox & Ranck, 1975). Complex spike cells tend to fire intermittent bursts of action potentials, often with long periods of silence between bursts, and with each action potential within a burst having progressively smaller peak amplitudes. The mean firing rate of a given pyramidal cell over the course of a recording session is typically under 5 Hz. In contrast, theta cells tend to fire more tonically, at rates of upwards of 150 Hz, and clearly increase their discharge rate in the presence of theta, firing phase-locked to

it. Fox and Ranck (1981) subsequently identified CA3 complex spike cells as pyramidal cells, based on the observation that these units could be antidromically driven by stimulating the ventral hippocampal commissure and therefore must be projecting (principal) cells. Conversely, most theta cells could not be driven in this manner, and were therefore suspected as being inhibitory interneurons.

Morphologically identified pyramidal cells and interneurons have been shown to have distinct extracellular action potential waveforms, with pyramidal cells exhibiting wider waveforms with longer after-hyperpolarisation phases (Henze et al., 2000). Kamondi et al. (1998) demonstrated that biocytin labelled CA1 pyramidal cells fired complex spikes in response to depolarising input currents. Pyramidal cells and interneurons also exhibit unique firing probabilities with relation to the local theta oscillation and SPWs (Skaggs et al., 1996; Csicsvari et al., 1999; Klausberger et al., 2003). Csicsvari and colleagues recorded putative interneurons and pyramidal cells during sleep and exploratory behaviour in rats, and used waveform shape and firing rate to define interneurons and pyramidal cells. In keeping with previous findings (Skaggs et al., 1996) they noted that pyramidal cells fired in time with the trough of the local theta oscillation, while interneurons tended to fire somewhat before them, and with a wider distribution of preferred phases. Pyramidal cells fired maximally at the peak of SPW events, while interneurons variously increased firing at the same time, decreased firing at the SPW peak or immediately afterwards, or, in some cases, were simply unaffected by it. Klausberger et al. (2003) confirmed these results using neurobiotin to identify pyramidal cells and three different classes of interneurons – basket cells, O-LM cells, and axo-axonic cells – each of which have a characteristic preferred theta phase and relationship with SPWs. It should be noted, however, that the temporal dynamics of pyramidal cell firing obscures a more complex relationship between spike timing and theta phase, which shall be discussed in more detail below.

1.5 The hippocampus as a spatial map

1.5.1 Internal representations of space

The study of cognitive spatial mapping arose from the observation that the wide variety and flexibility of behaviour that animals exhibit in everyday life cannot be explained in terms of classical learning theory, according to which, responses are

driven by specific stimulus inputs. For example, animals are capable of finding hidden caches of food in the absence of visibility of the cache or any markers immediately adjacent to it (e.g. Hampton & Shettleworth, 1996). Similarly, rats are able to find a submerged escape platform in a water maze based solely on the position of the platform relative to distal features of the experimental room (e.g., Morris, 1981). Tolman, Ritchie and Kalish (1946) observed that, faced with the blockade of the usual route to a goal, rats are capable of using entirely novel routes to reach the same destination. As suggested by Tolman (1948), understanding how animals accomplish these tasks requires the assumption that animals store a representation or map of their environment in memory, in order to plan appropriate behaviour. The inadequacy of S-R models was particularly highlighted by the ability of rats to make novel shortcuts to a goal location when the learned routes were blocked (Tolman et al., 1946), and the ability to acquire knowledge about the environment in the absence of any reward (latent, or incidental learning: Blodgett, 1929). Morris (1981) demonstrated that animals are capable of navigating to a learned escape position in a cylindrical "water maze", even in the complete absence of any marker at the position.

This is not to say that animals cannot or do not use non-spatial solutions to certain goal-oriented problems, because they can, and often do, where these solutions suffice (e.g., Morris et al, 1982; McDonald & White, 1993, Martin et al., 1997). Problems which simply require the animal to approach a visible cue or make a stereotyped behavioural response such as making a left turn, do not require any form of spatial representation. For the solution of more complex spatial problems, however, it is clear that an animal must use an allocentric representation of the environment and the significant features in it, irrespective of the animal's position at any time. To achieve this form of navigation, an animal must 1) identify the environment it is in and use the appropriate map, 2) confer an orientation onto the map, and 3) monitor its position and direction relative to the map as it moves about the environment.

The exact information encoded in a spatial cognitive map is open to debate, and has been the subject of numerous studies - but it is generally agreed that both sensory cues (landmarks) and the integration of self motion relative to a known starting point (path integration) contribute to the spatial map (O'Keefe & Nadel, 1978; Mittelstaedt & Mittelstaedt,1980; Gallistel, 1990; Jeffery & O'Keefe, 1999). Both sources of information have inherent deficiencies. For example, if an animal were to use visual stimuli which have no positional stability as landmarks, navigation would be impossible. Presumably the animal must have a mechanism for learning about the

stability of landmarks in novel environments. Path integration, on the other hand, is prone to cumulative errors (Barlow, 1964), because it is based on the summation of movement vectors over time. Consequently, maintenance of an accurate representation of current position during long periods of movement must require occasional reference to some sort of stable landmark.

In any case, the ability to accurately navigate in familiar environments, and to learn about spatial relationships in novel environments, is such a fundamental aspect of survival for motile species, one might expect that there are brain regions which have evolved to perform dedicated spatial mapping functions.

1.5.2 A firing rate code for position

One of the most remarkable features of the principal neurons of the hippocampus is the spatial selectivity of their activity during exploration and other theta-related behaviours. O'Keefe and Dostrovsky (1971) first observed that CA1 neurons increase their firing dramatically in some regions of an environment, independent of the animal's behaviour. Such cells are referred to as "place cells", and their preferred region of firing is referred to as the "place field". A place field is illustrated in Figure 1.4c. Place fields are not influenced by goal location in spatial learning and memory tasks (Speakman & O'Keefe, 1990). As a rat moves about an environment, most pyramidal cells are silent (Henze et al., 2000), but nearly all of the active subset are place cells (Thompson & Best,1989). Simultaneous recordings from large numbers of hippocampal neurons indicate that in a given environment, the active subset of place cells have overlapping fields which cover the entire environment (Wilson & McNaughton, 1994; O'Keefe et al., 1998). Place fields in a novel environment are established within the first few minutes of exposure (Hill, 1978; Wilson & McNaughton, 1993), and are stable between subsequent exposures for periods of weeks (Lever et al., 2002) or even months (Thompson & Best,1990). Place fields are attributable to all three of the principal cell types in the hippocampus - pyramidal cells in CA1 (O'Keefe & Dostrovsky, 1971) and CA3 (Olton et al., 1978; O'Keefe & Speakman, 1979;), and the granule cells of the dentate gyrus (Jung & McNaughton, 1993). Place-responsive cells, albeit with less sharply defined fields, have also been identified in the subiculum (Sharp & Green, 1994; Anderson & O'Mara, 2003), parasubiculum (Taube, 1995) and the medial entorhinal cortex (Quirk, et al., 1992). Given that the representation of space is most accurately defined in CA1, CA3 and DG, and given the nature of connectivity in

the HF and associated structures, it is not clear whether EC subiculum and parasubiculum contribute to the place code, or whether they passively inherit it from the hippocampus and DG. In any case, these findings, alongside other evidence (see below), support the notion that the HF is the physiological substrate for an internal map-like representation of space (O'Keefe and Nadel, 1978).

Cells recorded from adjacent wires in a tetrode (O'Keefe & Recce, 1993) are no more likely to have adjacent or overlapping fields than cells recorded from the more distant wires of separate tetrodes (O'Keefe et al., 1998; Redish, 2001; Hirase et al., 2001; but see also Hampson et al, 1999), which suggests that the representation is a distributed code. Assuming that the pyramidal cells being recorded at any moment represent only a fraction of the total active set, and based on the observation that simultaneously recorded cells sometimes have overlapping fields, it can also be assumed that the momentary activity of the entire hippocampal population forms a rate code for position. Provided a sufficient number of cells are recorded simultaneously, the rat's current position can be predicted with reasonable accuracy from the momentary firing rates of those cells (Wilson & McNaughton, 1993; Fenton & Muller, 1998; Zhang et al., 1998).

1.5.3 The hippocampus and spatial learning

Numerous studies have highlighted the particularly spatial nature of the deficits suffered by animals with hippocampal lesions. For example, lesioned rats fail to remember which arms of a radial arm maze they have already retrieved food from, making frequent "re-entry" errors (Olton et al., 1978). Harley (1979) observed that hippocampal lesions or scopolamine inactivation prevented acquisition of place preference on a radial arm maze. Morris et al. (1982) found that complete hippocampal lesions prevented rats from finding the hidden platform in their water maze, while navigation using taxon guidance strategies (based on approach to salient stimuli) were spared. That is, the rats successfully navigated to the platform when it was visible. By training rats to swim in an annular water maze, Hollup et al. (2001a) demonstrated that in addition to any impairment in navigation to the goal location, hippocampal lesions prevented recognition of the goal location when the rat inevitably arrived at it. Lesioned rats in their experiment failed to slow down at the portion of the annulus which normally contained the escape platform.

Other research has indicated that in rats, it is the dorsal hippocampus *in particular* which is required for spatial tasks such as learning in the Morris water maze (Moser et al., 1993), or delayed spatial alternation on a T-maze (Hock & Bunsey, 1998). Lesions which spare even a small portion of the dorsal hippocampus support new learning, (Moser et al., 1995) but impaired recall of spatial knowledge acquired previously with an intact hippocampus (Moser & Moser, 1998). This suggests that the hippocampal representation of space is sparse and distributed, and organised on the basis of the network connections within the hippocampus itself. The critical role of the rat dorsal hippocampus in spatial learning is supported by the observation that place cells are less common in ventral hippocampus than in dorsal hippocampus, and their fields are less spatially selective (Jung et al., 1994).

There is evidence of a role for the hippocampus in spatial learning in other species as well. For example, Hampton & Shettleworth (1996) demonstrated that black-capped chickadees, which store hidden caches of food, have proportionally larger hippocampi than non-caching juncos, and suffered impairments on a spatial non-matching-to-sample test following hippocampal lesions. Gagliardo et al. (2001, 2002) have identified navigational impairments in homing pigeons with hippocampal lesions. Place cells have been identified in mice (e.g. Rotenberg et al., 1996, 2000), monkeys (Hori et al., 2003), and humans (Ekstrom et al., 2003). Spatial view cells, which respond to the area being looked at, have also been identified in monkeys (Georges-Francois et al., 1999; Rolls, 1999). The existence of spatial view cells in primates (but not rodents) is particularly interesting, in that it suggests that animals with stereoscopic vision may be able to experience occupation of a familiar region of space simply by observing it - that is, they may be able to "project" themselves into that space.

1.5.4 Plasticity: Multiple maps for multiple environments

Studies in which recordings from the same population of place cells were made in two different environments demonstrate that the position of place fields for a given cell in one environment is not predictive of field positions in the other (Kubie & Ranck, 1983; Muller & Kubie, 1987;). Indeed, cells active in one environment may be almost completely silent in the other, and vice versa (O'Keefe & Conway, 1978). So, it seems the active subset of hippocampal neurons changes between environments in such a way as to create virtually orthogonal representations of each environment the rat is familiar with. This is consistent with the intuitive idea that animals do not create single,

detailed global maps incorporating all familiar environments – instead, internal representations of space are somehow parsed into more manageable, functional units (e.g. Hynes et al., 2000).

The nature of the differences between environments necessary for such "remapping" (Muller, 1996) are far from certain. Typically, remapping experiments involve recording the firing patterns of place cells in a familiar environment (apparatus) inside a relatively featureless curtained enclosure, and then replacing the familiar environment with a novel one prior to the next recording session. The change in the environment that produces remapping can be, to the casual observer, rather small. For example, cylindrical environments which differ only in terms of the colour of a cue card affixed to their inner surface can induce completely different hippocampal firing patterns (Bostock et al., 1991), although the effects are known to be rat-specific, in that not all rats will remap under the same conditions. Remapping has also been demonstrated between square and circular environments of the same size and colour (Muller & Kubie, 1987; Lever et al., 2002), and in approximately half of place fields recorded in scaled up versions of the same environment (Muller & Kubie, 1987). Lever et al. (2002) demonstrated that remapping between different shaped environments is not necessarily instantaneous, and that place cells may individually, gradually, modify their firing patterns over the course of multiple paired exposures to the familiar and novel environments. Remarkably, even in the exact same environment, it is possible to induce two different hippocampal representations, depending on the rat's just previous experience – presumably a reflection of the rat's expectations (Quirk et al., 1990; Skaggs & McNaughton, 1998). An important implication of these findings is that while visual features of the environment can be used to "call up" the correct spatial map, sensory aspects of the environment themselves do not have complete control of the firing of place cells.

The existence of remapping also indicates that the hippocampus is capable of plasticity - that is, there are mechanisms which enable change in the patterns of connectivity in the hippocampus, and the sensory/idiothetic inputs which drive individual place cells. The fact that well-defined place cells have not yet been identified outside the hippocampal formation suggests that the locus of the plasticity responsible for remapping is within the hippocampus itself - that is, it appears unlikely that the hippocampus passively inherits spatial selectivity, and plasticity thereof, from other brain regions. Long term potentiation (LTP: Hebb, 1949) is a form of synaptic plasticity which has been popularly nominated as a cellular mechanism of learning and memory -

including spatial learning and memory. It comes as little surprise, therefore, that robust LTP was first observed in the hippocampus, in the excitatory connections between the perforant path and DG granule cells (Bliss & Lomo, 1973). High-frequency stimulation to these pathways produced the coincident firing of pre- and post-synaptic neurons which Hebb postulated as being necessary for LTP, and indeed, Bliss and colleagues observed an abrupt and sustained increase in the efficiency of synaptic transmission.

LTP that occurs at the Schaffer collateral pathway connecting CA3 and CA1 pyramidal cells is dependent upon NMDA glutamate receptors (Bliss & Collingridge, 1993). Activation of NMDA receptors requires the depolarization of the postsynaptic cell coinciding with glutamate release from the presynaptic terminal. Depolarization results from the induction of action potentials, and given that hippocampal neurons fire preferentially to rhythmic inputs at theta frequency, it seems the theta oscillation may play an important role in plasticity through its ability to entrain excitatory inputs at these frequencies.

It has been demonstrated that pharmacological blockade of NMDA receptors not only inhibits spatial learning (Morris et al., 1986; Danysz et al., 1996), but also prevents the long term stability of newly formed hippocampal representations of novel environments (Kentros et al., 1998), and blocks experience-dependent anticipatory firing of place fields on familiar routes (Ekstrom et al., 2001). In mice with a selective knockout of CA1 NMDA receptors, both performance on a spatial task (Tsien et al., 1996) and CA1 place field specificity (McHugh, et al., 1996) are impaired. In summary, evidence suggests that mechanisms proposed to underpin learning and memory in general are not only expressed in the hippocampus, but blockade of them has detrimental effects on both spatial learning and the formation of stable place fields.

1.5.5 Human studies and episodic memory

In humans, the hippocampus has been implicated in the memory of personally experienced events, or "episodic memory" (O'Keefe & Nadel, 1978; Tulving, 1983). One of the unique features of episodic memory (as opposed to "semantic memory, the memory of simple facts) is that episodic memories have, as essential characteristics, aspects of time and space (O'Keefe et al., 1998). For example, when you remember a significant event in your life, it is remembered in the spatial context in which it originally occurred, and there is a (sometimes inaccurate!) sense of how long ago it was. Semantic memory for facts, on the other hand (4+6=?) are not fixed in a spatio-

temporal context. It is this spatial context which is of particular interest to spatial map theorists.

Probably the best-known human subject, "H.M.", suffered a profound anterograde amnesia following bilateral hippocampectomy to relieve epilepsy. His long term ability to remember new events was virtually eliminated, although his short term or working memory appeared intact, allowing him to engage in conversations, complete psychological assays, and so on (Scoville & Milner, 1957, reviewed by Corkin, 2002). While initial assays suggested that H.M. had retrograde amnesia spanning 2-3 years, he was later found to be impaired on recall of events up to 11 years prior to surgery (Sagar et al., 1985). While the effects of H.M.'s hippocampal lesion may be confounded with his previous history of epilepsy, a comprehensive review of 147 human amnesic patients with hippocampal damage (Spiers et al., 2001b) concluded that the human hippocampus is critical to both the formation of and long-term "storage" of memories, but particularly episodic memories.

And what of the spatial component of episodic memory in particular? People with hippocampal damage (particularly the right hippocampus) have been shown to have deficits on spatial tasks (Spiers et al., 2001a) and recognition of spatial scenes (Pigott, & Milner, 1993). Earlier brain imaging studies have shown preferential activation of the hippocampus and para-hippocampal regions during learning and recall of routes (Maguire et al., 1996; Maguire et al., 1997; Ghaem et al., 1997). More recently, Hartley et al. (2003) demonstrated that in a virtual reality task, correct use of novel shortcuts activated the right hippocampus, while accurately reproducing a familiar route in a novel environment did not. In a study somewhat analogous to those involving seed-caching birds, Maguire et al. (2000) found that London taxi drivers had larger hippocampi than non-cabbie controls, and that posterior right hippocampal volume was related to the amount of time spent driving taxis. Results like these suggest that, as with rats, the human hippocampus (or at least, the right hippocampus!) is particularly important for the encoding and retrieval of spatial information, and incorporating that information into long term "autobiographical" memories of personal experiences.

1.5.6 Spatial maps and nothing but?

Despite the wealth of data supporting the notion that the hippocampus' primary function is to serve as a substrate for a spatial map, it is by no means a debate which

has been resolved, and cognitive map theory has never ruled out the existence of second-order correlates of the firing of place cells (O'Keefe & Nadel, 1978; O'Keefe, 1999). Certainly, the imaging studies cited above indicate that other brain regions, in addition to the hippocampus, are activated during spatial tasks. Some tasks which are presumably spatial fail to activate the human hippocampus (e.g. Aguirre & D'Esposito, 1996), though this may be related to the difficulty in determining the novel strategies we clever humans can use in solving problems. In addition, human lesion studies are often problematic, because very rarely is naturally occurring damage confined to a particular brain region.

The firing of some CA1 and EC neurons recorded on "W" shaped tracks (Frank et al., 2000; Frank et al., 2001) varies on the same track segment, depending on the animal's future choice of arms to visit ("prospective" coding) or the arm the animal has just come from ("retrospective" coding). As with the direction and task specificity of place fields (see section 1.6, below), this suggests that hippocampal neurons may encode more than the current sensory information impinging upon them. However, we may assume that the hippocampal representation of space has behavioural relevance (e.g. Markus et al, 1995) and need not correspond with the precise geometric properties of the environment. Prospective and retrospective coding on "W" shaped tracks may reflect encoding of the same region of these tracks as completely different places, depending on the phase of the task. This holds in the case of the experiments by Frank and colleagues (2000, 2001) because the rats were trained to follow very stereotyped trajectories in which they always travelled from one particular arm to another in the same phase of the task.

There is also a body of animal lesion literature which suggests that the hippocampus is required for certain non-spatial memory or recognition tasks (e.g. Alvarez et al., 2002). Based on evidence of this sort, Eichenbaum (1994) has proposed an alternative "relational" model of hippocampal function, which proposes that the hippocampus encodes relationships between, well, just about anything, but particularly stimuli which are "discontiguous" - i.e., never experienced simultaneously. The encoding of relationships between sets of stimuli which define (say) environmental boundaries is not at issue - merely whether the hippocampus has evolved to encode this type of information *in particular*. Alternatively one might argue whether lower-order correlations with hippocampal pyramidal cell firing can really tell us much about its "main" function, given the seemingly overwhelming body of data which points to a primary role in spatial representation.

1.6 Place field properties

1.6.1 Size, shape, and firing rate

Place fields are typically described in terms of time-averaged spatial firing rate maps representing real space as viewed from an overhead camera. In this type of map, space is divided into discrete bins, and the firing rate in each bin is the total number of spikes fired in that bin corrected for bin dwell time (Muller et al., 1987). Place fields have been shown to resemble Gaussian tuning curves, exhibiting a peak firing region in the middle of the field, and lower firing rates towards the edges (O'Keefe & Burgess, 1996). This suggests that as a rat approaches a cell's place field, the cell gradually starts firing faster, reaches a peak in the middle of the field, and then the firing rate drops off gradually again as the rat exits the field. In some instances, place field shape can be shown to be specific to the shape of the environment they represent, such as the crescent-shaped place fields sometimes observed along the walls of cylindrical environments (Muller et al., 1987; O'Keefe & Burgess, 1996).

As described previously, most hippocampal pyramidal and granule cells are silent in any given environment, and silent in most regions of an environment in which they have a place field. As a result, place cells have relatively low mean firing rates compared with interneurons (~1.4 Hz as compared with ~14.1 Hz, Csicsvari et al., 1999). The exception is when the rat is in the place field of a cell, when firing rates can reach as much as 40 Hz (Muller, 1996) and sometimes more (personal observations, this study). The peak firing rate as a rat traverses a place field has been shown to depend on the rat's running speed (McNaughton et al., 1983; Wiener et al, 1989; Czurkó et al., 1999) - the faster the rat runs, the higher the in-field firing rate of the place cell (but see also Hollup et al., 2001b).

Calculations of place field sizes are subject to the vagaries associated with how the firing rate maps for place fields are generated. Things like the size of the bins into which the environment is divided for rate averaging, the minimum firing rates accepted for inclusion of a bin in the field, and whether any smoothing is applied to the firing rates, influence final estimates of place field size. Nevertheless, Muller (1996) arrived at a mean field size, based on his own data sets, of approximately 13% of the total size of the environment (range = 3% - 50%). There is intuitive appeal to the notion that place field size is proportional in size to the environment, and this is borne out by experiments which demonstrate that changing the size of the environment changes the

size of the place fields (Muller & Kubie, 1987; O'Keefe & Burgess, 1996). It is also worth considering that place field size varies as a function of the proximity of the field to environmental boundaries (O'Keefe & Burgess, 1996) which raises another possibility - given that animals may be more likely to move at higher speeds away from environmental boundaries, and given that movement next to boundaries is determined by the shape of the boundary, the size and shape of place fields might also be controlled by the behaviour of the animal in a given location. And finally, place fields are likely to be scaled to the animal in question. My own informal observation, broadly speaking, is that rat place fields are approximately rat-sized, give or take half a rat or so. This would seem to represent a functional scaling, and it seems unlikely (for example) that elephant place fields would encode position on a centimetre scale. This of course is speculation.

1.6.2 Directional sensitivity

Perhaps the strongest evidence that place cells are not responding to simple sensory stimuli is the observation that place fields can be omni-directional - that is, when the rat enters the place field, the cell fires regardless of the direction from which the rat enters the field, and regardless of head direction within the field (O'Keefe et al., 1998). This finding is typical of environments in which the rat's behaviour is not constrained to particular trajectories due to features of the environment. However, when place cells are recorded from environments in which the rat's behaviour is constrained to particular trajectories, place fields tend to be directionally specific. This phenomenon has been observed on t-mazes (O'Keefe, 1976), radial arm mazes (McNaughton et al., 1983), linear tracks (O'Keefe & Recce, 1993), running wheels (Czurkó et al., 1999), and even annular water mazes (Hollup et al., 2001a). For example, O'Keefe and Recce (1993) observed that on a linear track, most place cells fired robustly on a restricted region of the track when the rat was running in one direction, but remained virtually silent as the rat passed the same point running in the opposite direction. Interestingly, place cells with omni-directional fields in a given environment can adopt novel, directional place fields when task demands are changed so that the rat traverses the environment along a stereotyped trajectory (Markus et al., 1995). This suggests that the directional specificity of place cells on apparatuses like the linear track are related to the nature of the animal's behaviour, and not features of the apparatus itself or an impoverished experience of the environment due to

stereotyped behaviour. It also serves as a further example of remapping without alteration of the environment.

A physiological substrate for directional information has been identified in the form of "head direction" (HD) cells, found in the postsubiculum (Ranck,1984; Taube et al., 1990a,b), anterodorsal thalamic nuclei (ADN) (Taube, 1995), lateral dorsal thalamic nuclei (Mizumori & Williams, 1993), retrosplenial and medial prestriate cortex (Chen et al., 1994), and the lateral mammillary nuclei (Stackman & Taube, 1998). These HD cells behave something like an internal compass, each cell having a preferred direction corresponding to the orientation of the rat's head in the horizontal plane. Moreover, HD cells seem to behave in a unitary fashion - that is, while each HD cell has a preferred direction, any changes in the preferred direction of one cell is reflected by a corresponding change in any others which are simultaneously recorded. This internal compass, the HD system, is under the control of sensory stimuli in familiar environments, and is carried relatively intact with the animal as it enters novel environments (Taube & Burton, 1995), using idiothetic information derived from the vestibular system (Stackman & Taube, 1997). It is reasonable to postulate that the HD system conveys the necessary directional information to the hippocampus in order for place cell firing to be direction-specific (e.g. Knierim et al., 1995), although the communication is likely to be two-way, given that the hippocampus appears to be important for conferring environment-specific preferred directionality to the HD system (Golob & Taube, 1999).

1.6.3 Orientation and location of place fields

If we assume that the hippocampus acts as a spatial map, then given the evidence that navigation is based on both sensory landmarks and path integration, we might expect that a similar mix of information contributes to the firing of place cells in the hippocampus (O'Keefe & Nadel, 1978). Certainly, the wealth of cortical and subcortical information which converges on the hippocampus supports this hypothesis. In 1978, O'Keefe and Conway demonstrated that rotation of an array of controlled cues in a visually impoverished environment (inside a curtained area) led to a corresponding rotation of hippocampal place fields in rats trained on a T-maze. This study and subsequent ones (Martin & O'Keefe, 1998; Hetherington & Shapiro, 1997) demonstrated that when rats were trained with an array of orientation cues, a subset of those cues could continue to determine place field orientation following removal of one

or more of the others. Muller and Kubie (1987) demonstrated "cue control" using an even more simplified environment - a grey cylinder with a single white cue card attached to the inside surface. These results provide strong evidence that visual cues can act to control the angular orientation place fields. Furthermore, up to 50% of the cues from a cue array which controls place cell firing can be removed, and control can be maintained by the subset of remaining cues (O'Keefe & Conway, 1978; Pico et al., 1985), suggesting that it is the spatial configuration of the cues, and not the individual cues themselves, which control orientation of the place fields. Of course, it should be noted that control of place field orientation may well be indirect, via the HD system, which responds in a similar way to these cue-rotation experiments (reviewed by Taube et al., 1996). Indeed, like HD cells, place fields which rotate in response to cue rotation tend to do so in unison (e.g. Jeffery et al., 1997). This coherent, simultaneous rotation of place fields ensures that the topological relationships between them (and by extension, the integrity of the spatial map) are preserved.

Certain classes of visual cues appear to be endowed with particularly powerful control over map orientation. If rats have no access to orienting cues beyond the boundaries of the testing environment (such as a rectangular box), the geometry of the environment overrides other salient aspects of the environment (like a pattern on a wall) in determining spatial choices (Cheng, 1986; Margules & Gallistel, 1988). Interestingly, Hermer and Spelke (1996) obtained similar results in young children. O'Keefe & Burgess (1996) highlighted the importance of geometry in determining the position and size of fields within a square or rectangular environment. Transforming the box in which the animals were tested from a horizontal (E-W oriented) rectangle to a vertical (N-S oriented) rectangle caused translations and changes in the size of place fields which are consistent with the notion that place cells receive converging inputs which are tuned to distances and directions from the boundaries of the environment (Hartley et al., 2000). Interestingly, the transformation of the environment, which could be interpreted as a rotation, failed to produce rotation of the hippocampal map. Presumably the orientation of place fields in the O'Keefe & Burgess (1996) study remained under the control of the HD system, and was anchored to the visual cues in the room beyond the box. Cressant et al. (1999) found that a triangular array of three objects controlled the orientation of place cells if they were placed at the periphery of the cylindrical training apparatus, while the same objects failed to exert control when they were clustered in the middle of the apparatus. An intriguing explanation for this finding is that animals must first learn that visual stimuli are stable before they gain

control of the representation of space. If an array of cues is positioned at or beyond the periphery of an environment, the apparent relationship between them is always the same, no matter where in the environment the rat observes them from. For example, the rat could know with certainty that if cue "A" were in front of it, then he should be facing north. If, however, an animal can move around the array of cues, then there is no way for the view of a particular cue, or array of cues, to unambiguously signal direction. In other words, the rat can never experience the cue as stable, or reliable.

When one discusses the perceived stability of visual stimuli, one must as "stable relative to what"? The "what" in this case would appear to be complimentary information on current position and orientation derived from idiothetic sources, including the head direction system. McNaughton et al. (1996) have proposed that when a rat first enters a novel environment, it has no knowledge of the stability of features in that environment - the only information available to it is that based on the integration of self motion from the point of entry. According to this theory, control of the spatial firing of place cells is determined entirely by path integration upon initial exposure to the environment, with salient landmarks only added to the spatial map later. Once the stability of certain sensory features of the environment has been established, only then they may gain control of the spatial map. Key evidence comes from a study which indicates that if rats are always disoriented just prior to exposure to an environment, visual cues in the environment fail to control the orientation of place fields (Knierim et al., 1995). Instead, the fields rotate together by a random amount on each successive trial. McNaughton and colleagues (1996) suggest that primary moment-to-moment firing of individual place cells remains determined by self-motion cues, with landmarks being referred to only occasionally to correct for the cumulative errors inherent in path integration.

Traditionally, experimental evidence for idiothetic control of place cell firing has come from studies conducted in darkness (O'Keefe, 1976; Quirk et al., 1990; Markus et al., 1994; Bures et al., 1997), or using animals which are blind (Save et al., 1998) or deaf (Hill & Best, 1981). There are three fundamental problems with simply using darkness or blindness to infer idiothetic control of place cell firing. First, eliminating visual cues does not eliminate information from other sensory modalities, which may remain intact and signal the rat's position. For example, Save et al. (2000) demonstrated that olfactory cues play an important role in maintaining place fields in darkness. Second, it is impossible to infer what the self-motion cues are indicating about position or orientation, so there is no way of making predictions about what firing

under idiothetic control should look like. Jeffery et al. (1997) attempted to address this issue using slow rotation in darkness, presumably below the rat's vestibular threshold. By using controlled amount of rotation, they demonstrated that they could predict place field locations when the rat was subsequently placed in a rectangular box. And finally, experiments involving darkness or blindness generally examine the effects in place field orientation - a feature presumed to be inherited from the head direction system, and perhaps unrelated to momentary processes like the ones involved in determining whether a given cell will fire at a particular position on a linear track.

In any case, it is most useful to think of the hippocampus as being continually under the direction of a wide array of sensory and idiothetic inputs, providing redundant information on the animal's position in space. The opportunistic way in which the hippocampus can switch between the use of spatial information from either of these two broadly defined sources has been highlighted by Best and Thompson (1989) and Huxter et al. (2001).

1.6.4 Place fields and behaviour

It is fair to say that one of the most obvious evolutionary purposes of a spatial map would be to guide goal-directed behaviour. So far I have outlined several lines of evidence that physical or pharmacological hippocampal pathology interferes with the learning and execution of spatial tasks, and we have seen that the hippocampal rate code can be used to predict a rat's momentary position. But what of direct comparisons of place fields and choices? O'Keefe & Speakman (1987) noted that when an array of cues inside the maze was rotated across trials, rats who learned to use the cues to locate the food had place fields whose positions were defined by the orientation of the cue array. Similarly, Dudchenko & Taube (1997) demonstrated that animals failed to find a food reward on trials in which the preferred firing direction of HD cells did not rotate in accordance with the rotated position of a visual cue. Lenck-Santini et al. (2002) found that poor performance on a place preference task was only associated with rotated place fields when the task could only be solved using a spatial hypothesis. However, there is only one study I am aware of which attempted to match field location with particular behavioural choices on a trial by trial basis. Huxter et al. (2001) found concordance between place field position and behavioural choice on 38/52 trials on which rats ran to a corner of a box they had learned contained a reward, followed by five minutes of random foraging for food throughout the box. Discordance was found

primarily on trials in which rats were disoriented and cues were rotated, if the rat made choices which corresponded with neither the original goal location or the location defined by the rotated cue. On these discordant trials, the place field was usually in the predicted location, while choice behaviour was more variable. Jeffery et al. (2003) didn't make trial by trial choice-field comparisons, but also noted discordance - in their case, preserved choice behaviour despite hippocampal remapping induced by changing the colour of the environment. What both of these papers demonstrate is that while it is commonly assumed that the hippocampal representation of space is used to guide behaviour, the fact is that animals probably have multiple hypotheses which can be used to make choices, spatial hypotheses being only one of them. Consequently, spatial learning experiments should be designed to eliminate or restrict the utility of alternative hypotheses as much as possible.

A fundamental weakness in all the aforementioned studies is that learning could be supported by directional information alone - the goals are invariably at the periphery of the environments, so no knowledge of distances is required, as goal location is always unambiguously signalled by direction. Of course, the head direction system lies outside the hippocampus proper, so it is not inconceivable that head-direction-guided choices could be dissociated from hippocampal place field orientation. The solution would seem to be to compare behaviour and place fields on spatial tasks which require knowledge about both angles and distances to goals from different starting positions, such as the Morris water maze or a hole-board task.

1.7 The phase precession effect

1.7.1 O'Keefe & Recce, 1993

One of the most remarkable features of place cell firing, and a major focus of this thesis, is the phase precession phenomenon. In 1993, O'Keefe and Recce noticed that when rats shuttle on a linear track for food reward at either end, place cells fire not only on a restricted region of the track (as expected), but also at particular phases of the local theta oscillation, in a position-dependent way. Specifically, they found that as a rat first entered a place field, the firing of the first spike occurred near the positive peak of the local theta. As the rat traversed the field, spikes or bursts of spikes tended to occur at successively earlier phases of each subsequent theta cycle (phase

precession), indicating that the inter-burst interval of the place cell was shorter than the interval between theta cycles. When spikes which fired on multiple passes through the field are plotted together as a function of position and theta phase, it is clear that there is something approximating a linear relationship between firing phase and position. Figure 1.4 describes the phase precession effect on both single traversals of the place field, and as it emerges over multiple passes.

O'Keefe and Recce suggested that this asymmetrical temporal code for position (as distinguished from the symmetrical, Gaussian firing rate code) could significantly improve the ability of the hippocampus to signal the rat's momentary position. This prediction was borne out by a subsequent study by Jensen and Lisman (2000), who demonstrated a dramatic 43% improvement in the accuracy of position reconstruction when firing phase was included in calculations based on the firing rates of large numbers of simultaneously recorded neurons. One of the revelations from the discovery of phase precession is that previously documented "mean firing phase" values for hippocampal pyramidal cells (e.g. Buzsáki et al., 1983) are affected by, but fail to account for, the spatio-temporal dynamics of place cell firing as the rat traverses a place field.

O'Keefe and Recce (1993) made a number of interesting observations about the nature of the phase precession. First, they noted that phase shifts ranged from 100^0 to 355^0, as calculated by multiplying field size by the slope of the best fit line describing the relationship between phase and position on the track. The apparent limitation of phase precession to less than 360^0 means that the phase of the theta cycle, as a unit of time, can serve as a unique carrier of spatial information. Second, O'Keefe and Recce noted that phase precession always appeared to begin at the same phase of the theta cycle – specifically, just after the positive peak of the locally recorded theta oscillation. Third, the authors observed that firing phase was better correlated with position than time, which suggests that phase precession is not simply a temporal effect which appears as a spatial effect due to the stereotypy of the rat's running behaviour. And finally, the authors found no correlation between field size and the slope of the phase precession. Now, this last point is one of the topics investigated in this thesis, and so, I feel it is important to point out what appears to be an oversight on the part of O'Keefe and Recce. Using the values from their Table 1, and using the absolute value of the slope measures, I found there to be a very robust correlation between field size and phase precession slope indeed ($\underline{R} = -0.779$, $\underline{F}_{1,14} = 21.601$, $\underline{p} < 0.001$). It is necessary to use the absolute value of the slope values (degrees/metre)

because the slope is positive or negative depending on whether the rat is running west or east, respectively, when the place cell fires – that is, position values in cm are either decreasing or increasing as the rat crosses the place field, assuming the track is aligned horizontally relative to the overhead camera. In short, based on my calculations from the O'Keefe & Recce data, the smaller the field, the steeper the slope of the phase precession.

1.7.2 Skaggs et al., 1996

Three years later, Skaggs et al. (1996) provided collaborative evidence that place cell firing undergoes ~360^0 of precession beginning from a relatively constant starting phase, and expanded upon the original observations of phase precession made by O'Keefe & Recce as follows. First, Skaggs and colleagues noted that the phase precession appears to accelerate in the later portions of the fields – that is, the rate at which firing shifts to earlier phases of the theta cycle as the rat exits the field is higher than the rate of firing rate change as the rat enters the field, and the variability in firing phase is also much greater as the rat exits the field. Together, this gives phase precession, in most cases, a curvilinear (as opposed to linear) appearance. Second, Skaggs et al., observed phase precession in a two-dimensional environment, as well as on a track. Although there were complications surrounding the analysis of the 2-D phase dataset with omni-directional place fields, the authors present fairly convincing evidence that phase precession is not a phenomenon restricted to experimental paradigms in which the rat runs in a very stereotyped manner. Third, the authors identified phase precession in DG granule cells. This suggests that at least in theory, that CA3 and CA1 pyramidal cells may inherit the temporal organisation of spiking activity from earlier portions of the hippocampal circuit. However, given the truncated nature of the precession reported by Skaggs et al., this may not account for the degree of precession observed in CA1 and CA3. And finally, of major significance to LTP-based models of learning and memory, Skaggs et al. (1996) demonstrated that phase precession resulted in the repetition, in every theta cycle, of the sequence of cell firing as the rat traverses a series of overlapping place fields. NMDA receptor mediated LTP is limited to making associations between cellular "events" separated by no more than ~ 50 ms (reviewed in Skaggs et al., 1996), so this compressed representation of the sequence of places the rat visits on the track could be a potent mechanism for creating associations between "memories" for the *sequences* of positions the rat visits on the track, and lead in-turn to anticipatory firing of the neurons before the place field proper

has been reached. This later prediction has been confirmed by (Mehta et al., 1997, 2000), who observed that place fields undergo asymmetric expansion (opposite the direction of motion) over the course of the first few stereotyped traversals of a linearised environment. While Ekstrom et al. (2001) appear to confirm the role of the NMDA receptor in this expansion process, is should be noted that the phenomenon they observed (which was blocked by CPP) appears to resemble more of a shift in the field position, rather than a developing asymmetry.

1.7.3 Models of phase precession

O'Keefe and Recce (1993) proposed a dual oscillator model to explain the phase precession effect. According to this model, the precise timing of action potentials is a result of the interference pattern produced by the summation of two slightly detuned oscillatory inputs to the neuron. One input was presumed to be the rhythmic modulation provided by the theta oscillation itself, and the other, possibly, an intrinsic membrane oscillation whose frequency is dependent on the degree of depolarisation of the cell. If the second oscillator is normally 180^0 out of phase with theta outside the place field (when the cell is not excited) the two would cancel each other out. Upon entering the field, however, the second oscillator presumably increases frequency and the two begin to act cooperatively, the phase of peak excitation gradually shifts relative to the phase of the theta oscillation, and the familiar Gaussian shape of the place field emerges. If one further assumes that the second oscillator is sensitive to running speed, there is a built in mechanism for maintaining the size constancy of place fields under different running speeds. It should be noted that the locus of one or both of the oscillators in this model may be remote from the site at which the phase precession is recorded, and spike timing in CA1 may be inherited, at least in part, from upstream structures (Skaggs et al., 1996). Figure 1.6 presents a very simple model of phase precession driven by a dual oscillator whose summed input determines the firing rate of a cell. Two important observations can be made from models of this type. One is that they can only ever account for up to 180^0 of phase precession. The other is that as little as a 10% change in the frequency of one of the oscillators can compensate for a doubling (or halving) or running speed.

Several alternative models have been proposed to explain the phase precession model, most assuming that the timing of spike firing is derived from the organisation (multiplexing) of environmental sensory inputs based on a gamma-cycle

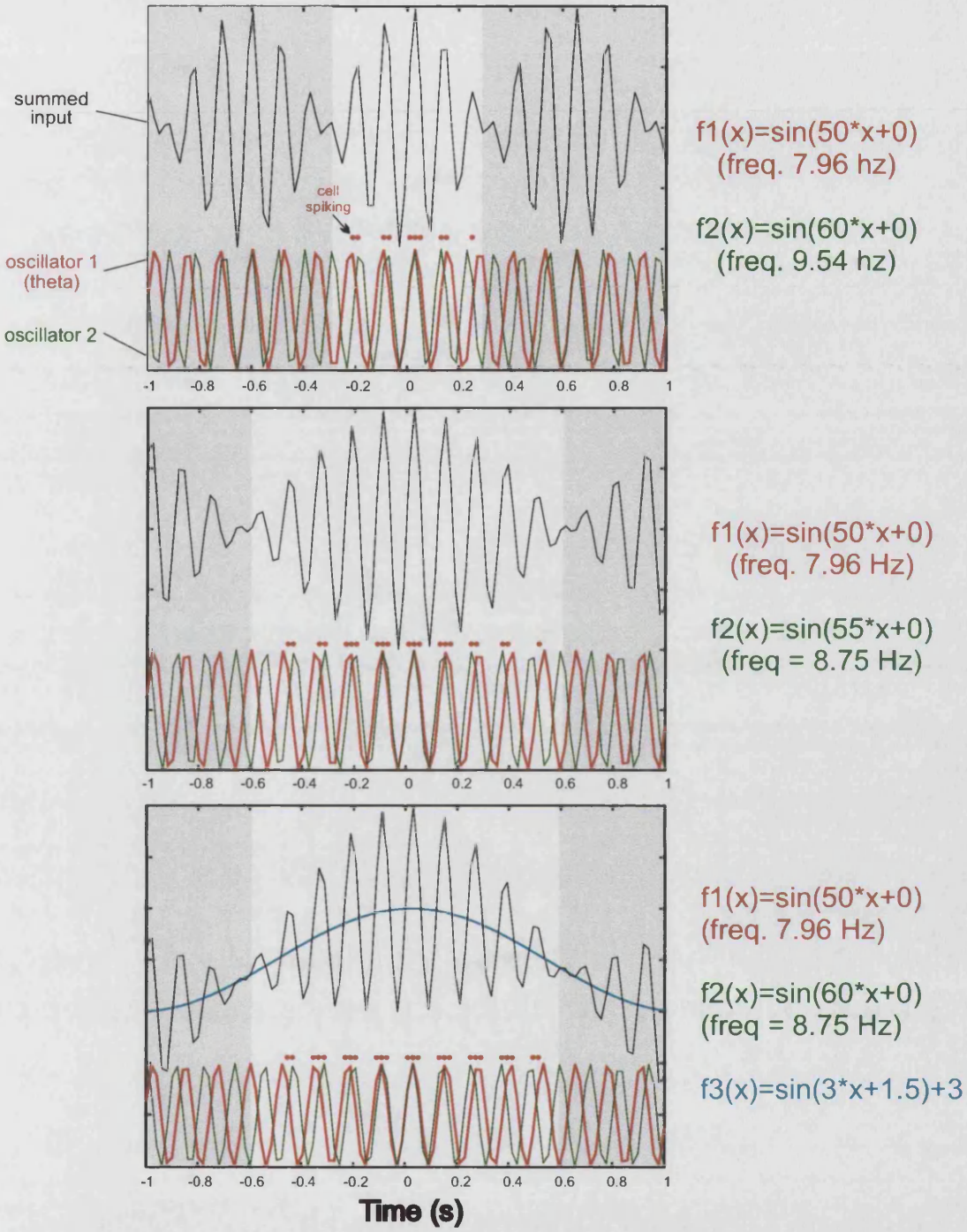

Figure 1.6. A dual oscillator model of phase precession, adapted from O'Keefe & Recce, 1993. Formula for generating the oscillations are presented at right, along with the corresponding frequency. Note the beat frequency produced by the two detuned oscillators. The dual oscillators are actually assumed to remain 180^0 in the grey areas. The white areas represents the place field, within which excitatory "place" input drives oscillator to its velocity-defined higher frequency. Spiking occurs when the summed input exceeds an arbitrary threshold.Note the approximately 180^0 of phase precession in spike firing within the field. **a**: fast run though the field (approximately 0.6 seconds). **b**: slow run through the field, in which the second oscillator's frequency is reduced by about 10%. Spiking occurs for about 1 second, which would compensate for a halving in running speed. The amount of phase precession is preserved. **c**: As in **b**, with the addition of an excitatory "place" input which, in theory, initiates the change in frequency of the second oscillator.Note that the underlying dual oscillators still determine spike timing, and that the phase precession still encompases ~ 180^0.

timescale (Jensen & Lisman, 1996; Tsodyks, et al., 1996; Wallenstein & Hasselmo, 1997; Lisman, 1999). Bose et al., (2000) have also proposed a model based on the temporal dynamics of inhibition in local pyramidal-interneuron networks, modulated (of course) by running speed. However, two recent publications present the compelling argument that the momentary firing phase of place cells, and hence, phase precession, are best explained in terms of the net excitatory input to the place cell (Harris et al., 2002; Mehta et al., 2002). Harris and colleagues support their argument by demonstrating that phase precession appears to occur in non-spatial tasks in a manner dependent on the firing rate of accelerating spike trains. Mehta and co-workers show that a skewed, or ramp-shaped depolarisation envelope will produce phase precession of spike firing, and that improvements in the spatial and temporal correlations with firing phase coincide with experience-dependent skewing of place fields.

These models are fundamentally based on the observation by Kamondi et al. (1998) that applying an increasingly large depolarising current to CA1 pyramidal cell dendrites against a background of oscillatory somatic inhibition (simulating theta) results in the cell firing at successively earlier phases of the inhibitory cycle (Kamondi et al.,1998). This phenomenon was also observed in hippocampal slices by Magee (2001), who substituted tonic depolarisation at the dendrites with an oscillatory input in antiphase to the somatic input, mimicking the two major theta dipoles in CA1 in vivo. The notion is that if the theta rhythm reflects rising and falling levels of somatic inhibition of pyramidal cells (Fox, 1989), then there is a preferred phase of theta at which place cells will begin firing in response to depolarisation. Firing at earlier phases involves overcoming the higher levels of inhibition at these phases, and may require the kind of increased depolarisation that is reflected in the increased firing rate of place cells as they approach the centre of the place field. Testing this hypothesis is one of the principal purposes of this thesis, and the models are discussed a little further in Chapter 5: Firing Rate Analysis.

1.8 The current study

To a certain degree, this study was conceived as a replication of O'Keefe & Burgess' 1996 experiment, in which they demonstrated that changing the geometry of an environment alters the size and distribution of place fields in the environment. One of the questions I wanted to address was whether these changes in field size produced concomitant changes in the slope or the extent of phase precession within those

altered place fields. A demonstration that this is the case would build on previous work suggesting that firing phase encodes spatial information, by demonstrating that changes in the space produces changes in the temporal code. Covariance of theta phase precession with other properties of place fields was also investigated using population statistics for all recorded place fields on trials in which no manipulations were formed.

This thesis also addresses the question of whether changes like the ones observed by O'Keefe and Burgess (1996) could be attributed to a particular sensory aspect of the altered environment, like the visual angle to the height of the environmental boundaries. Alternatively, are these changes attributable to changes in the rat's behaviour, or running speed, which coincide with alterations of the environment? To answer these questions, I investigated the effects of simply lowering the height of the walls at the ends of the runway, and analysed the contributions of running speed to place cell properties and positions, in some detail.

A third purpose of this thesis was to investigate the hypothesis that the phase of the local theta oscillation at which place cells fire is directly related to the momentary depolarisation of the cells. This was achieved by using momentary firing rate as an indicator of depolarisation, and determining how momentary firing rate changes as a function of position, what the concomitant changes in firing phase are, and whether random or controlled events which influence firing rate have any influence on the slope or the extent of phase precession.

And a final goal was to determine whether there is solid evidence of a path-integration based determinant of place cell firing. I wanted to determine whether, as a rat moves about an environment, the information encoded by hippocampal place cell firing could be affected by manipulations of a particular class of idiothetic input - in the current case, motor-related cues concerning self motion.

Chapter 2: General Methods

In this chapter, experimental methods are discussed which are applicable to all rats, regardless of the particular manipulations performed. Detailed discussion of the methods used in each individual experiment are discussed in the appropriate chapters.

2.1 Subjects

Nine adult male Lister Hooded rats were used, weighing between 309 and 423 g (mean = 363 g) at the beginning of the experiment. Prior to training and between training or testing sessions, all rats were individually housed in plastic home cages with wire covers, in a holding room. Temperature in the room was kept between 19^0 and 23^0 C, and illumination was provided on a reverse 12 h / 12 h light/dark cycle, with lights off at 8 am. Water was provided ad lib, while food was restricted to maintain rats at 90% of their initial weight, plus 3 g/week allowable weight gain. The health and weight of all rats was monitored daily over the course of the experiment.

2.2 Experimental room and apparatus

Training and experiments were conducted in a 4.81 m x 2.35 m air-conditioned room, kept at 20^0C, and illuminated by a single 60 watt incandescent lamp directed towards the ceiling. The room could be completely darkened by extinguishing the light and covering the door frame with heavy black cotton curtains. Black duct tape was used to cover any point light sources such as the power indicators on electrical equipment. The experimental room and its contents are presented in Figure 2.1.

The main apparatus consisted of a linear track (254 cm long, 10 cm wide) with a motorized treadmill for a floor. A linear track was the apparatus on which phase precession was originally described (O'Keefe & Recce, 1993) and is best expressed (Skaggs et al., 1996; Harris et al, 2002). Rats running on linear tracks exhibit clear, high amplitude theta oscillations, and make the large number of place-field traversals essential for analyses which use subsets of the data collected on a given trial. Despite the availability of non-spatial solutions to linear track tasks, as with pellet-foraging tasks, the prevalence of place fields in these experimental paradigms suggests that

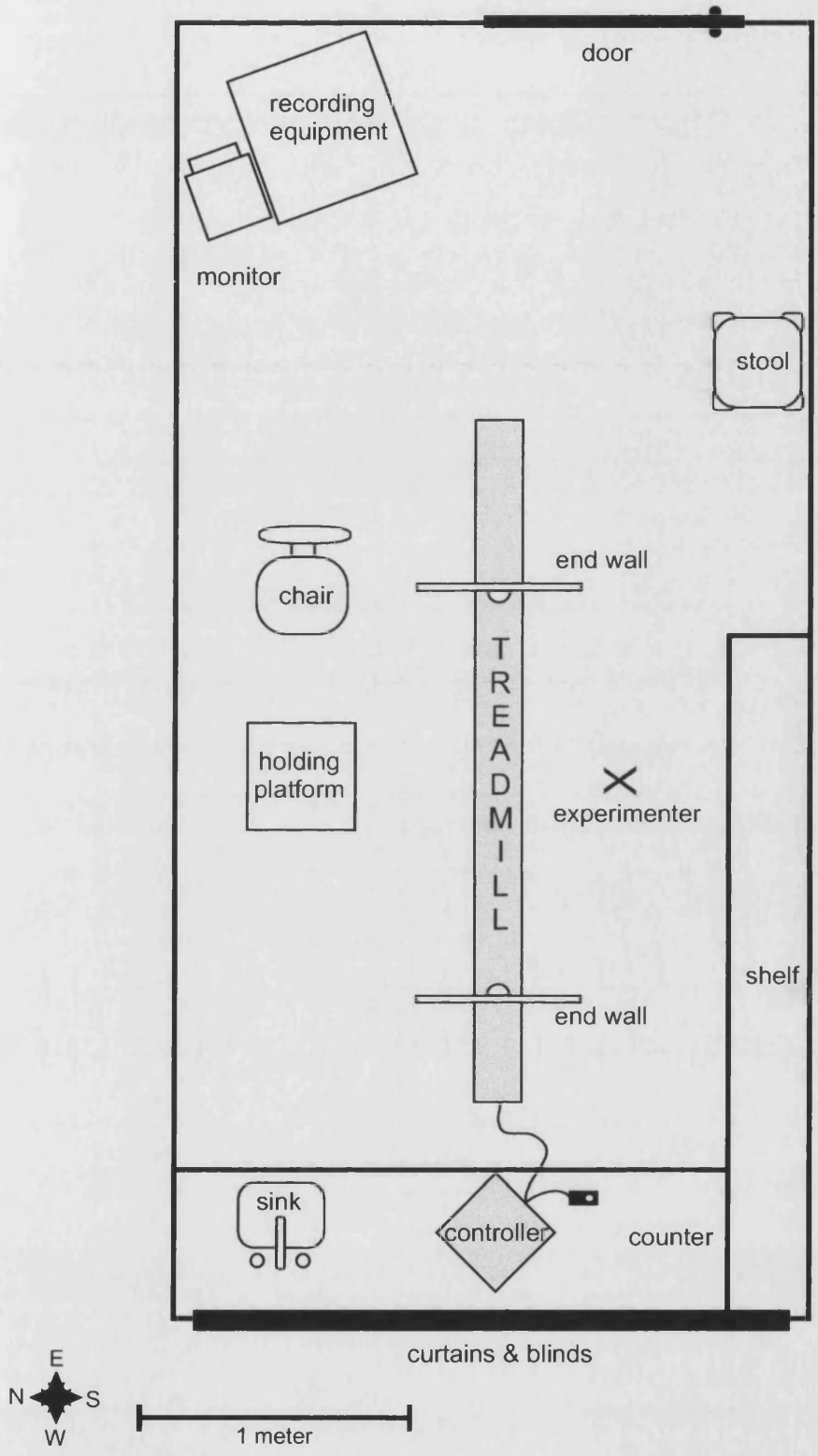

Figure 2.1: Scale drawing of the experimental room, showing the position of the treadmill and its controller (grey). The middle 150 cm of the treadmill is the runway used by the rats, bounded on either end by the end walls. The protrusions on the end walls are the food wells. The end walls can be moved one towards the other to shorten the length of the runway as required . Not shown are the walls bounding the north and south sides of the runway, the camera suspended over the mid-point of the runway, and the air conditioning and pre-amplifier units on the north wall of the room.

rat's map their environments, whether or not the task demands it. Indeed, they may prefer a spatial solution, even when other solutions are available (Tolman et al., 1946).

The track was oriented east-west and positioned in the middle of the room. The treadmill was made of light grey suede, which, while impossible to clean, was durable, non-reflective, and provided excellent purchase for running rats without generating static charge. The treadmill could be made to run in either direction, at speeds of up to 25 cm per second or more. A 25.5 cm high wall made from particle board coated in grey plastic was clamped along the full length of each side of the treadmill, forming a 14.3 cm wide runway channel. The middle 150 cm of the channel was bounded by end walls made of the same material. The end walls had slots cut in them so they could slide down over the side walls, thus being held in place with the aid of a clamp. This configuration also allowed the end walls to be positioned anywhere along the length of the treadmill, effectively changing the length of the runway as required. Two 8.4 cm diameter plastic Petri dishes, cut in half, served as food wells, and were attached to the bottom of each end wall, facing towards the middle of the runway.

The room contained numerous other salient visual stimuli, including the black curtains in the west, rows of shelves in the south, a door in the east, and the recording equipment in the north-east corner. While no attempt was made to obscure these things from the rats view, objects below the level of the side or end walls were generally invisible to the rat during running on the track, unless he stopped and reared to peer over the side walls. A 40 cm x 40 cm box with 2 cm high walls and filled with 1 cm of sawdust served as a holding platform where the rat was kept during training and testing sessions between trials. The box was placed atop a stool, 44 cm north of the midpoint of the runway. A black open-topped plastic box with sawdust on the floor was used to transport the rat from the holding room to the experimental room. This transport box typically sat at the foot of the holding platform during screening, training, and testing.

2.3 Electrodes

Recording electrodes consisted of strands of H-ML insulated, 25µm platinum-iridium fine wire (California Fine Wire), each 40 mm long, twisted together at a rate of 2 turns/mm to form a "tetrode" (O'Keefe & Recce, 1993). Harris et al. (2000) have confirmed that the use of tetrodes dramatically improves the accuracy with which

extracellular signals are attributed to the correct neuron. The upper 10 mm of the strands remained untwisted, with 3-5 mm of insulation removed from the tips using an alcohol flame. Typically, the entire length of the twisted portion of the tetrode was coated with cyanoacrylate to add strength. The twisted end was then blunt cut with surgical scissors, so that the tips of all four wires were separated only by the diameter of the insulation.

2.4 The "poor lady" microdrive

Figure 2.2 illustrates the microdrive assembly used to manipulate the position of the electrodes in the brain. My former MSc. supervisor, Dr. Carolyn Harley, was the "poor lady" for whom the drive was named. Upon completion of a sabbatical with Prof. John O'Keefe in the 70's, she requested a microdrive design suitably robust and yet simple and inexpensive enough so that even a "poor lady" like herself could make them. This incredibly stable and reusable microdrive became the standard for hippocampal rat implants in the O'Keefe lab, and indeed, has since been miniaturized for use with mice as well.

The drive consists of two L-frames made from 17 gauge stainless steel tubing, soldered at the mid-point of the feet. The feet were at right angles to each other, the vertical posts were parallel to each other, and a hollow stainless steel screw was mounted over the vertical post of one of the L-frames (the screw post). A stainless steel flange bridging the top of both posts kept them parallel to one another, and was used to apply steady pressure to the screw via an interposed high tension spring cut from 14 gauge tubing. This pressure prevented vertical movement of the screw relative to the opposite post (the guide post), while permitting rotation of the screw on the screw post. The screw and the guide post were bridged in the middle by a two-hole nut made from dental acrylic. Lubricated heat-shrink tubing formed a durable, custom-fit interface between the acrylic and both the steel screw and guide post. A 12 mm long piece of 23 gauge stainless steel cannula for carrying the electrodes was fixed to one side of the nut, running parallel to the screw. A 360^0 counter-clockwise turn of the screw lowered the nut, cannula, and electrodes by 0.200 mm. Similarly, the nut could be raised by turning the screw clockwise. A 7 mm long piece of 19 gauge stainless steel sleeve covered most of the exposed portion of the cannula below the nut, and was held in place by a small amount of petroleum jelly.

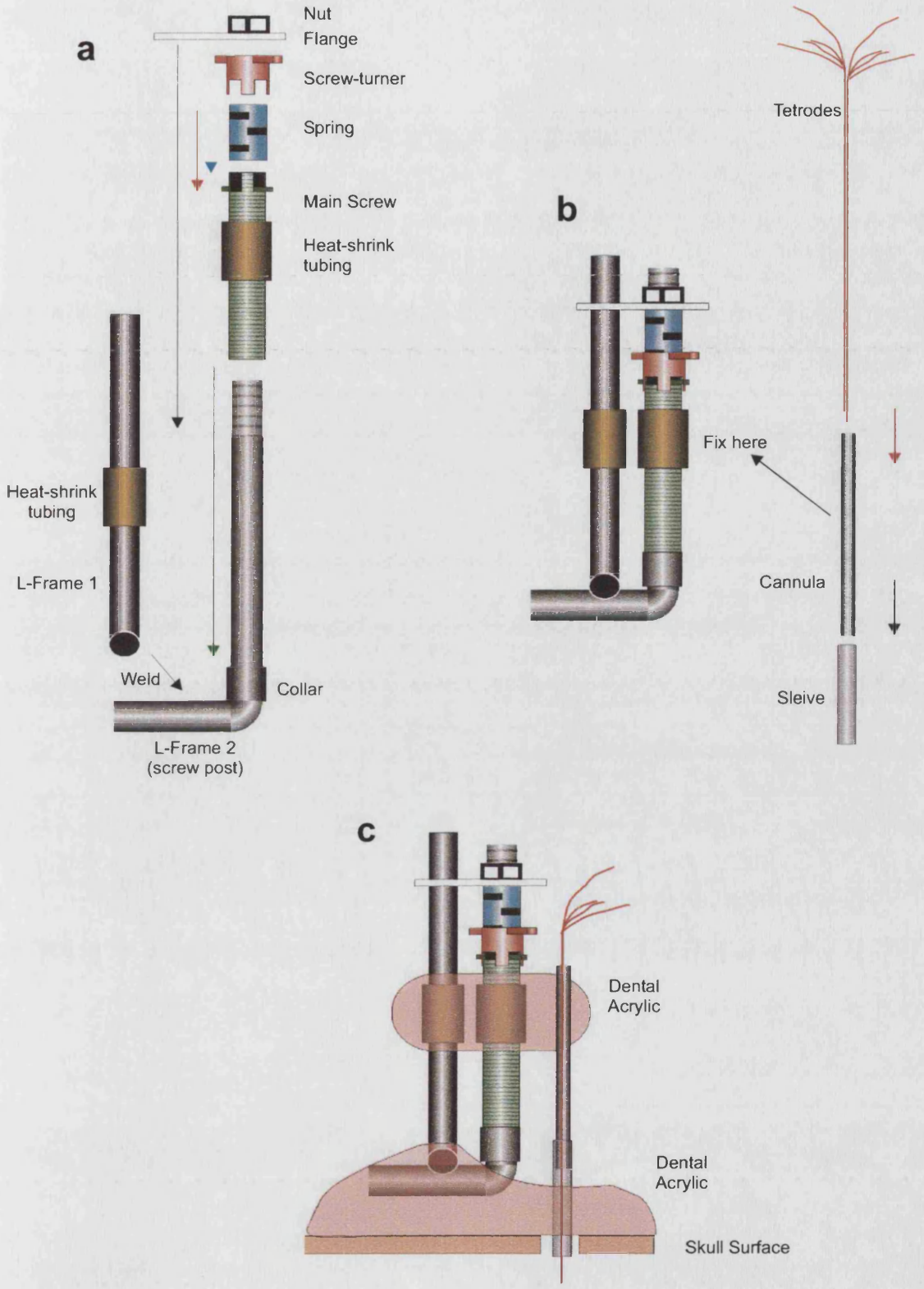

Figure 2.2. The "Poor-Lady" microdrive, in false colour. **a:** Assembly of the drive, shown with the floating collar and heat-shrink tubing already in place. **b:** The cannula is attached to the assembled drive, tetrodes are inserted, and the sleeve is fitted over the cannula. **c:** The complete assembly is positioned with the electrodes in the cortex, and the sleeve lowered to touch the brain surface. Dental acrylic fixes the assembly in place. The brain surface is protected from the dental acrylic by absorbable sponge. The wiring of the electrodes to the drive and the plug connecting the drive to the recording cable are not shown.

Prior to surgery, two tetrodes were fed tip-first into the top of the cannula. Their uninsulated, untwisted ends were wrapped around the ends of stainless steel leads from a connector plug mounted on the opposite side of the microdrive, and silver conductive paint was applied to improve the connection between the electrodes and the leads. Conductivity of the tetrodes was tested by submerging the tips in saline solution, and looking for the bubbles indicative of current passage as a 9 V potential was applied across each pin of the connector and the saline solution. If any wire of either tetrode failed to show evidence of current passage, the tip of that tetrode was re-cut with surgical scissors. Testing was repeated until satisfactory results were obtained from both tetrodes. The tips of the tetrodes were then carefully manipulated so that one was positioned approximately 0.3mm below the other, and the two tetrodes were fixed in position relative to one another with cyanoacrylate. After the silver paint had cured, the tetrodes were fixed to the cannula, and the connections were protected, using multiple coats of nail varnish. The tips of the electrodes extended below the feet of the microdrive by about 6 mm.

The spacing of the electrodes in the dorso-ventral plane was critical. As can be seen from Figure 1.5, pairs of recording sites with this separation above or below the pyramidal cell layer exhibit little noticeable discrepancy in phase. However, when the deeper tetrode passes below the pyramidal cell layer so that the two tetrodes straddle it, the discrepancy between the tetrodes becomes apparent as a partial phase-inversion. This permits rudimentary real-time localisation of paired recordings.

2.5 Recording techniques

During recording sessions, three types of data were recorded simultaneously: 1) position, 2) EEG, and 3) extracellular action potentials (spikes) from individual neurons (units). Individual records in each file were time stamped, so that the three types of data could be recombined for offline analysis on a SUN workstation.

2.5.1 Position tracking.

Typically, dual clusters of infra-red (i.r.) light emitting diodes (LEDs) were used to represent the position of the rat. The LED array was attached to a plastic post fixed to the rat's head (see surgery, below) so that the larger cluster (4-7 LEDs) was about 5 cm above the rat's nose, and the smaller cluster (2-3 LEDs) was about 7 cm posterior,

just behind the neck. In some instances, a single 3-LED cluster array was used, with the LEDs positioned 5 cm above the rat's head, between its eyes. The larger LED array was interpreted as the rat's position, with the smaller array serving as an optional indicator of head direction and inclination (but see section 2.10.2).

A video camera suspended 198 cm above the middle of the runway and a multi-spot video tracking system were used to identify the position of the LED clusters, and hence the position of the rat. For dual cluster tracking, position was taken as the coordinates for the larger cluster. Position was sampled at 50 Hz. The camera resolution was 768 x 574 pixels (x-y), and the optical zoom was adjusted to cover 230 cm of the treadmill. This zoom level was necessary to ensure that tracking would continue normally if the rat reared at the ends of the 150cm runway. The resulting theoretical tracking resolution was 333 pixels per metre (3mm accuracy), but see section 2.10.6 for further discussion on this point. The data acquisition software was used to restrict tracking to a 768 x 90 pixel window centred on the runway. The lower left corner of the tracking window became the 0,0 (x,y) tracking coordinates.

2.5.2 Unit and EEG recording.

A dual op-amp headstage was attached to the plug of the microdrive during recording, providing 8 channels of unity gain buffer amplification for the electrical brain activity picked up by the two tetrodes. The headstage served to isolate the electrodes from the wires connecting the headstage to the recording equipment, and improved the signal to noise ratio of the signal in transit by increasing the current drive without altering the voltage. Lightweight hearing aid wire (270 cm long) carried the output from the headstage to a 100 x preamplifier, and from there, a 450 cm length of ribbon cable carried the signal to the recording equipment. There were eight independent channels of electrophysiological unit recording data (four from each tetrode), two of which (one from each tetrode) were "split" to serve as additional EEG channels. Unit and EEG channels underwent different filtering and amplification, as described below.

Unit data was recorded differentially - that is, each of the eight unit channels was subtracted from another "reference" unit channel, removing the signals (usually noise or artefacts) common to both channels. Unit recordings were, therefore, inverted, with action potentials identified as positive (instead of negative) deflections in the voltage trace. References were chosen from channels which had little or no unit activity, so that these units were not added to the other channels as "reference

artefacts". Unit data was saved as discrete 1 ms spike-captures, triggered only when the voltage on any one of the four wires of a given tetrode exceeded a threshold. Signals were digitised at 48 KHz, low pass filtered at half this rate (24 KHz) to prevent aliasing, band-pass filtered between 500-6700 Hz, and digitally amplified 20,000-50,000 times. The trigger threshold was typically set at between 72 and 94 μV. When the threshold was exceeded, the voltage from all four wires of the tetrode was recorded for the 0.2 ms before and 0.8 ms after the trigger event. The resultant records typically captured the entire spike waveform which triggered recording. Digital noise rejection based on template matching was used to redirect spikes with waveforms resembling a square wave (likely to be artefacts) to a separate file for later analysis, if required.

Unlike the unit signals, EEG was referenced to the skull-screw ground (see below), and was not inverted. EEG signals were digitised at 250 Hz, low-pass filtered at 125 Hz, and high-pass filtered at 0.34 Hz. In addition, a 101-tap Von Hann-windowed finite impulse response filter was applied to minimise 50 Hz mains interference. EEG signals were digitally amplified 7000-25,000 times, and were recorded continuously over the course of a recording session.

2.6 Surgery

Rats were anaesthetized with a combination of isoflurane/N_2O/O_2, and the top of the head was shaved and prepared with antiseptic (povidone-iodine). Rats were given injections of a prophylactic (enrofloxacin, 0.10 ml s.c.) and a long-lasting analgesic (buprenorphine hydrochloride, 0.07 ml i.m.) to improve recovery. Once under deep anaesthesia, rats were fixed in a stereotaxic frame. Respiration and depth of anaesthesia was monitored regularly, and over the course of the surgery, isoflurane concentration was gradually reduced from 3.0% to 0.8%. An incision was made along the midline of the skull, extending from between the eyes to the muscles at the back of the neck. The incision was widened using haemostats and the surface of the skull was exposed and cleaned using the scalpel and sterile cotton swabs. A small burr drill was used to make six tapping holes in the skull. Six stainless steel jewellers screws were screwed into the holes. These screws would be used to anchor the microdrive to the skull. One of the screws was also soldered to a gold pin, which would serve as an electrical ground.

A trephine drill was used to make a hole in the skull at the implant coordinates: 3.8-4.0 mm posterior, and 2.5-2.7 mm lateral to bregma. The dura and pia were removed, and the brain surface was kept moistened with sterile saline solution until completion of the implant. The microdrive was placed in a micromanipulator (Narashige) and positioned so that the tips of the tetrodes were directly over the implant coordinates. Care was taken to ensure that the microdrive screw and the cannula were vertical relative to the skull surface. The microdrive and electrodes were then lowered until the tips rested 1.5 mm below the brain surface. The sleeve on the microdrive cannula was lowered to protect the portion of the electrode below the cannula which remained exposed. The surface of the brain around the sleeve was then packed with moistened absorbable surgical sponge. Dental cement was poured over the exposed skull surface, fixing the feet of the microdrive and the protective sleeve to the anchor screws in the skull. The edge of the incision was cleaned with sterile saline and treated with a topical prophylactic powder (neomycin and becitracin zinc). The skin was then pulled up over the edge of the dental cement "cap" and an additional thin layer of dental cement was applied to seal the wound to the cap. Anaesthetic delivery was then stopped, two 2.5 ml injections of sterile saline (s.c.) were administered, and the rat was allowed to recover for up to 24 hours in a clean recovery cage in the holding room before being returned to its home cage. All rats were then given a further seven days of recovery time before cell screening began.

2.7 Cell screening

The purpose of the cell screening phase was to move the electrodes into the pyramidal cell layer of CA1, and into close proximity to the soma of one or more pyramidal cells (putative place cells), so that its activity could be recorded. Screening was conducted on each tetrode separately, beginning with the deeper tetrode.

Over the first two days of screening, the electrodes were advanced about 200 μm per day, in 50 μm steps, bringing, the electrode to an estimated depth of 1.9 mm below brain surface. Thereafter, advancement was usually restricted to 100 μm per day, in 25 μm steps. From the beginning, the experimenter looked for evidence of 200 Hz "ripple" oscillations in the unit recording trace. Ripples (O'Keefe, 1976). are typically observed in or just above the pyramidal cell layer, while the animal is sleeping or during periods of waking rest. When ripples were first observed, the rat was returned to its

home cage until the following day, to allow time for the electrodes to achieve a stable position in the brain. Electrodes tend to drag the brain tissue down slightly when they are being lowered, so some time is required for the tissue to spring back up, especially after a period of rapid electrode movement. During this period, the tetrodes were effectively drifting down into the brain, and stable recordings would have been difficult to achieve.

Following the observation of ripples, it was assumed that the electrodes were in the vicinity of the pyramidal cell layer, so they were subsequently advanced by no more than 50 μm per day until suitable place cells were found. The researcher looked for evidence of burst firing cells with a signal to noise ratio of 3:1 or better on the unit channels on which ripples were detected. No waveform-based exclusion criterion was set, although an attempt was made to classify all recordings as having come from the soma of either principal cells or interneurons, or from dendritic or axonal processes. Because place cells that are active in one environment may not be active in another (O'Keefe & Conway, 1978; Kubie & Ranck, 1983), screening at this stage was often conducted at the same time as behavioural training on the runway, as described below. Screening for cells on the runway ensured that no potential candidate for recording was missed. Moreover, for a cell to be considered for inclusion in the study, its pattern of firing on the runway had to meet several additional criteria, outlined in the Preliminary Analysis section, below.

If a good candidate for recording was identified, electrode movement was halted, and a combination of training and test trials were conducted. If at any point during training or testing suitable place cell could no longer be isolated, the electrode was advanced 25 μm per day until such time as another suitable cell was found. If the deeper tetrode passed below the cell layer, as indicated by the phase inversion of the locally recorded theta oscillations on the two tetrodes (see Figure 1.5) the shallower tetrode was screened. When this tetrode passed through the cell layer, as indicated by the observation of in-phase local theta recordings from the two tetrodes, then the electrodes were advanced approximately 800 μm and recordings were attempted from CA3.

2.8 Training sessions

Rats were trained to shuttle between the food wells at either end of the runway, for food reward. Each rat was removed from its home cage in the holding room, weighed, carried to the experimental room in the transport box, and placed on the holding platform. A single moist grain of pre-cooked white rice, flavoured with honey, was placed in both food wells in the runway. The rat was then placed in the middle of the runway, facing west, while the experimenter stood at the south side of the track. Once the rat had found and eaten both pieces of rice, the piece in the food well the rat had eaten from first was replaced. Thereafter, the rat had to eat from one food well before another grain of rice was placed in the other food well. On the first and second day of training, rats were typically given two or three 10 minute trials in which to learn the reward contingency. By this time, all rats had begun to shuttle, and trials were reduced to 8 minutes. At the end of the trial, the rat was returned to the holding platform. When all training trials for a given day were completed, the rat was placed back in the transport box and returned to its home cage in the holding room.

Training was considered complete when the rat reliably shuttled (ran) between the food wells at the ends of the runway approximately 100 times in an 8-minute trial. A good run was one in which the animal did not stop or alter its direction of movement once the run was initiated. Most rats had completed training long before suitable place cells were identified for recording, although some rats needed additional training before the recording phase began. It was considered crucial that the rats' behaviour be reliable before conducting recording sessions. Otherwise, place-specific firing might simply be attributed to place-specific behaviours, and changes in firing patterns on trials in which manipulations were made might be the result, not of the manipulations themselves, but of spontaneous or induced changes in behaviour.

2.9 Recording sessions

The recording phase of the experiment usually involved an extended period of recording from several discrete cell populations in each rat. Recordings were made from a given population until either a) a complete series of manipulations had been performed, or b) the cells could no longer be isolated. At this point, the electrodes were moved and screening for different cells would begin. Recordings could generally be divided into two types – baseline, in which conditions are similar to those during the

training phase, and probe trials, on which manipulations were performed. Only baseline recording methods are discussed here, as probe trials are discussed in detail in the appropriate chapters to follow.

Baseline trials were used to assess general properties of the neurons, to provide a data base from which observations of the effects of normal variability in behaviour could be assessed, and for comparison with probe trials, on which manipulations were performed. As mentioned previously, it was also not unusual for some baseline trials to be recorded before training was complete, as part of the cell screening process. However, these baseline trials were not used for the formal assessment of the properties of place fields for analysis; they were simply used to determine whether place cells were present in the vicinity of the electrodes. Lighting conditions and the position and height of the end walls bounding the runway were exactly the same as during training.

Because some of the probe manipulations involved having the treadmill move, it was necessary to ensure that any effects of these manipulations were not due to the translation in space of olfactory cues associated with the floor of the moving runway. Therefore, on recording trials (including baseline trials) in which the treadmill was categorized as "stationary", it was actually kept running at an extremely slow speed. - less than 0.4 cm/s. The direction of movement was randomised across trials. This movement appeared to go unnoticed by the rats, but resulted in a translation of any point of the floor between one half and one full length of the runway over the course of an 8 minute trial, and ensured that any stable place cell recordings were not dependent on stationary floor-cues.

Trials on which probe manipulations were performed (P) were interspersed with baseline trials (B), the most common trial patterns being B-P-P-B or B-P-B-P-B. On some days, multiple series like this were conducted, with different manipulations, while on other days, only baseline trials were recorded. Trials were always 8 minutes long, except when a session began with two or more baseline trials, in which case the first trial was sometimes only 4 minutes long. The inter-trial-interval was typically around 2 minutes, but varied. During the recording phase, the manner in which rats were carried to the experimental room and placed on the runway was unchanged from the training phase. The rat was connected to the recording equipment prior to the first baseline trial of the session, and usually remained connected between trials. If, over the course of the trial the wires connecting the wires connecting the headstage to the preamplifier

became overly twisted, the rat was disconnected to untwist the wires. Data acquisition was initiated within 5 seconds of the rat being placed on the runway.

2.10 Pre-analysis

The main purposes of offline pre-analysis was to attribute spikes to particular cells, to determine the spatial firing characteristics of these cells, and to characterise the local EEG recording from each tetrode. These preliminary measures were used during the screening phase to determine whether the electrode was correctly positioned to record from place cells, and to determine whether cells met the criteria (described below) for inclusion in the study. TINT (Tetrode Interface, Neil Burgess) was used to recombine position, unit and EEG data, to calculate momentary speed, direction, and LED separation, and to assign theta phase values based on EEG records. TINT was also used to sort spikes on the basis of waveform characteristics, to conduct preliminary evaluation of the degree to which spikes from individual neurons had been correctly isolated, and to determine when the isolated units had suitable place fields for further analysis.

2.10.1 Position.

Position samples were boxcar averaged using a 400 ms sliding window, and camera X and Y pixel-coordinates were converted to cm. Momentary dropouts in the position record were corrected by interpolation between existing position samples. Such dropouts were usually caused by unusual posturing of the rat, or obstruction of the camera view of the LEDs by the recording cable. Trials were identified on which camera resolution and position had been adjusted; scaling and shifting adjustments were made on these trials to ensure that position data accurately reflected the range of visited positions on the runway and the rat's position in the room.

2.10.2 Direction.

In tasks where rats run in stereotyped trajectories as in the current experiment, place fields tend to be directional (McNaughton et al., 1983). Therefore, it was necessary to filter position data based on the direction in which the rat is running, in order to disentangle the direction-specific fields of a given place cell. When the dual

cluster LED array was used, the direction in which the rat's head was facing in the horizontal plane could be determined by comparing the relative positions of the two LED clusters. However, some place cells fired at the end of the track as the rat turned to run in the opposite direction. Under these circumstances, the rat's head typically swept through 180 degrees during passage through the place field, so conventional direction filtering was inappropriate. Direction estimates based on the relative positions of the large and small LED clusters also suffered on some occasions when the large and small clusters could not be differentiated, when head tilt prevented tracking of the small cluster, or when the large and small LEDs were confused. All of these problems were accentuated at the ends of the runway. Therefore, momentary direction was defined as the direction the large LED cluster was moving, based on the comparison of consecutive position samples. This also proved to be the more reliable predictor of whether a given cell would fire in a given position. Direction values ranged from 0-359 degrees, with 0 corresponding to heading due east.

2.10.3 Speed.

Momentary speed was calculated by dividing the distance separating consecutive position samples by the time interval between the samples. Speeds over 4.0 m/s were considered artefactual and replaced by linear interpolation.

2.10.4 Theta phase.

Recorded EEG values ranged from 0-255 (arbitrary units), and theta cycles were modelled as half-sinusoids (144 EEG units high) fit to the EEG and aligned to negative-going crossings at EEG value 128 (mid-range). Consequently, fitting was applied to the troughs of the theta cycle, as the troughs in the CA1 pyramidal cell layer "are of more reliable shape than the peaks, and should be used as the landmark identifying a new cycle.... the peaks are often bimodal" (Neil Burgess, personal communication). This fitting method was previously used by O'Keefe & Recce (1993).

Half sinusoids were varied in two dimensions until the best least-squares fit with the data was obtained: half-period was varied from 32-80 ms (full cycle frequency = roughly 6-16 Hz) and zero-offset was varied from 0-64 EEG units. If the mean-square difference between the best fit sinusoid and the data exceeded 192 EEG units (3/4 of the potential EEG range), the fit was rejected. A further limitation was that successive

cycles could be no less than 48 ms apart, as this would correspond with an "impossible" momentary theta frequency of roughly 20 Hz. Phase values from 0-359 were assigned to the EEG samples between mid-range crossings associated with good fits, with the crossings themselves arbitrarily defined as the beginning of each cycle (phase = 0^0). The theta phase corresponding with the time at which any given spike was fired was referred to as the firing phase of that spike.

2.10.5 Spike sorting and cell isolation.

Spikes recorded from different tetrodes were analysed separately. Spikes were sorted primarily on the basis of their relative peak to peak amplitude on each of the four tetrode wires. This principle works on the assumption that, given the spatial arrangement of the tetrode wires, spikes from a given cell will appear larger on some wires than others, as a function of proximity (Harris et al., 2000). Comparing the relative amplitude of a spike on each wire of the tetrode permits, in essence, triangulation of the signal in space. In a scatter-plot projection of multi-cell spike amplitudes on any two wires, points representing different neurons will tend to form discrete clusters. TINT allows the user to assign groups of spikes to a cluster by manually drawing a polygon around them. Such clusters could be defined in any of the six possible projections comparing two of the four tetrode wires. A discrete cluster, as defined in one projection, may appear as two or more clusters in another projection, allowing further refinement of the cluster in multi-dimensional spike amplitude space. In addition to amplitude, peculiarities of the spike waveforms were used to identify spikes from different neurons. For example, some waveforms had a distinctive notch on the ascending phase of the spike. In the 1 ms window surrounding the trigger point for any spike, the voltage on a particular wire at a particular time (V_t) could be used to create additional projections on which clusters could be isolated. A sample of cluster-cut data is presented in Figure 2.3.

Relative amplitude and V_t projections represent two complimentary methods of unit isolation, based on proximity, and a limited form of template matching, respectively. When a cluster was refined to the point that the experimenter was satisfied that no further projections could produce bimodal distributions of spikes, a temporal autocorrelation was performed on the spikes from that cluster. If, and only if, the autocorrelation showed clear signs of a 2 ms refractory period, that cluster was defined as a "cell", and proceeded to the next phase of analysis. Otherwise, it was

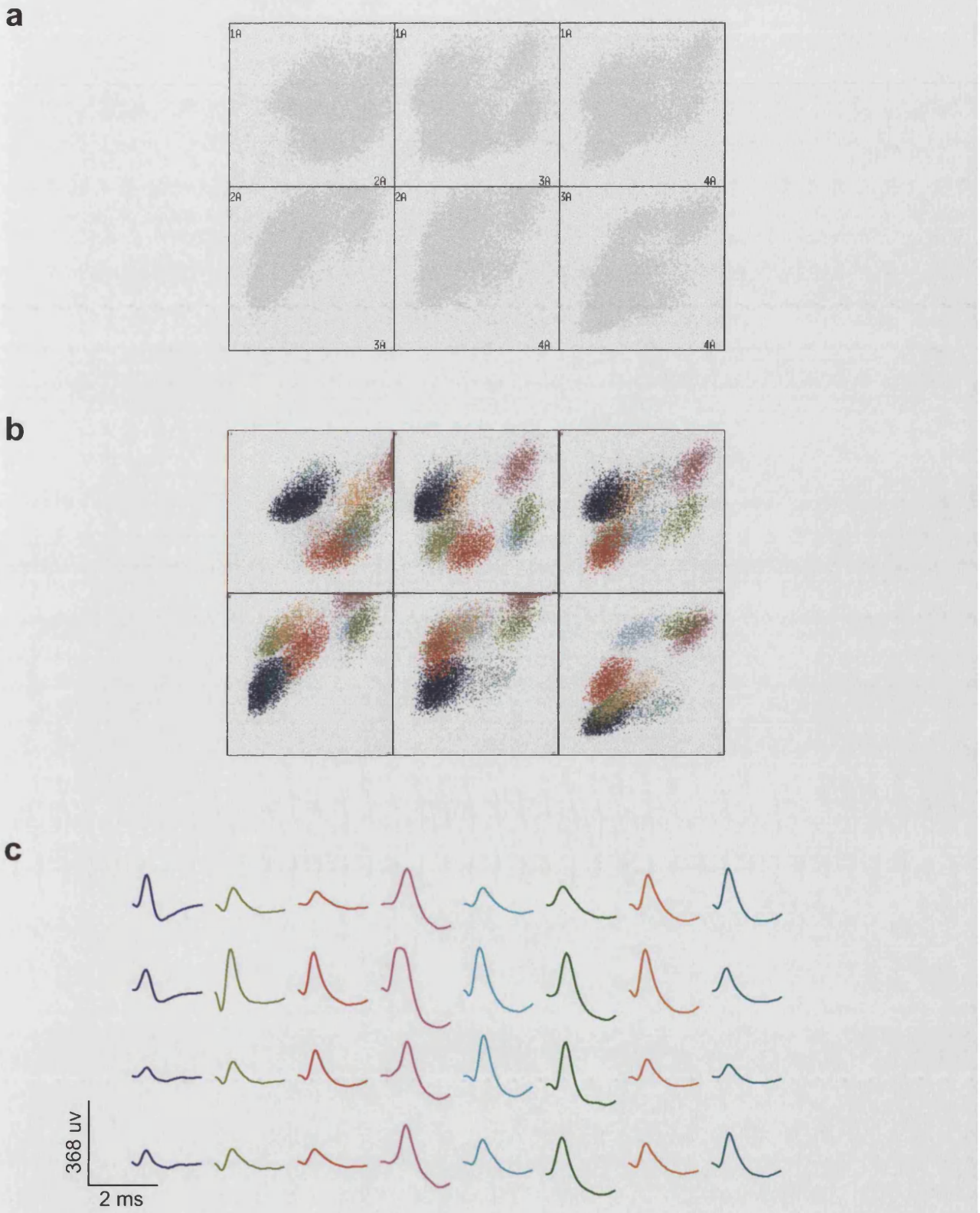

Figure 2.3. Cluster cutting. **a:** Unclustered spikes plotted as a function of each of six possible peak amplitudes on pairs of wires in a tetrode. Note the tendency for spikes to form eliptical clusters in each projection, with axes oriented towards the plot origin. **b:** The same data, with clusters identified. Note that clusters which overlap in some projections are distinct in others. **c:** Mean resultant waveforms in each cluster. Each column represents an individual neuron, while each row represents the waveform as recorded on a given wire of the tetrode. Note that neurons with waveforms similar on some wires differ considerably on others - the differences in amplitude are reflected in **b**.

deemed likely that the cluster actually represented the activity of two or more indistinguishable units, and thus had to be rejected. It should be noted, however, that use of the autocorrelation is not a failsafe way of determining if spikes are from single or multiple neurons, because if two neurons have non-overlapping place fields, they will also fail to exhibit coactivity within the time it takes for the rat to travel from one field to the other.

2.10.6 Place field definition.

For each well isolated cell, a firing rate map was constructed to determine whether the cell had a place field on the runway. The tracking coordinates were scaled down by a factor of 2, so that the range of pixels visited in the tracking window fit within TINT's 512 x 512 pixel plotting window. This resulted in a plotting resolution of approximately 167 pixels per meter, or 0.60 cm per pixel. Note that it is possible that the accuracy of the tracked positions may be somewhat less than this, due to errors relating to jitter or estimation of centre of the large (60 pixel) LED array. The plotting window was then divided into a 128 x 128 array of bins, each bin measuring 4 x 4 pixels, and representing a 2.40 x 2.40 cm area of the runway. For each bin, firing rate was calculated using the formula RATE = S/(P/F), where S is the number of spikes recorded when the rat's position corresponded with the bin (occupancy), P is the number of position samples collected during occupancy of the bin, and F is the position sampling frequency. In other words, bin firing rate is the number of bin spikes divided by the bin dwell time.

In addition, a boxcar averaging technique was used to smooth the firing rate map, in order to correct for temporal variability in cell firing and bin occupancy, and to better represent what the rate map might look like if recording was extended for an infinite amount of time with infinite occupancy in all parts of the environment. The firing rate for each bin was redefined as the mean firing rate for the block of 25 (5 x 5) bins centred on it, not including bins in which occupancy was zero. The peak firing rate was defined as that of the bin with the highest firing rate. For the purpose of plotting the rate map, firing rate of each bin was then autoscaled and colour coded as a percentage of the peak firing rate, with a white mask applied to regions of the tracking window which the rat never visited (zero occupancy). At this stage, the place field(s) for a given cell was simply defined as a group of contiguous bins with firing rates exceeding 20% of the peak.

2.10.7 Inclusion criteria.

Cells were accepted or rejected for analysis on the basis of their place field characteristics. Separate rate maps were calculated for when the rat was travelling in either direction (due east or west, $\pm 90^0$) on the runway, so cells could be selected on the basis of having suitable fields specific to either or both directions. Cells with peak firing rates of less than 1.0 Hz or which fired fewer than 10 spikes over an 8 minute trial were either excluded or simply considered silent for that trial. Analysis of phase precession slope was restricted to trials on which at least 100 spikes had been fired.

Rate maps of ideal candidates also generally exhibited a single 2-dimensional firing rate gradient of contiguous bins representing from 100% of the peak firing rate at the centre to 0% at the periphery. The region(s) where the firing rate exceeded 20% of the peak rate was defined as the cell's place field(s). Cells with extremely spatially constrained fields, such as those which only fire when the animal poked its nose into a corner, were excluded from analysis. Movement within such fields was virtually impossible, and consequently, theta EEG was unreliable. Conversely, fields which covered more than ¾ of the runway were excluded from further analysis due to their low spatial selectivity (i.e., they could hardly be considered "place" cells).

Cells with multiple place fields were not excluded, provided that no more than two fields were evident when the rat was running in a given direction, and that such fields were clearly separated by a region of null firing. In these cases, spikes comprising the discrete fields were reassigned to different clusters. During screening, these criterion were used to determine whether the cells being recorded were suitable for further analysis, in which case movement of the electrode was halted, and training (if required) was continued until the rat was ready to begin recording trials.

2.11 Data extraction and detailed analysis

While TINT provided the necessary tools for cluster cutting and preliminary place field evaluation, the data had to be exported to custom software (GOODRUN, John Huxter, 2001) for more detailed analyses, and this also required reconstruction of place fields based on the interpolated position records produced by TINT. It was possible for fields previously deemed acceptable in the preliminary analysis to be rejected at this phase, following changes in field parameters due to the linearising of the data, the combined speed and direction filtering, and/or the slight differences from

the binning and smoothing regimens used in preliminary analysis, all of which are described in detail below. TINT was used to generate an ASCII output file containing the following momentary information, sampled from the original data at the EEG sampling rate: time since the start of the trial in seconds, x- and y-position in cm, direction in degrees (east = 0^0, north = 90^0, etc.), EEG voltage (0-255), theta phase (0^0-359^0, -1 = poor fit), LED separation in pixels, and the number of spikes fired by each isolated cell.

2.11.1 Redefinition of place fields.

Given that single cells often had multiple fields on the runway, the fields themselves were subsequently treated as the principal unit of analysis. Basic place field characteristics were recalculated using the GOODRUN program, which reads TINT output file. Data was filtered so that spikes and positions were only counted when the rat was moving at greater than 10 cm/s in the preferred direction of the field ($\pm 45^0$), as determined from the preliminary analysis. On trials when the treadmill was moving at above-baseline speeds, the minimum speed requirement was raised or lowered as needed to account for passive displacement. For example, on eastward runs when the treadmill was moving east at 7 cm/s, the minimum velocity of the rat was raised to 17 cm/s. However, 1 cm/s was the lowest permissible minimum velocity value, under any circumstances. Given the one-dimensional nature of movement on the runway, all position data points were collapsed in the y-dimension (north-south). Position was then sorted into a single row of 2 cm bins.

The firing rate for each bin was calculated as the boxcar averaged firing rate for the row of five bins centred on it, in a manner similar to that described previously. Again, bins contributing to the boxcar average had to have been visited by the rat (occupancy > zero). Similarly, peak firing rate could only be derived from a bin the rat had actually visited. The place field was then defined as the series of all contiguous bins flanking the peak bin, and having rates $\geq$ 20% of the peak. It was occasionally found that using the 20% criterion to define the edge of the field resulted in exclusion of spikes which were clearly part of the field. Therefore, very infrequently, the field edge was redefined as 10% of the peak to include these spikes. Conversely, for fields consisting of a main field (containing the peak) and one or more closely spaced subfields, it was occasionally necessary to raise the edge threshold to 30% of the peak rate in order to exclude spikes from the subfield(s). A record was made of all these

exceptions. Redefined place fields no longer meeting the inclusion criterion described previously were excluded from further analysis at this point.

2.11.2 Extraction of runs through the field.

For each place field identified on a given trial, a separate copy of the data was made which only included records from uninterrupted runs through the place field meeting the speed and direction requirements. In most cases, runs which did not cover a distance equal to at least the length of the field minus one bin (2 cm) were excluded. The only exception to this rule was when fields abutted one of the end walls, often due to the field-enlarging effects of the boxcar averaging. A valid run through such a field would require the rat to maintain the minimum velocity right up until the point at which the rat contacted the end wall, which was virtually impossible. Under these circumstances, the minimum run length requirement was relaxed to allow a greater number of runs to be included in the data set. Typically, minimum run length was lowered until at least 10 valid runs through the field of the specified length were recorded. A record was kept of all the times these exceptions were made. The complete set of good runs through a given field on a given trial was stored in a unique file. Insofar as the different place fields recorded on a given trial overlapped, these "runs" files contained overlapping data records.

2.11.3 Momentary variables and run statistics.

Additional variables were calculated for each record in the runs files: the current run number, the elapsed time and cumulative distance travelled since the run began, the current angular distance from the centre of the place field, and the momentary frequency of the theta oscillation. Momentary theta frequency at t_2 was defined as follows...

$$1 \Big/ \frac{(t2 - t1) + (t3 - t2)}{2}$$

...where *t1*, *t2* and *t3* are the time at phase-zero of the previous, current, and next theta cycle, respectively. In other words, frequency was calculated from the mean time separating three consecutive cycles. Frequency was only calculated for a cycle if theta fitting was good for the entire period from *t1* to *t3*.

Momentary running speed was calculated by Tint in the pre-analysis phase, as described above. However, it was desirable also to obtain a measure of momentary changes in running speed, or acceleration. Such a measure is indirectly related to the amount of physical effort the animal exerts during locomotion. Momentary acceleration was calculated as $\frac{v2-v1}{t2-t1}$, where *v1* and *v2* are any two successive measures of the rat's running speed, and *t1* and *t2* are their corresponding timestamps. Acceleration was only calculated if *v1* and *v2* fell between 5-200 cm/s, and if there was an actual change in velocity between samples. Because the EEG sampling rate was higher than the video capture rate, it was normal for a data file to contain multiple consecutive records in which the rat's position and velocity was exactly the same. In the event of an exact match between *v1* and *v2*, acceleration values were inherited from the previous sample.

Instantaneous firing rate (IFR) was calculated for each spike fired as the rat traversed the place field. The IFR for any given spike is the number of spikes in a time window up to one theta cycle on either side of the reference spike, divided by the size of the window (Harris et al., 2002). The firing phase of each spike could then be correlated with the IFR at that time. A measure of the momentary change in IFR (the temporal derivative of the IFR, TDIFR) was also defined, as the difference between the IFR for any two consecutive spikes, divided by the time interval between them. This measure was only calculated for successive firing rates based on time windows of not less than 100 ms. The TDIFR permitted the determination of whether individual spikes occurred while the IFR was increasing or decreasing, or neither.

The temporal derivative of the firing phase (TDPHASE) was calculated for each theta cycle. This variable measured the change in firing phase from one theta cycle to the next. The circular mean phase at which spikes in each theta cycle fired was calculated, and TDPHASE for a given cycle was taken as the angular difference between its mean phase and the mean phase of the preceding cycle, divided by the duration of the preceding cycle. Cycle pairs for which fitting in one cycle was of poor quality were excluded.

In addition to momentary statistics, each pass, or run, through the place field could also be said to have characteristic features. The following variables were calculated for each run: run duration, cumulative distance travelled, mean running speed, number of spikes fired, number of theta cycles, position at which the run began,

position at which the first and last spikes were fired, and firing phase of the first and last spikes. For example, the characteristic running speed for any given run is the average of the momentary speeds for each sample in that run.

2.11.4 Calculating basic field statistics.

Basic field statistics included the peak firing rate (Hz), place field size (cm, x-dimension only), peak position (cm), centroid (cm), field skew, the slope of the phase precession (cm/s), the mean firing phase of the first and the last spike on each run through the place field (degrees), mean phase shift (degrees), characteristic running speed, and characteristic theta frequency. Peak firing rate and field size are described in section 2.11.1. Peak position was defined as the midpoint of the bin with the highest firing rate. The centroid (centre of mass) and skew of the field were calculated as a function of the dwell time corrected spike distribution. This distribution consisted of values representing the x-position at the midpoint of each bin considered to be a part of the place field. Each of these unique values was replicated 100 times per 1 Hz firing rate in that bin. For example, a bin whose centre was at x-position 5.25 cm, and who's firing rate was 8.73 Hz, contributed 873 data points of value 5.25 to the data set. The total number of data points (N), mean (μ) and standard deviation (σ) of the distribution were calculated. The mean corresponds with the field centroid, while the following formula yields the field skew...

$$\frac{\sum(X-\mu)^3}{N\sigma^3}$$

While peak position and centroid were expected to be similar, each has its advantages as an indicator of field position. Peak position is a more accurate indicator of maximal cell excitability when the field is skewed, while measures of the centroid are less prone to variability introduced by the arbitrary positions at which bin boundaries fall.

The firing phase of the first (phase_a) and last (phase_z) spike in each run was averaged across all runs in the first baseline trial for each field, using statistical methods for circular data (Mardia, 1972). The accuracy of all phase data depends on the quality of the original EEG recording. For 48/94 place fields, EEG data and theta fitting was worse on the tetrode from which unit activity was being recorded. This was often due to the low amplitude of theta in the pyramidal cell layer itself. Consequently,

for these fields, the theta used for estimation of phase values was not the local theta, but the best quality theta from the adjacent electrode. To correct for potential phase differences between tetrodes arising from the known depth profile of the theta oscillation, the estimated phase offset between electrodes was applied as a correction to phase_a and phase_z values. The correction was determined by the amount of shift required to align the peaks and troughs in a representative, simultaneously recorded three second epoch of theta from both tetrodes. Consequently, phase_a and phase_z should always be taken to refer to the phase of the local theta EEG, or the best possible estimation thereof. The correction was not applied to analyses of phase precession slope, total phase shift, or the temporal derivative of phase (see below), as phase offset affects the firing phase of all spikes equally, and therefore will not alter these variables.

Phase_z minus phase_a was taken as an estimate of the total phase shift (degrees) for a given field. It is mathematically equivalent to taking the mean of the shift on each run. Based on preliminary evaluation of the data, it was assumed that phase shift values should always be negative (indicating precession) and less than 360^0. Consequently, shift values greater than zero were adjusted by -360^0.

Characteristic speed, acceleration and theta frequency for fields were taken as the means of each of these momentary variables during runs through the field.

2.11.5 Analysis of theta phase precession.

Several variables were calculated to describe the phase precession effect for each trial. A regression line was used to describe the overall relationship between the rat's position and the theta phase at which any given spike fired. The mean phase of the first spike and the last spike of each run through the field gives an estimate of the phase at which cell firing in the field begins & ends, and the mean difference between those values describes the extent of the precession. Fitting a regression line to phase shift data presents special challenges, and is described in more detail below.

The firing phase of each spike was compared with the cumulative distance the rat had travelled in a given run through the place field - the run distance - rather than absolute position on the runway. This simplified the comparison of the precessions for different cells and different trials, because it ensured that the slope was always negative, and the y-intercept always corresponded with the firing phase of the first spike at the start of each run (i.e. as the rat entered the field). Of course, run distance

is highly correlated with absolute position on the runway, because the beginning of each run generally corresponds with the leading edge of the place field, ± 2cm. Due to the phase precession effect, spikes will occur at a progressively earlier phase of each subsequent cycle as the place field is traversed.

Because phase precession can subtend a full 360^0 of the theta cycle, and because phase precession sometimes begins considerably less than 360^0 after the beginning of the current cycle, spike firing often precesses until it actually occurs at phase zero (the beginning) of a particular cycle, and the cell fires again before the beginning of the next cycle. Technically, at this point, firing phase has become negative, but firing phase values are constrained to positive integers from 0-359. As a result, a plot of firing phase versus time or position yields what appears to be a discontinuous function, with firing phase reducing to zero, and then suddenly jumping to 359 before continuing to precess from there. To solve this problem, the firing phase data was linearised. First, a new origin was defined and all firing phase values above it were adjusted by -360^0 - a process referred to as "rolling" the data. This was considered a valid manipulation, because assuming the theta oscillation resembles a sine function with a constant frequency, the phase in any given cycle corresponds to the phase of the subsequent cycle minus 360^0. The new origin was defined using one of two methods. Both techniques take advantage of the fact that phase precession tends to be less than 360^0, creating a natural discontinuity in the firing phase data which usually corresponds to values just greater than the mean firing phase at the beginning of each run. Rolling data points above this discontinuity creates a continuous distribution which includes negative firing phase values, making the data better reflect the true temporal dynamics of cell firing, and permitting the application of traditional regression analysis.

The first technique, which tended to produce the best results, involved simply identifying the mean firing phase of the first spike on each run through the field. All data points greater than the mean plus one standard deviation (Mardia, 1972) were rolled by -360^0. Occasionally, however, this resulted in rolled data sets with outliers in the firing phase domain, which drastically affected the regression fit. This most often occurred for low peak-rate fields characterised by sparse firing at the leading edge (beginning of the run). For these cells, estimates of the firing phase of the first spike in each run tended to suffer from the high variability inherent in small samples. Fields with very shallow precession also tended to suffer when this technique was used, as the origin would often dissect a large portion of the data points. Under these circumstances, the second

technique was used, which took advantage of the fact that rolling the data to eliminate the natural discontinuity also tends to minimise the variance. Rolled data sets were created using all possible integer values for the new origin from $0\text{-}359^0$, and the rolled data set with the origin which produced the smallest variance was used.

The significance of the curvilinear fit of the rolled data served two additional purposes. First, if the slope of the regression line was non-significant ($p>0.05$), positive, or had an absolute value less than 1, firing was said not to precess. Second, for data sets which demonstrated precession, the data was "wrapped" around the curvilinear regression line. For each value of run-distance, an inclusion zone representing firing phase values within $\pm 180^0$ of the regression line was defined. Data points falling outside this inclusion zone were adjusted by $\pm 360^0$ to bring them within the inclusion zone. This had the effect of further reducing the variance in the data set. It was justified based on the presence of a significant trend in the data, and the possibility that some outliers not contributing to the trend were simply phase-matched to the wrong theta cycle. In some cases, this procedure also corrected for outliers produced by the rolling technique.

The rolled, wrapped data set was used for all subsequent analyses. A simple linear regression fit was used to describe the precession at this stage. The curvilinear fit used in the data processing stage better matched the data and ensured maximum inclusion of data points prior to wrapping. However, inclusion of the quadratic trend in a stepwise regression where the linear component was entered first never resulted in a significant increase in the amount of variance explained by the model. Moreover, describing the precession as a linear function enabled a straightforward comparison of the slope of the precession for different cells or different trials, as described below.

2.11.6 Analysis of responses to manipulations.

All manipulation (probe) trials were preceded and followed by baseline trials. The effect of the manipulations on place field characteristics were evaluated only if the baseline trials before and after exhibited a high degree of similarity in place field size and position (Pearson's $r > 0.90$). Otherwise, any changes in the fields could be attributed to uncontrolled factors, like the passage of time. In short, if a probe trial was not followed by a baseline trial in which firing was "normal", that probe trial was dropped from all subsequent analyses.

Chapter 3: Non-Experimental Observations

3.1 Introduction

This chapter deals with histological results, general observations on the behaviour of the rats, the description of general place field properties, and the relationships between those properties. Data from the first 8 minute recording of any given field were used to assess basic properties of the place fields. Note that these do not represent the first exposure of the rat to the runway – by the first recording, any given rat was already familiar with the environment. The objective was to make some general observations about place field characteristics in the absence of any experimental manipulations - that is, under "normal" conditions in an environment the rat was familiar with. It was also deemed necessary to quantify the differences in the rat's behaviour on different parts of the runway - a well documented feature of tasks requiring goal directed behaviour - in order to interpret how these differences might influence characteristics of the rat's representation of space.

Data were collected from a total of 9 rats with 73 putative pyramidal cells exhibiting spatially selective firing patterns, as described in the General Methods (inclusion criteria). From these cells, a total of 94 place fields meeting the inclusion criteria were analysed. Any given rat yielded between one and five unique place fields on a given day, and on average, 2.106 fields were recorded simultaneously.

3.2 Histology and recording localisation

Following experimentation, rats were killed by sodium pentobarbitone overdose (Euthatal™, 1ml, i.p.), and immediately perfused. The brains were removed, quick frozen, cut into 40 μm thick sections, stained using cresyl violet, and mounted for inspection. Histological results are presented in Figure 3.1. Unfortunately, sections from rat 1131 were too damaged to permit localisation of the electrode tract. In the remaining rats, electrodes clearly passed through the CA1 pyramidal cell layer. Tracts from each tetrode (deep and shallow) in a given rat are usually indistinguishable due to the proximity of the electrodes, a notable exception being rat 1089. Observation of the depth profile of the theta EEG as the electrodes were lowered, and in particular the theta phase inversion when the deep and shallow tetrodes straddled the CA1

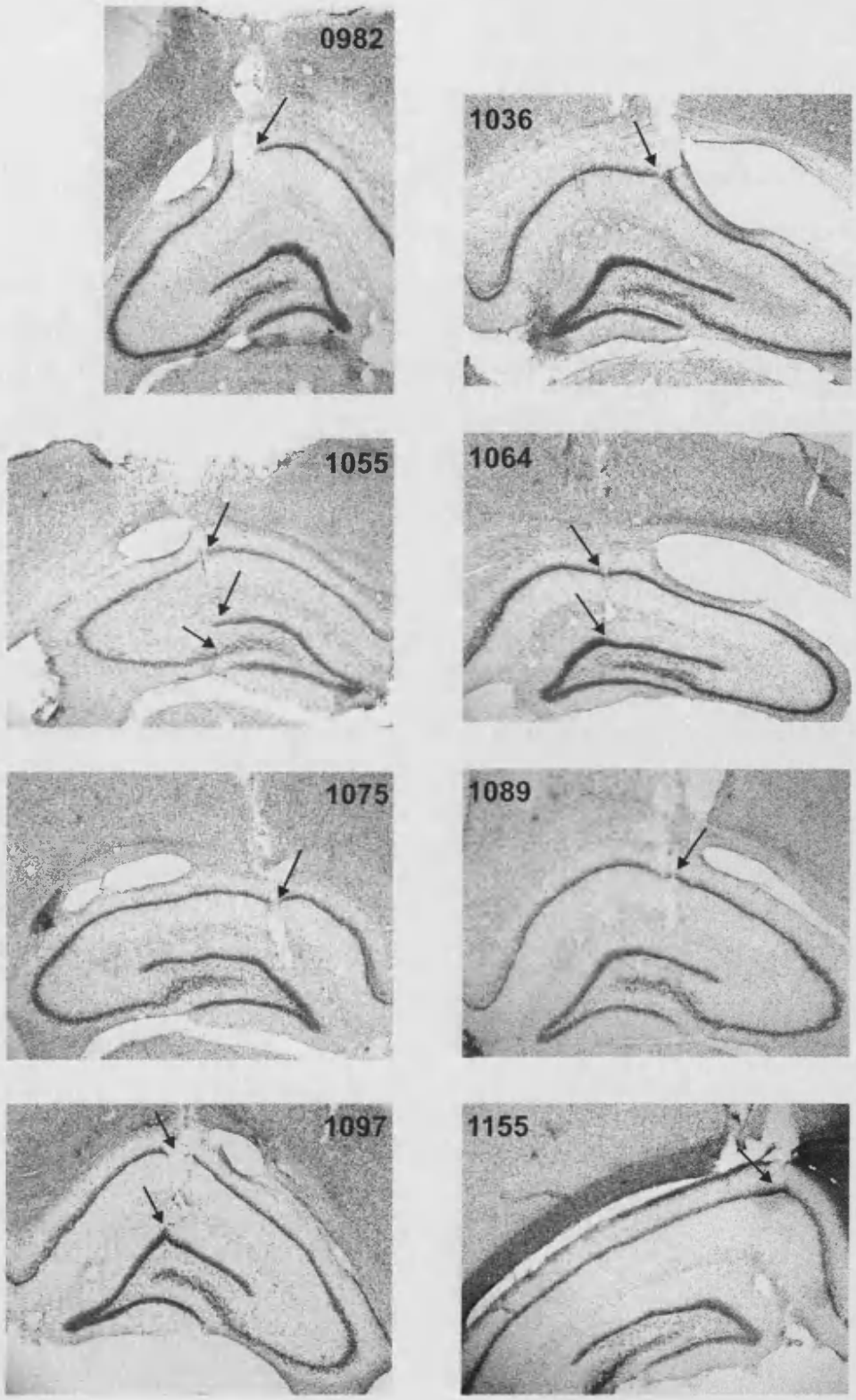

Figure 3.1. Histological results from eight of the nine rats used in the current study. Arrows indicate where electrodes entered the cell layer(s). Damage to the sections from rat 1131 prevented localisation of the electrode tract.

pyramidal cell layer, provided additional confirmation that recordings were made from CA1 in all rats, including rat 1131.

The electrode trajectories suggest that deeper recordings (rats 1064 and 1097) could have been made from the dentate gyrus or polymorph layer, but not CA3. No current was passed before the brains were removed, so it was difficult to determine the final depth of the recording electrode, and because recordings were obtained from cells at multiple depths for each tetrode, it was not possible to histologically determine the precise depth of any given recording.

The theta phase inversion zone (as described in section 1.3.3) permitted reasonably good localisation of recordings from CA1, but no such clear physiological marker is known to differentiate the dentate gyrus from the polymorph layer. Therefore, shallow recordings (just above or below the theta inversion zone) were attributed to CA1, while deep recordings (800 μm or more below the inversion zone) were more ambiguously classified as dentate gyrus/polymorph layer (DG/P). A total of 75 fields were recorded from CA1, while the remaining 19 were recorded from DG/P. Of the 75 CA1 fields, five were presumed to have been recorded just below the pyramidal cell layer, perhaps from dendritic processes, or cell bodies which were dragged along with the electrodes.

3.3 Behaviour

All rats quickly learned to shuttle between either end of the runway for food reward. It was not unusual for a rat to make 50 traversals of the runway in each direction, over the course of an eight-minute trial. One of the most remarkable features of the rats' behaviour was the distribution of running speed across regions of the runway, as illustrated in Figure 3.2. Running speed tended to decline over the course of each trial, and over successive trials on a given day (probably due to satiation). However, on each run, all rats began running slowly, reached peak speeds mid-runway and decelerated as they approached the other end. This results in place fields in different regions of the runway having different characteristic running speeds - that is, a rat will tend to run through one field at a different speed than it runs through another. The acceleration phase is more gradual than the deceleration phase, as rats tended to come to a fairly abrupt halt upon reaching the end of each run.

Figure 3.3 illustrates composite plots of speed, acceleration, and theta frequency as a function of position on the runway. The data are broken down into plots for eastward and westward runs, for all nine rats combined. Position data for each rat are standardised to values ranging from 0-1 before being combined, after which it is sorted from a continuous range into 100 bins. In addition to running speed, the composite acceleration data is presented, showing that the rat is accelerating for roughly the first half of the journey down the runway, and decelerating for the second half. The acceleration plots also highlight another behavioural characteristic - at the very beginning of the run, the rat's angular velocity and acceleration are fairly high, as the rat must turn around to face in the direction of the opposite end of the runway. Then there is a slight reduction in speed as the rat stops turning and engages in forward movement. Beyond this point, the velocity profile has a relatively parabolic shape, and consequently, the relationship between position and acceleration is approximately linear.

These observations of the rats' behaviour have serious implications for the way subsequent data are analysed. The most obvious of these is that, given the confounding of running speed and rat position, any investigation of the relationship between field characteristics and field position must be balanced by an analysis of the corresponding relationship with running speed. As an added measure, an attempt was made to quantify the relationship between running speed and field characteristics, independent of position and manipulations. This analysis is treated separately, in Chapter 5.

3.4 Theta frequency

Figure 3.2 illustrates how the frequency of the hippocampal theta oscillation changes as the rat traverses the runway. For each field, runway position is confounded with running speed, and although there were noticeable differences between rats, theta frequency was generally proportional to running speed. For some rats, theta frequency was correlated with changes in running speed (acceleration) as well – theta frequency was higher when the rat was gaining speed than when it was coming to a halt. Although this effect was not observed in all rats, it contributes to the observation that the change in theta frequency is most pronounced in the region of the runway where the rat is coming to a halt – where the separate effects of low speed and deceleration appear to summate.

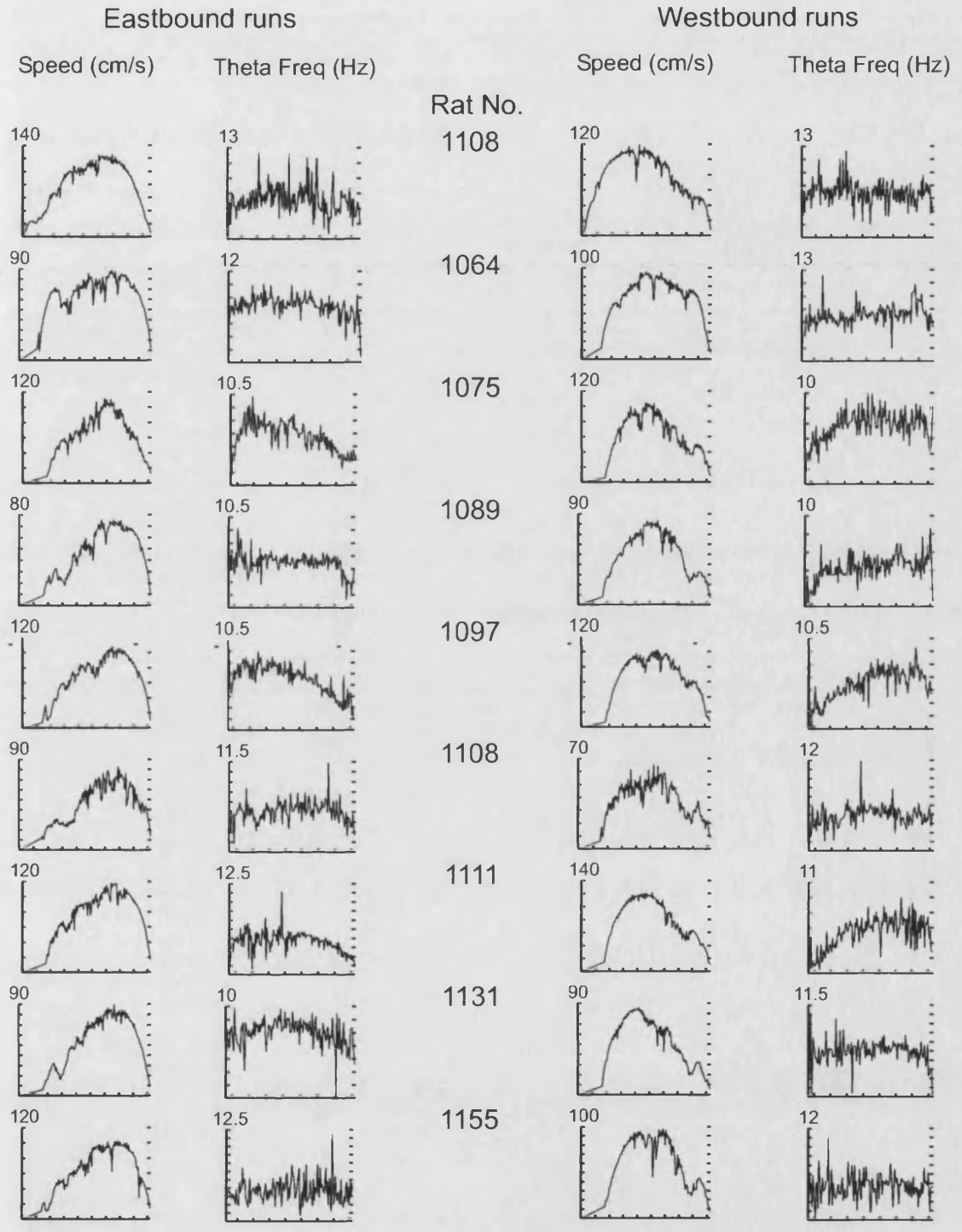

Figure 3.2. Mean momentary velocity and theta frequency for all nine rats, plotted as a function of position on the 150 cm runway. The plots are divided into eastbound and westbound data sets, in which the rat's speed never dropped below 5 cm/s and direction never deviated more than 45^0 from the specified cardinal direction. The rat number is indicated at left, and peak values for each plot appear in the top left corners.

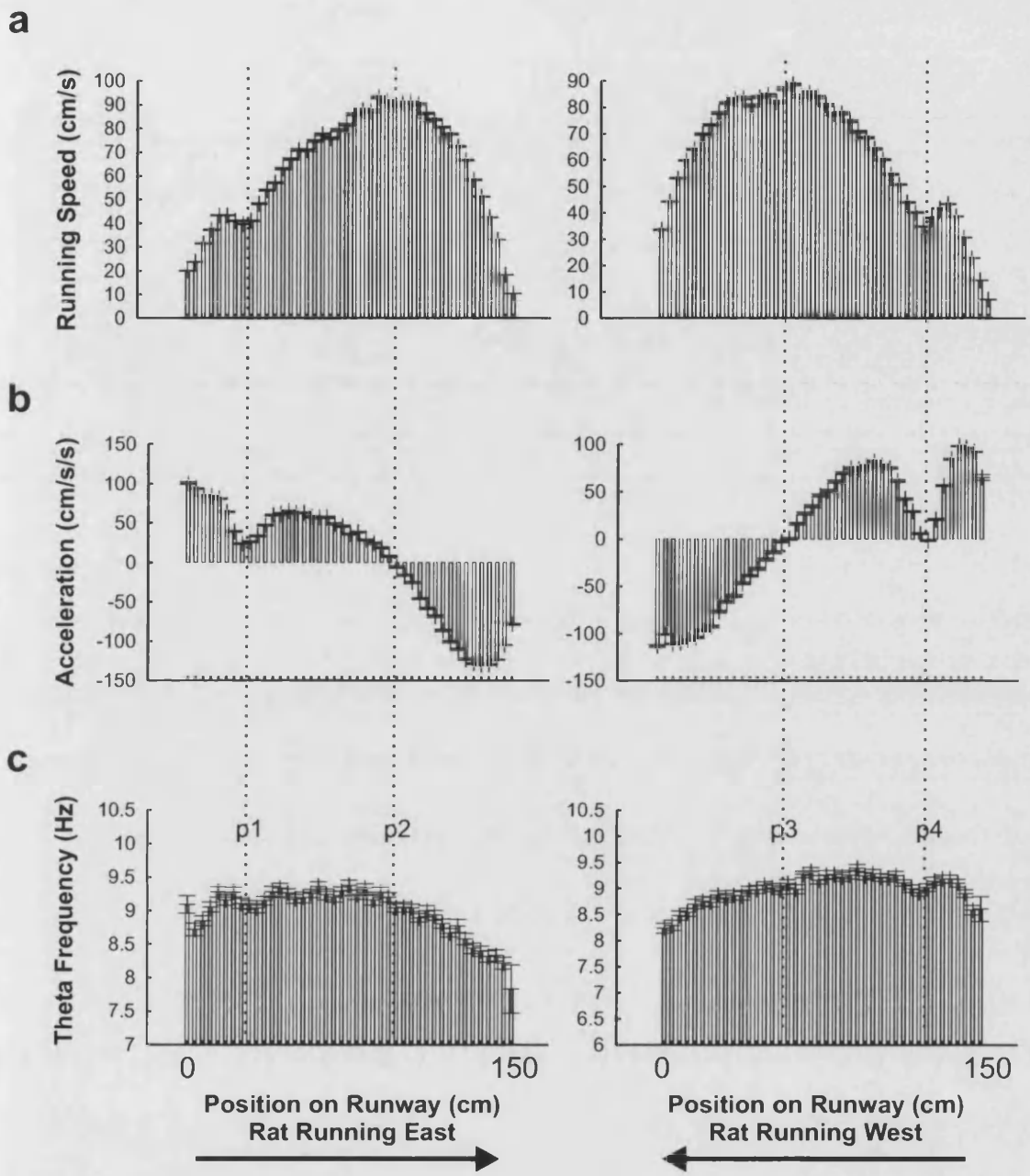

Figure 3.3. Composite plots of running speed (**a**), acceleration (**b**), and theta frequency (**c**) as a function of position. Data from all nine rats was combined, with position data normalised for each rat and boxcar averaged (100 bins). Error bars are SEM. Two positions on the runway correspond with significant behavioural events. P1 and P4 indicate the point at which the rat finishes turning around, just prior to running straight towards the opposite end of the runway. Note the dip in running speed, the reduction in acceleration, and the momentary reduction in theta frequency. P2 and P3 indicate the point at which the rat switches from acceleration to deceleration. Note that it is beyond this point that a negative trend in theta frequency becomes apparent.

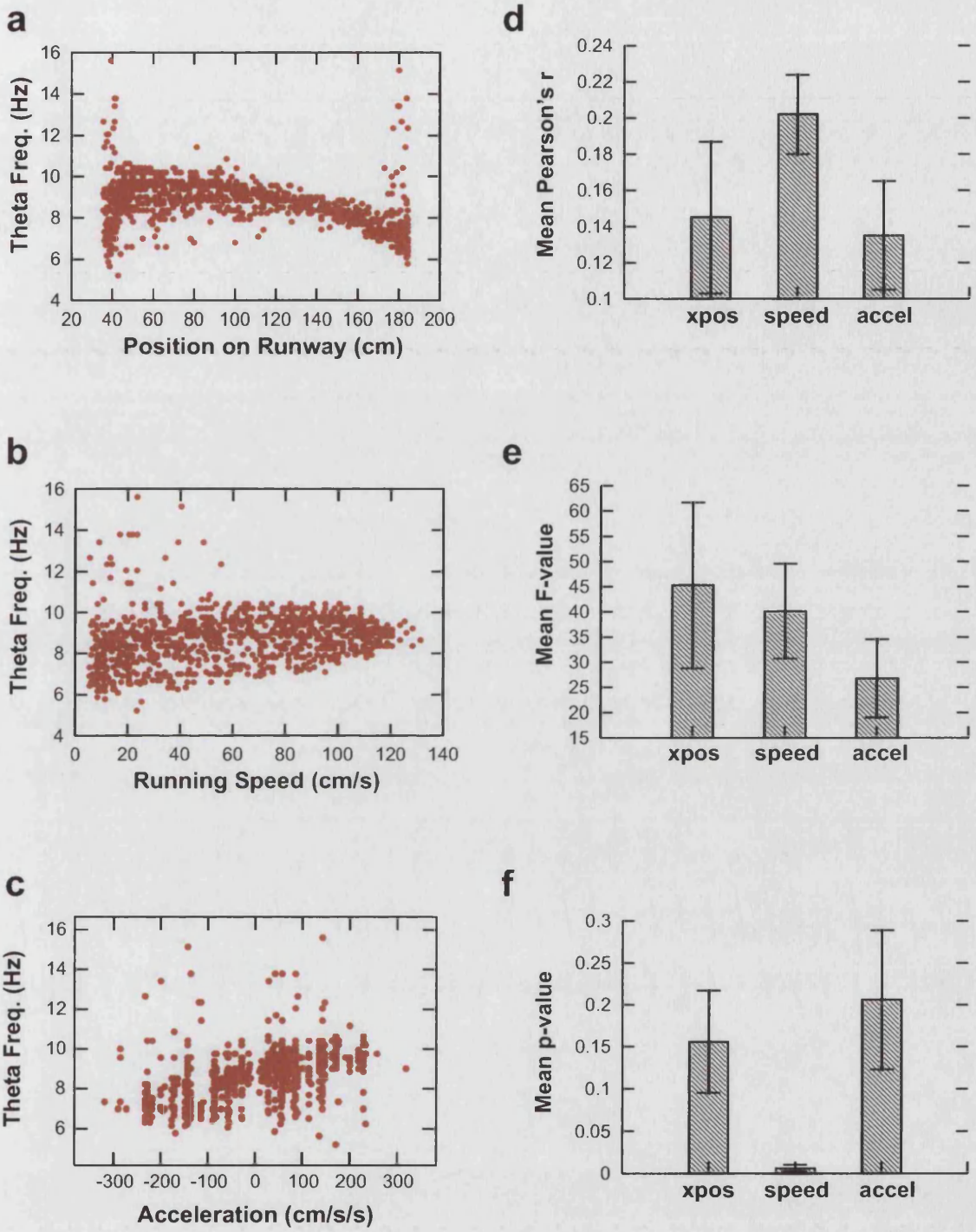

Figure 3.4. Correlations with theta frequency. The left hand column illustrates examples for one rat (1097) during eastbound runs along the entire length of the track. Theta frequency (**a**) drops over the course of the traversal, with a brief period increase at the beginning. Speed (**b**) and acceleration (**c**) are both positively correlated with theta frequency. However, variability between rats was fairly high. The right hand column shows the population mean Pearson's r (**d**), F-values (**e**) and p-values (**f**) for correlations between theta frequency and each of momentary position, speed, and acceleration. Overall, speed appears to be the best predictor of theta frequency, and the only predictor which consistently produced a significant correlation. Error bars are SEM.

Figure 3.3 shows the average relationship between running speed, acceleration, and theta frequency, with data from all nine rats combined. The stereotyped behaviour of all the rats is further emphasized by the speed and acceleration profiles, and theta frequency can be seen to increase in regions of the track where running speed peaks, and declines as running speed drops, with acceleration becoming negative. Dotted lines at P1 and P4 indicate a dip in theta frequency as the rat's head slows during the transition from angular movement (turning out of the end of the runway) to linear movement (running to the opposite end). P2 and P3 indicate the points beyond which the rat begins to run more slowly, and a corresponding reduction in theta frequency is observed.

Correlations between theta frequency and momentary position, speed, and acceleration were conducted for each of the nine rats. The results are summarized in Figure 3.4 . Overall, velocity is the best predictor of theta frequency. For example, while five of the nine rats exhibited a significant ($p < 0.05$) correlation between theta frequency and acceleration, all nine rats exhibited a significant correlation with velocity.

3.5 Basic place field properties

3.5.1 Overview

Basic field statistics are summarised in Figure 3.5. As described previously, only the first 8 minute baseline recording from each field contributed to the data sets on field properties and the relationships between them.

While all fields showed directional bias, there was no apparent overall "preferred direction", with 49 fields firing preferentially when the rat was running east, versus 45 when the rat was running west. Mean field size was 53.79 cm (SD = 19.57). Firing rates ranged from 2.09 Hz to 40.27 Hz (mean = 14.76 Hz), although it should be noted again that some putative fields were excluded because they did not meet the 1 Hz minimum peak firing rate criterion.

Of the 94 place fields analysed, 65 fields were considered suitable for phase shift slope analysis, having been comprised of at least 100 spikes. Linear fits using less than 100 points tended to be unreliable. However, all fields were included in every other analysis, including the comparisons of the mean firing phase of the first and last spike on runs through the field, and the total phase shift.

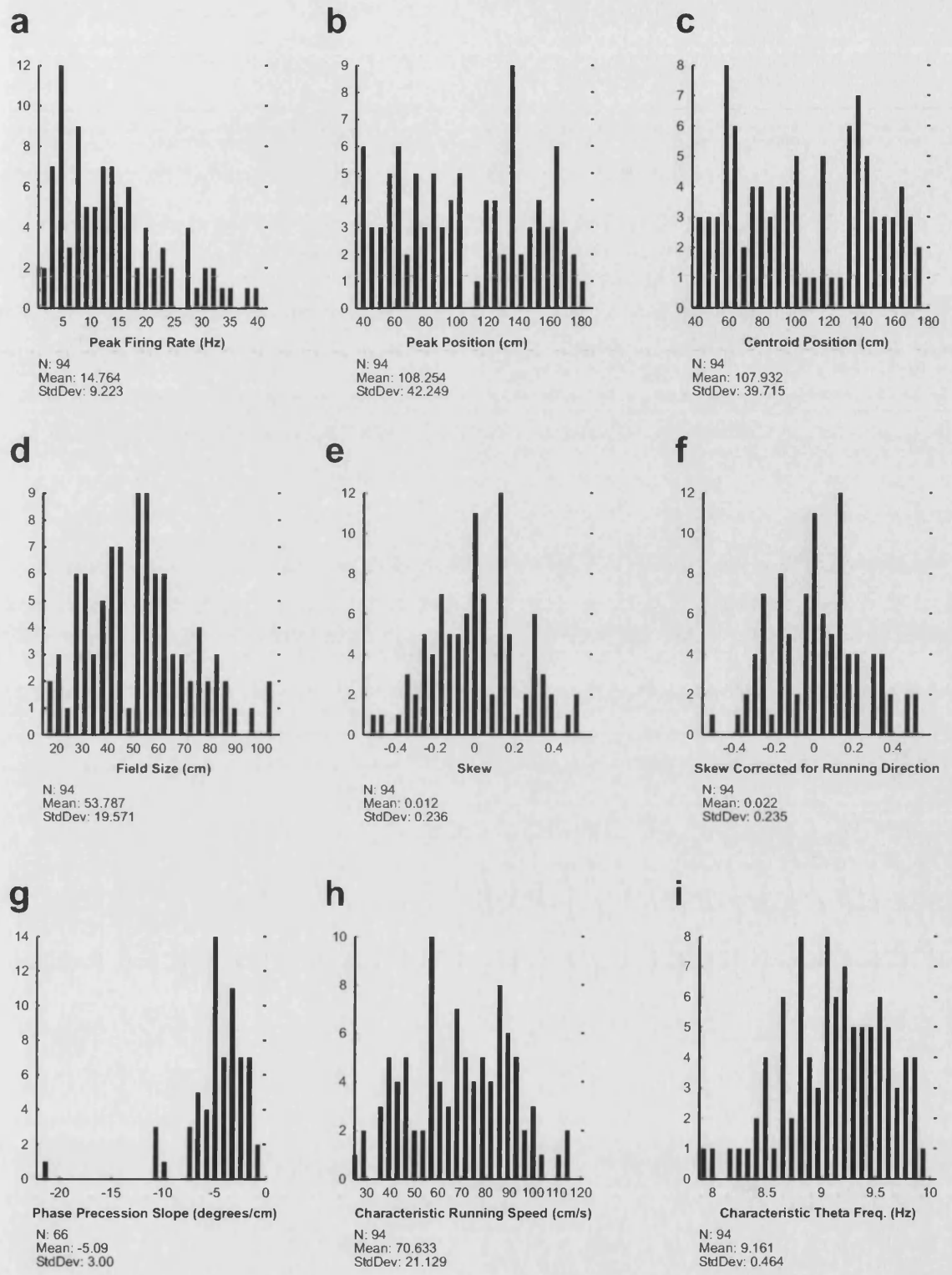

Figure 3.5. Frequency histograms of basic field characteristics from the first recorded baseline trial for all fields. Note that most field characteristics appear to have a gaussian distribution, with the exception of the indices of field position, peak (**b**) and centroid position (**c**). Characteristic running speed (**h**)and theta frequency (**i**) are averaged values from multiple passes through the place fields. Phase precession slope (**g**) only includes data from fields in which a cell fired at least 100 spikes on the first recorded baseline trial. Positive corrected skew values (**f**)should be interpreted as a skewed field with the "tail" pointing in the preferred direction for that field - that is, the direction the rat runs when the cell fires.

For comparison of results from different cell layers, only fields recorded above the theta EEG inversion point (as described in section 2.4) were included in the CA1 set, and only cells from at least 0.5 mm below the inversion point were included in the DG/P data set. This was to avoid any ambiguity about which layer the fields were recorded from. It should be noted, however, that the sample size from dentate/CA3 was relatively small (19 fields), and so the power of the tests comparing the two populations may be somewhat compromised.

3.5.2 Field distribution does not differ from uniformity

As can be seen in Figure 3.5b and c, indices of field position did not appear to exhibit any "clustering", and were certainly not normally distributed like other characteristics. Kolmogorov-Smirnov tests indicate that neither the peak ($Z = 0.693$, $p = 0.723$) nor the centroid ($Z = 0.637$, $p = 0.812$) position distributions differed significantly from uniformity. Unlike peak firing bin position, the calculation of the centroid is not prone to errors resulting from the arbitrary assignment of spikes to position bins. For this reason, centroid measures of field position are the preferred measure for subsequent analyses. Nevertheless, peak bin and centroid were very highly correlated (Pearson's $r = 0.99$, $F_{1,92} = 3523.65$, $p < 0.001$).

3.5.3 Firing phase is a function of position

As rats traversed any given place field, each successive spike of the corresponding place cell was seen to occur at successively earlier phases of the theta cycle. This appeared true of all fields, and the correlation between firing phase and position was significant for 80 fields out of 94. The remaining 14 fields either exhibited no significant relationship between firing phase and position, or consisted of fewer than 100 spikes, making linear fits of the data unreliable. The relationship between firing phase and position on the runway often appeared curvilinear, accelerating as the rat exited the field. However, regression analyses consistently failed to demonstrate that inclusion of the quadratic trend significantly increased the predictive value (r-change) of the linear model. Therefore, phase shift was always analysed as a linear function.

As can be seen in Figure 3.5g, phase precession slope, when significant, was always negative – i.e., cells always fired at progressively earlier phases of the local theta cycle as the rat traversed the place field. Phase shift is accurately described,

therefore, as a "precession". Only considering fields with significant correlations with position which were also based on at least 100 spikes (66 fields), the mean slope was -5.09 degrees/cm (SD = 3.00). There appeared to be a single outlier at slope -21.45, but it is not clear that the result was spurious, so it is included in all subsequent analyses. It should also be noted that these slope values tend to be over-estimates, having been calculated after the linearising procedure described previously.

It should be noted that crossing of the place field occurs simultaneously in both the temporal and spatial domains, and represents an apparently Gaussian distribution of firing rates. Consequently, phase precession could be described as either a spatial, temporal, or rate-related phenomenon. To test this, correlation coefficients were calculated for firing phase versus each of distance-travelled-in-field (position), time-in-field (time), and IFR. The results are summarised in Figure 3.6. While significant negative correlations were observed between firing phase and each of position (distance in field), time, and IFR, the relationship with IFR was clearly the least robust. Phase correlates better with position than IFR in 66/77 fields ($\chi^2 = 39.286$, $p < 0.001$), and better with time than IFR in 63/77 fields ($\chi^2 = 31.182$, $p < 0.001$). In keeping with findings by O'Keefe & Recce (1993), the correlation was more often stronger between phase and position than between phase and time (47/77 cases), but the difference was not significant ($\chi^2 = 3.75$, $p = 0.052$). For this reason, unless otherwise specified, the terms "phase precession" or "phase precession slope" will subsequently refer to firing phase as a function of the distance travelled through the field.

3.5.4 Phase precession was less than 360^0

Although there were exceptions, the range of phases represented typically spanned 360^0 as the rat traversed a place field multiple times. However, the mean extent of the phase precession for all fields was considerably less than 360^0. That is, on any one pass through any given place field, the mean difference between the firing phase of the first and last spike was only -168.11^0 (s.d. = 101.84). Care had been taken not to define fields too restrictively, which would have resulted in omitting large numbers of spikes far from the field centre in the analysis. Therefore, conservative definition of fields cannot be used to explain the surprisingly small degree of phase shift on individual runs through the field.

Figure 3.7 illustrates the mean extent of phase precession during traversal of a representative place field (number 17), and how firing phase is related to position on

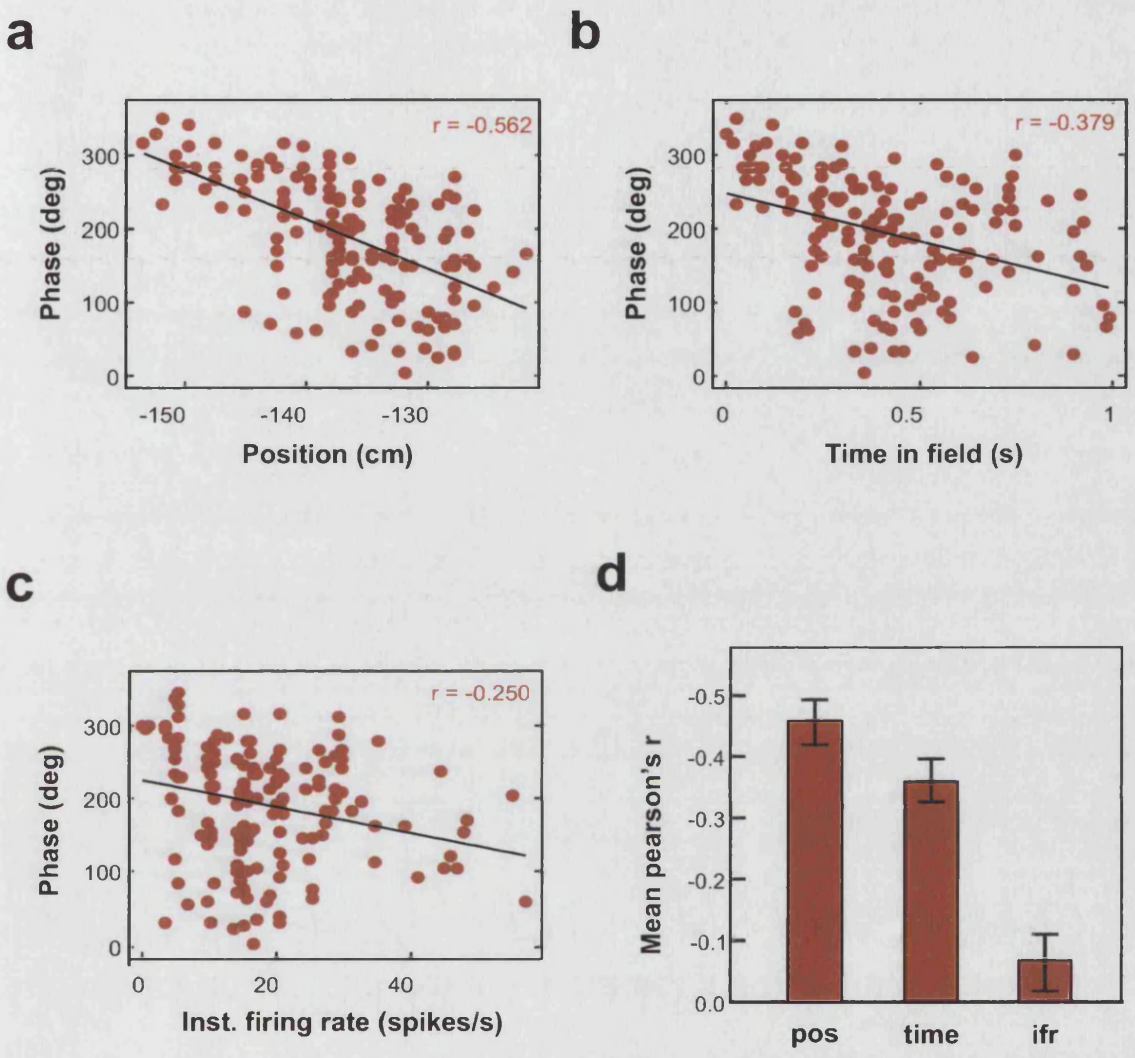

Figure 3.6. Correlates with momentary firing phase . Examples (field 23) of correlations with position in field (**a**), time in field (**b**) and instantaneous firing rate (IFR, **c**). **d**: Mean Pearson's r values for the correlations with firing phase. Data is taken from initial baseline trials for 77 fields comprised of at least 100 spikes. Note that correlations are stronger between phase and position than between phase and time, and that the mean correlation with IFR is particularly weak. Position values in **a** are reversed to reflect the fact that this is a field which fires when the rat runs from east to west.

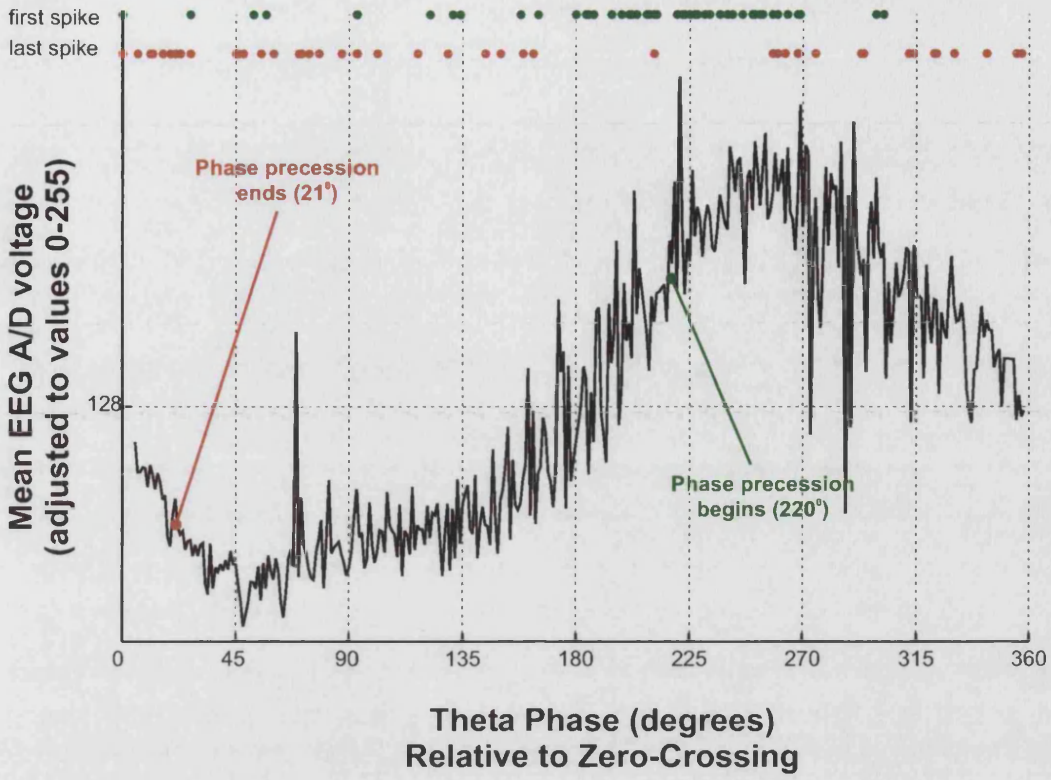

Figure 3.7. Firing onset and offset relative to the locally recorded theta EEG oscillation (field 17). The line graph illustrates the relationship between portions of the theta wave represented as voltage values, and the mean corresponding phase values derived from the theta fitting algorithm over the course of a singel eight-minute trial. Note that the negative-going crossing at EEG value 128 (mid-range) corresponds with phase zero. Green and red dots represent the firing phase of the first and last spikes fired, respectively, on each traversal of the place field. Note the spread of spike firing over the full 360^0 range, while the mean onset and offset of firing define only approximately 200^0 of the theta cycle.

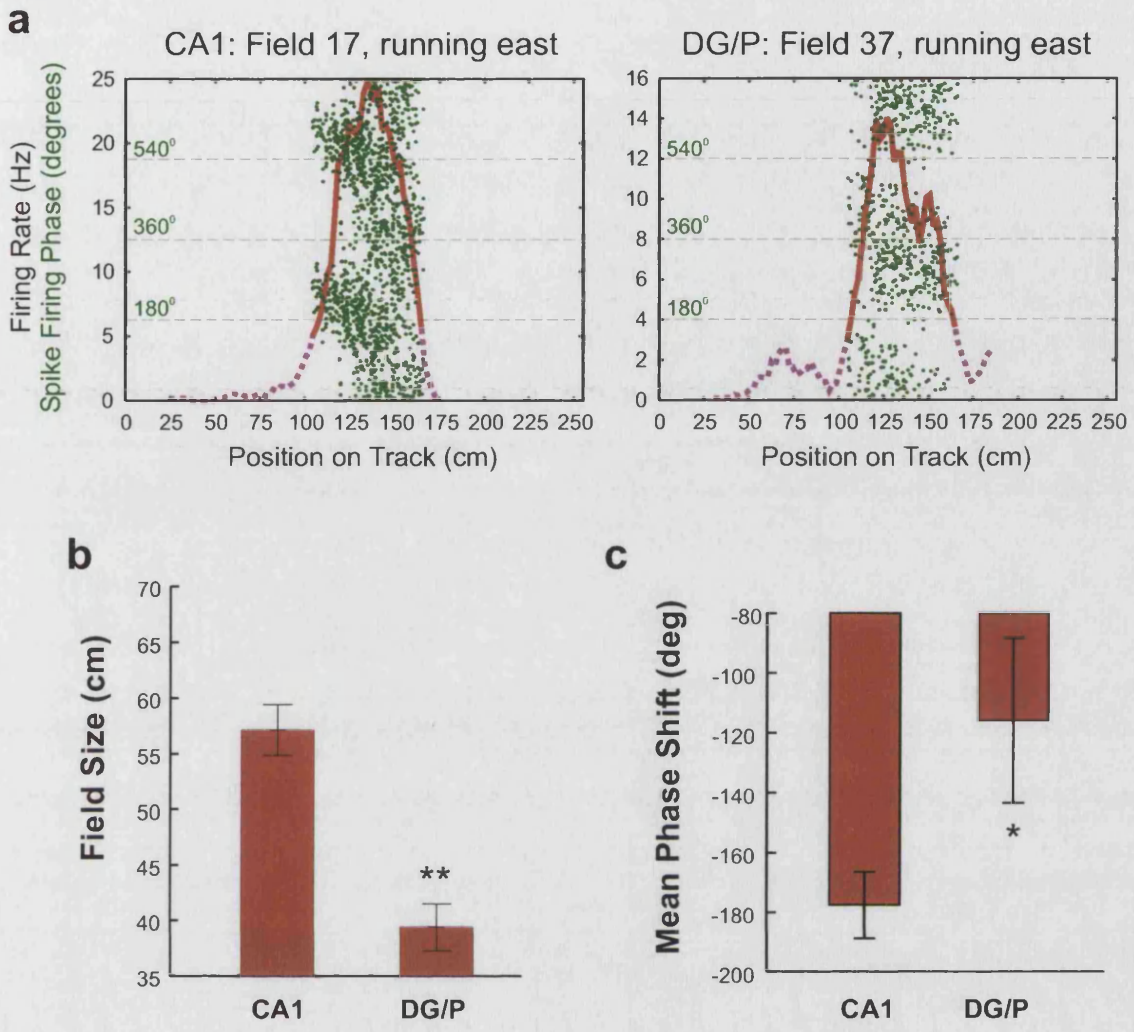

Figure 3.8. A comparison of place fields recorded from CA1 and dentate gyrus/polymorph layer (DG/P). **a:** Sample fields from each region. Fields of roughly the same size were selected for comparison purposes. Firing rate and firing phase of individual spikes is plotted as a function of position on the runway. Firing rate within the place field is represented as a solid red line. In order to better illustrate the phase precession in a circular data set which wraps around a $0^0/360^0$ origin, each firing phase point is replotted after adding 360^0. Note that upon entry into the place field, spikes fire earlier in the theta cycle but with higher variability in the DG/P field. **b:** Fields from DG/P tend to be smaller than CA1 fields. ** $p < 0.001$. **c:** Population mean phase shift in CA1 vs. DG/P fields. Individual shift values are were calculated on a per-field basis - for each field, shift was taken as the difference between the mean firing phase of the first and last spikes fired on multiple passes through the field. CA1 fields undergo significantly more phase precession. *$p < 0.05$.

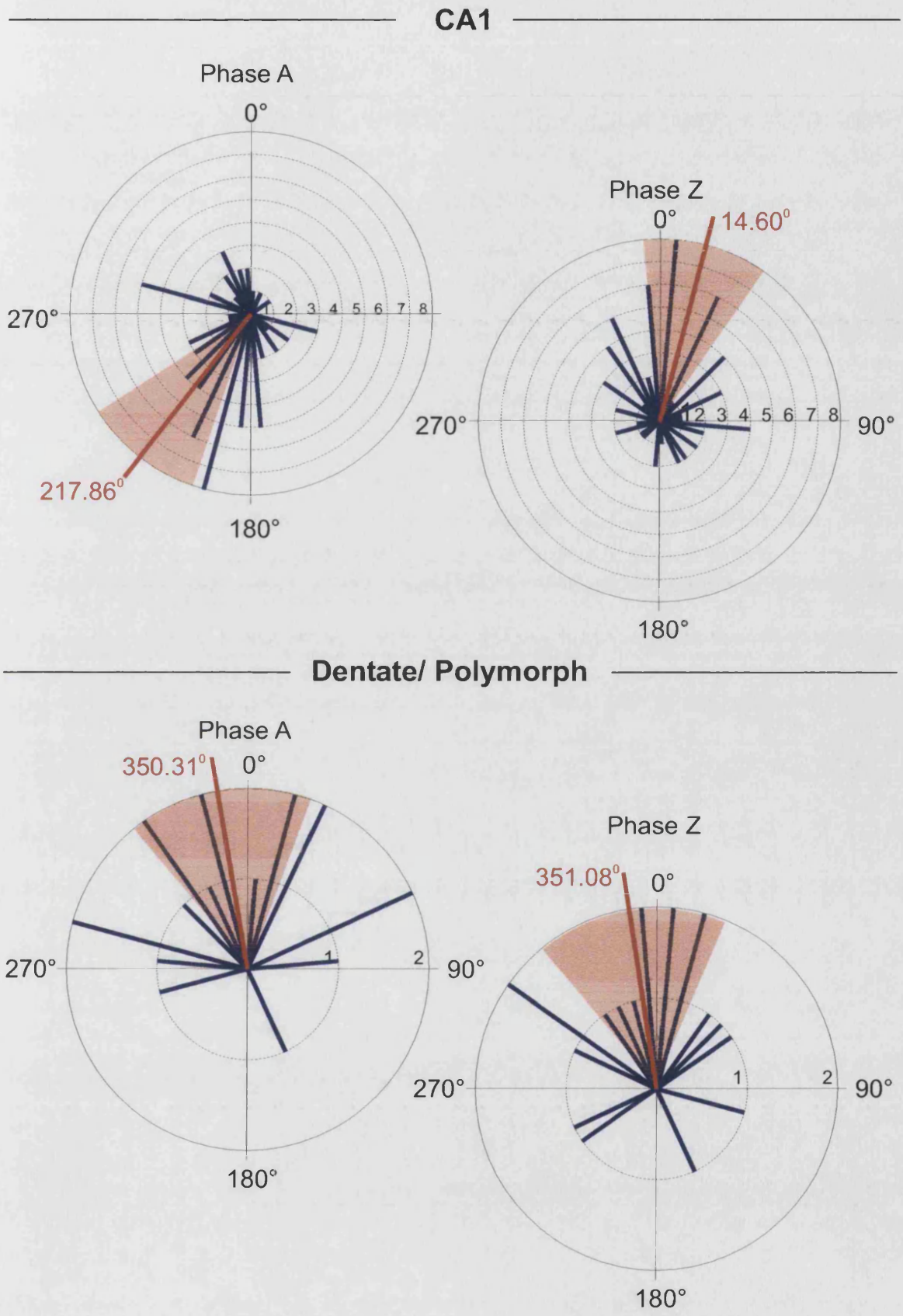

Figure 3.9. Mean firing phase histograms for the first (Phase A) and last (Phase Z) spikes on runs through each place field. Results from CA1and DG/Polymorph place fields are presented separately. Population means are given in red, with shaded areas representing 95% confidence intervals. There is a clear difference between Phase A and Phase Z in CA1. Results from DG/Polymorph are more variable, but suggest reduced precession.

the local theta wave. The assignment of phase values is clearly representative of position on the sinusoidal theta oscillation. Phase zero, as described in the General Methods, corresponds with the negative-going crossing at the middle of the EEG value range (value 128 in the range of 0-255). This place cell, fairly typical of the CA1 sample (see below) begins firing at phase 220^0, just before the positive peak in the local EEG. Firing occurs at successively earlier phases of the theta cycle until the rat exits the field, at which point mean firing phase is 21^0, or just prior to the trough in the local EEG.

3.5.5 Differences between CA1 and DG/P fields

There was no apparent difference in the proportion of cells from CA1 or DG/P which exhibited theta phase precession. Precession was observed in 56/70 (80.0%) of CA1 place fields, and 14/19 (73.7%) of DG/P place fields. Figure 3.8a shows two typical fields, one from each of CA1 and DG/P. A multivariate analysis of variance (MANOVA) was used to investigate whether fields recorded from CA1 versus dentate/CA3 differed in terms of peak firing rate, field size, phase precession slope, direction-corrected field skew, and total phase shift. Significant differences were only observed in field size and total phase shift. As illustrated in Figure 3.8b, CA1 place fields (mean = 57.11 cm) tend to be larger than DG/P place fields (mean = 39.37 cm, $F_{(1,61)} = 7.35$, $p < .01$). CA1 fields exhibited a mean total phase precession of -177.60^0, while DG/P fields only precessed on average by -115.90^0. The difference is significant ($F_{1,87} = 5.79$, $p = 0.018$), as illustrated in Figure 3.8c.

Circular statistics were used to further investigate differences in phase shift between CA1 and DG/P. Figure 3.9 compares the mean firing phase of the first and last spikes on runs through each of the fields recorded from CA1 and DG/P. Fields recorded from CA1 place fields begin phase precession at 217.86^0 and end at 14.60^0. The difference between the mean firing phase of the first and last spikes is significant ($F_{1,138} = 89.050$, $p < 0.001$). In contrast, DG/P fields began precession at 350.31^0 and ended at 351.08^0, and the difference was not significant ($F_{1,36} = 0.001$, $p = 0.972$). DG/P place cells appear to begin phase precession significantly later in the theta cycle than their CA1 counterparts ($F_{(1,87)} = 40.580$, $p < 0.01$), while there was no difference in the firing phase of the last spikes on passes through a place field ($F_{(1,87)} = 1.538$, $p = 0.218$). Of course, the means are so close to the zero/360^0 origin, the judgement of "earlier" or "later" seems somewhat arbitrary. In truth, the validity of the mean phase values for the first and last spikes from the DG/P data set are questionable because

the distribution of the values tends towards uniformity. If anything can be said about these cells, it is that their phase precession begins and ends at widely differing theta phases for different cells, with no apparent clustering of the values. The circular analysis does not correct for this inter-rat variability, so I am inclined to put more faith in the phase shift results presented in Figure 3.8c, which demonstrate a more believable value than the approximately 1^0 of precession suggested by the circular analysis.

3.6 Relationships between field characteristics

The characteristics of individual fields were compared to determine whether certain characteristics were associated with each other. As illustrated in Figure 3.10a, a preliminary test confirmed that field peak and centroid position were highly correlated ($F_{1,92} = 3523.65$, $p < 0.001$). Therefore, centroid was chosen as the indicator of field position for subsequent analyses. Figure 3.10b-d illustrates that the stereotyped behaviour of rats performing the shuttling task conferred on each field a position-dependent characteristic running speed, acceleration, and theta-frequency. The relationship between field position and characteristic acceleration or theta frequency depends on the direction the rat is running – therefore, the relationship is actually best described as a function of the rat's position within a run in a given direction, rather than position on the track per se. Inclusion of characteristic running speed, acceleration, and theta frequency in the analyses permits a simple assessment of the effect of these variables on "true" properties of the place fields, like size and skew.

Characteristics of all 94 fields were first plotted against one another in order to determine whether any potential linear or curvilinear relationships existed. Only promising linear or curvilinear relationships, were investigated statistically, using regression analysis. A set of 24 candidate analyses were identified, including comparisons between combinations of field size, centroid position, skew, skew corrected for running direction, phase precession slope, total phase shift, firing phase of the first spike, and characteristic in-field running speed, acceleration, and theta frequency. A Bonferroni correction was applied, adjusting the critical p-value to 0.05 / 24 = 0.00208. Significant relationships are presented in Figure 3.10e-l. Several patterns quickly emerged – the most notable was the complete interrelatedness of four variables – field position (centroid), characteristic running speed, field size, and the slope of the phase precession, as described below.

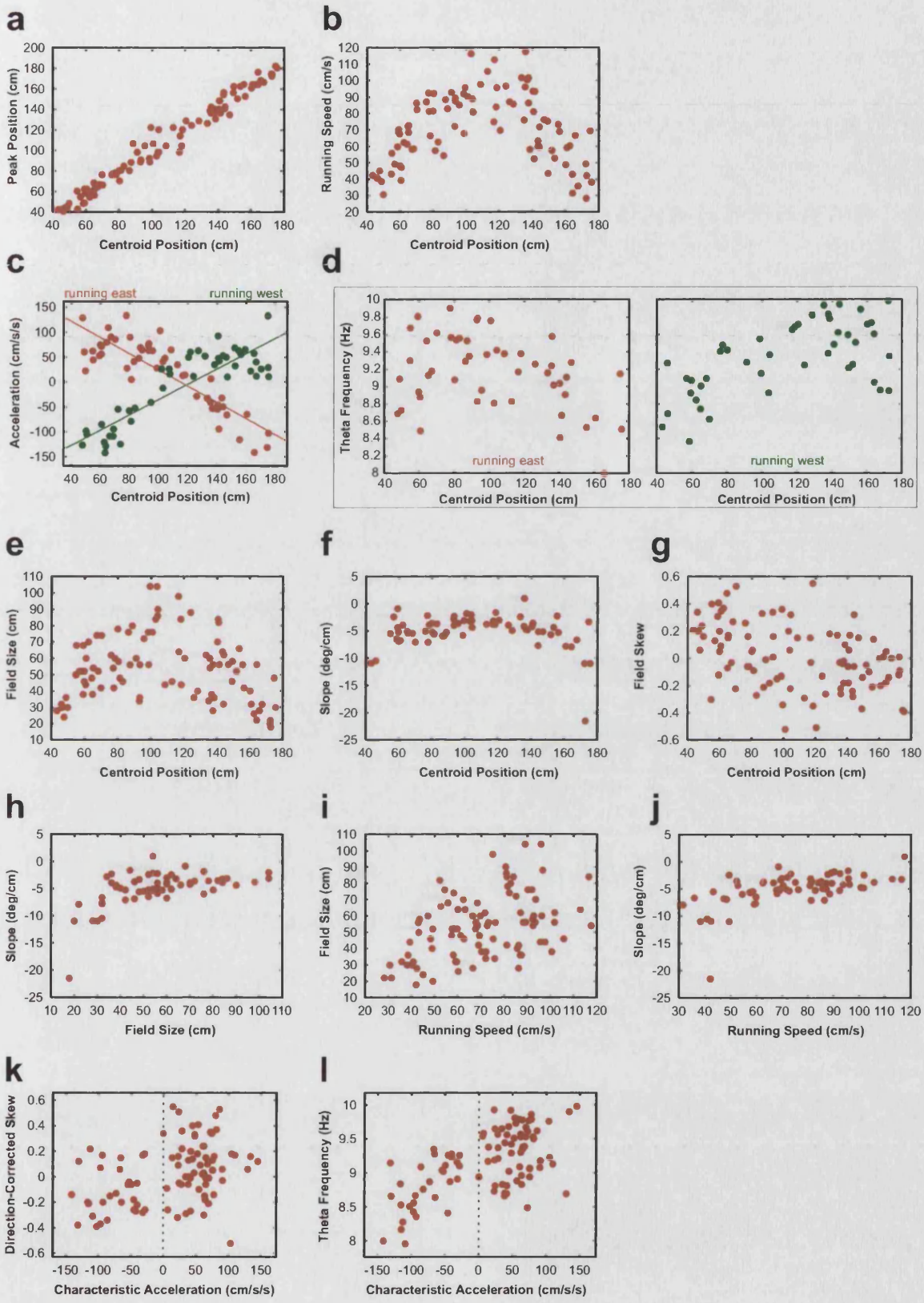

Figure 3.10. Significant correlations between field characteristics, from first baseline trials for each field. **a:** The high correlation between two measures of field position (centroid and peak). **b-d:** Field position (centroid) indirectly confers a characteristic running speed, acceleration, and theta frequency. Field position is related to field size (**e**), precession slope (**f**) and skew (**g**). **h-j:** field size and precession slope are correlated, and both are correlated with running speed. **k,l:** direction corrected field skew and theta frequency are correlated with characteristic acceleration. See text for detailed discussion.

3.6.1 Larger mid-runway fields have shallow phase precession slopes

There was a significant quadratic relationship between field centroid position and the size of the place field (Figure 3.10e, $R^2 = 0.366$, $F_{2,91} = 26.26$, $p < 0.001$), with some mid-runway fields being as much as three times larger than fields at either end. A similar relationship holds for phase precession slope (Figure 3.10f, $R^2 = 0.394$, $F_{2,63} = 20.45$, $p < 0.001$), with mid-runway fields exhibiting much more gradual phase precession. Consequently, it is of little surprise that field size and phase precession slope are themselves highly correlated (Figure 3.10h, $R^2 = 0.478$, $F_{2,63} = 28.81$, $p < 0.001$), with larger fields exhibiting more shallow phase precession slopes. Interestingly, this is best described as a curvilinear relationship, suggesting that for larger field sizes, the relationship between size and precession slope is weaker. A stepwise linear regression revealed that addition of the quadratic coefficient significantly increased the predictive power of the model (F-change $_{1,63} = 20.21$, $p < 0.001$), and this held true even when the apparent steep-slope outlier was omitted.

There is a strong quadratic correlation between field position and characteristic running speed (Figure 3.10b, $R^2 = 0.606$, $F_{2,91} = 69.93$ $p < 0.001$). That is, as anticipated, fields in the middle of the runway have a higher characteristic running speed than those in the periphery. Consequently, the characteristic speed of each field was also linearly correlated with field size (Figure 3.10i, $R^2 = 0.200$, $F_{1,92} = 22.98$ $p < 0.001$) and phase precession slope (Figure 3.10j, $R^2 = 0.304$, $F_{1,64} = 27.90$, $p < .001$), Fields in regions of the track where the rat ran quickly tended to be larger and exhibit more gradual phase precession slopes.

As Figure 3.10c illustrates, there is also a strong relationship between centroid position and characteristic acceleration, whether the rat is running east ($R^2 = 0.769$, $F_{1,47}) = 137.310$, $p < 0.001$) or west ($R^2 = 0.769$, $F_{1,43}) = 143.310$, $p < 0.001$).

3.6.2 Fields are skewed towards the middle of the runway

There was a strong linear relationship between centroid position and field skew (Figure 3.10g, $R^2 = 0.181$, $F_{1,92} = 20.30$, $p < .001$), such that west-most fields were skewed west (negative), east-most fields were skewed east (positive), and mid-runway fields tended not to be skewed at all. In other words, fields at the ends of the runway exhibited skewed firing rate distributions with tails pointing towards the middle of the runway.

Characteristic in-field acceleration also proved to be linearly correlated with direction-corrected field skew (Figure 3.10k, $R^2 = 0.182$, $F_{1,92} = 20.52$, $p < 0.001$). This means that regardless of which direction the rat was running, fields in regions where the rat was accelerating exhibited skewed fields with tails extending in from of the direction of motion, while deceleration produced skewed fields with tails pointing opposite the direction of movement. It should be noted, however, that this follows logically from the correlations between centroid position and both field skew and acceleration, as described above.

3.6.3 Characteristic running speed does not predict peak firing rate

The speed at which rats typically crossed place fields did not have any bearing on the peak firing rate in that field ($R^2_{1,91} = 0.036$, $p = 0.184$). That is, higher firing rate fields were not any more or less likely to be found in regions of the track where the rat ran quickly. Relationships with skew ($R^2_{1,91} = 0.037$, $p = 0.176$), corrected skew ($R^2_{1,91} = 0.012$, $p = 0.578$) and mean phase shift ($R^2_{1,91} = 0.015$, $p = 0.506$) also proved to be non-significant.

3.6.4 Firing rate is unrelated to other field characteristics

The peak firing rate of a cell during traversal of its place field(s) may be taken as a measure of the cell's net excitatory input, if we assume the basic membrane properties of all hippocampal place fields to be roughly the same. To this end, the relationships between peak firing rate and a variety of field characteristics were analysed, as summarised in Figure 3.11. No significant relationship emerged. Of particular interest were the absence of any relationship between the firing rate of a cell and the typical speed with which the rat ran through its place field ($R^2 = 0.005$, $F_{1,92} = 0.425$, $p = 0.516$), the total phase shift ($R^2 = 0.010$, $F_{1,92} = 0.919$, $p = 0.340$), or the phase precession slope ($R^2 < 0.0001$, $F_{1,64} = 0.0002$, $p = 0.989$).

3.6.5 Phase precession slope is unrelated to direction-corrected field skew

Corrected field skew took into account the direction the rat ran when a given field was active. A positive corrected skew indicates a firing rate distribution with the "tail" pointing in the direction of motion (rapid firing onset, gradual offset), while a field with a negative corrected skew would a relatively gradual onset of firing and a rapid

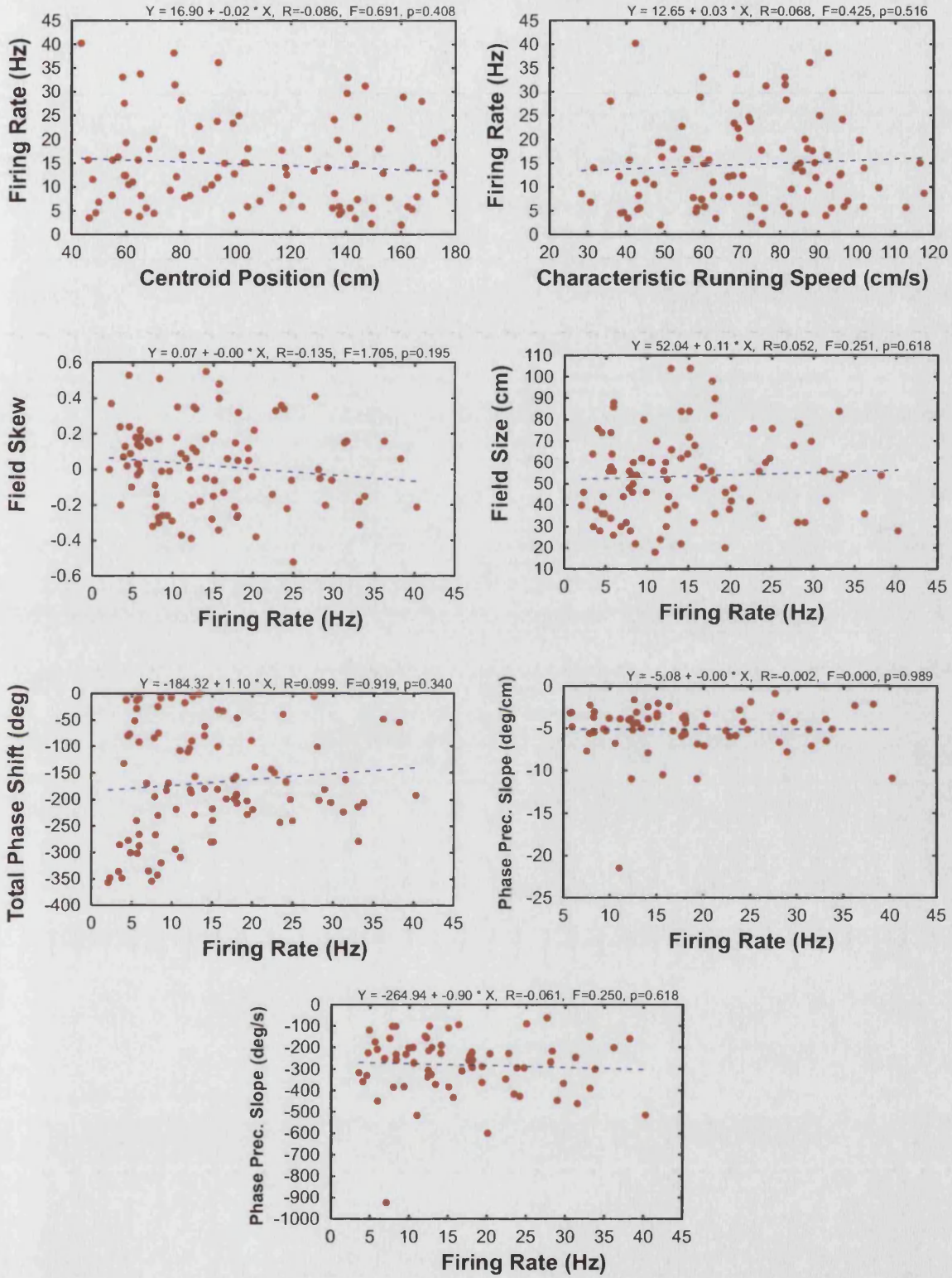

Figure 3.11. Correlations with firing rate. Neither field position nor the typical running speed through a given field were predictive of firing rate. Firing rate itself was not correlated with and other characteristics of the place field, including phase precession slope measured as a function of either position or time. Plots include a best fit line, with the regression equation of the linear fit and corresponding Pearson's-r, F, and p values displayed in the topright hand corner.

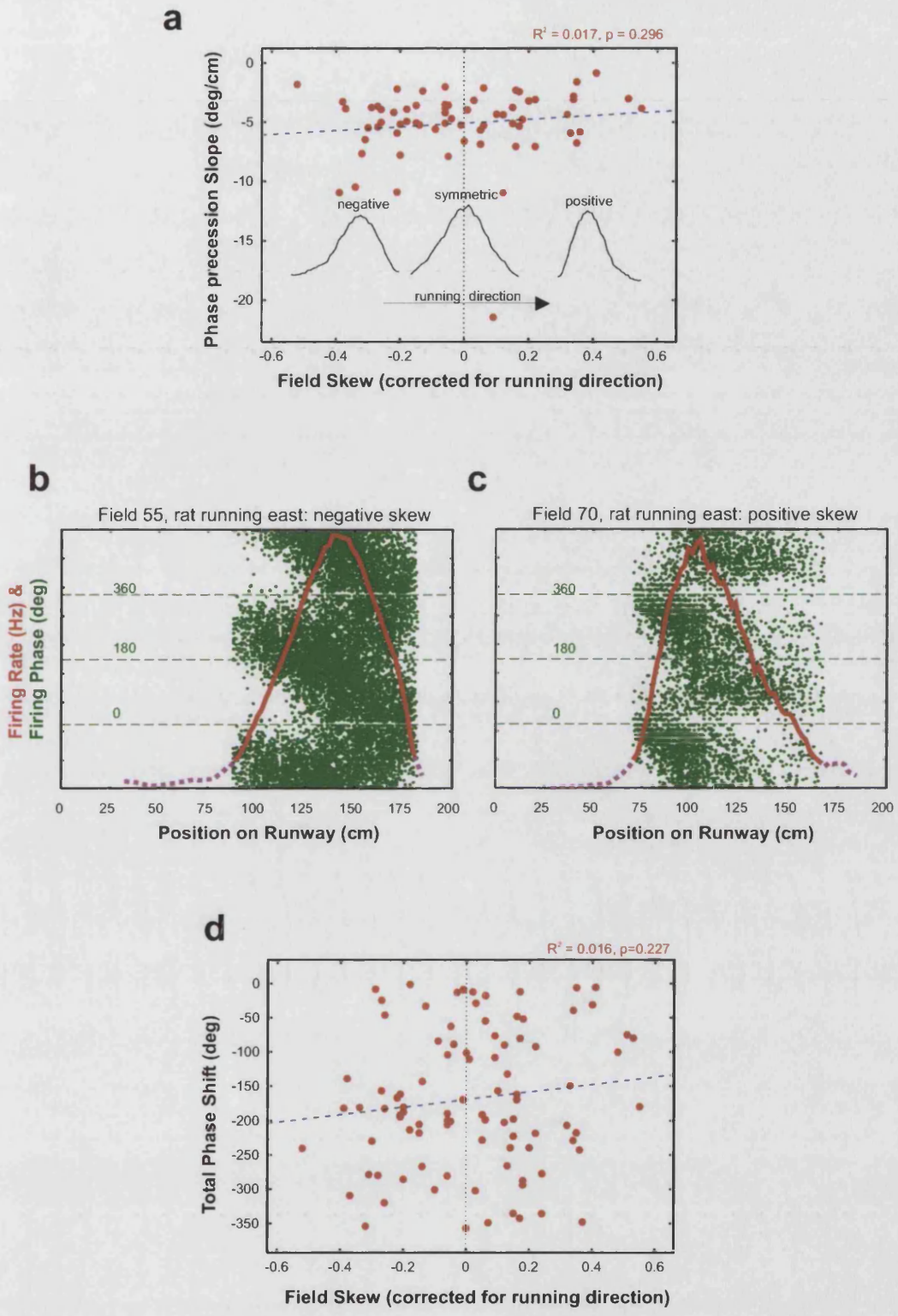

Figure 3.12. Phase precession slope and the total extent of phase precession are not related to the skew of the place field firing rate distribution. **a:** Phase precession slope as a function of field skew, corrected for running direction. A schematic representation of a field with negative and positive skew (assuming eastbound trajectory) are also presented. **b,c:** Positive and negatively skewed place fields exhibiting robust phase precession. Data for each field was taken from 290 runs through the field across multiple trials on which the place fields were highly correlated (Pearson's r >= 0.9). **d:** Total phase precession as a function of field skew, corrected for running direction.

offset. There was no evidence that the magnitude or direction of field skew (corrected for running direction) bore any relationship with either the slope of the phase precession ($R^2 = 0.017$, $F_{1,64} = 1.113$, $p = 0.296$), or the total magnitude of the phase precession ($R^2 = 0.016$, $F_{1,92} = 1.482$, $p = 0.227$). In other words, phase precession was unrelated to field asymmetry as indicated by the firing rate envelope. Figure 3.12 illustrates these findings.

3.6.6 Characteristic theta frequency is related to changes in running speed

The characteristic frequency of hippocampal theta during traversal of any given place field was unrelated to the characteristic speed at which the rat crossed the field ($R^2 = 0.040$, $F_{1,92} = 3.868$, $p = 0.052$). However, characteristic theta frequency was positively correlated with characteristic in-field acceleration (Figure 3.10l, $R^2 = 0.382$, $F_{1,92} = 53.8295$, $p < 0.001$). This robust correlation can be seen in Figure 3.10l. Upon inspection, however, it seemed as though there might be a qualitative difference in the relationship depending on whether the rat was typically speeding up (acceleration > 1) or slowing down (acceleration < 1) during traversal of a given field. Indeed, when the data was divided on this basis, it became clear that the relationship between characteristic acceleration and characteristic theta frequency was robust for fields in regions of the track where the rat was slowing down (left side of Figure 3.10l, $R^2 = 0.392$, $F_{1,30} = 19.302$, $p < 0.001$), but non existent for fields where the rat was gaining speed (right side of Figure 3.10l, $R^2 = 0.017$, $F_{1,60} = 1.008$, $p = 0.320$).

3.7 Discussion

3.7.1 Stereotyped behaviour

The relationship between stereotyped behaviour and position on the runway in a shuttling task like this one obviously has important consequences for the interpretation of results. The most serious is that cell firing may be correlated not with position, but with behaviours associated with position. However, omitting data from periods during which the rat ran at less than 10 cm/s effectively eliminates epochs during which the rat was doing anything but running along the track.

The most notable behavioural correlate with position, and one which is impossible to eliminate, is running speed. Therefore, any relationship between place field position and other parameters like size, phase precession slope, or skew is hopelessly confounded by running speed. Despite the strong stereotypy of behaviour, on any given run along the runway, a rat's running speed could be quite variable. This natural run-to-run variability in running speed provided an opportunity to investigate exactly how running speed influences factors like field size, shape, and phase precession. These tests are treated in detail later, in Chapter 5.

3.7.2 Theta frequency, running speed, and acceleration

The relationship between theta frequency and behaviour was highlighted by observations of both momentary theta frequency and the characteristic theta frequency during traversal of place fields. As rats ran the full length of the runway, momentary theta frequency was correlated with running speed (Figures 3.2, 3.3, and 3.4). This is consistent with previous studies which found a relationship between theta frequency and the velocity of movement (Bland & Vanderwolf, 1972; McFarland et al., 1975; Oddie & Bland, 1998; Rivas et al., 1996; Shin & Talnov, 2001; Slawinska & Kasicki, 1998). The relationship with acceleration was significant for some rats, but not others. In fact, in some instances, there was a significant correlation when the rat ran in one direction, but not the other. From these results, it appears that momentary running speed is the most robust predictor of theta frequency during behaviours distributed across the entire runway.

There was a tendency for fields through which rats ran quickly to exhibit higher characteristic theta frequencies, but it was not a significant effect. In contrast, the relationship between characteristic theta frequency and characteristic acceleration was strong, as illustrated in Figure 3.10l. This relationship only really holds for fields in portions of runway in which the rat tends to be decelerating, although "accelerating" fields clearly have a higher characteristic theta frequency than "decelerating" ones. This follows logically from the relationship between centroid position and both acceleration and theta frequency, as can be seen in Figure 3.10c,d. The relationship between theta frequency and acceleration is not entirely unexpected, given that acceleration is proportional to force, and is therefore indicative of the animal's exertion. Shin & Talnov, (2001) hypothesised that deceleration in the running wheel produced an increase in theta because the rats have to exert effort to maintain equilibrium in the

wheel as it comes to a stop. Whishaw & Vanderwolf (1973) observed that the frequency and amplitude of theta just prior to jumping was proportional to the size of the jump. The latter experiment observed this relationship during observations of atropine sensitive theta, although it is possible that atropine-sensitive and atropine-insensitive theta both contribute to theta frequency in the awake, behaving rat.

It should be noted, however, that the results of the in-field analysis may differ from the whole-runway analysis because of the way the data was assigned to place fields. Comparing characteristic theta frequency and other characteristics of place fields essentially takes the continuous data and groups it into place-field-sized chunks for comparison. While the characteristics of place cell firing (rate, skew, firing phase, etc.) are only meaningful within the place field, grouping the running speed, acceleration, and theta frequency data in this way is arbitrary. As a result, the relationship between running speed and theta frequency may be obscured when these variables are treated as field characteristics.

It is also worth noting that the composite theta-frequency vs. position plot in Figure 3.3c doesn't exactly resemble the dramatically curvilinear speed vs. position plot in Figure 3.3a. It may be that theta frequency is determined by a combination of both running speed and acceleration. This is in keeping with the observation that theta frequency tends to decline in a position-dependent manner as the rat completes a run, when both running speed and acceleration may be acting synergistically (both are declining). Theta frequency may be high at the beginning of a run, despite slow running speed, because the rat is quickly accelerating. This would be consistent with previous experiments demonstrating an increase in theta frequency at the onset of movement (Vanderwolf 1969; Bland & Vanderwolf 1972; Whishaw & Vanderwolf 1973).

Despite the mathematical relationship between running speed and acceleration, the two factors may provided independent types of input which influence theta frequency. Acceleration on the runway is a result of physical exertion. In contrast, steady-state running requires very little exertion, but results in the generation of speed-dependent motion cues. Such cues include optic flow, air flow, the change in visual angles, and motor efference copy, and there is evidence to suggest they contribute to theta frequency. Czurkó et al. (1999) failed to find any relationship between running speed and theta frequency in the running wheel. However, the rat does not translate through space in the running wheel, and it may be this absence of sensory motion cues which resulted in the lower mean theta frequencies Czurkó et al. observed (7.7 Hz,

versus 9.0 Hz in the current study). This is despite the fact that rats in their experiment achieved speeds in the running wheel comparable to those observed in the current experiment on the runway. It may be that these motion cues contribute critically to theta frequency, increasing it in a speed-dependent manner when the rat is running through space. While the documented relationship between core temperature and theta frequency (Whishaw & Vanderwolf, 1973) may also explain the discrepancy in mean theta frequencies between the two experiments, it cannot account for the observation of speed-modulation in one, but not the other.

3.7.3 Do all place cells exhibit phase precession?

Theta phase precession was observed in most place fields, and approximately equally amongst CA1 and DG/P populations. The fact that some place fields failed to exhibit phase precession requires some explanation, given that O'Keefe & Recce (1993) observed that all 15 of the putative pyramidal cells they recorded exhibited phase precession. Similarly, Skaggs et al. (1996, p. 155) report that the phase precession effect was "invariably present".

There are two likely reasons why phase precession was not observed in some fields in the current study on the initial baseline trial – that is to say, two reasons why the linear regression of firing phase versus position was not significant. First, low firing rates and inter-trial variability may result in spurious cases of fields failing to exhibit phase precession robust enough to produce a significant firing phase vs. position correlation. In some cases, the baseline trial used in initial assessment of the fields was anomalous, and subsequent trials produced better results. Fields 33, 38, 60 and 69 are good examples. In other cases, fields had a consistently low firing rate across multiple trials. While phase precession may have been present, the trial length was too short for sufficient spikes to be recorded on which to perform a reliable correlation analysis. An example is presented in Figure 3.13b, in which superimposing data from four trials makes the precession apparent.

The second possibility is that some of the cells actually have multiple overlapping sub fields. Several examples are presented in Figure 3.13c-e. Field no. 14 was the product of what appeared to be a well-isolated cell with a pronounced 2 ms refractory period. Nevertheless, the place field clearly had a bimodal firing rate distribution, and what appeared to be not one but **two** overlapping phase precessions, which precluded any success in putting a linear fit to it. It is possible that some fields

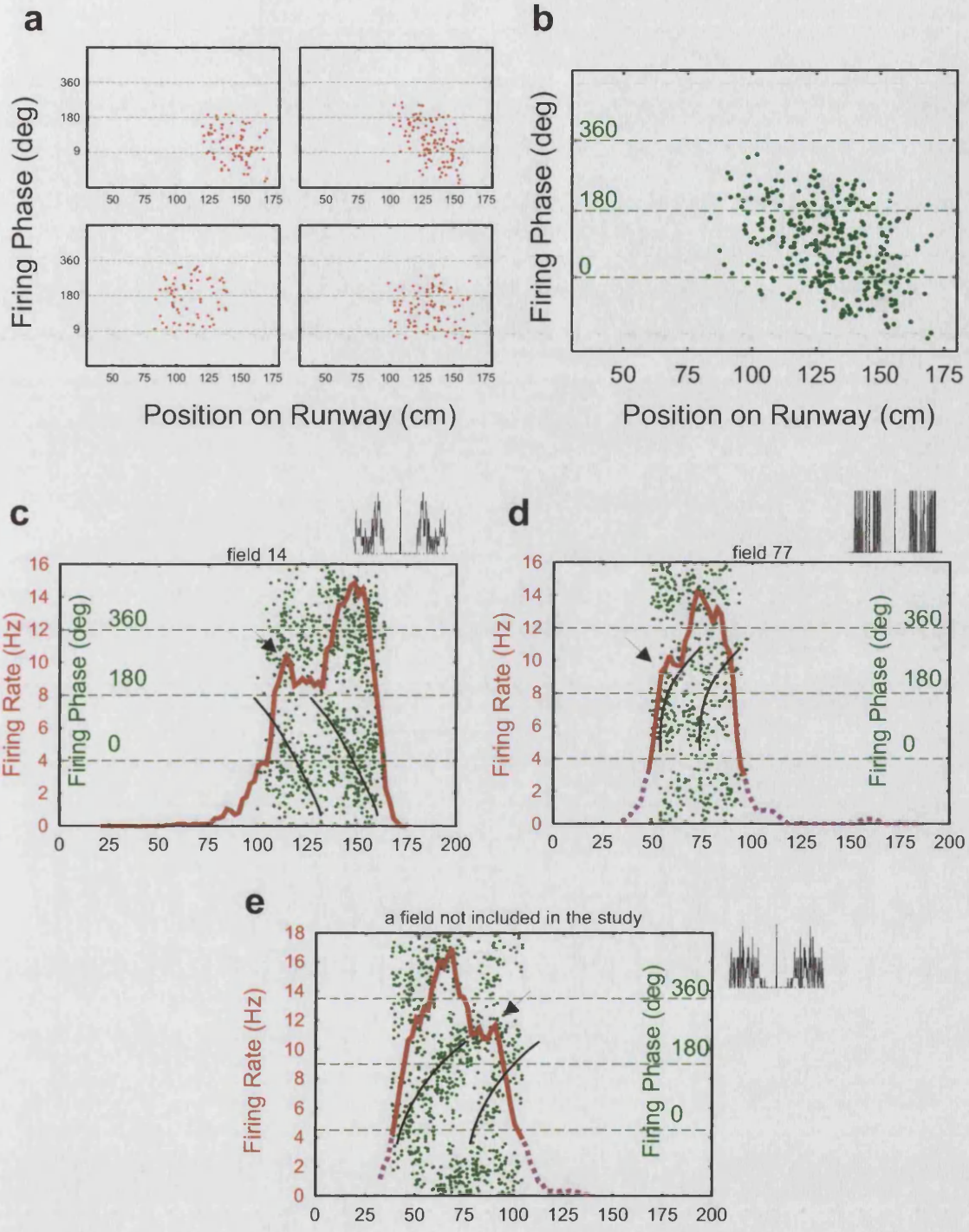

Figure 3.13. Some fields fail to exhibit phase precession. **a,b:** Failure to exhibit phase precession is relsometimes related to low firing rates and inter-trial variability. **a:** firing phase as a function of position on the runway on four consecutive trials for field 90. On only one of the trials is the spike density deep enough for phase precession to be apparent. **b:** But when the four trials are superimposed, the phase precession is evident. **c-e:** Poor phase precession fit due to dual phase precession in a single place field. This suggests that the place fields were comprised of two overlapping sub-fields. Firing rate is indicated in red, firing phase in green, both as a function of position on the runway. Arrows indicate the apparent peaks of the subfields, while curves are a subjective estimate of the independent phase precessions. Temporal autocorrelations adjacent to each diagram (+/-10 ms window) illustrate the clear 2 ms refractory period for each cell.

had such a high degree of overlap that the firing rate distribution itself looked perfectly normal, and the only indication that it was a double field might have been the absence of an identifiable phase precession effect. It should be noted that "double precession" was only rarely observed, and sometimes only on a given trial for a particular place cell. Double precession may also arise from the existence of a "bump" in the theta oscillation, resulting in regular or occasional misidentification of the beginning of the theta cycle, and a consequential shift in the apparent firing phase for all spikes in those cycles. However, no such anomaly was noted in the EEG on trials where double precession was observed.

In any case, it seems likely that all place fields do exhibit phase precession, provided enough spikes are collected to perform an accurate regression fit, and provided any sub-fields can be isolated so their respective precessions can be fit accordingly. The possibility of dual simultaneous phase precession in a single pyramidal raises some interesting possibilities regarding the generation of phase precession, which will be discussed in more detail in the general discussion.

3.7.4 Phase precession is best described as a spatial phenomenon

The fact that the best correlate with firing phase is position, not time, is in keeping with previous observations by O'Keefe and Recce (1993). This strongly suggests that the phase shift phenomenon is fundamentally spatial, not temporal, in nature. That is to say, it appears as though the momentary firing phase of a given cell is determined by spatial information the rat receives, and not the amount of elapsed time since some event which triggers it. One possibility, as proposed by Booth, Bose & Recce (2000) is that the phase precession is a temporal phenomenon which is precisely modulated by running speed. Of course, such precise modulation would be indistinguishable from a complete transformation. But it is possible to dissociate running speed and spatial translation, and this was one objective of the moving treadmill experiment, as described in Chapter 9. It is also important to note that the correlation between phase and IFR is much weaker on average than the correlation between phase and position. This suggests that the former may in fact be derived from the latter. This possibility discussed in more detail in section 9.1.2.

3.7.5 Spike timing and the extent of precession

As typified in Figure 3.7, CA1 phase precession began just prior to the positive peak in the local EEG. This is consistent with observations by Skaggs et al. (1996) who noted that phase precession began 90^0-120^0 after phase zero, with phase zero in their study defined as the peak probability of population pyramidal cell firing, that in turn being shortly after the trough in the local theta EEG. My results are also consistent with observations by Csicsvari et al. (1999) who observed that CA1 inhibitory interneurons fired maximally just before the trough, making the ascending slope the region of the theta cycle in which inhibition is weakest. The fact that both Skaggs et al. (1996) and Csicsvari et al. (1999) observed maximum pyramidal cell activity just after peak interneuron activity, also approximately in the EEG trough, reflects the fact that this is where peak cell firing occurs during traversal of the place field, mid-way through both the field and the phase precession.

The data from DG/P was very variable in the current study, but it seems as though phase precession in this region began just before the trough in the local EEG. Given the approximately 180^0 inversion of the theta oscillation between the pyramidal layer and the fissure (Winson, 1974; Leung, 1984a; Bragin et al., 1995) , this suggests that the onset of firing in both CA1 and DG/P is synchronised by a common "clock". Fox, Wolfson, and Ranck (1986) made similar observations. The variability in firing phase results is certainly consistent with observations by Skaggs et al. (1996), but the latter noted that DG granule cells tended to start firing somewhat later than CA1 pyramidal cells.. This discrepancy is unsurprising given the uncertainty regarding the precise positioning of electrodes used for DG/P recording in the current experiment. The assumption that local theta in these regions is exactly 180^0 out of phase with theta in the CA1 pyramidal cell layer is also probably an over-simplification.

The extent of phase precession in the current experiment was, on a run-by-run basis, considerably less that 360^0. While previous studies have commented on the apparent 360^0 spread of firing phase over multiple traversals of the field (O'Keefe & Recce, 1993; Skaggs et al., 1996), it was clear that the mean amount of precession on any given traversal was closer to 200^0. The appearance of 360^0 precession arises from variability in the phase of firing from run to run - a phenomenon for which there is no explanation at this time. This may have implications for models of phase precession based on dendritic depolarisation (Kamondi et al., 1998; Magee, 2001), which have been based on the assumption that 360^0 of precession must be accounted for.

3.7.6 Place field distribution

There is no evidence from the current experiment that there is any clustering of place fields at the ends of the runway. This is consistent with previous research (Gothard et al, 1996b; O'Keefe et al., 1998; Redish et al., 2001) suggesting that place fields are evenly distributed throughout the environment, and do not show any clustering around regions of presumed behavioural significance, like the ends of the runway. Contrary to this finding, Hollup et al. (2001b) observed clustering of place fields near the platform location in a version of the Morris water maze. There are several possible explanations for this discrepancy. First, Hollup and colleagues made use of a task in which the behaviourally significant location was not marked by a visible feature of the environment. This may have necessitated allocation of additional hippocampal resources towards representation of the goal location which would not be required in most unit recording paradigms, where behaviourally significant regions of the environment (end walls of runways, corners of tracks and boxes, edges of cylinders, etc) are visually distinct. A second possibility is related to the fact that Hollup et al. only recorded place units on probe trials when the escape platform was not present. This condition, a spatially-specific failure of the rat's expectations based on the training protocol, may have led to recruitment of a particular class of hippocampal neurons which have previously been described as "mismatch cells" (Ranck, 1973; O'Keefe, 1976).

3.7.7 Place field size and shape

In contrast to the even distribution of place fields on the runway, there was a pronounced relationship between field position and size, as predicted by O'Keefe & Burgess (1996) - place fields near the ends of the runway were clearly smaller than place fields in the middle. An interesting consequence of this relationship, assuming even distribution of field centroids, is that fields towards the centre of the environment are generally more overlapping. This could be interpreted either as over-representation of position by the hippocampal place cell population in the middle of the runway, or an increased spatial precision of the information encoded by single neurons with place fields at the ends of the runway. Given the confounding of position on the runway and running speed, it is unclear at this point whether field size is truly determined by sensory information such as proximity to the end walls, or by the rat's behaviour.

However, it is worth noting that field skew is also a function of position, in that place fields towards the ends of the runway tended to be skewed towards the middle of the runway, regardless of the rat's running direction. Both size and skew effects could be explained by a single phenomenon - the rate of visual change in cues to distance. The closer the rat is to an object like the end wall, the more quickly it appears to loom or shrink as the rat approaches or recedes from it, respectively. Given the rat's wide range of vision and the large size of the end wall, it seems not unreasonable to suggest that fields close to the wall are smaller because the rate of change in cues like the angle to the top of the wall is faster, and this effect may also be reflected within a field, with the rate of firing rate change being reduced as the rat moves to portions of the field further from the wall. Mid runway, it may be that fields are large because their firing rate envelopes are determined by balanced and slowly changing stimuli from the walls at either end of the runway.

3.7.8 Phase precession slope is related to field size, but not skew

Phase precession slope, that is, the rate at which firing phase changed as a function of position on the runway, was triply correlated with field size, running speed, and centroid position. The correlation between field size and phase precession slope was of particular interest, because it suggests that the extent of place field precession is a constant. This is borne out by the observation that most place fields do show an approximately 360^0 spread of represented firing phase, and there is no correlation between field size and extent of the phase precession. O'Keefe and Recce (1993) noted that phase precession never exceeded 360^0, which seems to obviate the existence of mechanisms which not only control the rate of precession, but also the extent. Bose, Booth & Recce (2000) have suggested that the dynamics of the phase precession actually define the extent of the place field.

The "ramp" model proposed by Mehta, Lee and Wilson (2002) suggests that asymmetry in the place field is required for the appearance of phase precession. The assumption is that linear phase precession reflects an asymmetric spike firing envelope, in which firing rate increases gradually and stops abruptly (negative skew). However, there was no correlation between field skew and the slope of the phase precession (Figure 3.12). Indeed, many fields with a positive skew exhibited pronounced phase precession. It does not appear, therefore, that firing phase is

directly related to momentary levels of depolarisation. This hypothesis will be explored in more depth in Chapter 6 (Firing Rate Analysis).

The next logical question arising from this hypothesis, then, is what is it that controls the temporal or spatial dynamics of phase precession? Are place field size and phase precession slope jointly determined by the rat's running speed, or by the changing dynamics of the sensory information the rat receives as it traverses the runway? The experiments outlined in the following chapters will shed some light on these issues.

Chapter 4: Running Speed Analysis

4.1 Introduction

The running speed analysis was intended to address several ambiguities which arose from observations of the relationships between basic place field characteristics. Specifically, it was necessary to determine whether features like small field size, steep phase precession slope and field skew associated with the ends of the runway were directly related to the sensory information unique to those positions, or whether they were an indirect result of the fact that the rat ran more slowly at the ends of the runway. No attempts were made to manipulate running speed. Instead, natural variability in running speed was used, based on the observation that running speed could vary considerably from one traversal of the runway (or run) to the next.

4.2 Methods

The effects of running speed on place fields was assessed in two ways which decouple running speed from a particular region of the runway, as described below. Both methods restrict analysis to chunks of the data record in which the rat crosses the place field multiple times at varying speeds. Because the place field is defined as a discrete region in space, this is a way of looking at speed effects while essentially holding position constant. A simple correlation analysis was used to compare the firing rate map for a given field on the initial 8 minute baseline with the rate map of the same field on successive non-manipulation trials. All baseline trial pairs for which there was a strong place field correlation (Pearson's $r > 0.9$) were concatenated. This created as large a baseline data set as possible, from which the field was redefined specifically for the purposes of these analysis, and from which a large number of runs through the field could be extracted. The procedure for runs extraction and the derivation of field statistics is described in detail in the General Methods.

4.2.1 Run-correlation analysis

The *run-correlation analysis* looked at the effect of the speed at which a rat runs through a place field and characteristics of cell firing on that particular run. A separate

set of correlation analyses was done for each field. Data from each run through a given field was only included if at least two spikes were fired. Correlations were calculated for run speed versus the total number of spikes fired, the firing rate, the distance into the run at which the first and last spikes occurred, the firing phase of those spikes (phase-a and phase-z), the amount of phase shift on the run (phase-a minus phase-z), and the mean momentary theta frequency.

Correlations with the position of the first and last spikes in a run were corrected for the rat's running direction. That is, normally, if the rat was running east, a positive correlation would indicate a shift in the direction of movement (east) on faster runs, If the rat were running west, a positive correlation would also indicate an eastward shift, but in this case, it would reflect a shift opposite to the direction of movement. Consequently, all correlation (r) values from cells active when the rat ran west were multiplied by –1. In this way, positive correlations always came to reflect a shift in the direction of movement, while negative correlations indicated a shift opposite the direction of movement.

Phase shift was presumed to be negative, so positive values were adjusted by -360^0. Often, spurious significant correlation results were obtained for analyses based on fewer than 100 data points (runs). For this reason, only fields for which there were 100 or more runs through the field on which spikes fired were seriously considered.

This analysis permitted comparison of large numbers of values, like the position of the first spike fired as a function of run speed. However, because the number of spikes fired on individual runs could be very variable and often quite low, this analysis did not permit estimation of "higher order" field characteristics like centroid position, skew, or the slope of the phase precession.

4.2.2 Speed-field analysis

The *speed-field analysis* involved reconstruction of "slow run" versus "fast run" fields, comparing the field size, peak firing rate, centroid position, skew, and the slope of the phase precession. First, a composite field was defined, as in the first analysis, but with the field boundaries relaxed to include regions where the firing rate was as low as 5% of the peak rate. This ensured that virtually no spikes associated with the place field were excluded from the analysis, as might happen if the field shifted position on the slowest or fastest runs. Note, however, that the 5% lower limit was raised in a small

number of cases where it was evident that spikes from disparate regions of the runway were being included in the composite field.

This analysis was restricted to fields through which rats made no less that 100 runs. This criteria is slightly more inclusive than for the run-correlation analysis, as there was no requirement for spike firing on all included runs. Once all runs through the composite field were defined, they were sorted on the basis of the mean running speed. The fast- and slow-run subsets were then created from fastest and slowest runs (respectively) which contributed 25% of the total number of spikes. The only caveat was that no fewer than 200 spikes should be fired during runs from each subset. Preliminary analyses suggested that fields comprised of fewer than 200 spikes were prone to random irregularities which introduce artefacts into estimates of skew and centroid calculations. If fewer than 200 spikes were sorted into each set using the aforementioned method, then the composite set was simply divided in two at the 50^{th} speed percentile. This reduced the difference in the mean run speed between the sets, and therefore, the likelihood of detecting an effect. However, it was considered of higher priority to ensure that estimates of field characteristics were based on sufficient information. Paired t-tests were used to compare the mean field characteristics on "slow" versus "fast" versions of the place fields, and a Bonferroni correction was used to adjust the critical p-value.

Note that for this analysis, field size was *not* defined in the conventional manner, in terms of 20% of the peak firing rate on a given trial. Preliminary analysis determined that such auto-scaling to the peak rate on trials with very reduced rates can produce fields in which the firing rate in the periphery (5%) drops below "meaningful" levels – random cell firing would cause some fields to be interpreted as covering the entire runway. Instead, "fast" and "slow" fields were defined as the region in which the firing rate exceeded 20% of the peak firing rate of the composite field, not the peak firing rate of each of the "slow" and "fast" subsets. In other words, for each field and for each speed category, the same firing rate was taken as the cut-off defining the field edge for both the slow- and fast-field subsets. One of the consequences of this is that if firing rate drops, field size will inevitably be interpreted as smaller.

4.3 Results

Between 27 and 31 fields met the criterion for inclusion in the runs-correlation analysis, depending on the characteristic of the runs being investigated. Results are presented in Figure 4.1. Thirty four fields met the criterion for inclusion in the field-speed analysis. Figure 4.2 presents all of the slow and fast versions of the place fields which were subsequently analysed. Results from the runs-correlation and speed-field analyses are presented in Figures 4.3 and 4.4, respectively. Mean running speed in the "slow-field" data set was 61.87 cm/s, versus 84.93 cm/s in the "fast-field" data set. The mean difference between running speeds through individual fields was 23.06 cm/s, representing a 39% relative increase in the fast-field. This could also be interpreted as a relative 27% reduction in running speed in the slow-speed set.

4.3.1 Firing rate is modulated by running speed

On faster runs, the peak in-field firing rate increases. Twenty-nine fields exhibited a positive correlation, of which the relationship was significant for 23 ($p < 0.05$). As can be seen from Figure 4.1, this is by far the most consistent effect of running speed. When the mean correlations between run-speed and each of the variables studied are plotted (Figure 4.3), it can be seen that only the correlation with firing rate is meaningfully different from zero. An example for one field is given in Figure 4.4.

In 30 of the 34 fields meeting the inclusion criteria for the field-speed analysis, the peak firing rate was higher on the fast-run version of the place field, yielding positive difference scores. These results are summarized in Figure 4.5, as a function of the difference in the mean run speed in the fast and slow subsets. A paired t-test confirmed that fast-run fields exhibited higher firing rates than their slow-run equivalents ($t_{1,33} = -5.88$, $p < 0.001$). The mean difference in firing rate (fast-slow) was 5.52 Hz, representing a 49% mean increase in the fast-run set.

4.3.2 Running speed may influence theta frequency

A cursory glance at Figure 4.1 suggests that there is no tendency for correlations between mean velocity on a run and mean theta frequency to be either positive or negative - at least for fields through which there are at least 100 runs on which to base the correlation. Figure 4.3 reinforces this impression - the mean

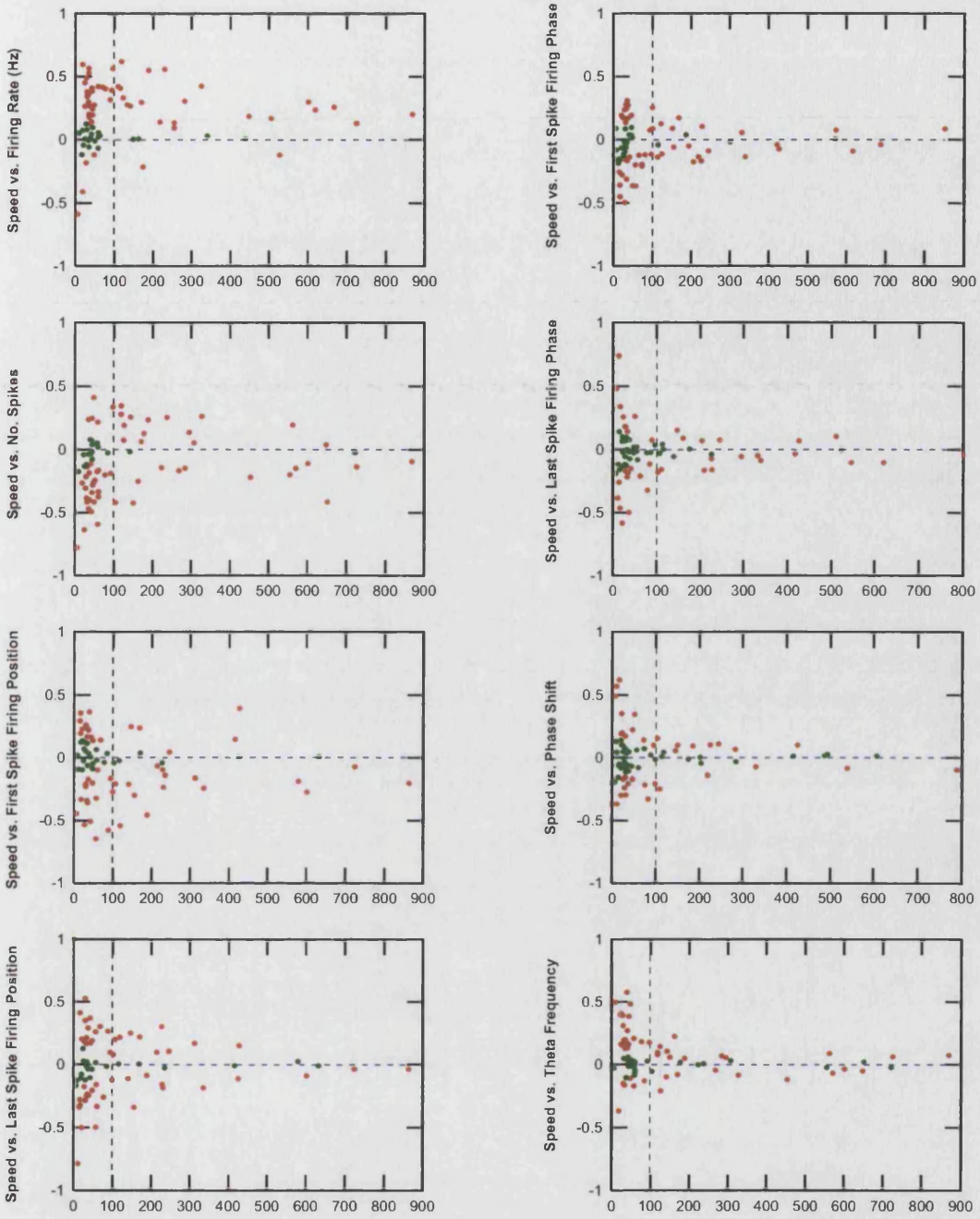

Figure 4.1. Each plot illustrates the correlations between the speed at which the rat ran through a given field, and features of the spike distribution on those crossings. Each dot represents a correlation (Pearson's r) for a single field, with red dots representing significant ($p < 0.05$) correlations. The X-axis in each plot is the number of passes (runs) through the field which were used to generate each correlation. Note that as the sample size increases, variability in the correlations is reduced in all cases. A sample size of 100 (vertical dotted line) was used as the lower cutoff for making meaningful interpretations of the correlation data. The distribution of points can be used to glean whether there are relationships between run speed and spike firing which are common to all or most fields. The relationship between the speed at which the rat runs through the field and firing rate (positive) appears to be robust. There is also the suggestion of a trend towards negative relationships between run speed and the position at which the first spike of the run fires. That is, the first spike occurs sooner (spatially) on faster runs for most fields.

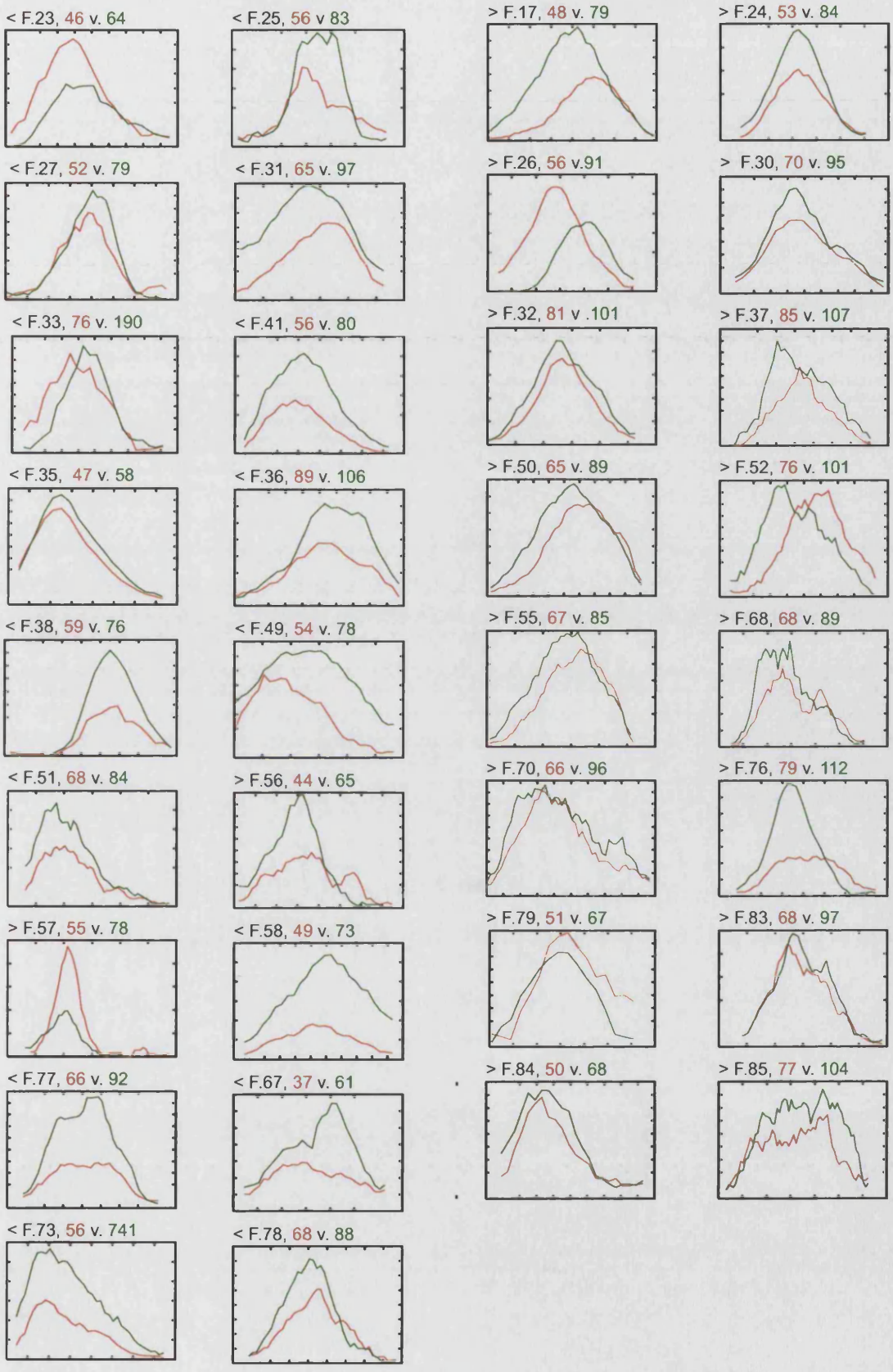

Figure 4.2. Results of redefining place fields on the basis of spikes collected during the slowest versus the fastest runs through the field. Each plot compares firing rate (Y-axis, Hz) with position on the runway (X-axis, cm). Position is centred on and restricted to the extent of the field. "Slow" fields appear in red, while "fast" fields are green. The "<" or ">" symbols above each plot reflect the preferred running direction for that field. Also presented are the field number and mean running speeds from the fast (green) versus slow (red) sets.

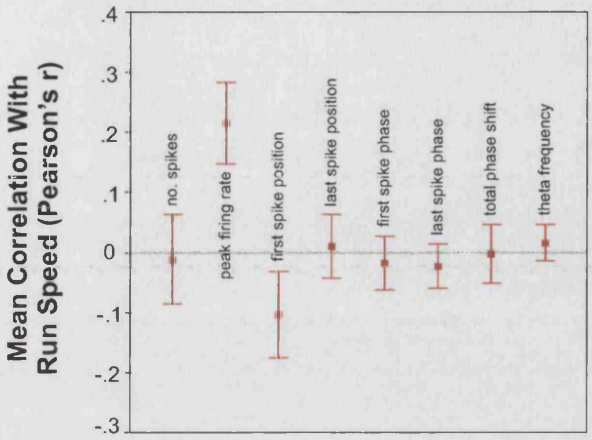

Figure 4.3. Summary of run-correlation analyses for 34 place fields for which at least 100 runs through the field were recorded. Non-significantcorrelations are included. Errors bars are 95% confidence intervals. Most correlations tend towards zero. The notable exceptions are correlations between run speed and peak firing rate (Hz), which are nearly universally positive. The negative correlations between run speed and the position of the first spike fired on the run also suggest a delay in spike firing on slower runs.

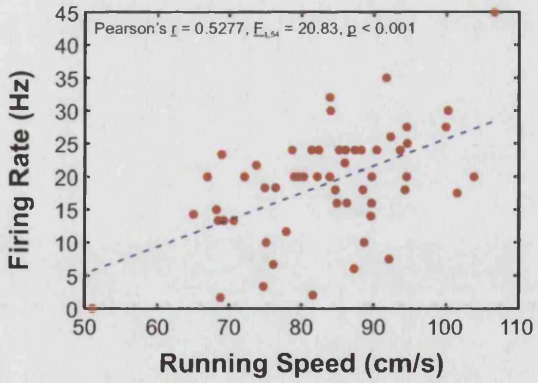

Figure 4.4. The correlation between the speed at which the rat traverses a cell's place field, and the firing rate of the cell on that pass. Data is for a single place field (No. 004).

correlation value for run-speed versus theta frequency is offset from zero by less than the 95% confidence intervals for the mean. However, the speed-field analysis revealed that theta frequency was lower on slow (mean = 9.10) versus fast (mean = 9.28) versions of the fields (t_{33} = -6.255, p < 0.001). The scatter plot comparing the differences between speed and theta frequency between the two versions of the field illustrates the consistency of the result.

4.3.3 Phase precession is independent of running speed

Neither the total amount of phase precession ($t_{1,33}$ = -0.432, p = 0.67), nor the slope of the precession ($t_{1,33}$ = 0.301, p = 0.77) were significantly different for slow- vs. fast-run versions of the place fields studied. Similarly, as illustrated in Figure 4.6, circular analysis revealed that there was no change in firing phase at the onset ($F_{1,32}$ = 0.066, p = 0.799) or offset ($F_{1,32}$ = 1.281, p = 0.266) of firing in CA1 fields. The same holds for the onset ($F_{1,28}$ = 0.258, p = 0.616) and offset ($F_{1,28}$ = 0.494, p = 0.488) of firing in DG/P fields. However, the distribution of firing phase at the onset of firing (phase-a) in both CA1 and DG/P fields approaches uniformity. That is to say, clustering of phase values around the mean is poor, and this makes interpretation of the absence of a significant effect somewhat problematic.

Figure 4.7a-c provides some examples of phase shift data for slow versus fast versions of place fields. In one field (17) it is evident that spike firing is delayed on slow runs, and there is some evidence that the whole field is shifted a little eastward. The other two examples show virtually identical phase precession in the slow- and fast-run fields. Figure 4.7d shows the results from a single field (number 073) for which it was possible to identify good runs through the field with widely varying run speeds. For this particular field, only the very slowest or very fastest runs were selected to produce the two alternate versions of the field. The end result was slow- and fast-run versions of the field which are virtually identical. Neither the phase precession nor the position of the field on the track were appreciably altered by the dramatic difference in mean run speed through the field (mean speed values for slow- and fast-run datasets were 33.40 cm/s and 78.90 cm/s, respectively.

4.3.4 Fields shift slightly, but size and skew are preserved

One interesting observation from the run-correlation analysis was that there appeared to be predominantly negative correlation between run speed and the distance into the run at which the first spike fired – that is, spikes tended to fire later on slower runs for most fields. The absence of a similar relationship between run speed and the position of the last spike in the run suggested that either 1) the field is smaller and more skewed on slow runs, with firing shifted towards later portions of the field, or 2) the field actually shifts forward beyond the space normally defined as the field on slow runs, resulting in the "cropping" of late spikes on slow runs.

The speed-field analysis resolved this issue. After applying a Bonferroni correction for multiple comparisons, there was no significant difference between slow and fast versions of the place fields in terms of skew ($t_{1,33}$ = -2.23, p = 0.03) or size ($t_{1,33}$ = -2.44, p = 0.02). The apparent difference in the mean skew values in Figure 4.5 appears to be largely dependent on a single outlier. This is consistent with the observation, from Figure 4.2, that fields can skew dramatically in either direction when the data is divided into slow- and fast-run subsets.

In contrast, the centroid shift scatter-plot in Figure 4.5 is strongly suggestive of a subtle negative shift in centroid position, opposite the direction of motion, for "fast-run" fields. For this analysis, separate t-tests were conducted for place fields when the rat was running east or west, as the shift in centroid position would be in opposite directions accordingly. However, despite a subtle suggestion of a backwards shift in the mean centroid positions, there was no significant difference between "fast" and "slow" versions of place fields (east, $t_{1,16}$ = 1.921, p = 0.073; west , $t_{1,16}$ = -1.695, p = 0.109). This discrepancy between what appeared to be a robust effect and the non-significant test results suggests that the large variance in centroid position between different place fields may be obscuring the subtle field shifts. A plot of the mean centroid shift in Figure 4.5 reveals that there is a strong tendency for fields to be shifted backwards, opposite the direction of motion on faster runs (or forward on slower runs), and this shift differs by more than the 95% confidence intervals for the distribution (mean shift = 2.102 cm). . These results are consistent with the shifting field interpretation of the results from the "run-speed" analysis - that is, the delay in the onset of firing on slow runs is related to a subtle shift in the place field in the direction of motion.

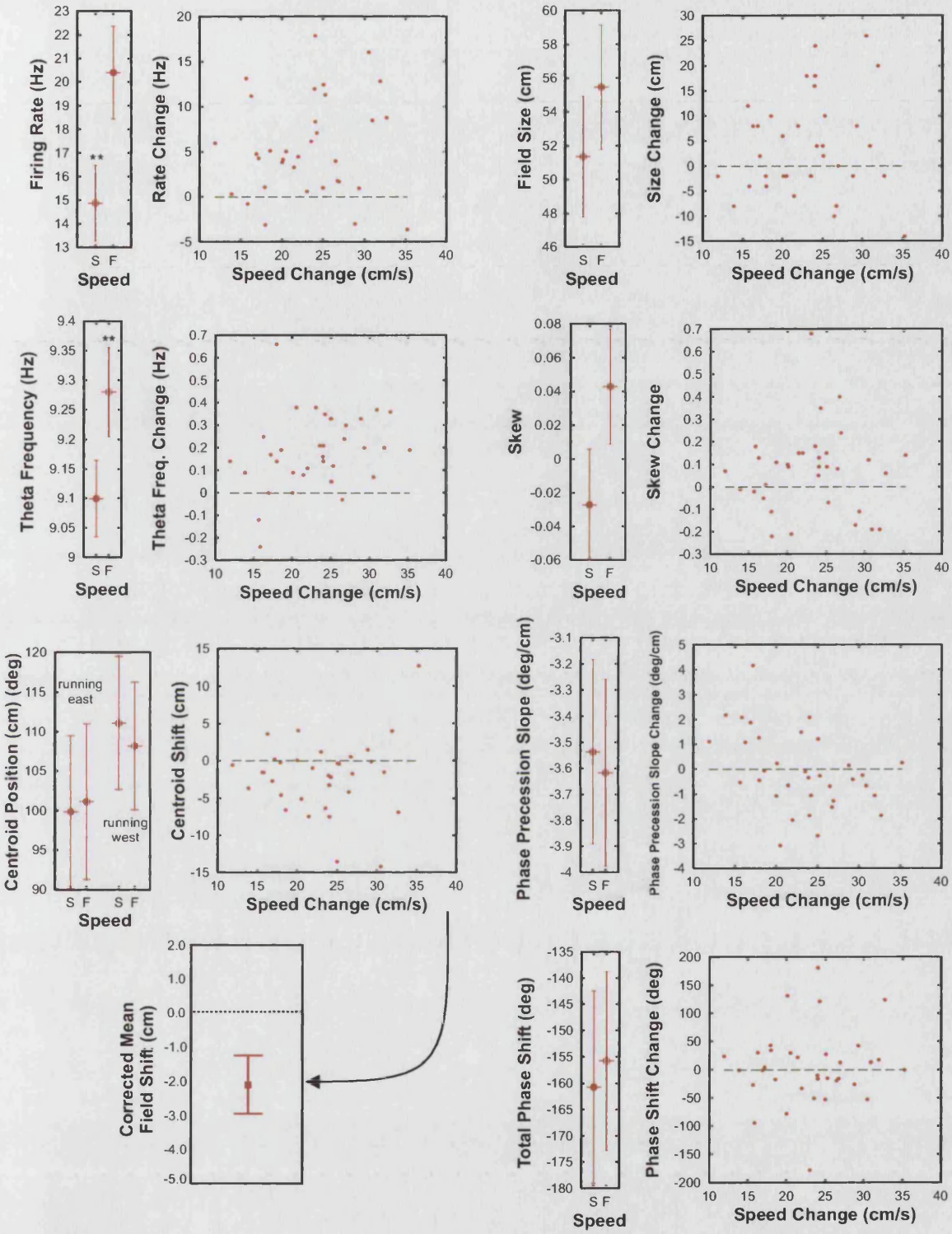

Figure 4.5. The speed-field analysis. “Fast” versions of place fields have a higher firing rate and characteristic theta frequency, relative to their “slow” counterparts. The apparent trends for high-speed fields to be larger and more positively skewed proved to be non-significant (Bonferroni criteria: * $p < 0.007$ **$p < 0.001$). Mean centroid position did not differ between slow and fast fields, but the mean per-field centroid shift was consistently negative (opposite running direction). Place fields generated using only data from the slowest (S) versus the fastest (F) runs were compared. On the left of each figure is a comparison of the slow-field and fast-field means, +/- SEM.Error bars in the plot of mean centroid shift are 95% confidence intervals. Scatter-plots illustrate the per-field differences between slow and fast fields. Centroid shift, phase precession slope change, and skew are corrected for running direction.

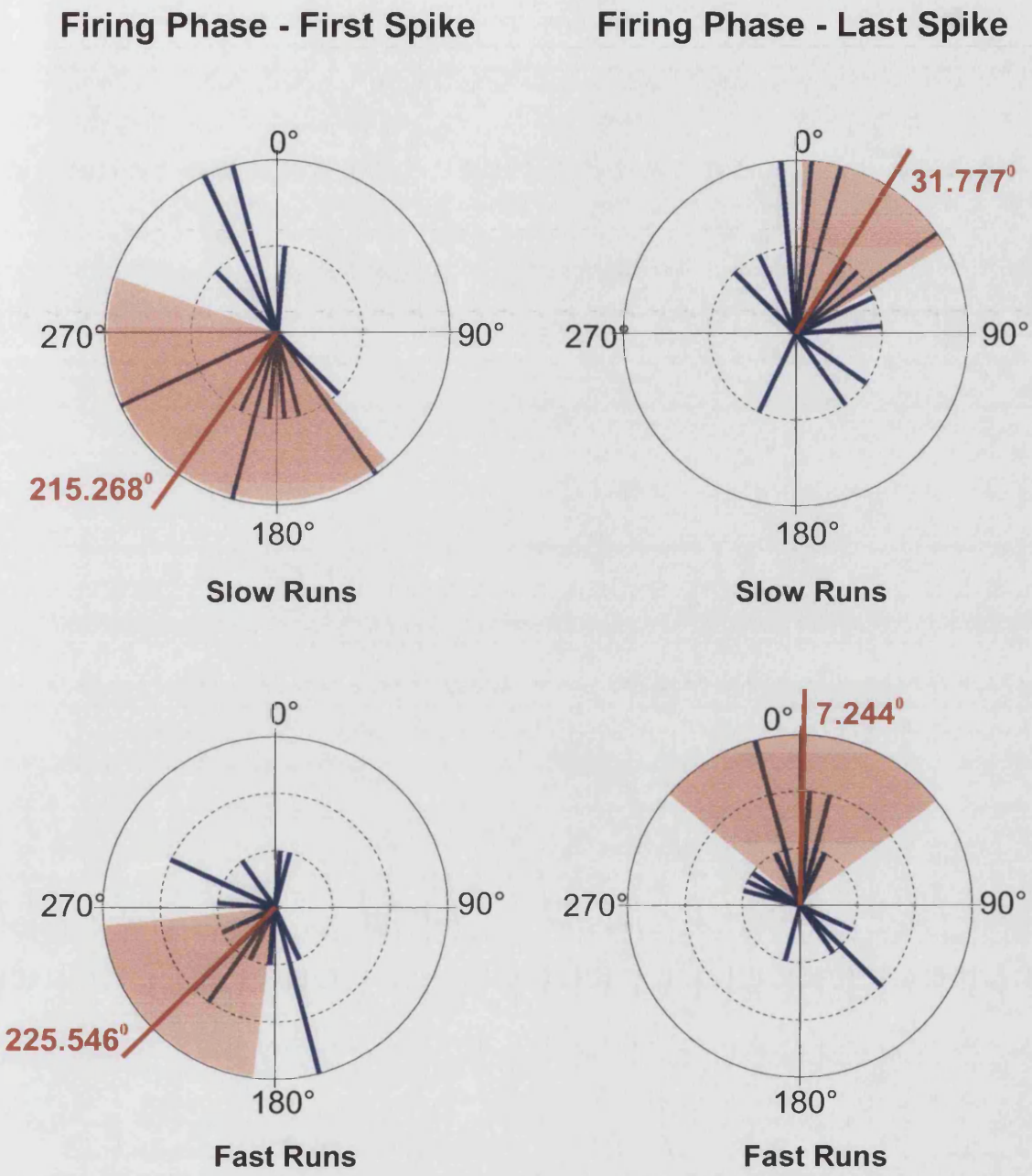

Figure 4.6. Results of the speed-field analyses for firing phase (CA1 place fields). The circular histograms illustrate the effect of running speed on the mean firing phase of the first (Phase-a) and last (Phase-z) spikes fired on runs through place fields. Data is broken down by cell layer. Each ring represents a count of one, and the circular mean phase of firing is indicated in red. Shaded regions represent the 95% confidence interval. While the ~180° difference between phase-a and phase-z is evident for CA1 (indicative of phase precession), there was no difference between slow-run and fast-run fields on measures of phase-a or phase-z, in either CA1 or DG/CA3. Note also the high variability and absence of a phase-a vs. phase-z difference within speed categories for the DG/CA3 resuts.

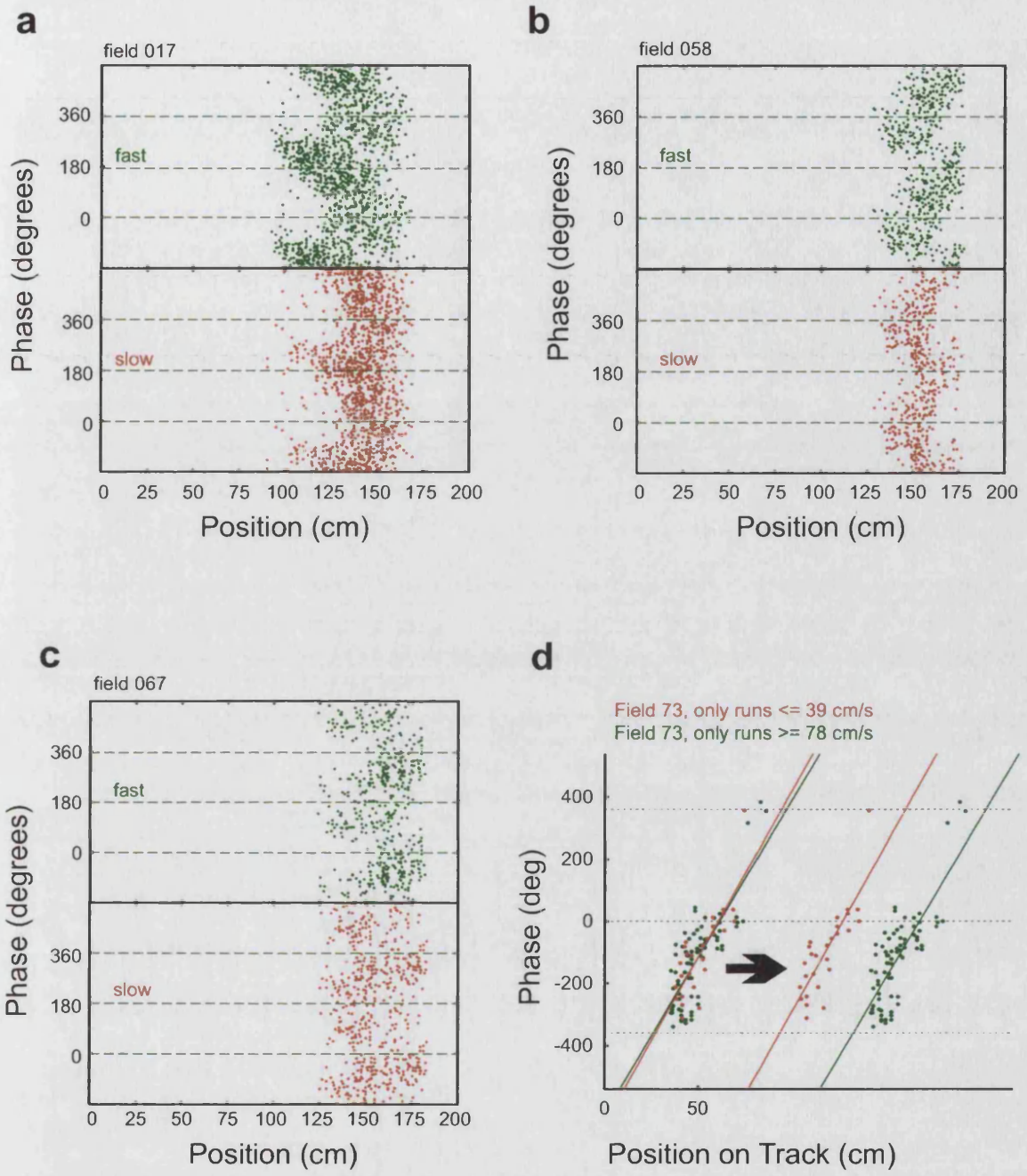

Figure 4.7. Examples of slow-run vs. fast-run versions of place field phase precession. **a-c:** Three typical place fields derived from slow (red) and fast (green) runs through the field, with slow and fast versions stacked to allow comparison. Data in each subset are further duplicated to show the continuity in the circular dataset. Field 017 is the most pronounced example of the delayed onset of firing seen in slow-run fields, resulting in a shifting of the field to the right. Note however that the overall shape and extent of the phase precession is preserved. **d:** A field for which the difference between fast- and slow-run subsets was as extreme as possible (in this case, mean speed on fast runs is more than twice mean running speed on slow runs). Results are plotted both together (left) and side by side (right) for comparison. Data have been linearised and the best fit line is shown. Note the striking similarity in the phase precession profiles, despite the obviously increased firing rate in the fast-run subset.

4.4 Discussion

4.4.1 A code for running speed?

The relationship between running speed and firing rate is the only effect which was robust enough to be discernable in both the run-speed and the speed-field analyses. The faster the rat ran through a place field, the higher the firing rate of the place cell. This is consistent with previous findings (McNaughton, Barnes & O'Keefe, 1983; Wiener et al., 1989; Kobayashi et al., 1997; Czurkó et al., 1999). The implication is that the firing rate of the cell, in addition to encoding information about the rat's position in the environment, may also provide information about the rat's running speed. This may play an important role in determining the temporal dynamics of phase precession (Harris et al., 2002), and perhaps even the extent of the place field itself (Bose, Booth & Recce, 2000).

In contrast, the results are at odds with those of Fenton & Muller (1998), who found place cell firing to be extremely variable from one traversal of a place field to the next, but no relationship between firing rate on a given traversal and the rat's running speed. There are several key differences between the two studies. For example, Fenton & Muller conducted their experiment in an open field, and excluded fields with peak firing rates of less than 10 HZ, whereas the current study looked at stereotyped behaviour on a runway, and the firing rate threshold was 1 Hz. They did not include traversals which lasted less than 1 second, whereas most field traversals in the current study lasted far less than a second, due to the high speed at which the rat's tended to run. Taken together, these differences suggest that while the current study included low firing rate fields through which the rat ran quickly, Fenton and Muller selected higher firing rate fields through which the rat tended to run slowly. But perhaps most importantly, Fenton and Muller did not filter the data to remove epochs during which the rat paused and engaged in non-exploratory behaviour. During such epochs, it is possible that the rat slipped into LIA state, in which large populations of pyramidal cells engage in synchronous bursting behaviour which is unrelated to the rat's position. If such bursting activity occurred during moments of immobility in the Fenton & Muller study, it would certainly have helped obscure any relationship between running speed and firing rate. Therefore, it remains possible that the variability in firing rate they observed was related to running speed.

4.4.2 The effect on theta frequency

The effect of running speed on theta frequency is most pronounced when "fast" and "slow" versions of place fields are compared on measures of characteristic theta frequency. It is clear from Figure 4.5 that selecting only the fastest (versus the slowest) runs to reconstitute a place field resulted in an increase in theta frequency. In other words, theta frequency was higher on the fastest runs than on the slowest. Why then was this not apparent from the correlations used in the run-speed analysis? One possibility relates to the fact that runs on which fewer than two spikes were fired were omitted from the run-speed analysis. While this makes a certain amount of sense for analysing place cell firing characteristics, it is unnecessary for estimates of theta frequency. Given the relationship between running speed and firing rate, we can assume that the run-speed analysis actually culled many low-speed runs, which may well have obscured any effect of running speed. In contrast, the speed-field analysis culls runs from the middle of the speed range, in order to accentuate the difference between slow- and fast-run fields.

4.4.3 Place field size is not determined by running speed

An important observation from the running speed analysis is that running speed did not appear to have a robust effect on field size. This can be taken as evidence that the speed at which a rat moves in different parts of the environment does not determine the size of the local place fields. The prevalence of smaller place fields at the ends of the runway (Non-Experimental Observations) must, therefore, be explained in terms of some phenomenon other than the tendency of the rat to run slowly in these regions.

In 1996, O'Keefe and Burgess proposed a model which could explain why fields near the environmental boundaries are small. Their model suggests that place fields represent the summation of multiple Gaussian tuning curves associated with the boundaries of the environment. Implicit in the model is the assumption that tuning curves which peak close to the boundaries they are associated with will be "higher and narrower than those peaked far from one" (p. 427). This is based on the increased rate of change in visual cues to the distance from the boundary as the rat approaches it -

cues such as the visual angle to the top or bottom of the wall. These ideas are explored more fully in Chapter 8.

Chapter 5: Firing Rate Analysis

5.1 Introduction

A major shortcoming of depolarisation-based models of phase precession is that they fail to account for the linear precession of firing phase as the rat traverses the place field. That is, insofar as firing rate reflects depolarisation, one would expect that as the rat passes the region of peak firing for a given place cell, depolarisation-dependent phase precession should reverse, so that the cell fires late in the cycle again as the rat exits the place field. The only way of overcoming this problem is if place fields themselves genuinely exhibit skewed firing rate distributions, either as a result of adaptation (Harris et al., 2002), or asymmetric place field expansion (Mehta et al., 2002).

I have already demonstrated that on a linear track, phase precession is not dependent on the magnitude or the direction of place field skew. However, an interesting possibility is that an asymmetry of momentary inputs to the hippocampus may not be reflected in asymmetry of the time-averaged place field firing rate map. If, on repeated traversals of the place field, firing rate continually ramped up and then abruptly shut off due to adaptation, the effect might be obscured by combining spikes from multiple runs to generate the place field map, provided onset and "offset" of firing shifts slightly from run to run. In other words, averaging misaligned asymmetrical phenomena may produce the illusion of a Gaussian firing rate distribution.

The purpose of the firing rate analysis, then, is to answer the following questions. Does firing rate actually increase linearly as the rat traverses the place field, or is the run-by-run firing rate envelope really an approximate Gaussian? And if the firing rate does tend to rise and fall on every traversal, can it be demonstrated that firing phase undergoes precession in the portion of the place field where firing rate is dropping? And finally, is it possible to show that momentary changes in depolarisation, as reflected by the firing rate of a place cell on a particular run, affect the rate or extent of phase precession in either the temporal or spatial domains?

5.2 Methods

5.2.1 Defining field portions

The extent of the place field was determined for initial baseline trials (section 2.11.1), and the range of x-position values representing the field was divided into three equal portions – early, middle, and late – according to the preferred direction of the field. Each spike was then assigned to one of these three field portions. For example, if a place field was defined as ranging from position 10cm to position 25cm and the cell fired when the rat was travelling west, a spike at position 24cm would be defined as "early", a spike at position 17 would be "middle", and a spike at position 12cm would be "late". For each portion of each field, the mean firing phase, TDPHASE, IFR and TDIFR were calculated (refer to section 2.11.3), and tests were conducted to compare the differences in these values across portions of the field. In addition, mean values were averaged across all fields for each portion of the field, and in this manner, population statistics were calculated.

Note that phase values were adjusted for this analysis to compensate for the inclusion of cells (some of them from DG/P) with widely varying phase precession profiles. For each field, after adjusting the origin to eliminate bimodality in the phase distribution, phase values were adjusted so that 360 represented the highest phase values. This aligns all fields to the phase at the beginning of their phase precession and redefines that value as "360". Therefore, mean phase values in the results will not be true, but the differences between the means will be.

5.2.2 Sorting runs by firing rate

Just as rats run through place fields at different speeds from run to run, so also does firing rate vary from run to run, as previously documented by Fenton and Muller (1998). This natural variability in within-run firing rate (spikes fired divided by duration of run) provides an opportunity to analyse the effects of depolarisation on phase precession, without the requirement of any experimental manipulation. Presumably, on runs in which the firing rate is low, the cell is less depolarised, even though the reasons may not be immediately evident.

In a similar fashion to the speed-field analysis, runs from composite baseline records for each field were sorted into either a low-rate or high-rate subset. In this

case, runs were sorted based on whether the firing rate was greater or less than the mean run firing rate. Only fields for which there were at least 100 valid runs in the composite record were included. Adjustment of the phase values for each field (as described above) permitted treatment of phase values as linear data for this analysis. However, as above, circular statistics were used to calculate the mean phase for each portion for each individual field, and it was these means which were used to calculate the population means and used in the linear analysis. A mixed design was used to analyse low-rate versus high-rate phase data across three levels of the repeated measure "field portion" (early, middle, and late).

5.3 Results

5.3.1 IFR is a Gaussian function of position

A total of 76 composite fields from both CA1 (64) and DG/P (12) were included in the analysis of IFR and TDIFR. The mean instantaneous firing rate (IFR) was calculated for the beginning, middle, and end of each place field, and the results for field portion were combined for all fields. A repeated measures ANOVA determined that IFR was higher in the middle of the field than either the beginning ($F_{1,74} = 63.10$, $p < 0.001$) or the end ($F_{1,74} = 115.59$, $p < 0.001$). This trend can be clearly seen in Figure 5.1c. Contrasts using polynomial coefficients confirmed that this is a significant quadratic relationship ($F_{1,74} = 153.46$, $p < 0.001$).

Figure 5.1d shows that the temporal derivative of the IFR (TDIFR) tended to be linear ($F_{1,74} = 54.77$, $p < 0.001$). TDIFR is positive as the rat enters the field, tends towards zero mid-field, and becomes negative in the later portion of the field. In other words, using measures which are not averaged in the spatial domain, it is clear that firing rate increases as the rat approaches the middle of the place field, and tapers off as the rat exits.

5.3.2 Phase precession continues while firing rate drops

Figure 5.1a illustrates that in the same portion of the field where firing rate is decreasing, firing phase continues to precess. Only data from CA1 are considered. Place cell firing occurs significantly earlier in the middle of the field than it does upon

entry ($F_{1,120}$ = 21.540, p < 0.001), and earlier again as the rat exits than mid-field ($F_{1,120}$ = 24.449, p < 0.001). In other words, the change in mean firing phase is significant in the latter portion of the place field. This is, of course, the well documented linear phase precession effect. Figure 5.1b further illustrates that within each portion of the field, TDPHASE is negative (early, 68/76 fields, p < 0.001; middle, 57/76 fields, p < 0.001; late, 46/76 fields, p < 0.05, binomial test). This means that in each part of the field, every spike tends to fire at an earlier part of the theta cycle than the preceding spike. Note that the phase values presented in Figure 5.1a differ from estimates of the mean phase values for the first and last spikes in runs through the place fields on baseline trials (phase_a and phase_z, Figure 3.9) because of the way the phase values were aligned (see section 5.2.1).

5.3.3 Phase precession is preserved on low firing rate runs

The results from comparing phase precession from low firing rate runs (mean rate = 6.123 Hz) with high firing rate runs (17.162 Hz) are summarized in Figure 5.2. The average jump in firing rate between the low-rate and high-rate subsets for each field was 11.039 Hz, a 503% increase.

As expected, from the observation of phase precession in the previous analysis using all baseline runs combined, there was an overall effect of field portion on firing phase ($F_{2,132}$ = 100.503, p < 0.001), with cell firing significantly precessed mid-field relative to early-field ($F_{1,66}$ = 95.022, p < 0.001), and late-field relative to mid-field ($F_{1,66}$ 35.509 = , p < 0.001), regardless of firing rate group (low vs. high). However, there was no overall effect of firing rate group membership on firing phase ($F_{1,66}$ = 0.938, p = 0.336), and no interaction with field portion ($F_{2,132}$ = 0.043, p = 0.958). In other words, whether cells fired rapidly or slowly on runs through the place field does not appear to have affected phase precession. Figure 5.2b presents a very robust example of this preservation of phase precession in the face of high momentary variability in depolarisation. In this particular example, the firing rate cut-offs used to assign runs to either the "low" or "high" firing rate category were shifted to exaggerate the difference between the two sets. In this case, a nearly 10-fold difference in firing rate has virtually no discernable effect on the extent of the phase precession or its slope as a function of position.

Phase precession may also be measured as a temporal function – that is, the rate of change in firing phase. However, it was not possible to properly analyse the

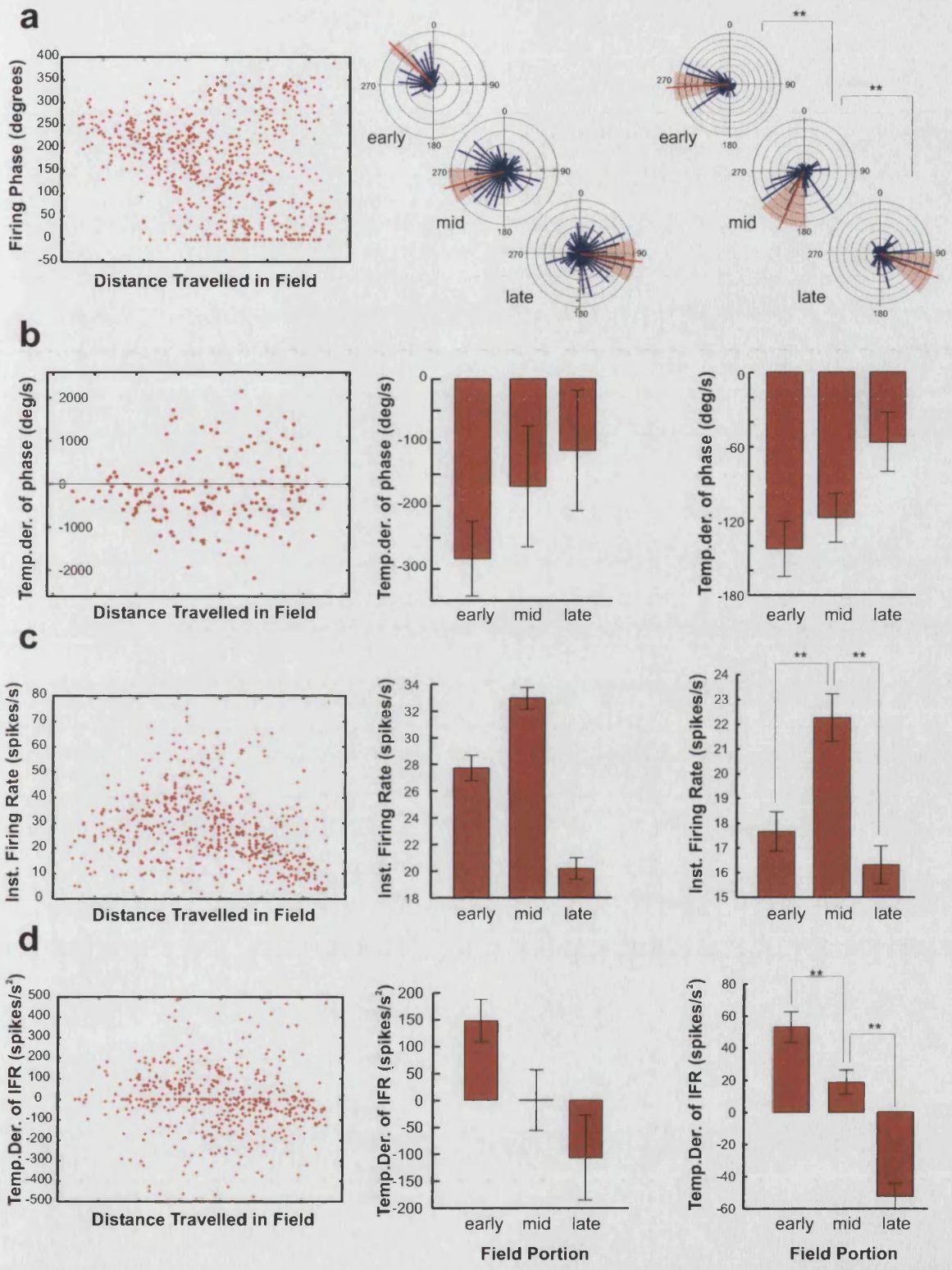

Figure 5.1. The relationship between position and each of phase (**a**), temporal derivative of phase (TDPHASE)(**b**), instantaneous firing rate (IFR)(**c**), and temporal derivative of IFR (TDIFR)(**d**). Scatter plots illustrate raw data for a single place field (field 017). In the middle column position is "binned" into early, middle, or late portions of the place field. Mean values are calculated for each portion of the place field in the middle column, and the population averages are presented in the right hand column. Bars are SEM. Phase precession is linear across the extent of the field, while firing rate begins low, reaches a peak mid-field, and falls again in the late portion of the field. TDPHASE results show that phase continues to precess within spike trains in all field portions, and TDIFR confirms that firing rate is genuinely falling in the late portion of the field. This proves that the relationship between firing rate and position genuinely is a quadratic function, while phase precession is linear. $^{**}p < 0.01$.

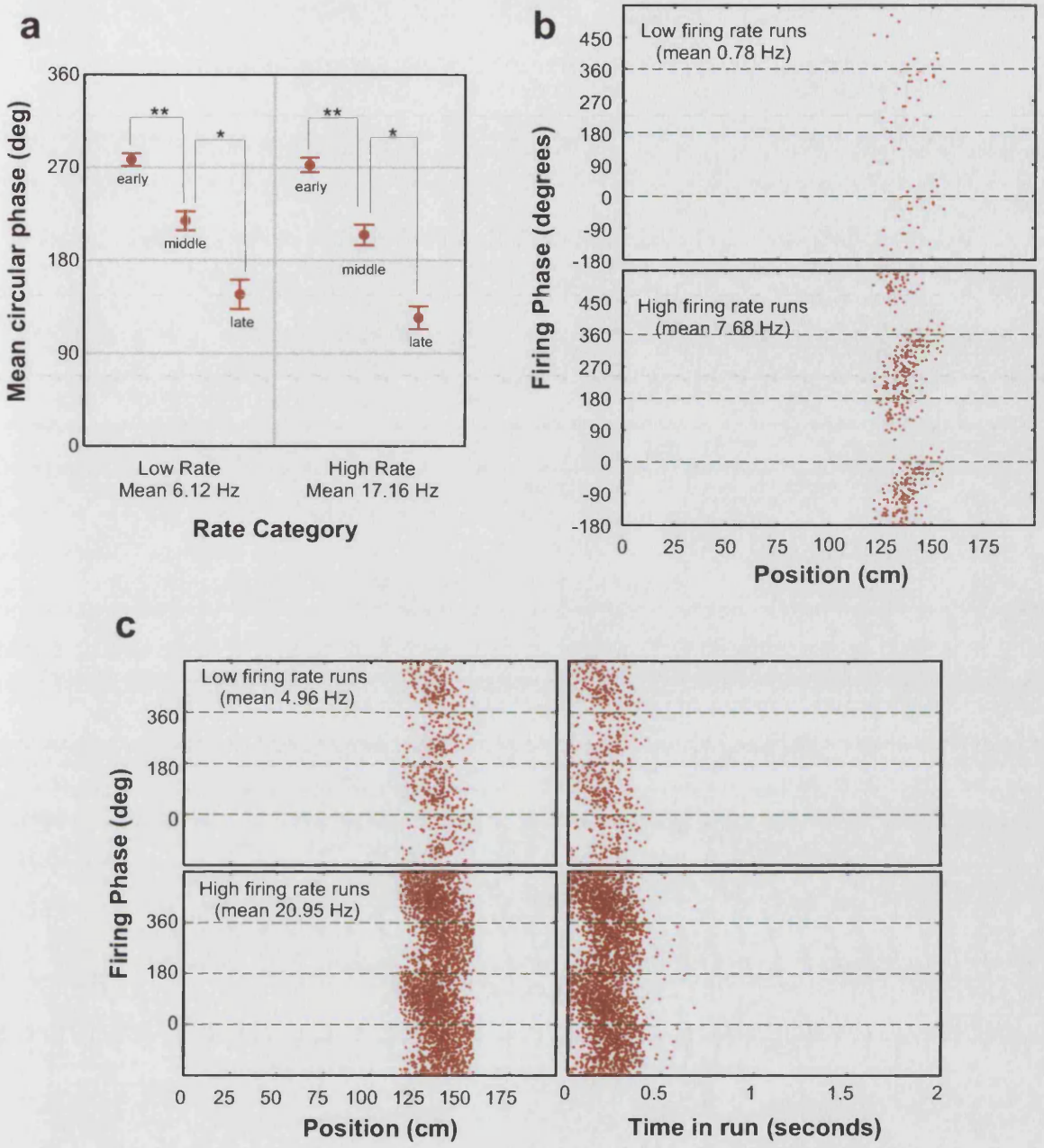

Figure 5.2. The influence of natural variation in firing rate on phase precession. Multiple baseline trials were combined to generate a large number of runs through a "composite" place field. Runs were then sorted into "low" or "high" rate categories and phase precession was compared on those runs. **a**: Mean firing phase for place fields as a function of rate category and field portion (early, middle, late). Significant phase shifts occur between field portions, regardless of firing rate category. Error bars are SEM. *$p < 0.05$, ** $p < 0.01$. **b:** Preservation of phase precession (firing phase versus position) on low- versus high-rate runs (field 023). Despite the nearly ten-fold difference in firing rate, the extent and slope of the phase precession is unaffected. The position of the field on the runway also appears to be unaffected. Note that this is a place field which fires only when the rat is running west (right to left). **c:** An unusual example of a place field (field 32) in which both spatial and temporal phase precession are preserved in the face of dramatic variation in firing rate.

effect of firing rate on temporal phase precession, because running speed, which affects the amount of time it takes the rat to traverse the field, is strongly correlated with firing rate. Therefore, in almost every case, the higher the firing rate, the more rapid the phase precession in the temporal domain. Nevertheless, it was possible to find examples of fields for which this relationship did not hold. One such example is presented in Figure 5.2c. The existence of examples like this suggests that it is possible for temporal phase precession to proceed "normally" despite conditions of heightened or lowered depolarisation. It also suggests that factors other than running speed contribute to firing rate variability on a run-by-run basis.

5.4 Discussion

Clearly, instantaneous firing rate begins low as the rat enters the field, peaks mid-field, and ends low as the rat exits the field. This alone does not prove that the mean values of IFR reflect the dynamics of IFR on each run. However, when it became clear that the temporal derivative of IFR (TDIFR) was consistently positive in the first third of the field, and consistently negative in the final third, there was no denying that the time averaged firing rate reflects the run-by-run firing rate dynamics of each cell. In other words, spikes as the rat enters the field are always part of an accelerating spike train, and spikes as the rat exits are part of decelerating trains. The Gaussian shape of place fields is not a result of the smearing effect of averaging the data over time or space - on each pass through the field, firing rate truly rises and falls.

There is unambiguous phase precession between the early, middle, and late thirds of the place field. Phase precession continues to occur in the same region of the field in which there is a consistent tendency for firing rate to be decelerating, as evidenced by the advancement in mean firing phase from theta cycle to theta cycle in the latter portion of the place field, this presents a serious challenge to the notion that phase precession is brought about by increased depolarisation of the cell. Firing rate and firing phase are further dissociated in the comparison of low- and high-firing rate runs. There is no indication that the shifts in firing phase between early, middle and late portions of the place field are affected by the difference in firing rate between the low and high firing rate data subsets, even though on average, each cell's firing rate is five times higher on the high-rate runs. If phase precession were critically dependent on the firing rate of the cell, such a difference ought to have some effect. Hirase et al. (1999) noted a similar dissociation between firing rate and firing phase in the running wheel -

in their case, in response to changes in running speed. They hypothesised that the rate/phase relationship may only manifest at the upper range of firing rates they observed (>11 Hz). Yet there was clearly no such rate-dependence of phase precession in the current experiment: significant phase precession occurred between field portions in the low-rate subset, in which the mean firing rate on each run was only 6.123 Hz. Moreover, as indicated by Figure 5.2b, even a ten-fold increase in firing rate does not seem to appreciably alter the spatial relationship with firing phase. In this example, while perhaps only a single spike is fired on the low-rate runs, that spike always seems to fire at the appropriate phase of theta for the current position of the rat. This suggests that the rate/phase dissociation observed by Hirase and colleagues was not due to the rates being too low, but some other difference between the running wheel and linear track experimental paradigms – like actual traversal of the place field.

It may well be that firing rate affects the rate of phase precession in the temporal domain - that is, on higher firing rate runs, the same amount of phase precession may occur in a short period of time than on low firing rate runs. However, firing rate on individual runs tends to be correlated with running speed. Given the strong preservation of the phase vs. position relationship regardless of the speed at which the rat runs through the field, it stands to reason that high firing rate (fast) runs will exhibit faster temporal phase precession. Indeed, this is the case, and it is almost impossible to find examples of low or high firing rate runs which are not associated with comparable differences in running speed. Nevertheless, there were several examples, one of which is illustrated in Figure 5.2c. Clearly, for this field, changes in firing rate are unrelated to changes in running speed - some other factor is obviously modulating the cell's firing rate from run to run. Consequently, phase precession is preserved in both the spatial and temporal domains. This is not evidence, of course, of a general mechanism - it merely shows that it is possible for phase precession, even in the temporal domain, to be dissociated from firing rate.

In summary, depolarisation (as indicated by firing rate) is dissociable from phase precession, and the temporal dynamics of spiking during individual passes through a place field do not appear to resemble the skewed spike distributions proposed by the adaptation model of Kamondi et al. (1998) or the asymmetric field model of Mehta et al. (2002). Consequently, the following chapters will be dedicated to identifying alternative determinants of phase precession, although attention will be paid to changes in firing rate induced by manipulations, and whether they induce concomitant change in the rate or extent of phase precession.

Chapter 6: Compressing the Runway

6.1 Introduction

The main purpose of the compressed runway experiment was to determine whether the types of environmental manipulations performed on two dimensional environments by O'Keefe & Burgess (1996) would have similar effects on place fields in the essentially one-dimensional linear runway (i.e. stretching, shrinking, or silencing), and to determine the effect on the theta phase precession. Moving the end walls actually accomplishes two things - it changes the dimensions of the physical space in which the rat performs the shuttling task, and it changes the visual angle to the top and bottom of the shifted end wall for a rat at a given position on the runway. These factors may affect place fields in different ways. Consider, for example, a rat running east with the east wall shifted west by 50 cm. When the rat arrives at the midpoint of the runway, its idiothetic senses and sensory cues from the experimental room suggest it is in the middle, but the visual information encoded by the visual angle to the top of the east wall suggests that it has travelled much further. One of the questions addressed by this manipulation is whether one or the other sources of information plays a more important role in determining the position of place fields.

Another issue addressed by this experiment is the mechanism which drives the phase precession itself. Given the fact that running speed and depolarisation/firing rate have no apparent effect on the phase precession effect, compressing the runway may provide insight as to whether the rate and extent of precession is a function of environmental sensory inputs, such as cues to distances from environmental boundaries.

6.2 Methods

6.2.1 Overview

These manipulations involved sliding one of the end walls towards the other, effectively shortening the length of the runway and restricting the rat's movement in space. For example, the eastern end wall might be shifted west by 50 cm, shortening the runway to 100cm. On days when two moving wall trials were conducted, each of

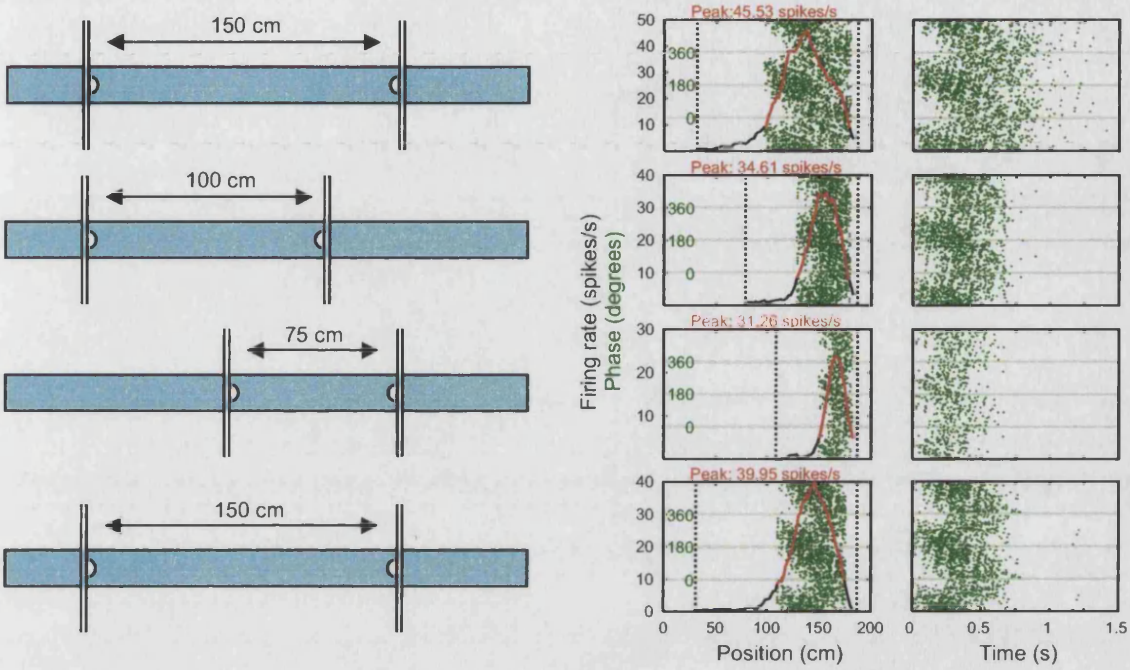

Figure 6.1. The effect of runway compression on one field. **a:** Sample compressed-runway manipulation series. The first and last trials are baselines, with the end walls in the normal position. On the second and third trials the runway is compressed to 100 and 75 cm, by shifting the east and the west walls, respectively. **b**:The response of field 55 to this series of manipulations. Vertical dashed lines represent the end walls. The red trace represents the extent of the field - that is, the region of cell firing exceeding the 20%-of-peak threshold. Peak rates are indicated at the top left of each plot. Green dots represent the spikes comprising the field, plotted versus firing phase. Phase values are indicated in green on the left of each plot. Left hand plots show firing as a function of position on the runway, while the right hand plot shows firing as a function of time. Note the increasing compression of the field and increased slope of the phase precession as the west wall is moved 50, then 75 cm to the east. Firing rate has dropped by over 25% by the third trial. In the right hand column, firing phase for the same four trials is plotted as a function of time since the rat entered the field. The compression of the field and increasing rate of precession in the temporal domain reflects the same trend in the spatial domain.

the two end walls were shifted on separate trials, with the order in which the walls were shifted randomised across days. The most common manipulations were to shift the east or west wall towards the centre of the track by 50 cm. However, 70 cm and 75 cm shifts were also conducted. Figure 6.1a illustrates a trial sequence with mixed wall shifts. Movement of the walls was completed before rats were placed on the maze.

6.2.2 Classification of remapping responses

Moving the walls at either end of the runway effectively altered the sensory and behavioural space of the rat. As might be expected, this occasionally resulted in qualitative changes in place fields which could not be accounted for in terms of the specific manipulation. Types of responses falling into this category, which were referred to as "remapping", included the cessation of firing (or dropping below the 1 Hz firing rate criterion), or the adoption of a firing pattern which could not be readily explained in terms of the manipulation, such as a cell with a field on the west end of the runway switching to firing on the east end. If cell firing on probe trials involved a shift in the position of the field which corresponded closely with the shift of one of the walls, this was considered a parametric response to the manipulation, and not a remapping event.

6.2.3 Analysis of responses to runway compression

A repeated measures design was used for the analysis of the effects of moving the end walls (compressing the runway). Four consecutive trials were considered for each field: an initial baseline trial on which the walls were in the normal position and the runway was 150 cm in length, two trials on which one of the end walls was moved, and a final baseline trial. There was often an additional baseline trial between the two probes, but in the interest of balancing the design, these baselines were omitted. In nearly all cases, the first probe trial involved moving one wall, while the second involved moving the other. In two cases, both probes involved moving the same wall. As described above, the precise amount by which the runway was compressed varied from probe trial to probe trial, but all probe manipulations were considered equivalent for this analysis.

Effects were analysed as trends in the data, analysed using polynomial contrasts, with curvilinear trends interpreted as an indication of change on the probe trials relative to the baselines, and linear trends as an indication of a change in time,

across the four trials. Linear trends would be indicative of effects which were potentially independent of the manipulation. This analysis was used to examine the effect of compressing the runway on running speed, field size, firing rate, field skew, phase precession slope, and the total phase shift for each field. A Bonferroni correction for multiple comparisons was used to adjust the critical value of p.

Movement of the place field in response to the manipulation was not analysed using the repeated measures analysis. As observed in the running speed experiment, the large range of potential place field centroid positions is capable of completely obscuring subtle place field shifts. Also, because the wall which was moved was likely to affect the direction in which the fields shifted, and because the order in which the walls were moved was randomised, any effect of moving an end wall might be further obscured. So instead, field shifts were defined as the difference between the centroid position on any given trial and the centroid position on the most recent preceding baseline. Trials were categorised as being either another baseline, on which neither wall was moved, an "east-wall-moved" probe, or a "west-wall-moved" probe. A one-way ANOVA was used to compare field shifts on west-wall, east-wall, and "neither-wall" moved trials. It should be noted that this data set was more inclusive than the set used for the repeated measures analysis, as all baseline-probe and baseline-baseline pairs within a day's trials were included, not just a baseline-probe-probe-baseline series.

Phase_a and phase_z (mean firing phase of the first and last spikes fired across multiple field traversals) were not analysed using repeated measures ANOVA either, due to the circular nature of the phase data. Instead, a 2-sample Watson's F-test was used to compare phase_a and phase_z on baseline versus compressed runway probe trials. The same trials were utilised for this analysis as were used for the repeated measures analysis, so each field contributed two sets of values. Only CA1 fields were included in the analysis.

In addition to determining the effect of the manipulation on field characteristics, it was also of interest to determine if a change in one characteristic was related to changes in another. Like the field-shift analysis, these analyses were conducted on a larger data set which was not restricted to the sets of four trials used for the repeated measures ANOVA. Change values were calculated as the ratio of values on compressed-track trials to the preceding baseline. For change in phase precession slope, only trial pairs for which the slope values met the inclusion criteria (see General

Methods) were included. Simple correlations were used to compare ratio scores for different field characteristics.

6.3 Results

6.3.1 Remapping on the compressed runway

The runway compression (moving walls) manipulation was tested on 38 fields from 31 place cells in seven rats. Seven of the 38 fields exhibited remapping when the walls were moved. In five of these seven cases, it appeared to be the result of preventing the rat from entering the place field coordinates as defined in the laboratory frame. Place cell firing in these fields appears to have been controlled by features of the environment external to the runway – perhaps features of the laboratory room. The remaining two remapping fields were normally in regions of the runway unobstructed by movement of the walls, and therefore appear to have been principally controlled by features of the runway. It is worth noting that in some cases in which a neuron had more than one place field on the runway, one field would remap in response to the manipulation while another did not. Therefore, it seems as though different fields of the same place cell can behave in different ways in response to the same manipulation. The remaining 31 of the 37 fields studied exhibited persistent firing patterns before, during and after the moving walls manipulation, although there were often subtle differences in field characteristics.

6.3.2 Run speed and firing rate are reduced

Figure 6.1b illustrates a typical response of a place field on the compressed runway. Figure 6.2 presents the results of the repeated measures ANOVA used to investigate the response of individual field characteristics. Moving one of the walls to shorten the runway significantly reduced mean characteristic running speed in the field on probe trials (quadratic $F_{1,29} = 12.536$, $p = 0.001$), and running speed tended to be reduced over the course of the series of trials (linear $F_{1,29} = 12.812$, $p = 0.001$). Mean in-field running speed was 71.29 cm/s on baseline trials, versus 61.66 cm/s on probe trials - a 15% reduction.

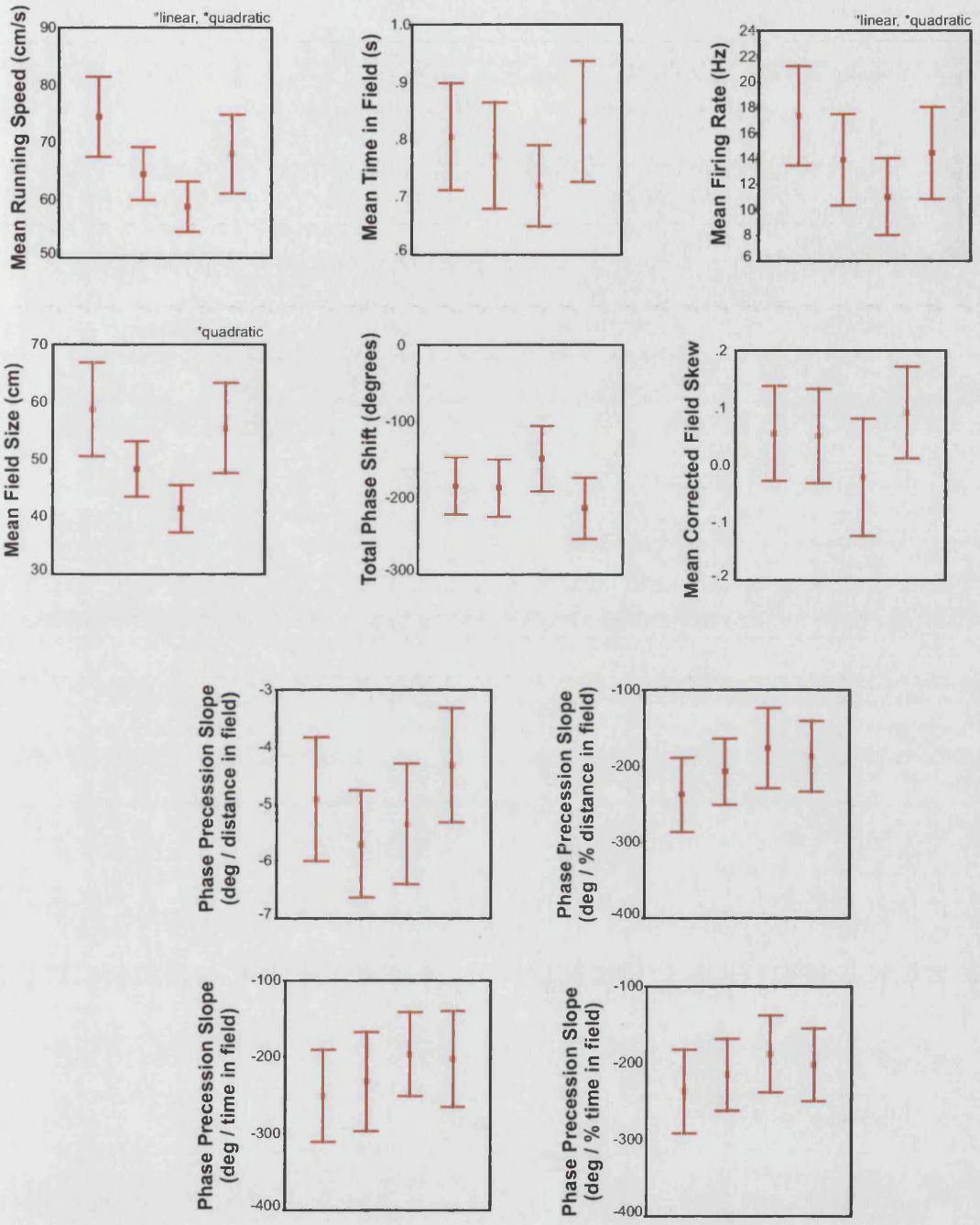

Figure 6.2. Effects of moving the walls on place field characteristics. Data is analysed using a repeated measures ANOVA, across four trials (baseline-probe-probe-baseline). On the two middle probe trials, one of the two walls are moved to shorten the runway. Polynomial contrasts were used to identify linear (time-related) or quadratic (probe-related) trends. A Bonferroni multiple-comparison correction was used, setting the critical p-value at 0.005. Labels above plots indicate whether trends meet this criterion. Probe effects are evident for running speed, firing rate, and field size.

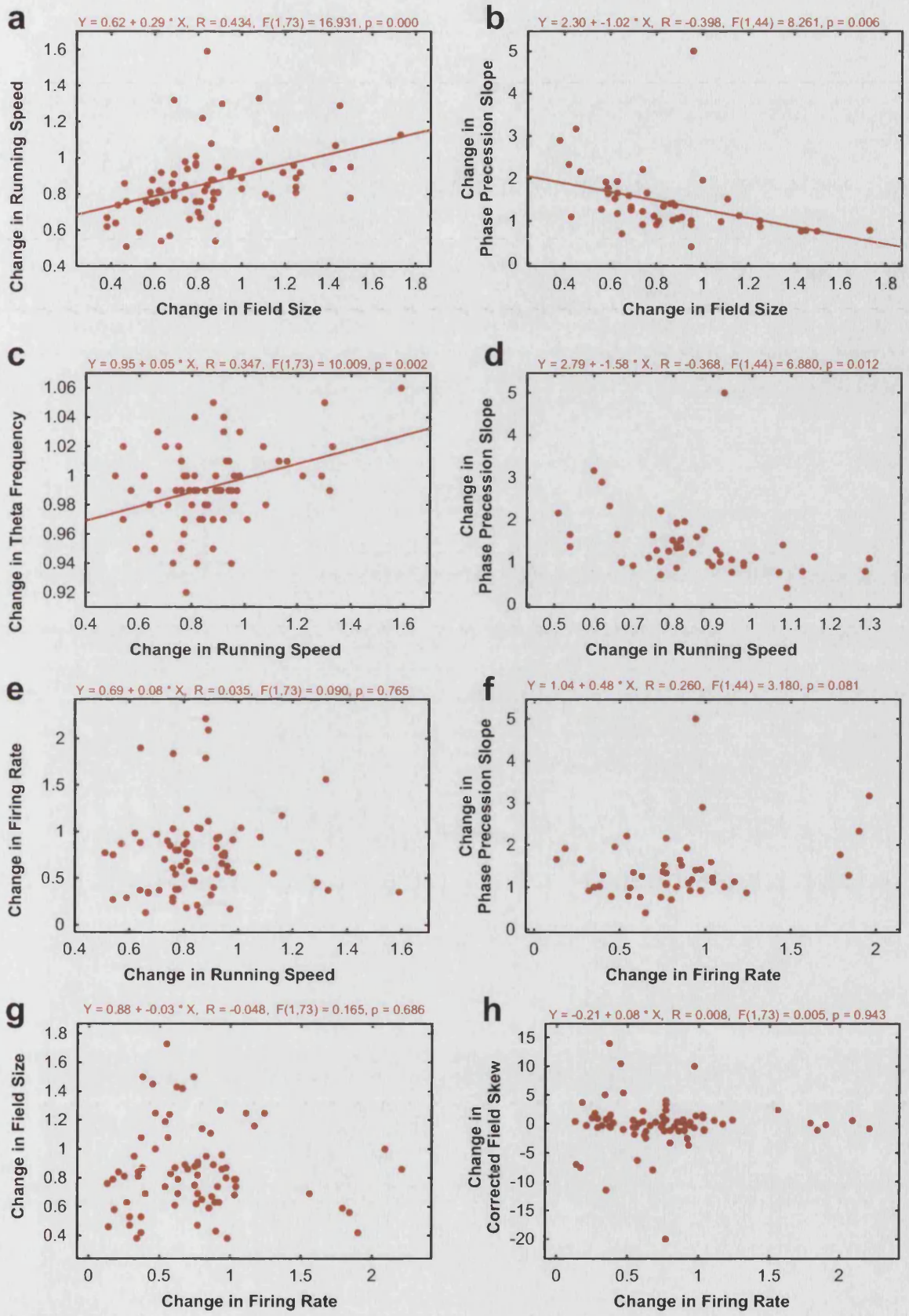

Figure 6.3. Correlations between responses to the compressed runway. Change values are taken only from manipulation trials, and are expressed as a proportion of the value from the preceding baseline trial. Data for phase precession slope is further restricted to trial pairs on which at least 100 spikes were fired on both baseline and probe trial. Linear regression equations and significance values appear above each plot, with best fit lines shown for significant correlations ($p < 0.006$).

a

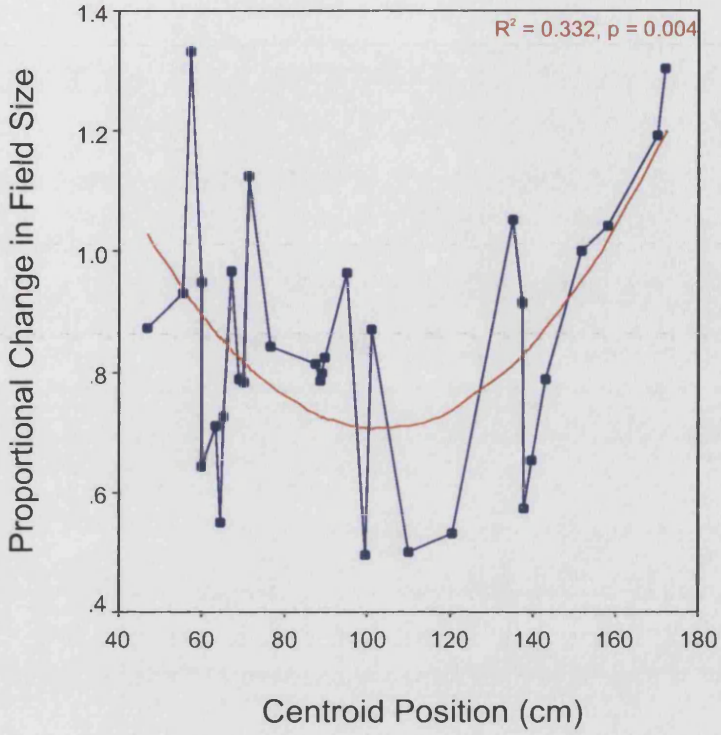

b

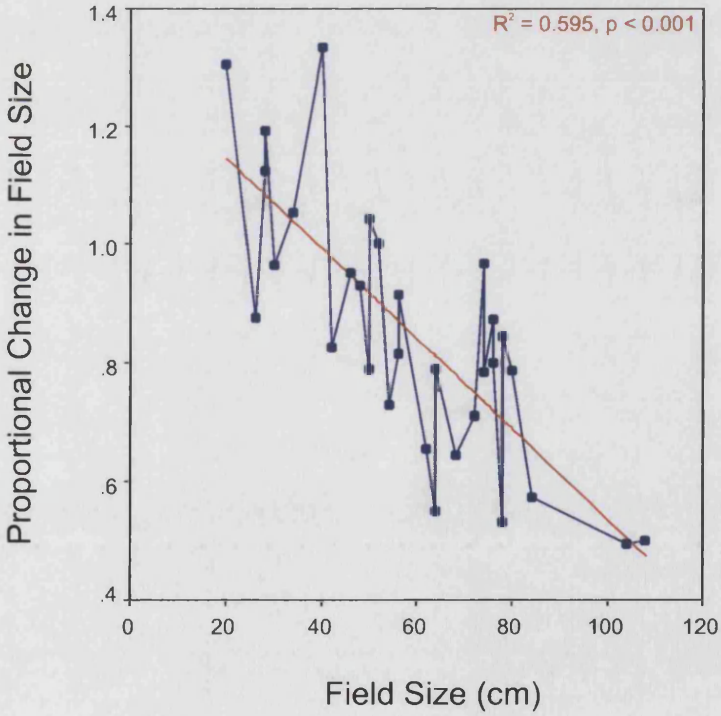

Figure 6.4. The change in field size (delta size) in response to the compressed runway manipulation is related to the original size (**a**) and position (**b**) of the field on baseline trials. Delta size is the proportional change in field size on probe trials, M_P / M_B, where M_p = mean field size on probe trials, and M_B = mean field size on baseline trials. Best fit lines are presented in red. The relationship with field size is the most robust.

Based on previous observations of the relationship between running speed and firing rate(Chapter 5), a reduction in firing rate was expected on probe trials as a consequence of the reduction in running speed. Mean firing rate on probe trials dropped 21%, from 15.93 Hz to 12.55 Hz. The quadratic trend was significant ($F_{1,29}$ = 11.068, p = 0.002), but the linear trend for declining firing rates over the course of the trials just failed to meet the Bonferroni criterion ($F_{1,29}$ = 8.913, p = 0.006).

Figure 6.3 presents the correlations between the proportional change in pairs of place field characteristics on the compressed runway. It is clear that the change in the characteristic running speed for a given place field is correlated with the change in characteristic theta frequency during traversal of the field (Pearson's r = 0.347, $F_{1,73}$ = 10.009, p = 0.002). That is, the greater the drop in running speed, the greater the reduction in theta frequency. Unexpectedly, there was no relationship between the magnitude of the changes in running speed and firing rate (Pearson's r = 0.035, $F_{1,73}$ = 0.090, p = 0.765), and the correlation with the change in phase precession slope failed to meet the Bonferroni criterion of $p < 0.0063$ (Pearson's r = -0.368, $F_{1,44}$ = 6.880, p = 0.012). The magnitude of changes in firing rate was not related to changes in phase precession slope (Pearson's r = 0.260, $F_{1,44}$ = 3.180, p = 0.081) or direction-corrected field skew (Pearson's r = 0.008, $F_{1,73}$ = 0.005, p = 0.943).

6.3.3 Place fields are reduced in size

There was a significant quadratic trend in field size across the baseline-probe-probe-baseline trial series (quadratic $F_{1,29}$ = 16.834. $p < 0.001$), with mean field size reduced 21%, from 57.16 cm on baseline trials to 45.16 cm on probe trials. The resulting tendency for the rat to spend less time in the place field on compressed-track probe trials proved to be non-significant (quadratic $F_{1,31}$ = 4.749, p= 0.037).

The magnitude of the shrinking response varied depending on both the field size and position on the runway – variables which are themselves confounded. A regression analysis revealed a quadratic trend between field size change and position on the runway (quadratic $R^2_{2,28}$ = 0.595., $F_{2,28}$ = 6.970, p = 0.004). There was also a linear trend between field size and field size change: the larger the field, the greater the reduction in field size as a result of compressing the runway (linear $R^2_{1,29}$ = 0.595, $F_{1,29}$ = 42.518, $p < 0.001$). In other words, when the runway is compressed by moving one of the end walls, large fields in the middle of the track shrink more than smaller fields in the periphery. The relationship between field size and shrinkage was the more robust

of the two. This effect is illustrated in Figure 6.4. The magnitude of the change in place field size was also related to the magnitude of the change in running speed. The more a place field shrank, the more the speed at which the rat traversed the field was reduced (Pearson's $r = 0.434$, $F_{1,73} = 16.931$, $p < 0.001$). These results are presented in Figure 6.3.

6.3.4 The phase precession response is ambiguous

As is evident from Figure 6.2, the slope of the phase precession (firing phase vs. position) tended to become more negative on the compressed track, but the effect did not pass the $p < 0.005$ Bonferroni criterion for significance (quadratic $F_{1,11} = 7.796$, $p = 0.018$). The low number of samples contributing to this analysis is related to the strict inclusion criteria – only slopes from significant linear fits of the phase precession were included, and only from trials in which at least 100 spikes were fired by the cell.

As previously noted, phase precession can be measured in other ways – for example, as a temporal (instead of spatial) function. However, there was no significant effect of compressing the runway on phase precession slope when measured as a function of the proportion of the field traversed ($F_{1,15} = 1.153$, $p = 0.300$), the time spent in the field ($F_{1,15} = 1.040$, $p = 0.324$), or of the percentage of the total amount of time spent in the field on each run ($F_{1,15} = 0.007$, $p = 0.934$). While non-significant, the only measure of slope which appeared sensitive to runway compression was phase versus position. Each slope value is derived from a regression fit between firing phase and the respective measure of time or position. Figure 6.5 shows a comparison (baseline vs. probe) of the mean Pearson's r-values for the fit between firing phase and each of position-in-field and time-elapsed-in-field. It is clear that on both baseline and compressed runway probe trials, the correlation with position is better.

However, despite the non-significant change in phase precession slope (as a function of position), the magnitude of the change in slope was directly related to the magnitude of the change in field size. The more the field shrank on the compressed runway, the steeper the phase precession slope became (Pearson's $r = -0.398$, $F_{1,44} = 8.261$, $p = 0.006$). This effect is illustrated in Figure 6.3b. It should be noted that the preceding analyses were based on change values for every valid baseline-probe pair, and included a small amount of data which was not included in the 4-trial between-subjects analysis: from two cells for which probe trials were conducted on two days, and for one cell on which three probe trials were conducted on one day. Nevertheless,

even using ratio scores from the repeated-measures analysis (mean probe / mean baseline) yielded a significant correlation between field size change and slope change (Pearson's r = -0.561, $F_{1,20}$ = 9.202, p= 0.007). This is provided that the slope-change outlier at value 5.00 is removed (field 31).

A second ambiguity surrounds the effect of track compression on the mean extent of the phase precession. The results are presented in Figure 6.6. There was no significant difference between baseline and probe trials in terms of firing phase upon entry to the place field ($F_{1,97}$ = 0.209, p = 0.649). The uniformity of the distributions of values, however, makes it uncertain as to whether an effect is being masked. In contrast, phase_z values were reasonably clustered around their means, and there was a significant difference between baseline and probe trials – on the compressed runway, the last spike as the rat exits the field occurs later in the theta cycle than on baseline trials ($F_{1,97}$ = 5.388, p < 0.022). This ought to result in the reduction of the total amount of phase precession on the compressed runway. However, the repeated-measures analysis, which compared phase shift (phase_z – phase_a) on baseline vs. compressed runway trials, indicates that there is no effect (quadratic $F_{1,29}$ = 2.454, p = 0.128). Mean phase shift on the baseline trials was -198.468^0 (s.d.= 70.687), versus -167.702 (s.d. = 84.247) on probe trials.

6.3.5 Compressing the runway shifts field centroids

Movement one of the walls to compress the runway clearly had an effect on the position of the field's centroid, but the direction of the field shift depended on which wall was moved. The effect of trial type on field shift was significant ($F_{2,158}$ = 111.690, p < 0.001), as illustrated in Figure 6.7a. Moving the east wall westward nearly always produced westward field shifts, while moving the west wall eastward nearly always produced eastward centroid shifts. On baseline trials, the null-change value of zero fell within the 95% confidence interval for field shifts.

The relationship between the original field position and field shift was also investigated. For each category of wall movement (east or west), regression analyses were conducted to compare the magnitude of the field shift to the original position of the field on the runway. Field shifts were calculated as the difference between centroid positions on probe versus baseline trials, and thereby compensated for the large variance in centroid position between different fields. The closer the field to the wall which was moved, the more the field shifted in the same direction, whether the west

Figure 6.5. Firing phase is better correlated with distance travelled in the field (pos) than time elapsed (time). This holds for both baseline trials and compressed-runway trials.

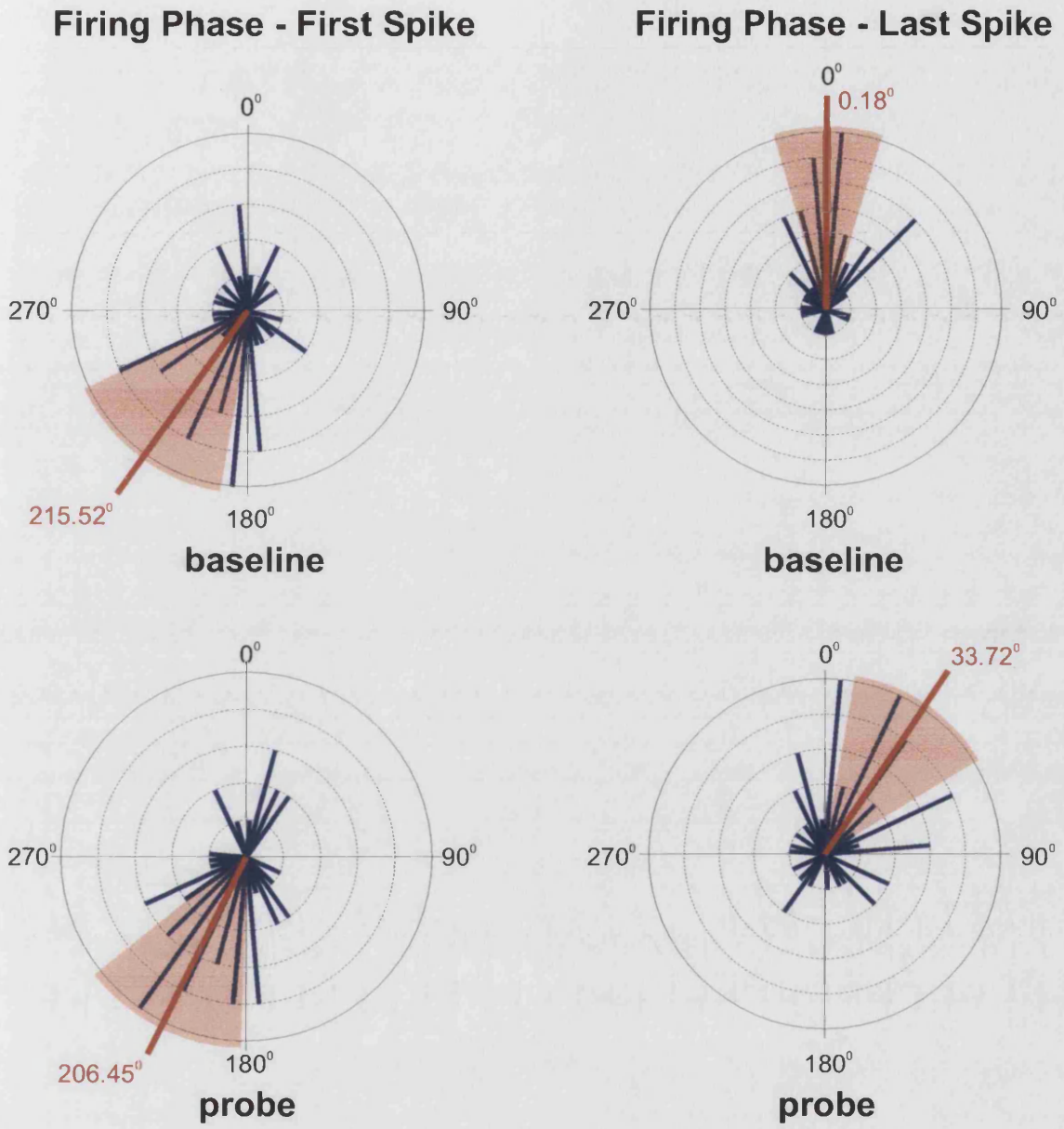

Figure 6.6. The effect of runway compression on firing phase. Plots are circular frequency histograms, with mean values indicated in red, and the 95% confidence intervals defined by the shaded areas. The firing phase of the first spike as the rat enters the field appears unchanged on probe trials, but last spikes tend to fire at a later phase ($p < 0.01$). Data from five DG/CA3 cells is omitted. Baseline and probe data are combined data from the two baseline and probe trials (respectively) which constitute the four-trial series from the repeated measures analysis.

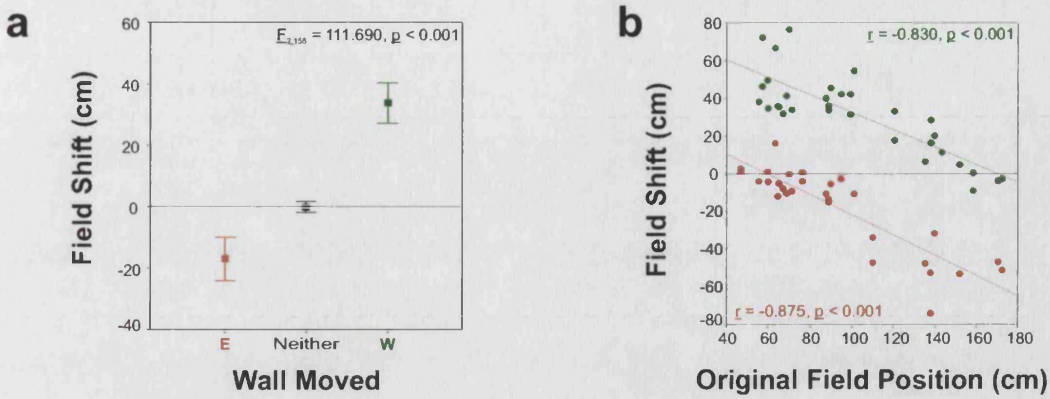

Figure 6.7. Analysis of field shift responses. **a:** Westward movement of the east wall produces negative (westward) field shifts, while moving the west wall to the east produces positive (eastward) field shifts. Field shifts for baseline trials, when neither wall was moved, are included to demonstrate the stability of field position in the absence of any manipulation. **b:** The magnitude of the shift is proportional to the proximity of the field to the wall which was moved. Shifts tended towards zero for fields which were furthest from the wall that was moved. Data is broken down depending on whether the east (red) or west (green) wall was moved. Coloured lines represent the least squares fit for each subset. Baseline trials are omitted. Error bars indicate 95% confidence intervals.

wall was moved east (R^2 = 0.689, $F_{1,30}$ = 66.570, p < 0.001), or the east wall was moved west (R^2 = 0.765, $F_{1,27}$ = 88.074, p < 0.001). In both cases, field shifts tended towards zero for fields furthest from the shifted wall. Conversely, fields closest to the shifted wall moved approximately by the same amount as the wall (50-75 cm). These results are presented in Figure 6.7b.

6.4 Discussion

6.4.1 The shifting of relative field positions

Few place cells remapped on the compressed runway, and those which did tended to normally have fields on regions of the runway made inaccessible by movement of the end wall. This suggests that these fields were defined by positional cues in the "room" reference frame. The multi-field cells in which only one field remapped on the compressed runway seem comparable to the "disjunctive cells" observed by Gothard et al. (1996a), and suggest that place cells are capable of encoding information from multiple reference frames, even simultaneously (see also Bures et al., 1997; Zinyuk et al., 2000).

However, the most dramatic and consistent effect of compressing the runway was the shifting of place fields in the direction of the wall which was moved, as illustrated in Figure 6.7. Fields closest to the wall being moved shifted by approximately the same amount as the wall shift itself (typically 75 cm), while fields furthest from the shifted wall, and closest to the opposite wall, tended not to shift at all. The fact that the amount of field shift was directly related to the fields "normal" position on the uncompressed track has a very important implication - namely, the topographical relationship between place fields is preserved, along with the number of place fields which are active. If, when the west wall was shifted eastward by 50cm, all fields also shifted 50 cm eastward, there would be some fields which would be pushed beyond the confines of the runway, and would therefore no longer contribute to the representation of the runway. If the fields shifted by random amounts, then the order of the fields would become disrupted, along with any ability of the hippocampus to accurately encode stereotyped sequences of positions visited. Phrased differently, this suggests that the inputs to place fields are not merely random constellations of visual inputs, but that inputs are weighted somehow on the basis of proximity to the field. These findings

strongly support the model proposed by O'Keefe and Burgess (1996), which predicts that Gaussian tuning curves peaking near the wall they are tuned to will be narrow and high. The height of the Gaussian is related to the degree it contributes to the firing of the place field, and consequently, is indicative of the degree of control over it. The further a field from a given wall, the weaker the influence of that wall on it, with mid-runway fields being influenced by both.

The field shift results of the current experiment are very similar to those of Gothard et al. (1996b), who also varied the distance rats shuttled on a runway. Gothard and colleagues interpreted the result as a switch in place field control from path integration to environmental cues at some point along the runway (Gothard et al., 2001). However, the imposition of a "switch" point is somewhat arbitrary and unnecessary - it is just as reasonable to assume that there is a gradual shift in the weighting of each type of information. Moreover, there is no reason to assume that the shift is from idiothetic to environmental cues, as opposed to from one end of the runway to the other. Indeed, there is no need to invoke idiothetic cues at all. Nevertheless, the possibility cannot be excluded, and a potential source of path integration information - motor efference copy - will be investigated in Chapter 9.

6.4.2 Field size and phase precession slope

Provided there was no remapping, place fields tended to shrink on the compressed runway. This reflects similar responses to changes in environmental geometry in open-field experiments (Muller & Kubie, 1987; O'Keefe & Burgess, 1996) and in previous linear track experiments (Gothard et al, 1996b). Phase precession slope also tended to become more negative on the compressed runway, although the effect failed to reach significance. Two things should be considered here, however. First, the mean change in slope was -1.027 degrees/cm (s.d. = 1.595), representing a 47% average increase (based on mean values for probe and baseline trials for each field) – this is a considerable change which might have passed the Bonferroni-adjusted F-test, provided a larger sample size. Second, the magnitude of the change in slope was directly related to the magnitude of the change in field size (Figure 6.3b), with fields whose size remained constant on the compressed runway exhibiting little or no change in phase precession. These were typically small fields with centroids near the ends of the runway (Figure 6.4), and including them in the analysis doubtless weakened the mean response to runway compression.

The relationship between changes in field size and slope is consistent with observations from Chapter 4, in which it was clear that field size and phase precession slope were correlated. It is also consistent with other studies (O'Keefe & Recce, 1993; Skaggs et al., 1996) which suggest that the range of firing phases subtended is usually about 360^0. Preservation of the extent of phase precession across fields of different sizes would necessitate a scaling of the slope of the precession, and given the current results, it is clear that inducing changes in the size of place fields results in a proportional change in the phase precession slope.

6.4.3 A Truncated precession?

It is not quite fair to say that the extent of phase precession has been preserved, on the compressed runway, however. The mean firing phase of the last spike during field traversals occurred significantly later in the theta cycle (Figure 6.6), suggesting a truncation of the phase precession by about 45^0. Superficially, given the 21% reduction in firing rate, these results support the notion that decreased depolarisation may have caused spike firing to "stall" in a portion of the theta cycle where it could no longer overcome the inhibition in earlier portions of the cycle. However, there is no evidence from the running speed and firing rate analyses in the previous chapters to suggest that either of these factors directly produce effects on the phase precession.

One possible explanation is that the latter portion of place fields, the portion apparently truncated or absent on the compressed runway, represents a different component of the spatial code from the earlier portion of the field. Wallenstein and Hasselmo (1997) proposed that late in the theta cycle, when place cell firing typically begins, there is a reduction in GABAergic inhibition specific to intrinsic hippocampal pathways which support the transmission of prospective spatial information - that is, early portions of the place field (late portion of the theta cycle) are dominated by anticipatory firing based on experience. This is consistent with the experience dependent asymmetric expansion of place fields observed by Mehta et al. (2000). Conversely, Wallenstein & Hasselmo suggest that late portions of the place field (early in the theta cycle), where GABAergic inhibition begins to rise again, are characterised by an inhibition of intrinsic hippocampal circuits, so that external inputs dominate. Such external inputs might be sensory input conveyed via the entorhinal cortex. Yamaguchi et al. (2002) observed that the phase precession of CA1 place cells is best described

as not one, but two Gaussian components - an early component (N1) which is roughly linear, and a late component (N2) which is more "amorphous" - a blob, if you will. Combined, N1 and N2 give the phase precession a curvilinear appearance, as described previously by O'Keefe & Recce (1993) and Skaggs et al. (1996). Indeed, the appearance of two components of phase precession, separated in phase but overlapping in space, can be seen in much of the data presented in those two works, and in the present experiment as well. Could the truncated fields on the compressed runway be missing the N2 component of the precession? In other words, is the early portion of the field, based on expectation, intact, while the late portion, dependent on the unique constellation of sensory cues which signal position, missing or severely attenuated?

Figure 6.8 presents a hypothetical model to explain the truncation of the phase precession on the compressed runway, in terms of suppression of the N2 component. Figure 6.8a,b shows actual recorded data from field 17 on a baseline and compressed-runway probe, respectively. Spikes are assigned to N1 or N2 based on firing phase, firing position, and the apparent discontinuity n the precession (Yamaguchi et al., 2002). On the compressed runway (Figure 6.8b) note the compression of the place field and the relative absence of early-phase spikes late in the field. Figure 6.8c,d presents a hypothetical model explaining the results. N1and N2 are presumed to arise from Gaussian inputs. Note that the N2 input could easily be the summation of multiple Gaussians from direct sensory inputs (O'Keefe & Burgess, 1996). N1 is assumed to be preserved on the compressed runway, based on previous learning of the sequence of events leading to arrival at a given location. However, when the rat arrives at the predicted location, there is a mismatch between any number of inputs contributing to N2 - for example, the rat's idiothetic senses may be informing the hippocampus that it ought to be at position "X", having moved the appropriate distance from the end of the runway, but the unusual appearance of the runway suggests otherwise - the end wall on the compressed runway will appear much closer than it ought to be. This mismatch results in net attenuation of the N2 drive to the place cell. The end result is a net reduction in firing and the near absence of N2 spikes as the spatial distribution of firing becomes biased towards the predictive N1 input. Note that no effort is made in this simple model to account for the compression of the field and the shift in the direction of wall motion - which are presumed to arise directly from changes in the dynamics of the N2 inputs.

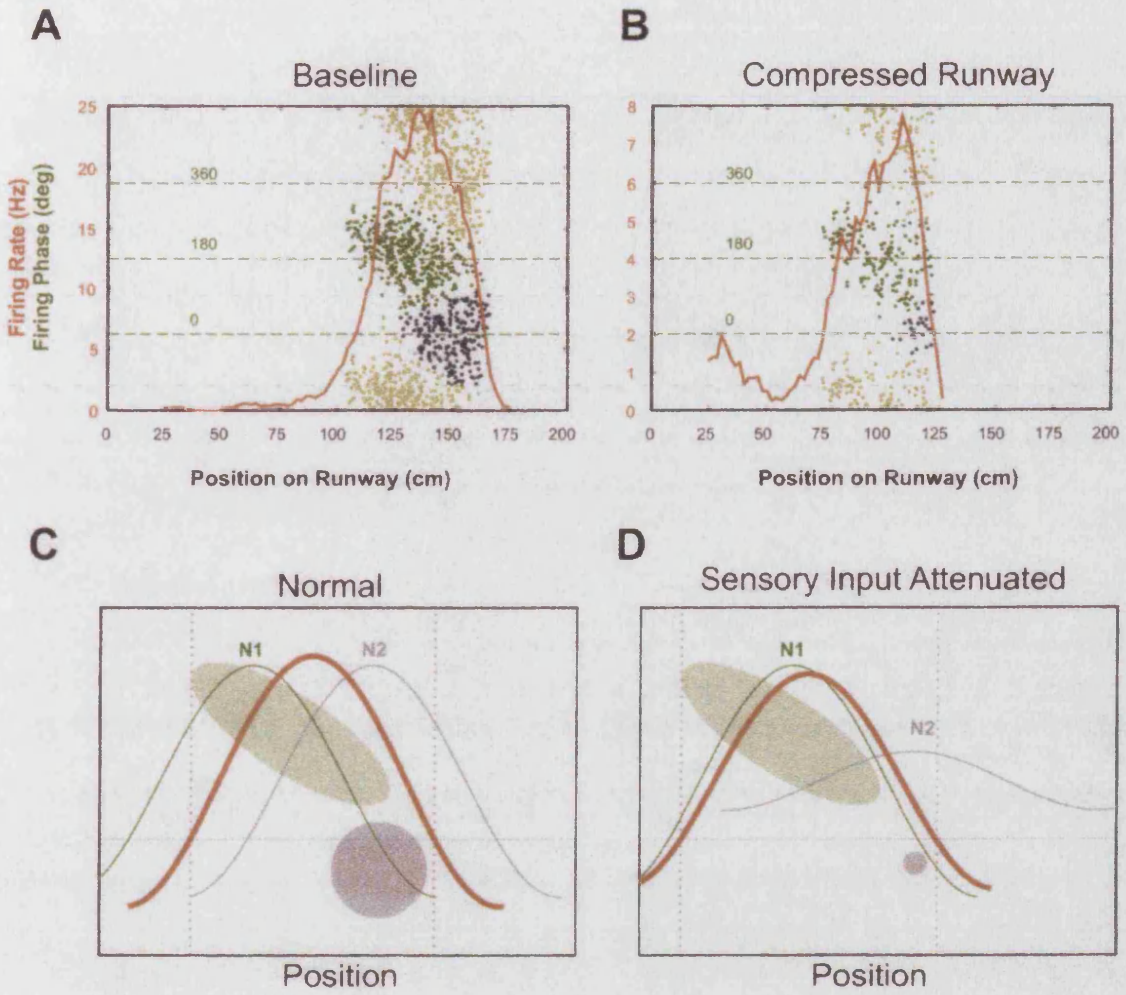

Figure 6.8. Panels A & B: Field 17 on a baseline and compressed runway probe trial, respectively. Firing rate (red line) and firing phase (green dots) are presented simultaneously. Phase data is duplicated so the origin doesn't obscure the phase precession effect. Unique points taken to best represent the phase precession are highlighted. These are colour coded to represent the putative N1 (green) and N2 (blue) portions of the precession, after Yamaguchi et al (2002). Assignment is based on the apparent discontinuity in the spike cloud, and the assumption that N1 spikes are driven by anticipatory inputs late in the theta cycle and early in the field, while N2 spikes are driven by sensory inputs, early in the theta cycle and late in the field (after Wallenstein & Hasselmo, 1997). On the compressed runway (Panel 8), note the reduced firing rate, relative preservation of the N1 portion of the phase precession, and the near absence of the N2 portion. Panels C: a proposed model, baseline condition. The curves N1 and N2 define independent inputs responsible for the two portions of the phase precession, which, when summed, determine the net excitation to the cell (red). Horizontal line: firing threshold of cell. Vertical lines: spatial extent of cell firing. Shaded areas: representations of N1 and N2 portions of the phase precession attributable to each input, bounded by the spatial extent of cell firing. Panel B: the response to N2 being attenuated by 75%. Cell firing is now driven principally by the intrinsic, anticipatory input (N1), and the N2-associated spikes are dramatically reduced. Increased control by N1 shifts the region of cell firing away from the N2 peak. Overall firing rate is reduced, but the Gaussian shape of the field is maintained.

6.4.4 Running speed effects

Running speed was significantly reduced (15%) on the compressed runway, and it is tempting to conclude that the change in running speed brings about a concomitant change in field size, given the relationship between field position, running speed and field size on baseline trials. However, I have already demonstrated that a 27% reduction in run-by-run running speed, produced by natural variability in the rat's behaviour, fails to have any effect on field size. Therefore, it seems unlikely that the reduction in field size seen here is the result of changes in running speed, even though the magnitude of the change in running speed is highly correlated with the change in field size (Figure 6.3a). And why might this be? Assuming the hippocampal representation of space is used to guide behaviour, and assuming stereotyped running is guided by the perception of distances, a compressed representation in a particular region of the runway ought to induce a compensatory reduction in running speed. It is not surprising and probably adaptive, therefore, that the fields which shrink the most on the compressed runway are those which are normally found in the region of the runway where the rat typically runs the fastest - in the middle (Figure 6.4).

The more a rat's running speed was reduced on the compressed runway, the more the rat's theta frequency was reduced. This relationship is apparent even though theta frequency itself is not significantly reduced on compressed runway trials. This may be because the relationship between theta frequency and running speed is more robust than the relationship between theta frequency and the manipulation. Indeed, for 10/31 fields, theta frequency increased on the compressed runway, while two fields exhibited no change, and theta frequency was reduced on the remaining 19 fields. This is by no means a consistent response, but is not inconsistent with a relationship to running speed changes which do exhibit more consistent responses.

Chapter 7: Lowering the End-Walls

7.1 Introduction

The results of the compressed runway experiment indicate that changing the dimensions of the environment alters the size and position of place fields, without altering their topographical relationship with one another. This is consistent with the notion that place fields are tuned to distances from environmental boundaries (O'Keefe & Burgess, 1996). One of the cues a rat might use to estimate distances to boundaries is the visual angle to the top (or side, or bottom) of the boundary.

In the current experimental paradigm, one way of manipulating the visual angle to the top of the end-walls, without actually changing the dimensions of the environment, is to alter its size. Under normal conditions, the walls at either end of the runway are more than twice as high as the walls on the sides. Reducing the size of the end walls by 50% would result in a dramatic change in the visual angle to the top of the wall at any given position on the track. If the rat used the angle as an estimate of distance to the wall it was approaching, reduced height should give the illusion that the rat is further away from the wall than it actually is. This would result in a shift in the position place fields, toward the lowered wall.

7.2 Methods

For this manipulation, one of the end walls was replaced by a half-sized wall made of the same material. This manipulation leaves the dimensions of the track unaltered, but like the moving walls manipulation, affects the visual angle to the top of the wall for a rat at a given position on the runway. It is designed to test the contribution to place cell firing of this particular source of information. One might expect, for example, that based on the visual angle to the top of the wall, a field which normally fires mid-runway when the rat is running east might be shifted east if the east wall is replaced by the half-sized wall.

A repeated-measures ANOVA was used to investigate the effect of changing the apparent height of either of the end walls. For each field, series of four trials (baseline-probe-probe-baseline) were analysed. Centroid position and skew (uncorrected for running direction), might have been expected to exhibit an asymmetric

response to the lowering of the west versus the east wall. The basic assumption is that if place cells respond to visual cues to distance related to the visual angle to the top of a wall, lowering the height of that wall should shift the field towards that wall, or cause it to become less skewed towards the middle of the runway. Consequently, for the analysis of these variables, trials were shuffled so that trial-2 always represented a lowering of the west wall, while trial-3 always represented a lowering of the east wall. A wall-specific response to the probe manipulation ought, therefore, to result in each probe differing from the baselines, but in opposite directions. Such cubic effects might be expected for variables whose units of measure correspond to the asymmetric distribution of firing in space: that is, centroid position and field skew. A Bonferroni correction for ten analyses put α at 0.005.

7.3 Results

Twenty place fields were studied under the lowered-wall condition. In no case did any of the place fields disappear or remap under this condition. The results are summarised in Figure 7.1. There were no significant quadratic effects of the lowered-walls manipulation on firing rate ($F_{1,16} = 0.771$, $p = 0.393$), place field size ($F_{1,16} = 1.099$, $p = 0.310$), direction-corrected field skew ($F_{1,19} = 0.025$, $p = 0.876$), phase precession slope ($F_{1,8} = 0.369$, $p = 0.560$), or total phase shift ($F_{1,16} = 0.084$, $p = 0.776$). The apparent increase in running speed on the lowered-wall probe trials ($F_{1,16} = 7.195$, $p = 0.016$) failed to pass the Bonferroni criterion of $p < 0.005$. There was neither a quadratic ($F_{1,16} = 0.500$, $p = 0.490$) nor a cubic ($F_{1,16} = 0.266$, $p = 0.613$) effect on uncorrected field skew. Similarly, there was neither a quadratic ($F_{1,16} = 1.099$, $p = 0.0310$ nor a cubic ($F_{1,16} = 0.169$, $p = 0.687$) effect on field position.

The effect of the manipulation on field position was further analysed by comparing the change in centroid position on each trial relative to the preceding baseline trial. This compensates for the large, uniform distribution of place fields on the runway, and the possibility that place field shifts were relatively small. However, a one-way ANOVA indicated that there was no significant effect of wall height on field position ($F_{2,70} = 1.894$, $p = 0.158$). A regression analysis was used to compare the magnitude of the response to the original position of the place field on the runway (from the first baseline trial of that day). In contrast to the compressed runway manipulation, lowering the walls did not produce responses which were related to the original field position.

This was true whether the lowered wall was in the west (r = 0.213, $F_{1,15}$ = 0.709, p= 0.413) or the east (r = 0.007, $F_{1,21}$ = 0.001, p= 0.974). The results are presented in Figure 7.2.

7.4 Discussion

Lowering the end walls appears to have no effect on any characteristic of the place fields. This was somewhat disappointing, given the general assumption that visual input plays an important roll in defining the position of place fields in an environment. Specifically, lowering the wall was expected to cause fields to shift in the direction of the wall, as the reduction in the visual angle to the top of the wall might be interpreted as a greater distance separating it from the rat at any given moment. It is worth noting that there was a non-significant trend in the data which was consistent with this hypothesis, and it may be that with a larger sample size, the test would have been significant. However, even the small shifts which were observed were in no way correlated with the proximity of the field to the lowered wall - a very robust relationship in the compressed runway trials.

Of course, it is reasonable to assume that rats make use of a wide variety of information sources when updating information about their current position. It may be that the visual angle to the top of the end walls is less important than other visual cues - for example, the visual angle to the junction of the end wall and the runway surface, or the apparent width of the end wall they are approaching. There is an abundance of evidence that rodents make preferential use of certain types of spatial cues (Gallistel, 1990; Alyan & Jander, 1994;McNaughton et al., 1996). Another possibility is that the weighting of particular sensory cues is not as important as the consistency of information provided by constellation of cues. Previous studies have shown that hippocampal representations of space tend to maintain their integrity when individual cues are removed from the environment (O'Keefe & Conway, 1978; Hetherington & Shapiro, 1997; Martin & O'Keefe, 1998), and even when cues from entire sensory modalities are put at odds with one another (Best & Thompson, 1989; Sharp et al., 1995; Huxter et al., 2001). In other words, the visual angle to the top of the end wall may well be an important source of spatial information, but in the presence of other sources of information which are consistent with one another, this particular source is insufficient to affect place fields in a significant way.

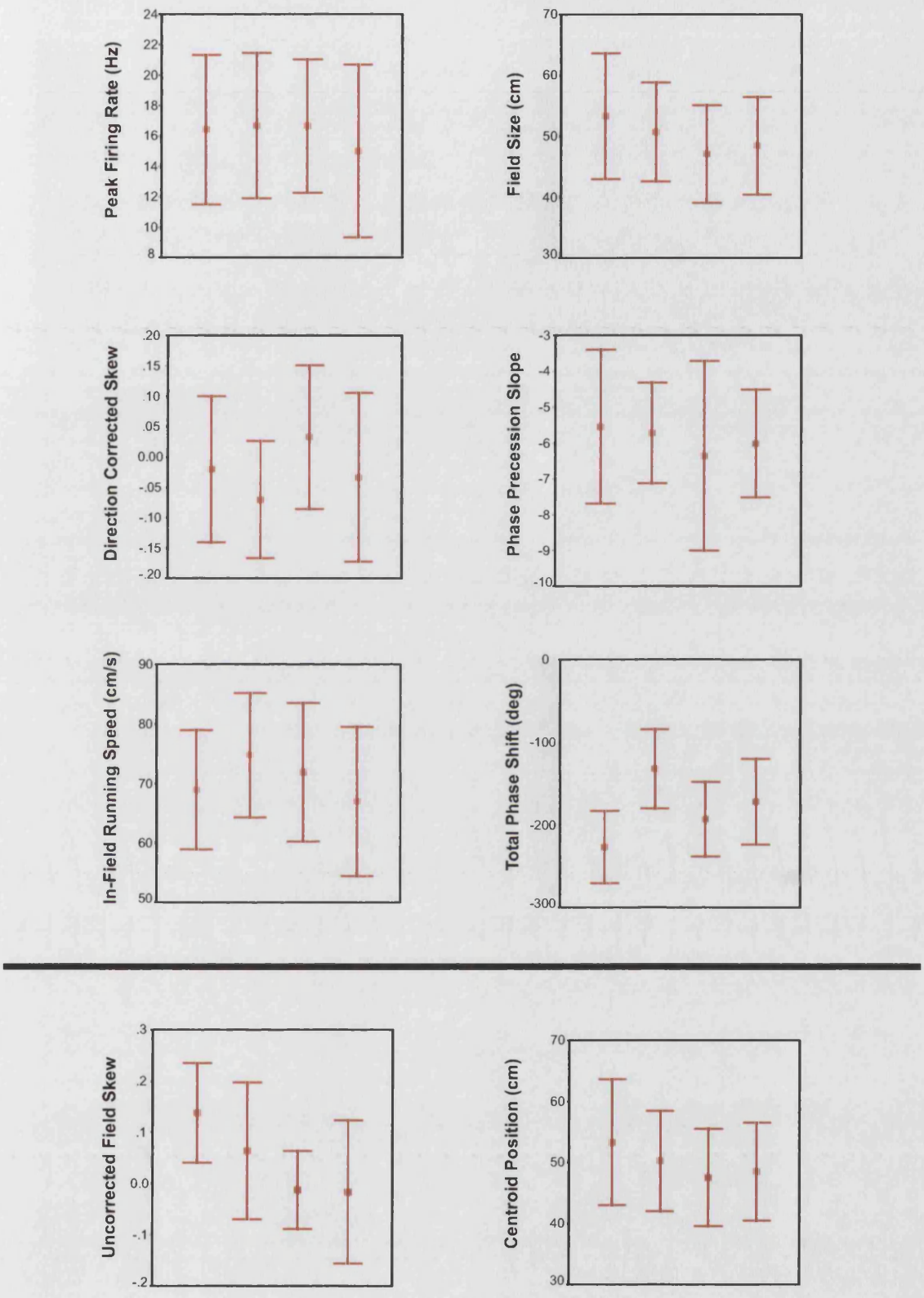

Figure 7.1. The effect of lowering one of the end walls. Four trials were compared - baseline, probe, probe, and baseline. In the bottom panel, trials are shuffled so that trial-2 reflects lowering of the west wall, while trial-3 reflects lowering of the right. This enables detection of the cubic trend that would result from a wall-specific effect on uncorrected field skew or centroid position (trial 2 & 3 should deviate from baseline trials 1 & 4 in opposite directions). There was no significant tendency (Bonferroni criterion: $p < 0.005$) for probe trials to differ from baselines on any of the measures. Error bars: 95% confidence intervals.

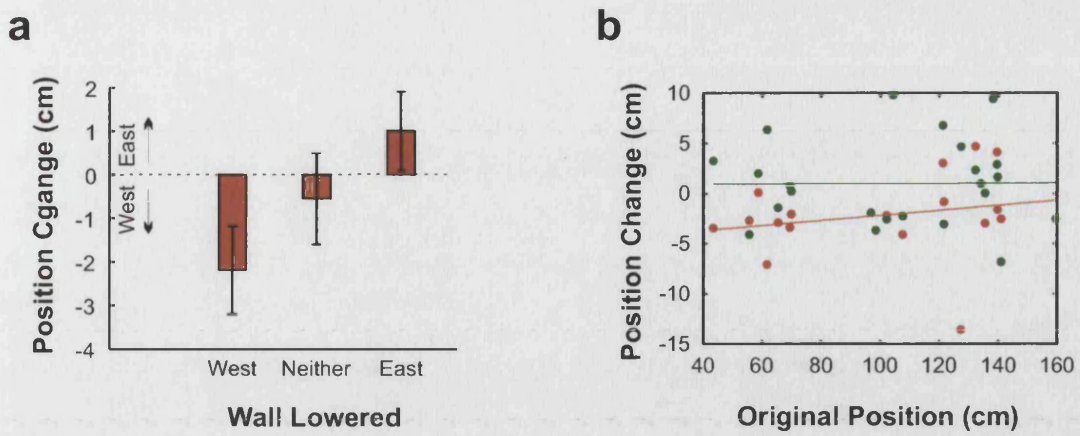

Figure 7.2. Field shifts in response to lowering one of the end walls. **a:** Field shifts as a function of the wall lowered. Change scores for baseline trials are also included. Field positions are compared with the previous baseline probe. Error bars are SEM. Lowering the west or east wall tended to produce westward or eastward field shifts, respectively. However, the effect was not significant. The right hand panel com. **b:** The magnitude of the shift as a function of the original position of the field on the runway. Data is categorised according to whether the west wall (red) or east wall (green) was lowered, and lines represent the best least-squares fit. Regardless of which wall was lowered, there was no relationship between field centroid position and the response to the manipulation.

Chapter 8: Moving Treadmill

8.1 Introduction

There is ample evidence that path integration plays a role in navigation (Barlow, 1964; Mittelstaedt & Mittelstaedt, 1980; Thinus-Blanc et al., 1987; Alyan & Jander, 1994; Collett & Collett, 2000) and very likely plays a role in the firing of place fields as well (O'Keefe, 1976; McNaughton et al., 1996; Save et al., 1998). While theories of place cell function have often treated sensory-based navigation and path integration as opposing models, spatial map theory has, from the start, acknowledged that both sources of information converge in the hippocampus, and both probably contribute to place cell firing (O'Keefe & Nadel, 1978). The question remains, however, whether it can be shown that hippocampal place cells encode idiothetic information.

Samsonovich and McNaughton (1997) have proposed an attractor network model of the hippocampus in which the "activity packet" of active neurons is shifted by information about the rat's momentary movements, with only periodic reference to sensory stimuli to correct for the cumulative error inherent in path integration. The moving treadmill experiment was designed explicitly to investigate whether idiothetic information contributes to the location of place cell firing in this manner - in particular, information derived from step counting or motor efference copy. Not only does this manipulation address the contribution of idiothetic information to the topography (versus the orientation) of the spatial map, but it permits direct predictions of the direction of the effects, based on the direction the treadmill is run.

8.2 Methods

8.2.1 Overview

On these trials, the treadmill was set to run at much higher speeds than during baseline trials (baseline speed < 0.4 cm/s, see section 2.9), so that the movement was clearly perceptible by the rat. The most common treadmill speed was about 7.5 cm/s, although speeds ranged from 2.50 cm/s to 11.25 cm/s. The direction in which the track moved was chosen in a pseudo-random fashion to ensure that both directions were used equally for each rat. As runway floor was always moving in a particular direction

within a trial, the rat was running with the track motion in one direction and against it in the other. When running in the same direction as the treadmill, the rat had to learn to walk in reverse at the end of the track to avoid being forced into the wall by the movement of the floor while eating. At the other end of the track, the rat would typically be passively transported towards the middle of the track while eating the rice before turning to run in the opposite direction.

This manipulation serves to dissociate motor efference and step-counting information about movement, from which the animal can determine its position, from all other sources of information. For example, the rat running east arrives at the mid point of the runway with visual cues, optic flow, and vestibular information all suggesting that he is indeed in the middle of the runway. However, if the treadmill is running east, the rat will have made less effort or taken fewer steps to get there, and we might expect, on the basis of this information, that place fields will be shifted in the direction of the movement of the treadmill. Given that only motor information has been altered, any observed shift in the place field relative to the baseline trials would have to be attributable to the role of information from motor efference copy. Assuming motor information contributes to the spatial firing properties of place fields, shifts in the direction of the treadmill's movement should be observed.

It should be noted that while the speeds at which the treadmill was run were fairly low, higher speeds generally proved too disruptive to behaviour, so the predicted shifts in place field position were relatively small. The predicted treadmill-induced shift was also proportional to the time (from the initiation of a run) that it takes the animal to reach the field under normal conditions, with longer times permitting larger amounts of passive displacement before the field is reached. This time is obviously directly related to the position of the field on the runway and the speed at which the rat runs.

8.2.2 Analysis

Remapping responses were categorised in the same manner as for the compressed runway experiment. Similarly, parametric responses to the moving treadmill manipulation were analysed using a repeated-measures ANOVA performed on blocks of four selected trials: baseline1, probe1, probe2, and baseline2. Only blocks of trials in which the treadmill was run in both directions (east and west) were included. Further limitations were imposed on cases included in the analysis of phase precession

slope - only slope values from significant linear fits of firing phase versus position were included, and only those values based on over 100 spikes.

If on either of the two probe trials the place field disappeared, or exhibited a remapping response, that field was omitted from the repeated measures analysis. Treadmill direction was coded as being either in the same direction or opposite the direction in which the rat ran when a given place field was active. Trial sequence was shuffled so that "opposite" probe trials always preceded "same" probe trials. This permitted detection of effects which were specific to the direction of treadmill motion as a cubic trend, and non-specific effects as quadratic trends. This analysis was used to investigate the effect of the manipulation on firing rate, place field size, direction-corrected field skew, phase precession slope, total phase shift, and theta frequency.

The moving treadmill was expected to have a fairly significant impact on the rat's behaviour. Preliminary tests suggest that it takes time for some rats to become comfortable shuttling under the probe conditions. They must also learn to "back-peddle" at the end of the runway when the treadmill is moving in the direction they run, to avoid crashing into the end-wall. In some cases, place cells failed to fire "normally" on initial moving-treadmill trials. Where several exposures to the manipulation were conducted for a given place field, if subsequent exposures suggested that the field "learned" to fire on the moving treadmill as behaviour improved, these trials were used instead of the initial ones. If the field showed no improvement, first-exposure trials were used.

Another consequence of the moving treadmill manipulation is that running speeds estimated from the fixed perspective of the video camera fail to capture the effort expended by the rat, or the rat's perceived rate of movement based on proprioceptive or motor efference information related to the movement of its legs. Therefore, another variable was created for inclusion in the repeated-measures analysis. "Corrected running speed" was calculated as camera-perspective running speed minus the speed of the treadmill relative to the direction the rat was running. For example, if the camera registered the rat as running east at 50 cm/s, and the treadmill was known to be moving west at 10 cm/s (-10 cm/s, by convention), then the rat's corrected running speed was taken as 50 – (-10) = 60 cm/s. This reflects the fact that the rat must overcome the motion of the treadmill to achieve its final real-world velocity.

The repeated measures design was not used for analysis of centroid and uncorrected field skew. These variables are defined in terms of the environment – that

is, the units of measure are directly related to space in the laboratory frame, and the effect of treadmill motion relative to rat motion would not yield meaningful results. Instead, difference scores were used to assess the response to the manipulation, because centroid position is defined on a scale with an arbitrary origin, and the sign of the skew value (and the resultant difference score) conveys important information about the shape of the field. Difference scores were calculated for both moving and stationary treadmill trials, providing there was a valid baseline trial (stationary treadmill) earlier in the same day to refer to. Treadmill movement was categorized as being either westward (-1), eastward (1), or stationary (0), and a multivariate analysis of variance (MANOVA) was used to investigate the effect on centroid position and skew. Running direction was included as a second factor to determine whether there was any interaction with the rat's behaviour.

A circular statistical analysis was used to compare firing phase of the first (phase-a) and last (phase-z) spikes as the rat traversed the place field under the three possible conditions – on the stationary treadmill, running with the treadmill, or running against the treadmill. The trials used in the repeated measures analysis were used again here, and as with previous analyses of phase_a and phase_z, only CA1 fields were included.

8.3 Results

8.3.1 Remapping on the moving treadmill

Thirty-three place fields were recorded while the rat ran both with and against the direction of motion of the moving treadmill, and of these, 20 passed the criterion for inclusion in the repeated measures analysis. The remaining 13 fields exhibited some form of remapping – they either stopped firing or adopted a novel firing pattern analysis. It is worth noting that 11 of the 13 remapping fields were recorded from DG/P, and only four of the 20 non-remapping fields were from DG/P. While there was no simultaneous recording of CA1 and DG/P fields during the moving treadmill trials, remapping DG/P fields were recorded from the same animals which had exhibited stable fields on the moving treadmill on previous trials. This suggests that CA1 and DG/P remapping results are not actually animal-specific. The two CA1 fields which remapped only did so when the rat ran against the runway. One DG/P field remapped

during running against the treadmill in one instance, six while running with the treadmill, and four fields remapped regardless of the direction of treadmill motion. A Chi-Squared test was used to determine whether remapping (in CA1 and DG/P fields combined) was dependent on the direction of treadmill motion. Remapping events were categorised as belonging to either "running with" or "running against" moving treadmill trials, with two entries made for fields which remapped on both. There was no tendency for remapping to occur on one type of manipulation versus the other ($\chi^2 = 0.529$, $p = 0.467$).

8.3.2 Fields shift in the direction of treadmill motion

Results of the MANOVA (field centroid shift and field skew versus treadmill motion and running direction) indicate that place fields tended to shift, relative to baseline trials, in the direction of treadmill motion ($F_{2,240} = 49.188$, $p < 0.001$). Figure 8.1 shows a typical response, and Figure 8.2a illustrates the population results, as obtained from centroid position difference scores. The consistency of the responses is evident – fields nearly always move west when the treadmill moves west, and east when the treadmill moves east. This shift occurs regardless of which direction the rat is running, as indicated by the absence of a significant interaction between treadmill direction and run direction ($F_{2,240} = 0.704$, $p = 0.495$). There was no effect of treadmill motion on field skew ($F_{2,240} = 0.540$, $p = 0.583$).

Figure 8.3 plots the centroid position of place fields on baseline trials against the magnitude of the deviation from the baseline position on the moving track. As can be seen, there is no relationship between the position of the place field and the magnitude of the centroid shift. All four correlations failed to reach significance. This stands in contrast to the response to compressing the runway, when proximity to the wall was a strong predictor of the magnitude of the centroid shift. It also runs counter to the expectation that a shift in cell firing induced by movement of the treadmill should be cumulative over the course of a run. For example, one might have expected that fields that are active when the rat runs east would be more shifted in the direction of treadmill motion the further east they normally are on the runway. This appears not to have been the case.

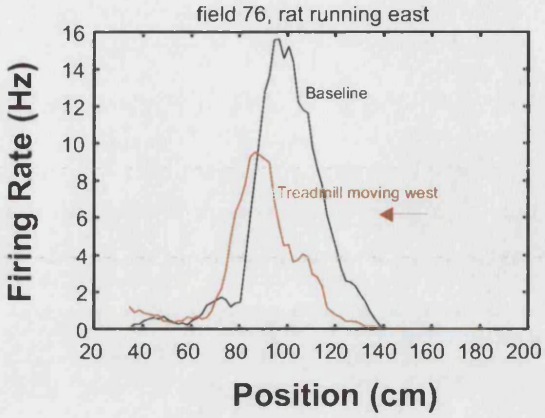

Figure 8.1. A typical place field response to running on the moving treadmill. In this particular example, the rat must run against the treadmill moving at 7.5 cm/s in order to traverse the place field. Note the shift of the place field in the direction of trreadmill motion.

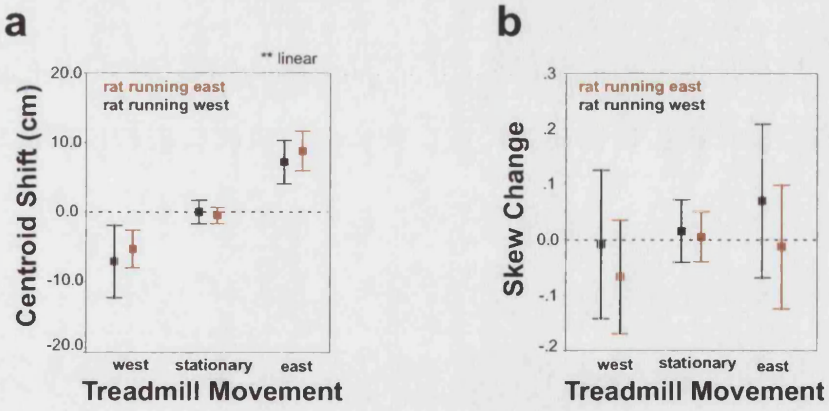

Figure 8.2. The effect of running on a moving treadmill, expressed as difference scores (probe minus preceding baseline). **a:** Regardless of the direction the rat was running, fields tended to shift in the direction the track moved. **b:** There was no effect on uncorrected (camera-relative) field skew. Error bars show 95% confidence intervals. Dotted lines show "no change" value. ** $p < 0.001$.

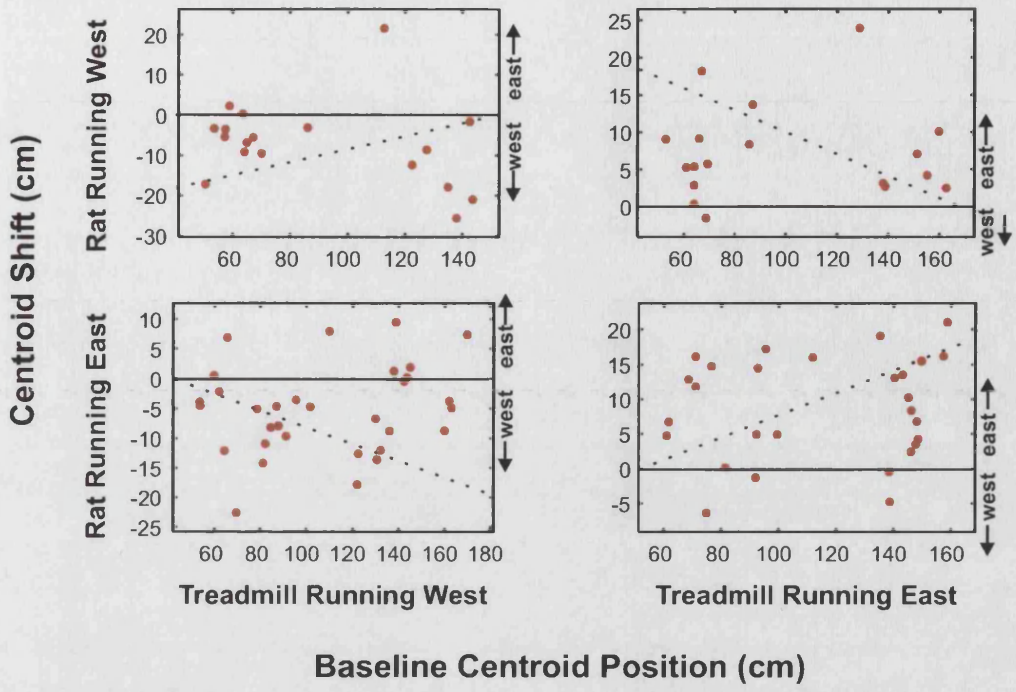

Figure 8.3. There is no consistent relationship between the baseline position of the field on the runway and the amount by which the field shifts in response to the moving treadmill. However, fields nearly always shift in the direction of the treadmill motion. Diagonal lines represent the hypothetical trend in centroid shift if shift was a cumulative function of the distance the rat had travelled on the moving treadmill. This is based on a "typical" treadmill speed of 7.5 cm/s and the mean running speed of the rat on probe trials (~60 cm/s).

8.3.3 Running speed and theta frequency were reduced.

Figure 8.4 illustrates the results of the repeated measures analyses. A Bonferroni correction was used to redefine p_{crit} as 0.006. The only variables which exhibited significant responses on probe trials were running speed (quadratic $F_{1,19}$ = 11.497, p = 0.003) and theta frequency (quadratic $F_{1,19}$ = 14.886, p = 0.001) – both were reduced when the treadmill was in motion. Mean running speed was 73.07 cm/s on baseline trials, versus 62.28 cm/s on moving treadmill trials. The mean speed reduction was 9.95 cm/s (11.40 %). Mean theta frequency was reduced from 9.21 Hz to 9.00 Hz, and the mean theta reduction was 0.20 Hz (2.06 %). The linear trend in running speed was also significant (linear $F_{1,19}$ = 11.301, p = 0.003), and is apparently attributable to the difference in running speed between the two baseline trials. This is consistent with previous observations that running speeds tend to be reduced over the course of a series of trials. The apparent reduction in firing rate (quadratic $F_{1,19}$ = 8.663, p = 0.008) and increase in in-field dwell time (quadratic $F_{1,19}$ = 7.057, p = 0.016) on moving-treadmill trials failed to pass the Bonferroni criterion. There was no evidence of a cubic trend in any of the variables, suggesting that the direction of observed effects were not dependent on whether the rat had to run against or with the motion of the treadmill.

Corrected running speed was also significantly reduced on probe trials (mean = 63.04 cm/s) relative to baselines (mean = 73.07 cm/s, quadratic $F_{1,19}$ = 11.393, p = 0.003). However, it is clear that correcting for track motion has a negligible effect on running speed, given that the adjustment is only on the order of $1/10^{th}$ the "original" uncorrected running speed. Certainly, there is no appreciable change in the relationship between running speed and the manipulation.

Correlations between the magnitude of responses to the moving treadmill manipulation are presented in Figure 8.5. The number of points in each plot exceeds the number of fields included because the analysis was based on all possible probe-baseline pairs. There was a significant correlation between the change in running speed and change in theta frequency (R = 0.353, $F_{1,98}$ = 13.974, $p < 0.001$). The more speed was reduced on the moving treadmill, the more theta frequency was reduced as well, as indicated in Figure 8.5c. This result was anticipated from the relationship between running speed and theta frequency observed previously.

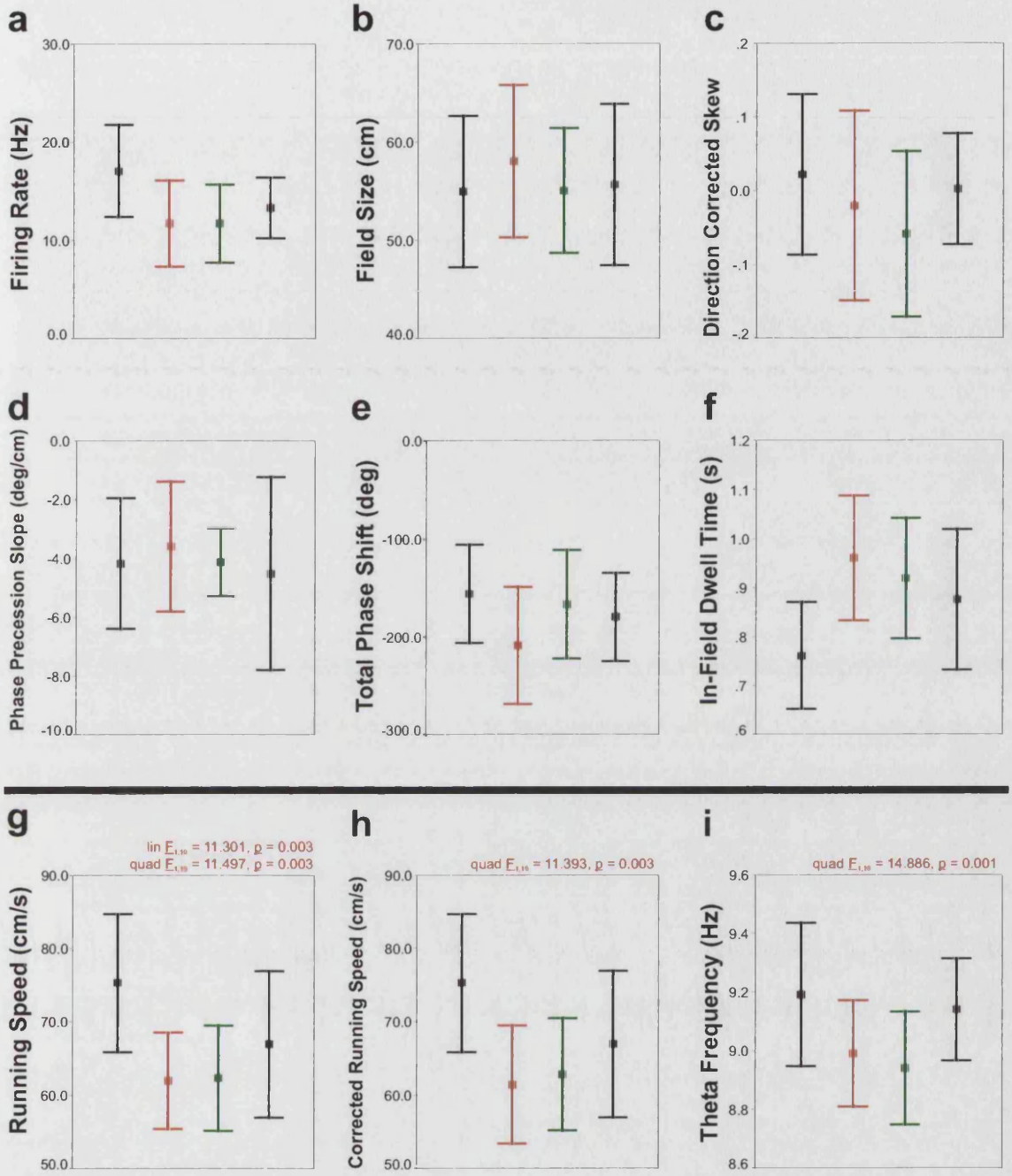

Figure 8.4. The effect of running on a moving treadmill. Results are sorted according to whether the treadmill moved counter to the rat's movement (red), moved in the same direction (green) or was stationary (black). A repeated measures analysis was used to detect linear, quadratic or cubic trends in each series. Significant results are presented in the bottom panel. Speed (**g**) and theta frequency (**i**) were reduced when the treadmill was in motion, but effects were not dependent on whether the track moved with or against the rat's running direction. Correction of running speed for track movement has a negligible effect on the mean running speed or the relationship with the manipulation (**h**). Error bars show 95% confidence intervals. Bonferroni-corrected critical $\underline{p}$ = * 0.006, **0.001.

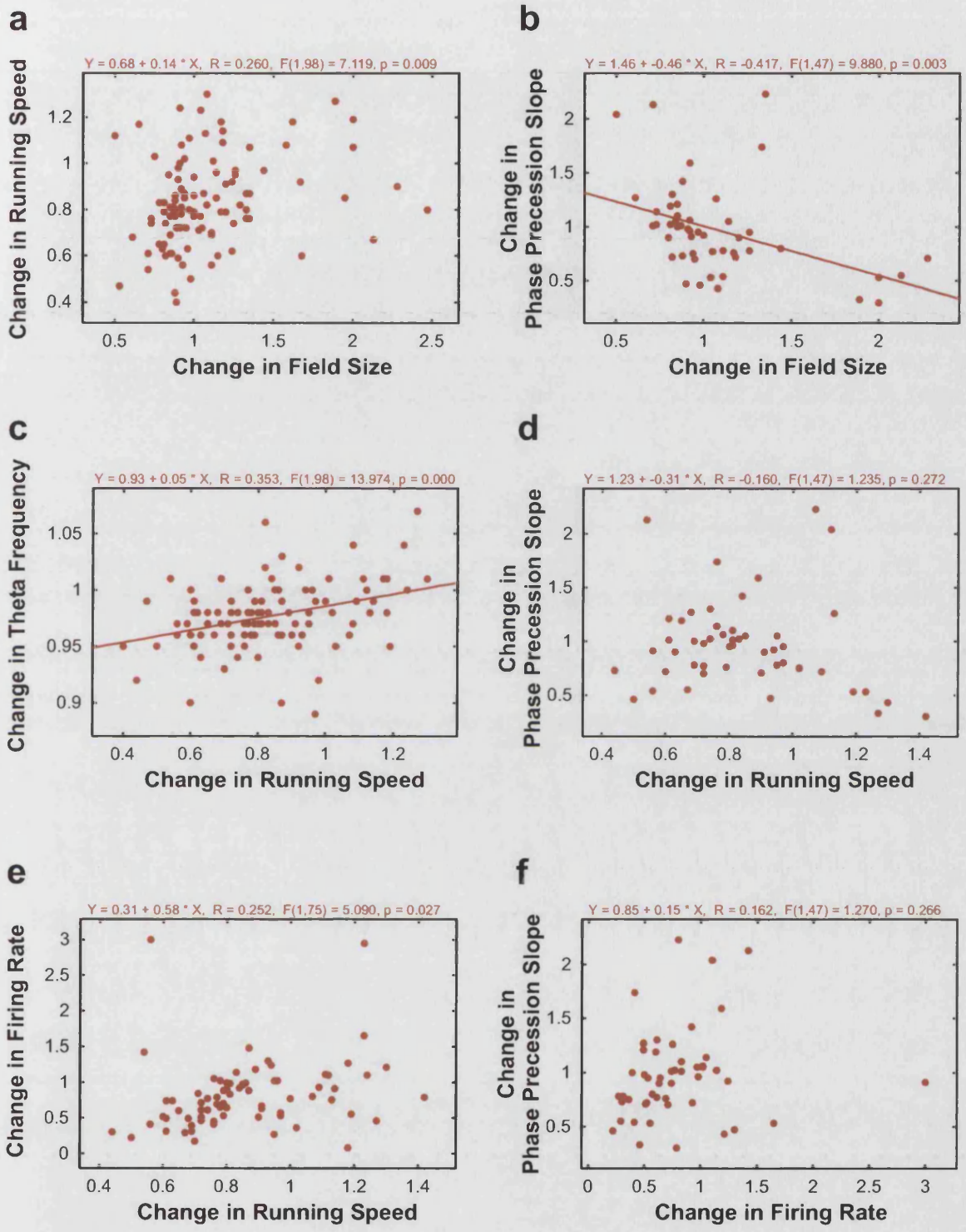

Figure 8.5. Correlations between responses to the moving treadmill. Change values are taken only from manipulation trials, and are expressed as a proportion of the value from the preceding baseline trial. Data for phase precession slope is further restricted to trial pairs on which at least 100 spikes were fired on both baseline and probe trial. Linear regression equations and significance values appear above each plot, with best fit lines shown for significant correlations ($p < 0.008$).

8.3.4 Phase precession was unaffected

The repeated measures analysis demonstrated that there was no manipulation effect on either the slope of the phase precession ($F_{3,15} = 0.557$, $p = 0.651$) or the total amount of phase shift ($F_{3,57} = 0.935$, $p = 0.430$). These overall results preclude any significant quadratic or cubic trends. However, as illustrated by Figure 8.5b, the magnitude of the changes in phase precession slope, while not significant themselves, are correlated with the magnitude of changes in field size ($R = -0.417$, $F_{1,47} = 9.880$, $p = 0.003$). In contrast to the compressed runway manipulation, on these probes most fields did not appreciably change size. As a result, the significance of the aforementioned effect is dependent on several fields which, for whatever reason, expanded on the moving runway.

For CA1 place fields, phase_a did not differ between baseline trials and trials on which the rat ran with ($F_{1,44} = 0.114$, $p = 0.737$) or against ($F_{1,46} = 0.237$, $p = 0.624$) the moving treadmill, nor was there a difference between "with" and "against" probe trials ($F_{1,28} = 0.001$, $p = 0.971$). Similarly, there was no difference between phase_z values on baseline trials versus "with" ($F_{1,44} = 0.225$, $p = 0.737$) or "against" ($F_{1,46} = 1.211$, $p = 0.277$) probe trials, and there was no phase_z difference between "with" and "against" probe trials ($F_{1,28} = 0.024$, $p = 0.878$). These results are summarised in Figure 8.6. The high degree of variability in the phase_a and (especially) phase_z values from trials when the rat ran with the moving treadmill may have reduced the power of tests involving these measures, although it did not prevent detection of a significant difference between phase_a and phase_z on "with" trials ($F_{1,26} = 7.749$, $p = 0.010$) or "against" trials ($F_{1,30} = 24.485$, $p < 0.001$). In other words, there is clearly a difference in the firing phase between the onset and offset of firing under both types of probe conditions, but no difference between the same measures in the different conditions.

8.3.5 Probe responses are not attributable to postural changes

Head tilt (nose up or down) when the rat occupies any given position on the runway results in a shift in the position of the tracking LED, and hence an apparent shift in the position of the rat from the camera perspective. Head tilt also affects the position of the rats eye, which is probably a reasonable indicator of position from the rat's perspective. However, head tilt does not affect the position of the LED and the eye in the same way, and can therefore produce changes in the rats apparent position (as

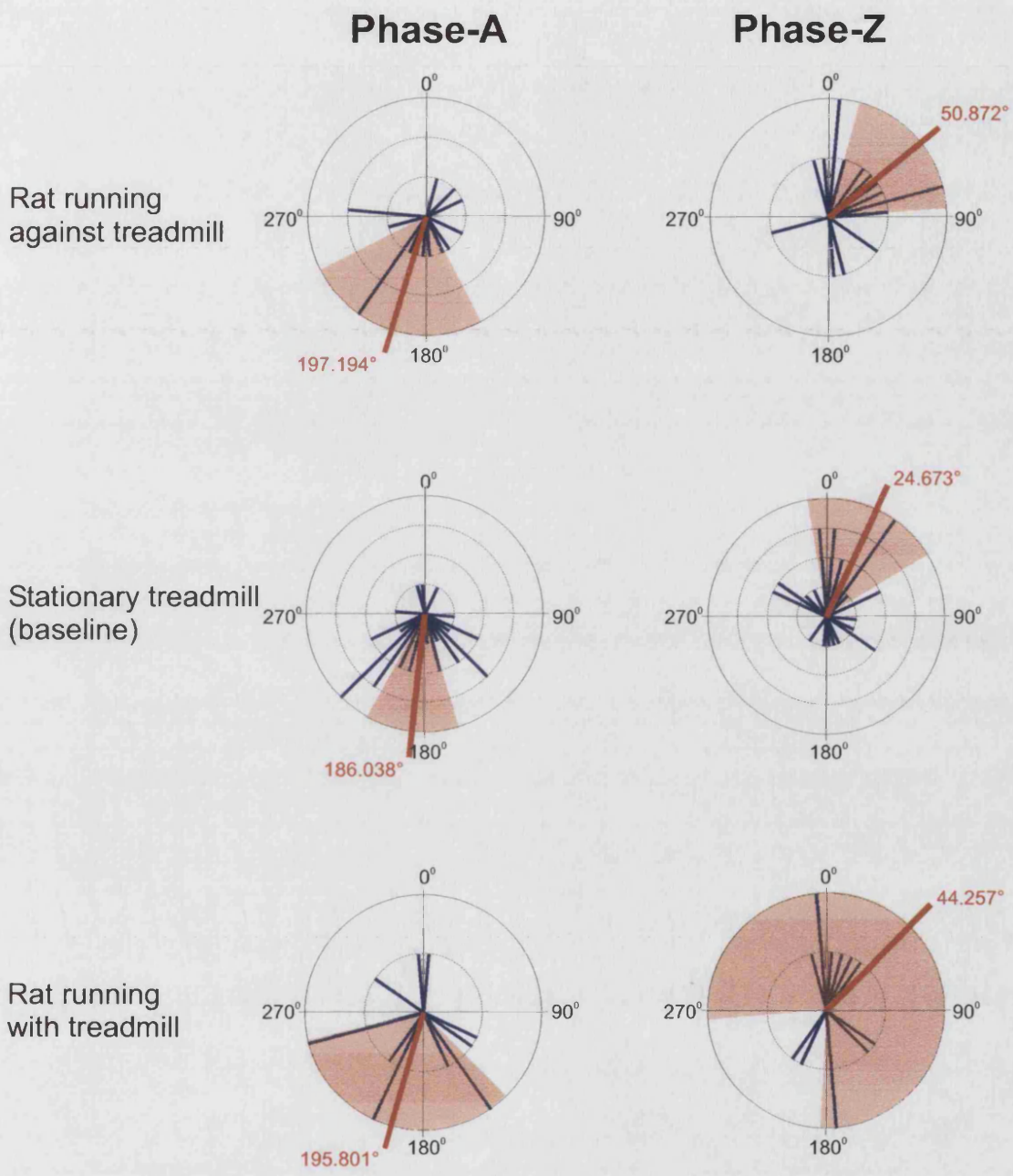

Figure 8.6. Running on the moving treadmill does not affect the mean firing phase of the first (phase_a) and last (phase_z) spikes on runs through the place field. Data are circular frequency histograms from CA1 fields, presented as a function of the direction the track was moving relative to the motion of the rat. Mean firing phases are shown in red. There were no significant differences between phase_a or phase_z values across manipulation types.

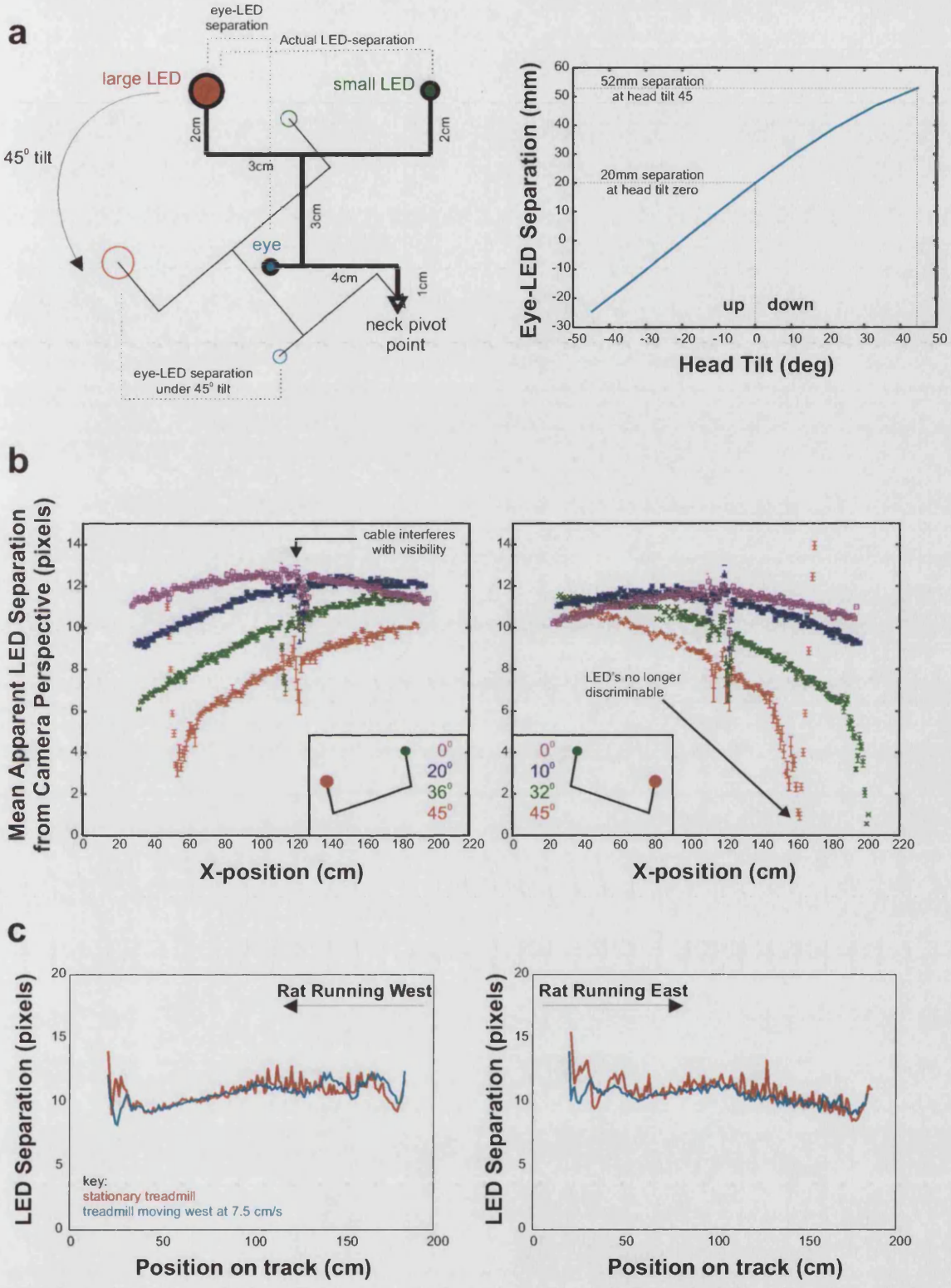

Figure 8.7. Testing the effect of head-tilt on errors in position tracking. **a:** the model used to represent the relative position of the rat's eye and the large LED array (in red) used for tracking position. A 45^0 downward tilt would increase the discrepency between eye and LED position by about 30mm. **b:** tests of the effect of tilting the LED array on the aparent distance between the large and small LED arrays. Position is taken as the position of the large array, which is generally tracked more reliably. **c:** composite records of LED separation on trials when the treadmill was moving west at 7.5 cm/s. Results suggest a slight downward head tilt in the direction of the rat's motion, but no change in head tilt between baseline and moving-treadmill trials. See text for further discussion.

registered by the overhead camera) which are not indicative of the rat's perceived position (as registered by the rat!).

A model was produced, using typical measures of distances between a rat's neck, eye, and the tracking LED, to determine the predicted error in position estimates produced by various degrees of head tilt, up or down. This model is presented in Figure 8.7a. It was determined that even a 45^0 change in head inclination would only produce a 3cm change in the usual discrepancy between the horizontal position of the rat's eye and the tracking LED.

Next, tests were conducted to determine the relationship between a known tilt of the dual LED array, and the apparent distance between the large and small LED clusters at different positions on the runway. The results are presented in Figure 8.7b. Apparent LED array separation was reduced at the west end of the runway when the array was inclined west, and at the east end of the runway when the array was inclined to the east. The steeper the incline of the array, the more pronounced the effect – so much so, that for 45^0 inclinations, the LED arrays became indistinguishable at the ends of the runway. From the camera perspective, once the visual angle to the array reached 45^0, a 45^0 incline would align the two LED clusters. The different position/separation profiles for each known tilt of the LED array provided a basis for estimating head tilt, and changes in head tilt from trial to trial .

Finally, LED separation data was compiled from multiple rats across multiple trials, to permit comparison of composite records from baseline trials and trials on which the treadmill was moving. Composite probe trials were drawn from individual trials on which the treadmill was moving 7.5 cm/s, as this happened to be the most common speed and best represents the "typical" moving treadmill manipulation. Results from when the treadmill was moving west are presented in Figure 8.7c. Composite baseline results are presented in blue, while data from probe trials is in red. Two facts are immediately apparent. First, the LED-separation/position profile is consistent with a slightly "head-down" posture, regardless of which direction the rat was running. This is consistent with casual observation of the rats during the shuttling task. And secondly, the baseline and probe trial composite profiles are virtually identical – certainly nothing even remotely like the difference between the 20^0 and 36^0 profiles from panel B can be seen here, let alone a difference indicative of the 45^0 change in head tilt required to produce a 3cm shift in rat position. Therefore, it seems clear that

the field shifts observed on moving-treadmill trials cannot be attributed to postural changes.

8.4 Discussion

8.4.1 A path integrator input to the hippocampus

Fields reliably shifted in the direction of treadmill motion on moving treadmill probe trials, providing strong evidence that the hippocampal representation of space is directly influenced by a particular class of self motion cues. Likely candidates are motor efference copy, proprioception, or step counting, all of which would have been rendered inaccurate position estimators on probe trials. It is possible that one of these inputs in particular is responsible for the observed effects, but it is just as likely that all three provide convergent (and incorrect) information about the rat's position on the moving treadmill. This is perhaps the first experiment to reliably demonstrate predictable control over place field topography (versus angular orientation) by idiothetic information.

I am confident that the observed field shifts on the moving treadmill were not artefactual. The analysis of head tilt effectively ruled out the possibility that these field shifts were produced by postural changes. The running speed analyses of Chapter 5 predicts that a reduction in running speed will produce field shifts in the direction of the rat's motion. But in the speed field analysis, a 39% reduction in running speed only produced a mean field shift of 2.10 cm. The moving treadmill produced, on average, a much smaller reduction in running speed (11.40 %) but a considerably larger place field shift – the mean magnitude of the field shift produced by the moving treadmill was 8.53 cm. It is unlikely, therefore, that this shift is produced by the change in running speed.

Despite the reliable shift in place fields, the magnitude of the shift is unrelated to the position of the field on the runway. Because idiothetic information is cumulative in nature, systematic manipulation of idiothetic information should produce systematic errors that are cumulative in nature as well. In other words, we would expect the magnitude of the place field shift to be directly related to the amount of time the rat spends running on the moving treadmill before entering the place field. For example, the most easterly fields which are active when the rat runs east should be the most

shifted in the direction of track motion. From Figure 8.3, we can see that there is no such relationship.

There are at least two possible explanations. The simplest is that when the data is broken down four ways to do this analysis, the power of the tests to detect an effect is severely reduced. A larger sample size might have yielded significant results, given that the field shifts involved are themselves so small. Alternatively, the systematic cumulative error may be balanced by increasing control of place field position by sensory cues as the rat approaches the wall at the opposite end of the run, consistent with the Gothard et al., 1996a,b). According to this model, most of the shift in field positions would be a result of passive displacement by the treadmill early in each run. The significance of this "early" displacement cannot be easily dismissed. When the rat is first turning to run *with* the treadmill, the rat's position can be shifted by several centimetres. When the rat is turning to run against the treadmill, it is often pressed up against the wall much more than usual by the movement of the track, because on "normal" trials, the rat frequently extends its head just far enough to retrieve the rice reward before turning to run the other way.

8.4.2 Phase precession

Insofar as a non-effect can be noteworthy, it is worth noting that the running treadmill manipulation failed to produce a significant change in the slope or the extent of the phase precession. Running speed was significantly reduced, while field size was maintained, and while the trend in mean in-field dwell-time failed to meet the Bonferroni criterion for significance, it was suggestive of an increase in the amount of time the rat spent in the place field on each run, as might be expected. Taken together, these observations support the notion that phase precession extent tends to be a constant, while slope is a function of field size, and firing phase is best described as a spatial (as opposed to temporal) function.

8.4.3 A few notes on response correlations

Reduced running speed was observed on both the moving treadmill and compressed runway probe trials, and in both cases the change in running speed was correlated with the change in theta frequency. This bolsters the argument that theta frequency is influenced by running speed. Changes in field size and phase precession

slope, while not significant themselves, were correlated with each other. This is consistent with observations on basic field statistics (Chapter 4) and on compressed runway trials (Chapter 7), and adds evidence to the notion that field size and phase precession slope are intimately related. Some anticipated correlations, like the one between changes in running speed and firing rate, proved to be non-significant. Interestingly, this is consistent with the observed absence of a relationship on the compressed runway, as well.

Chapter 9: Conclusions

9.1 Accounting for the phase precession effect

9.1.1 Is a depolarisation model sufficient?

Harris et al. (2002) and Mehta et al. (2002) have recently published evidence that the theta phase precession of place cell firing is, like firing rate itself, driven by spatially localised excitatory inputs. The model has certain advantages over detuned oscillator models (O'Keefe & Recce, 1993; Jensen & Lisman, 1996). For example, O'Keefe & Recce observed that if a rat stopped in the middle of a place field on the runway, when it resumed running, precession continued from the appropriate phase of theta until the rat exited the field. It is very difficult to account for such findings using detuned oscillators, without incorporating some mechanism for "remembering" the phase relationship between the oscillators during periods of motionlessness. Even precisely adjusting the frequency of the oscillators to compensate for running speed on every pass through the field presents some serious theoretical challenges. The depolarisation model solves these problem by doing away with the need for additional "clocks" altogether, and proposing a single spatial input which determines both firing rate and phase. Of course depolarization, as reflected by firing rate, would be expected to drop if the rat stopped in the field, reversing any precession up to that point.

Traditionally, the key weakness in depolarisation models has been a failure to account for the fact that phase precession is linear, while the firing rate of place cells tends to Gaussian. In response, Mehta at al. (2002) proposed that place fields are not symmetrical at all, but systematically skewed in the direction of motion, and that even this skew may fail to reflect an even more skewed underlying depolarisation envelope. The current experiment demonstrates that phase precession is *not* a function of field skew, that precession continues in portions of the field when firing rate is clearly dropping, and that manipulations which affect phase precession do not appear to produce a concomitant change in field skew. In other words, the two variables are completely dissociable.

Harris et al. (2002) proposed that the underlying depolarisation was symmetrical, but that the cell stops firing before excitatory input drops off due to adaptation. However, I have demonstrated that relationship between position and firing

phase is robust in the face of dramatic changes in momentary firing rate. Moreover, compressing the runway reduces firing rate, but produces a trend towards increased phase precession slope, not the predicted decrease. And finally, I have identified instances in which position-related phase precession occurs even when the firing rate is so low that only a single spike is fired, on average, per pass through the field. Under these circumstances, it is in fact impossible that adaptation could produce a dissociation between depolarization and firing phase.

Harris and colleagues reported a linear relationship between firing phase and instantaneous firing rate on a number of spatial and non-spatial tasks. I propose that the apparent linearity of the relationship may be an artefact of the nature of the phase precession and calculation of the circular mean. First, on spatial tasks, there is a curvilinear relationship between firing phase and time-averaged firing rate. That is, low rates correspond with both late and early phase values, as the rat is entering and exiting the place field, respectively. However, because the relationship between phase and position is strongest in the early portions of the place field (Skaggs et al., 1996), the fact that low rates are associated with early phases late in the field is obscured. Second, these early phase values, late in the place field, would be averaged with late phase values in a circular analysis, due to equivalence of points around the 0/360 origin (see Figure 9.1). In other words, points which are genuinely early firing phases may be lumped with late phase points for the calculation of a single circular mean for low instantaneous firing rate spikes. This might account for the relationship between firing phase and instantaneous firing rate in the two spatial tasks studied by Harris and colleagues. REM sleep may also be considered a quasi-spatial task, given the evidence that during REM, rats replay spike sequences experienced during previous waking epochs (Kudrimoti et al., 1999; Nádasdy et al., 1999). Which leaves the observation of phase precession in the running wheel. Previously, it had been suggested that phase advancement in the running wheel might be produced by actual translation of the rats position in the wheel (and hence, the place field) at higher speed (Czurkó et al., 1999). But Harris and co-workers (2002) demonstrated that the rat's head position remained stationary in the horizontal plane during observed phase precession. There is no simple way of reconciling this result with those of the current experiment, without resorting to something like vague speculation about the cognitive processes which may be occurring in a running wheel task!

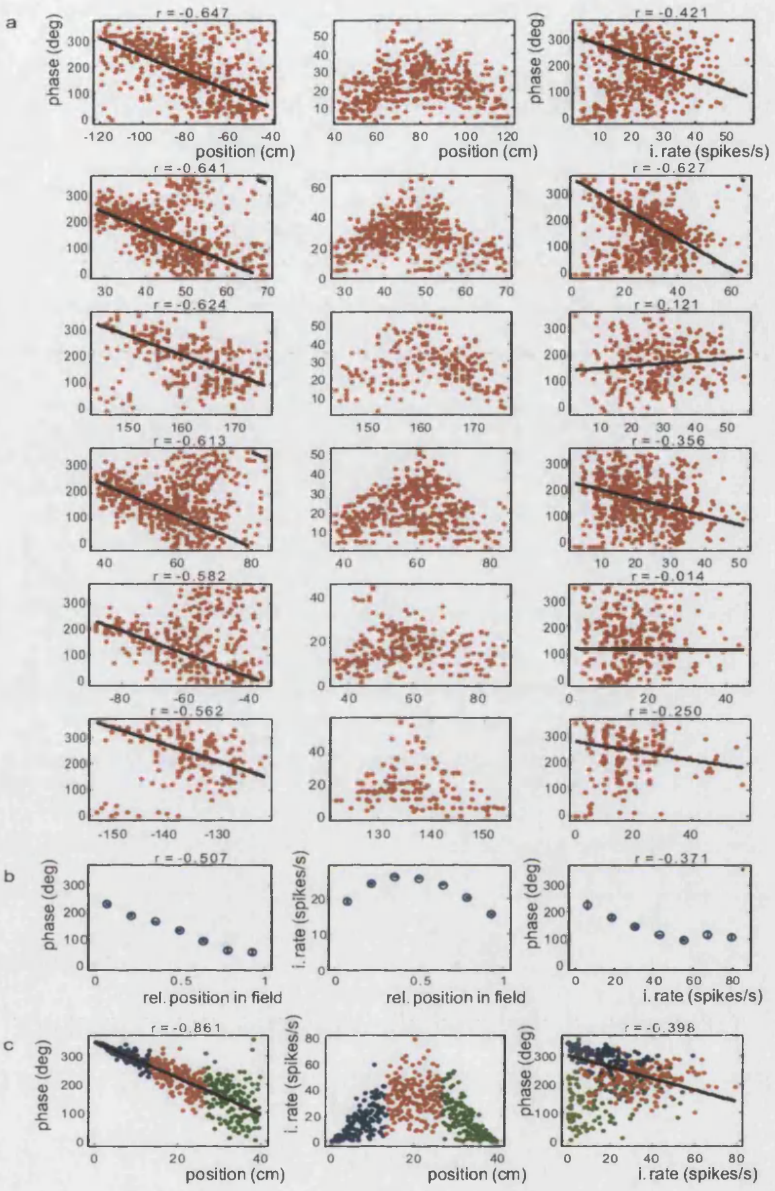

Figure 9.1. Apparent linear correlations between phase and instantaneous firing rate (IFR) may derive from the correlation of both variables with position. **a**: Data from six typical CA1 place fields showing the relationship between each of phase versus position, IFR versus position, and phase versus IFR. Correlation coefficients (r) and associated regression lines, take account of the circular nature of phase. Note the robust linear correlation with position, and the curvilinear relationship between IFR and position. Position data has been scaled to field size and, in the case of westbound fields, reversed so as to make position values reflect the distance travelled in-field. **b**: Analysis of 25158 spikes (77 fields) from the current experiment, pooled across cells as in Harris et al. (2002). The relationships between phase and position, rate and position, and phase and rate are illustrated. Points and circles show the appropriate mean (circular or linear) and standard error, respectively. Note the apparent linear relationship between phase and IFR. **c**: Simulation showing that the more robust phase vs. position relationship early in the field, due to lower phase variance, may result in a disproportionate contribution of these points to the phase versus rate correlation. Late field spikes (green) should contribute to a generally curvilinear phase vs. IFR relationship (only high rate spikes exhibit mid-range phase values), but due to circular averaging, points near phase zero may be combined with points near 360, artificially strengthening the apparent linear relationship. Data for phase f and instantaneous rate r were simulated as functions of position in the place field x according to $\{f, r\} = \{350 - 250x/L + 75\mu 1x/L, 15(1 - (2x/L - 1)2)(\mu 2 + 2.5(1 - (2x/L - 1)2))\}$, where $\mu 1$ and $\mu 2$ are drawn from a unit Normal distribution and L is the length of the place field.

9.1.2 Reconciling the findings

Field size is strongly correlated with phase precession slope, and when the runway is compressed, the change in field size is correlated with the change in precession slope. Moreover, on the compressed runway, position remains the best correlate of firing phase, which demonstrates the robust nature of the relationship. This presents a powerful argument that perceived changes in location play an important role in determining the firing phase of place cells. But it need not be the only factor involved. Magee (2001) demonstrated that increased depolarisation can produce phase precession in the hippocampal slice. So it may be that both depolarisation and perceived motion contribute to phase precession in a cooperative fashion. On a linear track, for example, it may be that precession occurs even while the firing rate is reduced, because the rat is moving through space and reactivating sequences of memories which were sorted on a gamma time-scale during learning (Jensen & Lisman, 1996). In the running wheel, in the absence of translation, it may be that firing rate alone is sufficient to drive a given cell to spike earlier in the theta cycle. It is worth noting that neither Harris et al. (2002) nor Czurkó et al. (1999) report additional cells being recruited during epochs of high running speed or high firing rate, which supports the notion that this phase precession is not the result of a translation through space, either real or perceived.

9.2 The hippocampus as a path integrating spatial map?

O'Keefe and Nadel (1978) proposed that the hippocampal representation of space ought to be based on information from a variety of sensory modalities, as well as idiothetic information regarding the animal's motion relative to an arbitrary starting point. McNaughton et al. (1996) proposed that representations of space are, in fact, based entirely on path integration on initial exposure to the environment, with salient sensory features being added to the map only later, after their reliability has been established. Indeed, the importance of self-motion to place cell firing is evident from the observation that strict restraint prevents cells from firing when the rat is passively moved through place fields (Foster et al., 1989). Attractor network models of hippocampal function (Samsonovich & McNaughton, 1997; Tsodyks, 1999) propose that self-motion cues (which may be derived from visual stimuli, such as optic flow) are

also involved in the moment-to-moment updating of the representation of position, with only occasional reference to sensory information to correct for cumulative errors.

Traditionally, it has been difficult to dissociate sensory and idiothetic sources of information regarding position. For example, O'Keefe and Burgess (1996) interpret place cell firing as a function of distances from boundaries, although there is no way of determining whether these calculations are based on internal or external sources of information. However, the moving treadmill manipulation affects a particular class of idiothetic information (relating to limb movement) in such a way as to allow prediction of the direction and magnitude of changes in place field position. Indeed, predictions regarding the direction of field shifts are borne out by the results, in keeping with the notion that self motion cues such as motor efference copy, or step counting, play an important role in determining place field firing. Clearly, however, the control is imperfect, and it seems likely that multiple sources of information – both internally and externally generated, contribute to the current state of the animal's spatial map. Given the degree of convergence in the hippocampus, of information from diverse brain regions, it would be surprising if it were otherwise. And so, while it has long been assumed that both path integration and sensory information play complimentary roles in driving place cells, the current experiment is an important demonstration that the contribution from a particular source (or subset of sources) can be effectively isolated.

But regardless of the balance of inputs which determine the firing pattern of hippocampal place cells, it appears from the current study that what the hippocampus is representing is the topography of the environment. The preservation of the topographical relationship between place fields on the compressed runway, and the proportional reduction in fields sizes, certainly have that effect, whether or not this is the "intended purpose" of the structure.

9.3 The effects (and determinants?) of running speed

9.3.1 Running speed and firing rate

The results of the current experiment generally support the view that running speed directly modulates the firing rate of hippocampal place cells within their place fields ((Czurkó et al., 1999) and during traversal of them (McNaughton et al., 1983). Within a trial, and from run to run, it is safe to say that the faster the rat runs while

crossing the field, the higher the mean firing rate during that traversal. This raises the possibility that pyramidal cell firing rate serves as a code for running speed – for example, the summed rate of all pyramidal cells at any given location within an environment should reliably reflect running speed, regardless of the subset of pyramidal cells most active at that time and place.

However, there was no relationship between the typical running speed through a given place field and its typical peak firing rate. In other words, individual place fields have "normal" firing rates which are determined by something other than the stereotyped behaviour in that portion of the environment – perhaps the nature of the constellation of positional cues impinging on that cell, or the nature of the local network as it is configured for a particular environment. Moreover, neither of the manipulations which lowered running speed (compressing the runway and the moving treadmill) produced changes in firing rate which were proportional to the change in running speed. This suggests that other factors play a more important role in determining firing rate, and that running speed effects are only really observable when all else is held constant.

9.3.2 Running speed and theta frequency

The relationship between running speed and theta frequency proved to be quite reliable, if weak. For a given rat, theta frequency was directly related to momentary running speed, and for a given place field, the typical theta frequency during traversal of the field was directly related to the location of the field on the runway. The speed-field analysis demonstrated that theta frequency was significantly higher on faster runs through the field, and the compressed runway and moving treadmill manipulations produced changes in running speed which predicted changes in theta frequency, even thought the changes in theta frequency were themselves not significant on the compressed runway. These results are consistent with previous observations of a relationship between running speed and theta frequency (Bland & Vanderwolf, 1972; McFarland et al., 1975; Oddie & Bland, 1998; Rivas et al., 1996; Shin & Talnov, 2001; Slawinska & Kasicki, 1998). The relationship with acceleration was significant for some rats, but not others. In fact, in some instances, there was a significant correlation when the rat ran in one direction, but not the other. From these results, it appears that momentary running speed is the most robust predictor of theta frequency during behaviours distributed across the entire runway.

The relationship between theta frequency and acceleration is not entirely unexpected, given that acceleration is proportional to force, and is therefore indicative of the animal's exertion. Shin & Talnov, (2001) hypothesised that deceleration in the running wheel produced an increase in theta because the rats have to exert effort to maintain equilibrium in the wheel as it comes to a stop. Whishaw & Vanderwolf (1973) observed that the frequency and amplitude of theta just prior to jumping was proportional to the size of the jump. The latter experiment observed this relationship during observations of atropine sensitive theta, although it is possible that atropine-sensitive and atropine-insensitive theta both contribute to theta frequency in the awake, behaving rat.

Despite the mathematical relationship between running speed and acceleration, the two factors may provide independent types of input which influence theta frequency. Acceleration on the runway is a result of physical exertion. In contrast, steady-state running requires very little exertion, but results in the generation of speed-dependent motion cues. Such cues include optic flow, air flow, the change in visual angles, and motor efference copy, and there is evidence to suggest they contribute to theta frequency. Czurkó et al. (1999) failed to find any relationship between running speed and theta frequency in the running wheel. However, the rat does not translate through space in the running wheel, and it may be this absence of sensory motion cues which resulted in the lower mean theta frequencies Czurkó et al. observed (7.7 Hz, versus 9.0 Hz in the current study). This is despite the fact that rats in their experiment achieved speeds in the running wheel comparable to those observed in the current experiment on the runway. It may be that these motion cues contribute critically to theta frequency, increasing it in a speed-dependent manner when the rat is running through space. While the documented relationship between core temperature and theta frequency (Whishaw & Vanderwolf, 1971,1973) may also explain the discrepancy in mean theta frequencies between the two experiments (perhaps our rats were "running hot"?), it cannot account for the observation of speed-modulation in one experiment, but not the other, unless core temperature varies sufficiently in the course of a single traversal of the runway (~ one second) to produce the effect. This seems unlikely.

It should also be noted that the relationship between running speed and theta frequency cannot be interpreted as a possible mechanism for a dual oscillator based phase precession effect – the speed-field analysis indicates that a 39% increase in running speed only produces a 2% increase in theta frequency – insufficient, for example, to maintain a constant degree of phase precession in the face of the reduced

time it takes to traverse the place field. If a detuned oscillatory inputs were responsible for phase precession, the second oscillator, as yet unidentified, would have to bear the bulk of the responsibility.

9.3.3 Behaviour may be determined by the spatial representation

One of the key issues raised in the current experiment is the degree to which the rat's behaviour in space affects the representation of space. For example, it may be that the speed at which a rat runs through a portion of the environment determines the size of the place fields in that region. Superficially, that appears to be the case in the baseline data set, in which larger fields tend to be found mid-runway, where the rat runs fastest. However, momentary changes in running speed appear to have no effect on field size – fields on faster runs are merely shifted backwards – opposite the direction of motion – by a small amount. Field size and running speed only co-vary on the compressed runway trials, where it can easily be argued that both changes are brought about by changes in the sensory environment. It seems probable, therefore, that the hippocampal representation of space, as defined by things like perceived distances to environmental boundaries, is used on a continual basis to modulate behaviour. A distinction should be made, however, between modulation of locomotor behaviour, and guidance of goal-directed behaviour. While it is widely assumed that the hippocampus is used to guide choice behaviour on spatial learning tasks, it is also clear from recent studies that dissociations between choice and spatial maps can be observed (Huxter et al., 2001; Jeffery et al., 2003).

9.4 Closing comments

The current experiment presents a number of important experimental findings, using novel experimental protocols, including the use of natural variations in behaviour to study the effects of running speed, and the use of a moving treadmill to study motor efference input to the hippocampal representation of space. The results demonstrate that idiothetic information contributes directly to the spatial firing properties of place cells. Path integration has long been proposed as an important mechanism for navigation, and its contribution to place fields often speculated upon but never conclusively demonstrated, until now. I have shown that place fields demonstrate a remarkable invariance in position in the face of widely varying running speeds and

levels of place cell excitation, in the absence of manipulation of the environment. In contrast, similar changes in speed and firing rate induced by changes to the environmental geometry accompany profound effects on place field position, size, and phase precession. And finally, cellular excitation and firing phase have been proven to be truly dissociable variables. Consequently, phase precession cannot be entirely explained in terms of depolarization models. Instead, hippocampal pyramidal cells are capable, in principal, of encoding different types of information simultaneously - in terms of both firing rate and firing phase. Firing phase encodes precise location within a region of space characterised by a supra-threshold firing rate, while the exact firing rate within the field is free to encode aspects of behaviour (such as running speed) and features of the environment within a particular region of it. This makes place cells a suitable substrate for episodic memories binding sensory and behavioural experiences in a spatiotemporal context.

Chapter 10: References

Aguirre, G.K., D'Esposito, M. (1997). Environmental knowledge is subserved by separable dorsal/ventral neural areas. Journal of Neuroscience, 17(7), 2512-2818.

Alonso, A. & Garcia-Austt, E. (1987). Neuronal sources of theta rhythm in the entorhinal cortex of the rat. I. Laminar distribution of theta field potentials. Experimental Brain Research, 67(3), 493-501.

Alonso, A. & Kohler, C. (1982). Evidence for separate projections of hippocampal pyramidal and non-pyramidal neurons to different parts of the septum in the rat brain. Neuroscience Letters, 31(3), 209-214.

Alvarez, P., Wendelken, L. & Eichenbaum, H. (2002). Hippocampal formation lesions impair performance in an odor-odor association task independently of spatial context. Neurobiology of Learning and Memory, 78(2), 470-476.

Alyan, S., & Jander, R. (1994). Short range homing in the mouse, Mus musculus: Stages in the learning of direction. Animal Behavior, 48, 285-298.

Amaral (1978). A Golgi study of cell types in the hilar region of the hippocampus in the rat. Journal of Comparative Neurology, 182(4 Pt 2), 851-914.

Amaral, D.G. & Witter, M.P. (1989). The three-dimensional organization of the hippocampal formation: a review of anatomical data. Neuroscience, 31(3), 571-591.

Amaral, D.G. & Witter, M.P. (1995). Hippocampal formation. In G. Paxinos (Ed.), The Rat Nervous System (2nd ed., pp. 443-493). New York: Academic Press.

Andersen, R.A., Snyder, L.H., Bradley, D.C. & Xing, J. (1997). Multimodal representation of space in the posterior parietal cortex and its use in planning movements. Annual Review of Neuroscience, 20, 303-330.

Andersen, P., Dingledine, R., Gjerstad, L., Langmoen, I.A., & Laursen, A.M. (1980). Two different responses of hippocampal pyramidal cells to application of gamma-amino butyric acid. Journal of Physiology, 305, 279-296.

Anderson, M.I. & O'Mara, S.M. (2003). Analysis of recordings of single-unit firing and population activity in the dorsal subiculum of unrestrained, freely moving rats. Journal of Neurophysiology, 90(2), 655-665.

Arnolds, D.E., Lopes da Silva, F.H., Aitink, J.W. & Kamp, A. (1979). Hippocampal EEG and behaviour in dog. I. Hippocampal EEG correlates of gross

motor behaviour. Electroencephalography and Clinical Neurophysiology, 46(5), 552-570.

Baisden, R.H., Woodruff, M.L., & Hoover, D.B. (1984). Cholinergic and non-cholinergic septo-hippocampal projections: a double-label horseradish peroxidase-acetylcholinesterase study in the rabbit. Brain Research, 290(1), 146-151.

Bakst, I., Avendano, C., Morrison, J.H., & Amaral, D.G. (1986). An experimental analysis of the origins of somatostatin-like immunoreactivity in the dentate gyrus of the rat. Journal of Neuroscience, 6(5),1452-1462.

Barlow, J.S. (1964). Inertial navigation as a basis for animal navigation. Journal of Theoretical Biology, 6, 76-117.

Beckstead, R.M. (1978). Afferent connections of the entorhinal area in the rat as demonstrated by retrograde cell-labeling with horseradish peroxidase. Brain Research, 152(2), 249-264.

Best, P.J., & Thompson, L.T. (1989). Persistence, reticence, and opportunism of place-field activity in hippocampal neurons. Psychobiology, 17(3), 230-235.

Blackstad (1956). Commissural connections of the hippocampal region in the rat, with special reference to their mode of termination. Journal of Comparative Neurology, 105, 417-528.

Bland, B. H., Andersen, P., & Ganes, T. (1975). Two generators of hippocampal activity in rabbits. Brain Research, 94(2), 199-218.

Bland, B.H., & Vanderwolf, C.H. (1972). Diencephalic and hippocampal mechanisms of motor activity in the rat: effects of posterior hypothalamic stimulation on behavior and hippocampal slow wave activity. Brain Research, 43(1), 67-88.

Bliss, T.V., & Collingridge, G.L. (1993). A synaptic model of memory: Long-term potentiation in the hippocampus. Nature, 361(6407), 31-39.

Bliss, T.V., & Lomo, T. (1973). Long-lasting potentiation of synaptic transmission in the dentate area of the anaesthetized rabbit following stimulation of the perforant path. Journal of Physiology, 232(2), 331-356.

Blodgett, H.C. (1929). The effect of the introduction of reward upon the maze performance of rats. University of California Publications in Psychology, 4, 113-134.

Boeijinga, P.H., & Lopes da Silva, F.H. (1988). Differential distribution of beta and theta EEG activity in the entorhinal cortex of the cat. Brain Research, 448(2), 272-286.

Bose, A., Booth, V., & Recce, M. (2000). A temporal mechanism for generating the phase precession of hippocampal place cells. Journal of Computational Neuroscience, 9(1), 5-3.

Bostock, E, Muller, R.U., & Kubie, J.L. (1991). Experience-dependent modifications of hippocampal place cell firing. Hippocampus 1(2), 193-205.

Bragin, A., Jando, G., Nádasdy, Z., Hetke, J., Wise, K., & Buzsáki, G. (1995). Gamma (40-100 Hz) Oscillation in the hippocampus of the behaving rat. Journal of Neuroscience,15(1), 47-60.

Buckmaster, P.S., & Schwartzkroin, P.A. (1994). Hippocampal mossy cell function: a speculative view. Hippocampus, 4(4), 393-402.

Buhl, E.H., Halasy, K., & Somogyi, P. (1994). Diverse sources of hippocampal unitary inhibitory postsynaptic potentials and the number of synaptic release sites. Nature, 368(6474), 823-828.

Bullock, T.H., Buzsáki, G., & McClune, M.C. (1990). Coherence of compound field potentials reveals discontinuities in the CA1-subiculum of the hippocampus in freely-moving rats. Neuroscience, 38(3):609-19

Bures, J., Fenton, A. A., Kaminsky, Yu., & Zinyuk, L. (1997). Place cells and place navigation. Proceedings of the National Academy of Sciences of the United States of America, 94, 343-350.

Burwell, R.D. & Amaral, D.G. (1998b). Cortical afferents of the perirhinal, postrhinal, and entorhinal cortices of the rat. Journal of Comparative Neurology, 398(2), 179-205.

Buzsáki, G. (1989). Two-stage model of memory trace formation: a role for "noisy" brain states. Neuroscience, 31(3), 551-570.

Buzsáki, G. (2002). Theta oscillations in the hippocampus. Neuron, 33(3), 325-40.

Buzsáki, G., Buhl, D.L., Harris, K.D., Csicsvari, J., Czeh, B. & Morozov, A. (2003). Hippocampal network patterns of activity in the mouse. Neuroscience, 116(1), 201-211.

Buzsáki, G., Leung, L.W. & Vanderwolf, C.H. (1983). Cellular bases of hippocampal EEG in the behaving rat. Brain Research, 287(2), 139-171.

Caplan, J.B., Madsen, J.R., Raghavachari, S., & Kahana, M.J. (2001). Distinct patterns of brain oscillations underlie two basic parameters of human maze learning. The Journal of Neurophysiology, 86(1), 368-380.

Chapman, C.A., & Lacaille, J.C. (1999). Intrinsic theta-frequency membrane potential oscillations in hippocampal CA1 interneurons of stratum lacunosum-moleculare. The Journal of Neurophysiology, 81(3), 1296-1307.

Chen, L. L., Lin, L. H., Green, E. J., Barnes, C. A., & McNaughton, B. L. (1994). Head-direction cells in the rat posterior cortex. I. Anatomical distribution and behavioral modulation. Experimental Brain Research, 101(1), 8-23.

Cheng, K. (1986). A purely geometric module in the rat's spatial representation. Cognition, 23, 149-178.

Chrobak, J.J., & Buzsáki, G. (1994). Selective activation of deep layer (V-VI) retrohippocampal cortical neurons during hippocampal sharp waves in the behaving rat. Journal of Neuroscience, 14(10), 6160-6170.

Cole, A.E., & Nicoll, R.A. (1983). Acetylcholine mediates a slow synaptic potential in hippocampal pyramidal cells. Science, 221(4617), 1299-1301.

Collett, T.S., & Collett, M. (2000). Path integration in insects. Current Opinion in Neurobiology,10(6), 757–762.

Colombo, M., Fernandez, T., Nakamura, K., & Gross, C.G. (1998). Functional differentiation along the anterior-posterior axis of the hippocampus in monkeys. Journal of Neurophysiology, 80(2), 1002-1005.

Corkin, S. (2002). What's new with the amnesic patient H.M.? Nature Reviews Neuroscience, 3(2), 153-160.

Cressant, A., Muller, R.U., & Poucet, B. (1997). Failure of centrally placed objects to control the firing fields of hippocampal place cells. Journal of Neuroscience, 17(7):2531-2542.

Cressant, A., Muller, R.U. & Poucet, B. (1999). Further study of the control of place cell firing by intra-apparatus objects. Hippocampus, 9(4), 423-431.

Crowne, D.P., & Radcliffe, D.D. (1975). Some characteristics and functional relations of the electrical activity of the primate hippocampus and a hypothesis of

hippocampal function. In: The Hippocampus, vol. 2 (Isaacson, R.L., & Pribram, K.H., eds), pp 185-206. New York: Plenum Press.

Csicsvari, J., Hirase, H., Czurkó, A., Mamiya, A., & Buzsáki, G. (1999). Oscillatory coupling of hippocampal pyramidal cells and interneurons in the behaving rat. Journal of Neuroscience, 19, 274-287.

Csicsvari, J., Hirase, H., Mamiya, A., & Buzsáki, G. (2000). Ensemble patterns of hippocampal CA3-CA1 neurons during sharp wave-associated population events. Neuron, 28(2), 585-594.

Csicsvari, J., Jamieson, B., Wise, K.D., & Buzsáki, G. (2003) Mechanisms of gamma oscillations in the hippocampus of the behaving rat. Neuron, 37(2), 311-322.

Czurkó, A., Hirase, H., Csicsvari, J., & Buzsáki, G. (1999). Sustained activation of hippocampal pyramidal cells by 'space clamping' in a running wheel. European Journal of Neuroscience, 11(1), 344-352.

Danysz, W., Zajaczkowski, W., & Parsons, C.G. (1996). Modulation of learning processes by ionotropic glutamate receptor ligands. Behavioural Pharmacology, 6(5 And 6), 455-474.

Dragoi, G., Carpi, D., Recce, M., Csicsvari, J. & Buzsáki, G. (1999). Interactions between hippocampus and medial septum during sharp waves and theta oscillation in the behaving rat. Journal of Neuroscience 19(14), 6191-6199.

Dudchenko, P.A., & Taube, J.S. (1997). Correlation between head direction cell activity and spatial behavior on a radial arm maze. Behavioral Neuroscience, 111(1), 3-19.

Eichenbaum, H. (1994). The hippocampal system and declarative memory in humans and animals: Experimental analysis and historical origins. In D.L. Schacter & E. Tulving (Eds.), Memory systems. Cambridge: MIT Press.

Ekstrom, A.D., Kahana, M.J., Caplan, J.B., Fields, T.A., Isham, E.A., Newman, E.L. & Fried, I. (2003). Cellular networks underlying human spatial navigation. Nature, 425(6954), 184-188.

Ekstrom, A.D., Meltzer, J., McNaughton, B.L., & Barnes, C.A. (2001). NMDA receptor antagonism blocks experience-dependent expansion of hippocampal "place fields". Neuron, 31(4), 631-638.

Engel, A.K., & Singer, W. (2001). Temporal binding and the neural correlates of sensory awareness. Trends in Cognitive Sciences, 5(1), 16-25.

Fellous, J.M., & Sejnowski. T.J. (2000). Cholinergic induction of oscillations in the hippocampal slice in the slow (0.5-2 Hz), theta (5-12 Hz), and gamma (35-70 Hz) bands. Hippocampus,10(2),187-197.

Fenton, A.A., & Muller, R.U. (1998). Place cell discharge is extremely variable during individual passes of the rat through the firing field. Proceedings of the National Academy of Sciences of the United States of America,95(6), 3182-3187.

Fisahn, A., Pike, F.G., Buhl, E.H. & Paulsen, O. (1998). Cholinergic induction of network oscillations at 40 Hz in the hippocampus in vitro. Nature, 394(6689), 186-189.

Fischer, Y., Wittner, L., Freund, T.F. & Gahwiler, B.H. (2002). Simultaneous activation of gamma and theta network oscillations in rat hippocampal slice cultures. Journal of Physiology, 539(Pt 3), 857-868.

Foster, T.C., Castro, C.A., & McNaughton, B.L. (1989). Spatial selectivity of rat hippocampal neurons: Dependence on preparedness for movement. Science, 244, 1580-1582.

Fox, S.E. (1989). Membrane potential and impedance changes in hippocampal pyramidal cells during theta rhythm. Experimental Brain Research, 77(2), 283-94.

Fox S.E., & Ranck, J.B. Jr, (1975). Localization and anatomical identification of theta and complex spike cells in dorsal hippocampal formation of rats. Experimental Neurology, 49, 299-313.

Fox, S.E., & Ranck, J.B. Jr. (1981). Electrophysiological characteristics of hippocampal complex-spike cells and theta cells. Experimental Brain Research, 41, 399-410.

Fox, S.E., Wolfson, S., & Ranck, J.B. Jr. (1986). Hippocampal theta rhythm and the firing of neurons in walking and urethane anesthetized rats. Experimental Brain Research, 62(3), 495-508.

Frank, L.M., Brown, E.N. & Wilson, M. (2000). Trajectory encoding in the hippocampus and entorhinal cortex. Neuron, 27(1), 169-178.

Frank, L.M., Brown, E.N. & Wilson, M.A. (2001). A comparison of the firing properties of putative excitatory and inhibitory neurons from CA1 and the entorhinal cortex. Journal of Neurophysiology, 86(4), 2029-2040.

French & Totterdell (2002). Hippocampal and prefrontal cortical inputs monosynaptically converge with individual projection neurons of the nucleus accumbens. Journal of Comparative Neurology, 446(2), 151-165.

Freund, T.F. & Buzsáki, G. (1996). Interneurons of the hippocampus. Hippocampus, 6(4), 347-470.

Freund, T.F., & Antal, M. (1988). GABA-containing neurons in the septum control inhibitory interneurons in the hippocampus. Nature, 336(6195), 170-173.

Georges-Francois, P., Rolls, E.T., & Robertson, R.G. (1999). Spatial view cells in the primate hippocampus: allocentric view not head direction or eye position or place. Cerebral Cortex, 9(3), 197-212.

Gagliardo, A., Ioale, P., Odetti, F., Bingman, V.P., Siegel, J.J. & Vallortigara, G. (2001). Hippocampus and homing in pigeons: left and right hemispheric differences in navigational map learning. European Journal of Neuroscience, 13(8), 1617-1624.

Gagliardo, A., Odetti, F., Ioale, P., Bingman, V.P., Tuttle, S. & Vallortigara, G. (2002). Bilateral participation of the hippocampus in familiar landmark navigation by homing pigeons. Behavioral Brain Research, 136(1), 201-209.

Gallistel, C.R. (1990). The Organization of Learning. Cambridge, MA: MIT Press.

Ghaem, O., Mellet, E., Crivello, F., Tzourio, N., Mazoyer, B., Berthoz, A., & Denis, M. (1997). Mental navigation along memorized routes activates the hippocampus, precuneus, and insula. Neuroreport, 8(3), 739-744.

Golob, E.J. & Taube, J.S. (1999). Head direction cells in rats with hippocampal or overlying neocortical lesions: evidence for impaired angular path integration. Journal of Neuroscience 19(16), 7198-7211.

Gothard, K.M., Hoffman, K.L., Battaglia, F.P., & McNaughton, B.L. (2001). Dentate gyrus and CA1 ensemble activity during spatial reference frame shifts in the presence and absence of visual input. Journal of Neuroscience, 21(18), 7284–7292.

Gothard, K.M., Skaggs, W.E., Moore, K.M., & McNaughton, B.L. (1996a). Binding of hippocampal CA1 neural activity to multiple reference frames in a landmark-based navigation task. Journal of Neuroscience, 16(2), 823-835.

Gothard, K.M., Skaggs, W.E., & McNaughton, B.L. (1996b). Dynamics of mismatch correction in the hippocampal ensemble code for space: Interaction between path integration and environmental cues. Journal of Neuroscience, 16(24), 8027-8040.

Green, J.D., & Arduini, A..A. (1954) Hippocampal electrical activity in arousal. Journal of Neurophysiology, 17, 533-557.

Groenewegen, H.J., Berendse, H.W., Meredith, G.E., Haber, S.N., Voorn, P., Wolters, J.G., & Lohman, A.H.M. (1991). Functional anatomy of the ventral, limbic system-innervated striatum. In: Willner, P., & Scheel-Kruger, J., editors. The mesolimbic dopamine system: from motivation to action. Chichester: John Wiley and Sons. p 19–60.

Gulyás, A.I., Hájos, N., Katona, I. & Freund, T.F. (2003). Interneurons are the local targets of hippocampal inhibitory cells which project to the medial septum. European Journal of Neuroscience, 17(9), 1861-1872.

Haberly, L.B. (2001). Parallel-distributed processing in olfactory cortex: new insights from morphological and physiological analysis of neuronal circuitry. Chemical Senses, 26(5), 551-576.

Halasy, K., Buhl, E.H., Lorinczi, Z., Tamas, G. & Somogyi, P. (1996). Synaptic target selectivity and input of GABAergic basket and bistratified interneurons in the CA1 area of the rat hippocampus. Hippocampus, 6(3), 306-329.

Han, Z.S., Buhl, E.H., Lorinczi, Z., & Somogyi, P. (1993). A high degree of spatial selectivity in the axonal and dendritic domains of physiologically identified local-circuit neurons in the dentate gyrus of the rat hippocampus. European Journal of Neuroscience, 5(5), 395-410.

Hampson, R.E., Simeral, J.D., & Deadwyler, S.A. (1999). Distribution of spatial and nonspatial information in dorsal hippocampus. Nature 402, 610-614.

Hampton, R.R., & Shettleworth, S.J. (1996). Hippocampus and memory in a food-storing and in a nonstoring bird species. Behavioral Neuroscience, 110(5), 946-964.

Harley, C.W. (1979). Arm choices in a sunburst maze: Effects of hippocampectomy in the rat. Physiology and Behavior, 23(2), 283-290.

Harris, K.D., Henze, D.A., Csicsvari, J., Hirase, H., & Buzsáki, G.(2000). Accuracy of tetrode spike separation as determined by simultaneous intracellular and extracellular measurements. Journal of Neurophysiology, 84(1), 401-414.

Harris, K.D., Henze, D.A., Hirase, H., Leinekugel, X., Dragoi, G., Czurkó, A. & Buzsáki, G. (2002). Spike train dynamics predicts theta-related phase precession in hippocampal pyramidal cells. Nature, 417(6890), 738-741.

Hartley, T., Maguire, E.A., Spiers, H.J. & Burgess, N. (2003). The well-worn route and the path less travelled: distinct neural bases of route following and wayfinding in humans. Neuron, 37(5), 877-888.

Hebb, D.O. (1949). The organization of behaviour. New York: Wiley-Interscience.

Henze, D.A., Borhegyi, Z., Csicsvari, J., Mamiya, A., Harris, K.D. & Buzsáki, G. (2000). Intracellular features predicted by extracellular recordings in the hippocampus in vivo. Journal of Neurophysiology, 84(1), 390-400.

Hetherington, P.A., & Shapiro, ML. (1997). Hippocampal place fields are altered by the removal of single visual cues in a distance-dependent manner. Behavioral Neuroscience, 111(1), 20-34.

Hill, A.J. (1978). First occurrence of hippocampal spatial firing in a new environment. Experimental Neurology, 62(2):282-297.

Hirase, H., Leinekugel, X., Csicsvari, J., Czurkó, A., & Buzsáki, G. (2001). Behavior-dependent states of the hippocampal network affect functional clustering of neurons. Journal of Neuroscience, 21:RC145 (1-4).

Hirase, H., Czurkó, A., Csicsvari, J., & Buzsáki, G. (1999). Firing rate and theta-phase coding by hippocampal pyramidal neurons during 'space clamping'. European Journal of Neuroscience, 11(12), 4373-4380.

Hock, B.J. Jr., & Bunsey, M.D. (1998). Differential effects of dorsal and ventral hippocampal lesions. Journal of Neuroscience, 18(17), 7027-7032..

Hollup, S.A., Kjelstrup, K.G., Hoff, J., Moser, M.B., & Moser, E.I. (2001a). Impaired recognition of the goal location during spatial navigation in rats with hippocampal lesions. Journal of Neuroscience, 21(12), 4505-4513.

Hollup, S.A., Molden, S., Donnett, J.G., Moser, M.B., & Moser, E.I. (2001b). Accumulation of hippocampal place fields at the goal location in an annular watermaze task. Journal of Neuroscience, 21(5), 1635-1644.

Holsheimer, J. (1982). Generation of theta activity (RSA) in the cingulate cortex of the rat. Experimental Brain Research, 47(2), 309-312.

Hori, E., Tabuchi, E., Matsumura, N., Tamura, R., Eifuku, S., Endo, S., Nishijo, H., Ono, T. (2003). Representation of place by monkey hippocampal neurons in real and virtual translocation. Hippocampus, 13(20, 190–196.

Huxter, J.R., Thorpe, C.M., Martin, G.M., & Harley, C.W. (2001). Spatial problem solving and hippocampal place cell firing in rats: control by an internal sense of direction carried across environments. Behavioural Brain Research, 123(1), 37-48.

Hynes, C.A., Martin, G.M., Harley, C.W., Huxter, J.R., & Evans, J.H. (2000). Multiple points of entry into a circular enclosure prevent place learning despite normal vestibular orientation and cue arrays: Evidence for map resetting. Journal of Experimental Psychology: Animal Behavior Processes, 26(1), 64-73.

Insausti, R., Herrero, M.T., & Witter, M.P. (1997). Entorhinal cortex of the rat: cytoarchitectonic subdivisions and the origin and distribution of cortical efferents. Hippocampus, 7(2), 146 –183.

Jay, T.M. & Witter, M.P. (1991). Distribution of hippocampal CA1 and subicular efferents in the prefrontal cortex of the rat studied by means of anterograde transport of Phaseolus vulgaris-leucoagglutinin. Journal of Comparative Neurology, 313(4), 574-58

Jeffery, K.J., Donnett, J.G., Burgess, N., & O'Keefe, J.M. (1997). Directional control of hippocampal place fields. Experimental Brain Research, 117, 131-142.

Jeffery, K.J., Gilbert, A., Burton, S., & Strudwick, A. (2003). Preserved performance in a hippocampal-dependent spatial task despite complete place cell remapping. Hippocampus, 13(2), 175-189.

Jeffery, K.J., & O'Keefe, J.M. (1999). Learned interaction of visual and idiothetic cues in the control of place field orientation. Experimental Brain Research, 127, 151-161.

Jensen, O., & Lisman, J.E. (1996). Hippocampal CA3 region predicts memory sequences: Accounting for the phase precession of place cells. Learning & Memory 3, (2-3) 279-287.

Jensen, O., & Lisman, J.E. (2000). Position reconstruction from an ensemble of hippocampal place cells: contribution of theta phase coding. The Journal of Neurophysiology, 83(5), 2602-2609.

Jung, M.W., & McNaughton, B.L. (1993). Spatial selectivity of unit activity in the hippocampal granular layer. Hippocampus, 3(2), 165-182.

Jung, M.W., Wiener, S.I., & McNaughton, B.L. (1994). Comparison of spatial firing characteristics of units in dorsal and ventral hippocampus of the rat. Journal of Neuroscience, 14(12), 7347-7356.

Kahana, M.J., Sekuler, R., Caplan, J.B., Kirschen M., & Madsen, J.R., (1999). Human theta oscillations exhibit task dependence during virtual maze navigation. Nature, 399(6738), 781-784.

Kamondi, A., Acsady, L., Wang, X., & Buzsáki, G. (1998). Theta oscillations in somata and dendrites of hippocampal pyramidal cells in vivo: activity-dependent phase-precession of action potentials. Hippocampus, 8(3), 244-261.

Kentros, C., Hargreaves, E., Hawkins, R.D., Kandel, E.R., Shapiro, M., & Muller, R.V. (1998). Abolition of long-term stability of new hippocampal place cell maps by NMDA receptor blockade. Science, 280(5372), 2121-2126.

Köhler, C., Chan-Palay, V. & Wu, J.Y. (1984). Septal neurons containing glutamic acid decarboxylase immunoreactivity project to the hippocampal region in the rat brain. Anatomy and Embryology, 169(1), 41-44.

Kiefer, S.W. & Braun, J.J. (1977). Absence of differential associative responses to novel and familiar taste stimuli in rats lacking gustatory neocortex. Journal of Comparative and Physiological Psychology, 91(3), 498-507.

King, C., Recce, M., & O'Keefe, J. (1998). The rhythmicity of cells of the medial septum/diagonal band of Broca in the awake freely moving rat: relationships with behaviour and hippocampal theta. European Journal of Neuroscience, 10(2), 464-77.

Klausberger, T., Magill, P.J., Marton, L.F., Roberts, J.D., Cobden, P.M., Buzsáki, G., & Somogyi, P. (2003). Brain-state- and cell-type-specific firing of hippocampal interneurons in vivo. Nature, 421(6925), 844-848.

Kloosterman, F., Witter, M.P. & Van Haeften, T. (2003). Topographical and laminar organization of subicular projections to the parahippocampal region of the rat. Journal of Comparative Neurology, 455(2), 156-171.

Knierim, J.J., Kudrimoti, H.S., & McNaughton, B.L. (1995). Place cells, head direction cells, and the learning of landmark stability. Journal of Neuroscience, 15(3), 1648-1659.

Kobayashi, T., Nishijo, H., Fukuda, M., Bures, J., & Ono, T. (1997). Task-dependent representations in rat hippocampal place neurons. The Journal of Neurophysiology, 78(2), 597-613.

Kocsis, B., Bragin, A., & Buzsáki, G. (1999). Interdependence of multiple theta generators in the hippocampus: a partial coherence analysis. Journal of Neuroscience, 19(14), 6200-6212.

Kosaka, T., Hama, K., & Wu, J.Y. (1984). GABAergic synaptic boutons in the granule cell layer of rat dentate gyrus. Brain Research, 293(2), 353-359.

Kosar, E., Grill, H.J. & Norgren, R. (1986). Gustatory cortex in the rat. I. Physiological properties and cytoarchitecture. Brain Research, 379(2), 329-341.

Kramis, R., Vanderwolf, C.H., & Bland B.H. (1975). Two types of hippocampal rhythmical slow activity in both the rabbit and the rat: relations to behavior and effects of atropine, diethyl ether, urethane, and pentobarbital. Experimental Neurology, 49(1 Pt 1), 58-85.

Kreiter, A.K., & Singer, W. (1996). Oscillatory Neuronal Responses in the Visual Cortex of the Awake Macaque Monkey. European Journal of Neuroscience, 4(4), 369-375.

Kubie, J.L., & Ranck, J.B., Jr. (1983). Sensory-behavioral correlates in individual hippocampus neurons in three situations: Space and context. In W. Seifert (ed.), Neurobiology of the Hippocampus (pp. 433-447). London

Kudrimoti, H.S., Barnes, C.A., & McNaughton, B.L. (1999). Reactivation of hippocampal cell assemblies: Effects of behavioral state, experience, and EEG Dynamics. Journal of Neuroscience, 19(10), 4090-4101.

Lee, M.G., Chrobak, J.J., Sík, A., Wiley, R.G., & Buzsáki, G. (1994). Hippocampal theta activity following selective lesion of the septal cholinergic system. Neuroscience, 62(4), 1033-1047.

Lenck-Santini, P.P., Muller, R.U., Save, E., & Poucet, B. (2002). Relationships between place cell firing fields and navigational decisions by rats. Journal of Neuroscience,22(20), 9035-9047.

Leung, L.S. (1984a). Model of gradual phase shift of theta rhythm in the rat. Journal of Neurophysiology, 52(6),1051-1065.

Leung, L.S. (1984b). Pharmacology of theta phase shift in the hippocampal CA1 region of freely moving rats. Electroencephalography and Clinical Neurophysiology, 58(5), 457-466.

Leung, L.W. & Borst, J.G. (1987). Electrical activity of the cingulate cortex. I. Generating mechanisms and relations to behavior. Brain Research, 407(1), 68-80.

Leung, L.S., Martin, L.A., & Stewart, D.J. (1994). Hippocampal theta rhythm in behaving rats following ibotenic acid lesion of the septum. Hippocampus, 4(2), 136-147.

Lewis, P.R. & Shute, C.C. (1967). The cholinergic limbic system: projections to hippocampal formation, medial cortex, nuclei of the ascending cholinergic reticular system, and the subfornical organ and supra-optic crest. Brain, 90(3), 521-540.

Lisman, J.E. (1999). Relating hippocampal circuitry to function: Recall of memory sequences by reciprocal dentate–CA3 interactions. Neuron, 22(2): 233-242.

Llinas, R., & Ribary, U. (1993). Coherent 40-Hz oscillation characterizes dream state in humans. Proceedings of the National Academy of Sciences of the United States of America, 90(5), 2078-2081.

Lorente de Nó, R. (1933). Studies on the structure of the cerebral cortex. Journal für Psychologie und Neurologie, 45, 381-438.

Lorente de Nó (1934). Studies on the structure of the cerebral cortex. II. Continuation of the study of the ammonic system. Journal für Psychologie und Neurologie, 46, 113-177.

Magee, J.C. (2001). Dendritic mechanisms of phase precession in hippocampal CA1 pyramidal neurons. The Journal of Neurophysiology, 86(1), 528-532.

Maguire, E.A., Frackowiak, R.S., & Frith, C.D. (1996). Learning to find your way: a role for the human hippocampal formation. Proceedings of the Royal Society of London. Series B: Biological Sciences B, 263(1377), 1745-1750.

Maguire, E.A., Frackowiak, R.S., & Frith, C.D. (1997). Recalling routes around London: activation of the right hippocampus in taxi drivers. Journal of Neuroscience, 17(18), 7103-7110.

Maguire, E.A., Gadian, D.G., Johnsrude, I.S., Good, C.D., Ashburner, J., Frackowiak, R.S.J., & Frith, C.D. (2000). Navigation-related structural change in the hippocampi of taxi drivers. Proceedings of the National Academy of Sciences of the United States of America, 97(8), 4398-4403.

Mardia, K. V. (1972). Statistics of Directional Data. London: Academic Press.

Margules, J, & Gallistel, C.R. (1988). Heading in the rat: Determination by environmental shape. Animal Learning and Behavior, 16(4), 404-410.

Markus, E.J., Barnes, C.A., McNaughton, B.L., Gladden, V.L., & Skaggs, W.E. (1994). Spatial information content and reliability of hippocampal CA1 neurons: effects of visual input. Hippocampus, 4(4), 410-421.

Markus, E.J., Qin, Y.L., Leonard, B., Skaggs, W.E., McNaughton, B.L., & Barnes C.A. (1995). Interactions between location and task affect the spatial and directional firing of hippocampal neurons. Journal of Neuroscience,15(11), 7079-7094.

Marr, D. (1971). Simple memory: a theory for archicortex. Philosophical Transactions of the Royal Society of London. Series B: Biological Sciences, 262(841), 23-81.

Martin, P.D., & O'Keefe, J. (1998). Place field dynamics and directionality in a spatial memory task. Brain Research, 783(2),249-261.

McBain, C.J., DiChiara, T.J. & Kauer, J.A. (1994). Activation of metabotropic glutamate receptors differentially affects two classes of hippocampal interneurons and potentiates excitatory synaptic transmission. Journal of Neuroscience 14(7), 4433-4445.

McDonald, R.J., & White, N.M. (1993). A triple dissociation of memory systems: Hippocampus, amygdala, and dorsal striatum. Behavioral Neuroscience, 107(1), 3-22.

McFarland, W.L., Teitelbaum, H., & Hedges, E.K. (1975). Relationship between hippocampal theta activity and running speed in the rat. Journal of Comparative and Physiological Psychology,88(1), 324-328.

McHugh, T.J., Blum, K.I., Tsien, J.Z., Tonegawa, S., & Wilson, M.A. (1996). Impaired hippocampal representation of space in CA1-specific NMDAR1 knockout mice. Cell, 87(7), 1339-1349.

McNaughton, B.L., Barnes, C.A., Gerrard, J.L., Gothard, K., Jung, M.W., Knierim, J.J., Kudrimoti, H., Qin, Y., Skaggs, W.E., Suster, M., & Weaver, K.L. (1996).

Deciphering the hippocampal polyglot: The hippocampus as a path integration system. The Journal of Experimental Biology, 199, 173-185.

McNaughton, B.L., Barnes, C.A., & O'Keefe, J. (1983). The contributions of position, direction and velocity to single unit activity in the hippocampus of freely-moving rats. Experimental Brain Research, 52, 41-49.

Meador, K.J., Thompson, J.L., Loring, D.W., Murro, A.M., King, D.W., Gallagher, B.B., Lee, G.P., Smith, J.R., & Flanigin, H.F. (1991). Behavioral state-specific changes in human hippocampal theta activity. Neurology, 41(6), 869-872.

Mehta, M.R., Barnes, C.A., & McNaughton, B.L. (1997). Experience-dependent, asymmetric expansion of hippocampal place fields. Proceedings of the National Academy of Sciences of the United States of America, 94(16), 8918-8921.

Mehta, M.R., Quirk, M.C., & Wilson, M.A. (2000). Experience-dependent asymmetric shape of hippocampal receptive fields. Neuron, 25, 707–715.

Mehta, M.R, Lee, A.K., & Wilson, M.A. (2002). Role of experience and oscillations in transforming a rate code into a temporal code. Nature 417(6890), 741-746.

Mitchell, S.J. & Ranck, J.B., Jr. (1980). Generation of theta rhythm in medial entorhinal cortex of freely moving rats. Brain Research, 189(1), 49-66.

Mittelstaedt, M.L. & Mittelstaedt, H. (1980). Homing by path integration in a mammal. Naturwissenschaften, 67, 566–567.

Mizumori, S.J.Y., & Williams, J.D. (1993). Directionally selective properties of the neurons in the lateral dorsal nucleus of the thalamus of rats. Journal of Neuroscience 13(9), 4015-4028.

Mogenson, G.J., Swanson, L.W., & Wu, M. (1983). Neural projections from nucleus accumbens to globus pallidus, substantia innominata, and lateral preoptic-lateral hypothalamic area: an anatomical and electrophysiological investigation in the rat. Journal of Neuroscience, 3, 189–202.

Morris, R. (1981). Spatial localization does not require the presence of local cues. Learning and Motivation, 12, 239-260.

Morris, R.G., Anderson, E., Lynch, G.S., & Baudry, M. (1986). Selective impairment of learning and blockade of long-term potentiation by an N-methyl-D-aspartate receptor antagonist, AP5. Nature, 319(6056), 774-776.

Morris, R.G.M., Black, A.H., and O'Keefe, J. (1976). Hippocampal EEG during a ballistic movement (abstract). Neuroscience Letters, 3, 102.

Morris, R.G. Garrud, P., Rawlins, J.N., & O'Keefe, J. (1982). Place navigation impaired in rats with hippocampal lesions. Nature, 297(5868), 681-683.

Moser, E., Moser, M-B, & Andersen, P. (1993). Spatial learning impairment parallels the magnitude of dorsal hippocampal lesions, but is hardly present following ventral lesions. Journal of Neuroscience, 13(9), 3916-3925.

Moser, M-B., Moser, E.I., Forrest, E., Andersen, P., & Morris R.G. (1995). Spatial learning with a minislab in the dorsal hippocampus. Proceedings of the National Academy of Sciences of the United States of America, 92(21),9697-9701.

Moser, M-B., & Moser, E.I. (1998). Distributed encoding and retrieval of spatial memory in the hippocampus. Journal of Neuroscience, 18(18), 7535-7542.

Muller, R. (1996). A quarter of a century of place cells. Neuron, 17(5):813-22.

Muller, R.U., Bostock, E., Taube, J.S., & Kubie, J.L. (1994). On the directional firing properties of hippocampal place cells. Journal of Neuroscience, 14(12), 7235-7251.

Muller, R.U., Kubie, J.L., & Ranck, J.B. Jr. (1987). Spatial firing patterns of hippocampal complex-spike cells in a fixed environment. Journal of Neuroscience, 7(7), 1935-1950.

Muller, R.U., & Kubie, J.L. (1987). The effects of changes in the environment on the spatial firing of hippocampal complex-spike cells. Journal of Neuroscience, 7(7), 1951-1968.

Naber, P.A., Lopes da Silva, F.H. & Witter, M.P. (2001). Reciprocal connections between the entorhinal cortex and hippocampal fields CA1 and the subiculum are in register with the projections from CA1 to the subiculum. Hippocampus, 11(2), 99-104.

Naber, P.A., Witter, M.P. & Lopes da Silva, F.H. (2001). Evidence for a direct projection from the postrhinal cortex to the subiculum in the rat. Hippocampus, 11(2), 105-117.

Nádasdy, Z., Hirase, H., Czurkó, A., Csicsvari, J., & Buzsáki, G. (1999). Replay and time compression of recurring spike sequences in the hippocampus. Journal of Neuroscience, 19(21), 9497-9507.

Oddie, S.D., & Bland, B.H. (1998). Hippocampal formation theta activity and movement selection. Neuroscience & Biobehavioural Reviews, 22(2), 221-231.

O'Keefe, J. (1976). Place units in the hippocampus of the freely moving rat. Experimental Neurology, 51(1), 78-109.

O'Keefe, J., & Burgess, N. (1996). Geometric determinants of the place fields of hippocampal neurons. Nature, 381, 425-427.

O'Keefe, J., Burgess, N., Donnett, J.G., Jeffery, K.J., & Maguire, E.A. (1998). Place cells, navigational accuracy, and the human hippocampus. Philosophical Transactions of the Royal Society of London, Series B, 353(1373), 1333-1340.

O'Keefe, J., & Conway, D.H. (1978). Hippocampal place units in the freely moving rat: Why they fire where they fire. Experimental Brain Research, 31, 573-590.

O'Keefe, J., & Conway, D.H. (1980). On the trail of the hippocampal engram. Physiological Psychology, 8(2), 229-238.

O'Keefe, J., & Dostrovsky, J. (1971). The hippocampus as a spatial map. Preliminary evidence from unit activity in the freely moving rat. Brain Research, 34, 171-175.

O'Keefe, J., & Nadel, L. (1978). The hippocampus as a cognitive map. London: Oxford University Press.

O'Keefe, J., & Recce, M.L. (1993). Phase relationship between hippocampal place units and the EEG theta rhythm. Hippocampus, 3(3), 317-330.

O'Keefe, J., & Speakman, A. (1987). Single unit activity in the rat hippocampus during a spatial memory task. Experimental Brain Research, 68, 1-27.

Oleskevich, S., Descarries, L., & Lacaille, J.C. (1989). Quantified distribution of the noradrenaline innervation in the hippocampus of adult rat. Journal of Neuroscience, 9(11), 3803-3815.

Olton DS, Branch M, Best PJ. (1978). Spatial correlates of hippocampal unit activity. Experimental Neurology 58(3), 387-409.

Pare, D. & Collins, D.R. (2000). Neuronal correlates of fear in the lateral amygdala: multiple extracellular recordings in conscious cats. Journal of Neuroscience 20(7), 2701-2710.

Pawelzik, H., Hughes, D.I., & Thomson, A.M. (2002). Physiological and morphological diversity of immunocytochemically defined parvalbumin- and cholecystokinin-positive interneurones in CA1 of the adult rat hippocampus. Journal of Comparative Neurology, 443(4), 346-367.

Petsche, H., & Stumpf, C.H. (1960). Topographic and toposcopic study of origin and spread of the regular synchronised arousal pattern in the rabbit. Electroencephalography and Clinical Neurophysiology, 12, 589-600.

Petsche, H., Stumpf, C.H., & Gogolak, G. (1962). The significance of the rabbit's septum as a relay station between the midbrain and the hippocampus. I. The control. of the hippocampus arousal activity by the septum cells. Electroencephalography and Clinical Neurophysiology, 14, 202-211.

Pico, R.M., Gerbrandt, L.K., Pondel, M. & Ivy, G. (1985). During stepwise cue deletion, rat place behaviors correlate with place unit responses. Brain Research, 330(2), 369-372.

Pigott, S., & Milner, B. (1993). Memory for different aspects of complex visual scenes after unilateral temporal- or frontal-lobe resection. Neuropsychologia, 31(1), 1-15.

Pike, F.G., Goddard, R.S., Suckling, J.M., Ganter, P., Kasthuri, N., & Paulsen, O. (2000). Distinct frequency preferences of different types of rat hippocampal neurones in response to oscillatory input currents. Journal of Physiology, 529 Pt 1, 205-213.

Quirk, G.J., Muller, R.U., & Kubie, J.L. (1990). The firing of place cells in the dark depends on the rat's recent experience. Journal of Neuroscience, 10, 2008-2017.

Quirk, G.J., Muller, R.U., Kubie, J.L. & Ranck, J.B., Jr. (1992). The positional firing properties of medial entorhinal neurons: description and comparison with hippocampal place cells. Journal of Neuroscience 12(5), 1945-1963.

Raghavachari, S., Kahana, M.J., Rizzuto, D.S., Caplan, J.B., Kirschen, M.P., Bourgeois, B., Madsen, J.R. & Lisman, J.E. (2001). Gating of human theta oscillations by a working memory task. Journal of Neuroscience 21(9), 3175-3183.

Ramón y Cajal, S. (1911). Histologie du systeme nerveux de l'homme et des vertebrates, tome II (L. Azoulay, Trans.). Paris: Maloine.

Ranck, J.B. Jr. (1973). Studies on single neurons in dorsal hippocampal formation and septum in unrestrained rats. I. Behavioral correlates and firing repertoires. Experimental Neurology, 41, 461-531.

Ranck, J.B., Jr. (1984). Head direction cells in the deep cell layer of dorsal presubiculum in freely moving rats. Society of Neuroscience Abstracts, 20, 1206.

Redish, A.D., Battaglia, F.P., Chawla, M.K., Ekstrom, A.D., Gerrard, J.L., Lipa, P., Rosenzweig, E.S., Worley, P.F., Guzowski, J.F., McNaughton, B.L., & Barnes, C.A. (2001). Independence of firing correlates of anatomically proximate hippocampal pyramidal cells. Journal of Neuroscience, 21(5):RC134.

Rivas, J., Gaztelu, J.M., & Garcia-Austt, E. (1996). Changes in hippocampal cell discharge patterns and theta rhythm spectral properties as a function of walking velocity in the guinea pig. Experimental Brain Research, 108(1), 113-118.

Rolls, E.T. (1999). Spatial view cells and the representation of place in the primate hippocampus. Hippocampus 9(4), 467-480.

Rose, G., Diamond, D. & Lynch, G.S. (1983). Dentate granule cells in the rat hippocampal formation have the behavioral characteristics of theta neurons. Brain Research, 266(1), 29-37.

Rotenberg, A., Abel, T., Hawkins, R.D., Kandel, E.R., & Muller, R.U. (2000). Parallel instabilities of long-term potentiation, place cells, and learning caused by decreased protein kinase A activity. Journal of Neuroscience, 20(21), 8096-8102.

Rotenberg, A., Mayford, M., Hawkins, R.D., Kandel, E.R., & Muller, R.U. (1996). Mice expressing activated CaMKII lack low frequency LTP and do not form stable place cells in the CA1 region of the hippocampus. Cell, 87(7), 1351-1361.

Rugg, M.D. & Dickens, A.M. (1982). Dissociation of alpha and theta activity as a function of verbal and visuospatial tasks. Electroencephalography and Clinical Neurophysiology, 53(2), 201-207.

Sagar, H.J., Cohen, N.J., Corkin, S. & Growdon, J.H. (1985). Dissociations among processes in remote memory. Annals of the New York Academy of Sciences, 444, 533-535.

Samsonovich, A., & McNaughton, B.L. (1997). Path integration and cognitive mapping in a continuous attractor neural model. Journal of Neuroscience, 17(15), 5900-5920.

Save, Cressant, Thinus-Blanc & Poucet (1998). Spatial firing of hippocampal place cells in blind rats. Journal of Neuroscience 18(5), 1818-1826.

Save, E., Nerad, L., & Poucet, B. (2000). Contribution of multiple sensory information to place field stability in hippocampal place cells. Hippocampus, 10(1), 64-76.

Scharfman, H.E., Kunkel, D.D. & Schwartzkroin, P.A. (1990). Synaptic connections of dentate granule cells and hilar neurons: results of paired intracellular recordings and intracellular horseradish peroxidase injections. Neuroscience, 37(3), 693-707.

Scoville, W.B., & Milner, B. (1957). Loss of recent memory after bilateral hippocampal lesions. Journal of Neurology, Neurosurgery, and Psychiatry, 20, 11-21.

Sharp, P.E., Blair, H.T., Etkin, D., & Tzanetos, D.B. (1995). Influences of vestibular and visual motion information on the spatial firing patterns of hippocampal place cells. Journal of Neuroscience, 15(1), 173-189.

Sharp, P.E. & Green, C. (1994). Spatial correlates of firing patterns of single cells in the subiculum of the freely moving rat. Journal of Neuroscience 14(4), 2339-2356.

Shibata, H. (1993). Direct projections from the anterior thalamic nuclei to the retrohippocampal region in the rat. Journal of Comparative Neurology, 337(3), 431-445.

Shin, J., & Talnov, A. (2001). A single trial analysis of hippocampal theta frequency during nonsteady wheel running in rats. Brain Research, 897(1-2), 217-221.

Siapas, A.G., & Wilson, M.A. (1998). Coordinated interactions between hippocampal ripples and cortical spindles during slow-wave sleep. Neuron , 21(5), 1123-1128.

Seidenbecher, T., Laxmi, T.R., Stork, O. & Pape, H.C. (2003). Amygdalar and hippocampal theta rhythm synchronization during fear memory retrieval. Science, 301(5634), 846-850.

Siegel, J.J., Nitz, D., & Bingman, V.P. (2000). Hippocampal theta rhythm in awake, freely moving homing pigeons. Hippocampus, 10(6), 627-631.

Sik, A., Penttonen, M. & Buzsáki, G. (1997). Interneurons in the hippocampal dentate gyrus: an in vivo intracellular study. European Journal of Neuroscience, 9(3), 573-588.

Sik, A., Penttonen, M., Ylinen, A., & Buzsáki, G. (1995). Hippocampal CA1 interneurons: an in vivo intracellular labeling study. Journal of Neuroscience 15(10), 6651-6665.

Skaggs, W.E., & McNaughton, B.L. (1998). Spatial firing properties of hippocampal CA1 populations in an environment containing two visually identical regions. Journal of Neuroscience, 18(20), 8455-8466.

Skaggs, W.E., McNaughton, B.L., Wilson, M.A., & Barnes, C.A. (1996). Theta phase precession in hippocampal neuronal populations and the compression of temporal sequences. Hippocampus, 6(2), 149-172.

Slawinska U., & Kasicki, S. (1998). The frequency of rat's hippocampal theta rhythm is related to the speed of locomotion. Brain Research, 796(1), 327-331.

Soriano, E. & Frotscher, M. (1989). A GABAergic axo-axonic cell in the fascia dentata controls the main excitatory hippocampal pathway. Brain Research, 503(1), 170-174.

Speakman, A, & O'Keefe, J. (1990). Hippocampal Complex Spike Cells do not Change Their Place Fields if the Goal is Moved Within a Cue Controlled Environment. European Journal of Neuroscience 2(6), 544-555.

Spiers, H.J., Burgess, N., Hartley, T., Vargha-Khadem, F., & O'Keefe, J. (2001a). Bilateral hippocampal pathology impairs topographical and episodic memory but not visual pattern matching. Hippocampus, 11(6), 715-725.

Spiers, H.J., Maguire, E.A. & Burgess, N. (2001b). Hippocampal amnesia. Neurocase, 7(5), 357-382.

Stackman, R.W., & Taube, J.S. (1997). Firing properties of head direction cells in the rat anterior thalamic nucleus: Dependence on vestibular input. Journal of Neuroscience, 17(11), 4349-4358.

Stackman, R.W. & Taube, J.S. (1998). Firing properties of rat lateral mammillary single units: Head direction, head pitch, and angular head velocity. Journal of Neuroscience 18(21), 9020-9037.

Stewart, M., & Fox, S.E. 1991. Hippocampal theta activity in monkeys. Brain Research, 538(1), 59-63.

Stewart, M., Luo, Y. & Fox, S.E. (1992). Effects of atropine on hippocampal theta cells and complex-spike cells. Brain Research, 591(1), 122-128.

Strata, F. (1998). Intrinsic oscillations in CA3 hippocampal pyramids: physiological relevance to theta rhythm generation. Hippocampus, 8(6), 666-679.

Szentágothai (1962). On the synaptology of the cerebral cortex. Structure and Function of the Nervous System. S. A. Sarkissov. Moscow, Medgiz: 6-14.

Szentágothai (1965). The synapse of short local neurons in the cerebral cortex. Modern Trends in Neuromorphology. J. Szentágothai Budapest, Akadémiai Kiadó: 251-276.

Szentágothai (1965). The use of degeneration methods in the investigation of short neuronal connections. Progress in Brain Research, 14, 1-32.

Taube, J. S. (1995). Head direction cells recorded in the anterior thalamic nuclei of freely moving rats. .Journal of Neuroscience, 15(1 Pt 1), 70-86.

Taube (1995). Place cells recorded in the parasubiculum of freely moving rats. Hippocampus, 5(6), 569-58.

Taube, J.S., & Burton, H.L. (1995). Head direction cell activity monitored in a novel environment and during a cue conflict situation. The Journal of Neurophysiology, 74(5), 1953-1971.

Taube, J.S., Goodridge, J.P., Golob, E.J., Dudchenko, P.A., & Stackman, R.W. (1996). Processing the head direction cell signal: a review and commentary. Brain Research Bulletin, 40(5-6), 477-484.

Taube, J.S., Muller, R.U., & Ranck, J.B., Jr. (1990a). Head-direction cells recorded from the postsubiculum in freely moving rats. I. Description and quantitative analysis. Journal of Neuroscience, 10(2), 420-35.

Taube, J.S., Muller, R.U., & Ranck, J.B., Jr. (1990b). Head-direction cells recorded from the postsubiculum in freely moving rats. II. Effects of environmental manipulations. Journal of Neuroscience, 10(2), 436-47.

Tesche, C.D., & Karhu, J. (2000). Theta oscillations index human hippocampal activation during a working memory task. Proceedings of the National Academy of Sciences of the United States of America, 97(2), 919-924.

Thinus-Blanc, C., Bouzouba, L., Chaix, K., Chapuis, N., Durup, M. & Poucet, B. (1987). A study of spatial parameters encoded during exploration in hamsters. Journal of Experimental Psychology: Animal Behavior Processes, 13, 418–427.

Thompson, L.T., & Best, P.J. (1989). Place cells and silent cells in the hippocampus of freely-behaving rats. Journal of Neuroscience, 9(7), 2382-2390.

Thompson, L.T., & Best, P.J. (1990). Long-term stability of the place-field activity of single units recorded from the dorsal hippocampus of freely behaving rats. Brain Research, 509(2), 299-308.

Tolman, E.C. (1948). Cognitive maps in rats and men. Psychological Review 5, 189-208.

Tolman, E. C., Ritchie, B. F., & Kalish, D. (1946). Studies in spatial learning. I. Orientation and the short-cut. Journal of Experimental Psychology: General, 121, 429-434.

Tóth, K., Borhegyi, Z. & Freund, T.F. (1993). Postsynaptic targets of GABAergic hippocampal neurons in the medial septum-diagonal band of broca complex. Journal of Neuroscience 13(9), 3712-3724.

Treves, A. & Rolls, E.T. (1992). Computational constraints suggest the need for two distinct input systems to the hippocampal CA3 network. Hippocampus, 2(2), 189-199.

Tsien, J.Z., Huerta, P.T., & Tonegawa, S. (1996). The essential role of hippocampal CA1 NMDA receptor-dependent synaptic plasticity in spatial memory. Cell, 87(7), 1327-1338.

Tsodyks, M.V., Skaggs, W.E., Sejnowski, T.J., & McNaughton, B.L. (1996). Population dynamics and theta rhythm phase precession of hippocampal place cell firing: a spiking neuron model. Hippocampus, 6(3), 271-280.

Tsodyks, M. (1999). Attractor neural network models of spatial maps in hippocampus. Hippocampus, 9(4), 481-489.

Tulving, E. (1983). Elements of episodic memory (Oxford: Clarendon Press).

Uchida, S., Maehara, T., Hirai, N., Okubo, Y. & Shimizu, H. (2001). Cortical oscillations in human medial temporal lobe during wakefulness and all-night sleep. Brain Research, 891(1-2), 7-19.

Vanderwolf, C. H. (1969). Hippocampal electrical activity and voluntary movement in the rat. Electroencephalography and Clinical Neurophysiology, 26, 407-18.

Vanderwolf, C.H. (1975). Neocortical and hippocampal activation relation to behavior: effects of atropine, eserine, phenothiazines, and amphetamine. Journal of Comparative and Physiological Psychology, 88(1), 300-323.

van Groen, T., & Wyss, J.M. (1990). The postsubicular cortex in the rat: Characterization of the fourth region of the subicular cortex and its connections. Brain Research, 529(1-2), 165–177.

Wallenstein, G.V., & Hasselmo, M.E. (1997). GABAergic modulation of hippocampal population activity: sequence learning, place field development, and the phase precession effect. The Journal of Neurophysiology, 78(1), 393-408.

Wenzel, H.J., Buckmaster, P.S., Anderson, N.L., Wenzel, M.E., & Schwartzkroin, P.A. (1997). Ultrastructural localization of neurotransmitter immunoreactivity in mossy cell axons and their synaptic targets in the rat dentate gyrus. Hippocampus, 7(5), 559-570.

Whishaw, I. Q, And Vanderwolf, C. H. (1971). Hippocampal EEG and behaviour: Effects of variation in body temperature and relation of EEG to vibrissae movement, swimming and shivering. Physiology and Behavior, 6, 391-7.

Whishaw, I. Q, And Vanderwolf, C. H. (1973). Hippocampal EEG and behaviour: changes in amplitude and frequency of RSA (Theta rhythm) associated with spontaneous and learned movement patterns in rats and cats. Behavioral Biology, 8, 461-84.

Wiener, S.I. & Berthoz, A. (1993). Forebrain structures mediating the vestibular contribution during navigation. In A. Berthoz (Ed.), Multisensory control of movement (pp. 427–456). Oxford: Oxford University Press.

Wiener S.I., Paul, C.A., & Eichenbaum, H. (1989). Spatial and behavioral correlates of hippocampal neuronal activity. Journal of Neuroscience, 9(8), 2737-2763.

Wilson, M.A., & McNaughton, B.L. (1993). Dynamics of the hippocampal ensemble code for space. Science, 261(5124), 1055-1058.

Wilson, M.A., & McNaughton, B.L. (1994). Reactivation of hippocampal ensemble memories during sleep. Science, 265(5172), 676-679.

Winson, J. (1972). Interspecies differences in the occurrence of theta. Behavioral Biology, 7(4),479-487.

Winson, J. (1974). Patterns of hippocampal theta rhythm in the freely moving rat. Electroencephalography and Clinical Neurophysiology, 36(3), 291-301.

Witter, M.P., Groenewegen, H.J., Lopes da Silva, F.H. & Lohman, A.H. (1989). Functional organization of the extrinsic and intrinsic circuitry of the parahippocampal region. Progress in Neurobiology, 33(3), 161-253.

Witter, M.P., Naber, P.A., Van Haeften, T., Machielsen, W.C.M., Rombouts, S.A.R.B., Barkhof, F., Scheltens, P., & Lopez da Silva, F.H. (2000). Cortico-hippocampal communication by way of parallel parahippocampal-subicular pathways. Hippocampus 10(4), 398–410.

Wood, E.R., Dudchenko, P.A., & Eichenbaum, H. (1999). The global record of memory in hippocampal neuronal activity. Nature, 397(6720), 613-616.

Wouterlood, F.G., Saldana, E. & Witter, M.P. (1990). Projection from the nucleus reuniens thalami to the hippocampal region: light and electron microscopic tracing study in the rat with the anterograde tracer Phaseolus vulgaris-leucoagglutinin. Journal of Comparative Neurology, 296(2), 179-203.

Yamaguchi, Y., Aota, Y., McNaughton, B.L., & Lipa, P. (2002). Bimodality of theta phase precession in hippocampal place cells in freely running rats. Journal of Neurophysiology, 87(6), 2629-2642.

Ylinen, A., Bragin, A., Nádasdy, Z., Jando, G., Szabo, I., Sik, A., & Buzsáki, G. (1995). Sharp wave-associated high-frequency oscillation (200 Hz) in the intact hippocampus: network and intracellular mechanisms. Journal of Neuroscience, 15(1 Pt 1), 30-46.

Zhang, K., Ginzburg, I., McNaughton, B.L., & Sejnowski, T.J. (1998). Interpreting neuronal population activity by reconstruction: unified framework with application to hippocampal place cells. The Journal of Neurophysiology, 79(2), 1017-1044.

Zinyuk, L., Kubik, S., Kaminsky, Y., Fenton, A.A., & Bures, J. (2000). Understanding hippocampal activity by using purposeful behavior: place navigation induces place cell discharge in both task-relevant and task-irrelevant spatial reference frames. Proceedings of the National Academy of Sciences of the United States of America, 97(7), 3771-3776.